Synaptic Vesicle Recycling *in Vivo*

Dissertation

in partial fulfilment of the requirements for the degree
"Doctor of Natural Sciences (Dr. rer. nat.)"
in the Molecular Biology Program
at the Georg August University Göttingen,
Faculty of Biology

submitted by

Annette Denker

born in

Aachen, Germany

Göttingen, September 2011

To my father

I hereby declare that I prepared this dissertation independently and with no other sources and aids than quoted.

Annette Denker

List of Publications

The results presented in this thesis are based on the following publications:

Denker A, Bethani I, Kröhnert K, Körber C, Horstmann H, Wilhelm BG, Barysch SV, Kuner T, Neher E, Rizzoli SO (2011)
A small pool of vesicles maintains synaptic activity in vivo.
Proc Natl Acad Sci USA *(epub ahead of print)*

Denker A, Kröhnert K, Bückers J, Neher E, Rizzoli SO (2011)
The reserve pool of synaptic vesicles acts as a buffer for proteins involved in synaptic vesicle recycling.
Proc Natl Acad Sci USA *(epub ahead of print)*

Denker A, Rizzoli SO (2010)
Synaptic vesicle pools: an update.
Front Synaptic Neurosci 2:135.

Denker A, Kröhnert K, Rizzoli SO (2009)
Revisiting synaptic vesicle pool localization in the Drosophila neuromuscular junction.
J Physiol 587:2919-2926.

Table of Contents

Acknowledgements

Abstract

The basic mechanism of neurotransmitter release at synapses is relatively well understood: upon arrival of an action potential, calcium influx into the nerve terminal triggers fusion of synaptic vesicles with the plasma membrane, resulting in the release of neurotransmitter from the vesicle interior into the synaptic cleft. The neurotransmitter diffuses to the postsynaptic cell, where it binds its respective receptors and evokes a change in membrane potential. At the presynaptic side, the vesicle membrane is retrieved and refilled with neurotransmitter, in what is termed vesicle recycling.

Surprisingly, synapses can contain up to half a million vesicles, most of which can be forced to undergo recycling under high frequency stimulation in many preparations *in vitro*. However, whether and how they are involved in neurotransmission *in vivo* is unknown. The aim of this project was therefore to determine the number of vesicles used by a living animal during a defined time period.

Vesicle use *in vivo* was monitored by three different approaches: first, the fluorescent dye FM 1-43 was injected into a living animal, which was then allowed to behave freely for a defined amount of time, during which the dye was taken up by recycling vesicles. At the end of the observation period, the organ of interest was dissected and photo-oxidized, a procedure that allows for the identification and quantification of labelled vesicles by electron microscopy. Using this technique, I found that only about 1-5% of all vesicles had undergone recycling over a few hours, in animal models ranging from nematodes and insects over fish, amphibians and birds to mammals. This limited vesicle use was confirmed by two independent experimental approaches, imaging of pHluorin *Drosophila* larvae combined with injection of the proton pump inhibitor bafilomycin and electron microscopy of the endocytic *Drosophila* mutant *shibire*.

To determine by what molecular mechanism the majority of the vesicles might be prevented from participating in recycling, a *Drosophila* knockout strain of the vesicle-associated protein synapsin was investigated. Synapsin was found to restrict the mobility of the non-recycling vesicle population. In addition, synapsin deletion resulted in a substantial increase in the percentage of vesicles recycling *in vivo*, indicating that synapsin is one of the molecular players involved in distinguishing actively recycling and inactive vesicles.

Finally, the functional role of the non-recycling vesicle population was investigated. It was shown that these vesicles might function as a molecular buffer, retaining soluble proteins involved in vesicle recycling in the synapse. Using immunostaining and stimulated emission depletion (STED) microscopy, the vesicle cluster (consisting largely of non-recycling vesicles) was found to concentrate many accessory molecules, and this interaction was also confirmed by immunoblotting. In line with the buffer model, vesicle cluster disruption

by black widow spider venom (BWSV) treatment resulted in protein loss into the axon. Further experiments using the calcium ionophore ionomycin indicated that molecular buffering is probably controlled by calcium, as was also confirmed biochemically. This would provide an explanation for how the vesicle cluster can provide these soluble molecules to a fused actively recycling vesicle upon demand.

In summary, this project revealed that the majority of synaptic vesicles do not function in neurotransmitter release *in vivo*. Instead, they support synaptic transmission indirectly by ensuring the availability of accessory molecules for the recycling of the few active vesicles.

List of Figures

List of Tables

List of Abbreviations

AAA+	ATPases associated with diverse cellular activities
ACV	*Adductor caudalis ventralis*
AOTF	Acousto-optical tunable filter
AP	Adaptor protein
APS	Ammonium persulfate
ATP	Adenosine triphosphate
BCA	Bicinchoninic acid
BWSV	Black widow spider venom
BSA	Bovine serum albumine
CaMK	Calcium/calmodulin-dependent protein kinase
CCD	Charge-coupled device
CHAPS	3-[(3-cholamidopropyl)dimethylammonio]-1-propanesulfonate
CME	Clathrin-mediated endocytosis
CNS	Central nervous system
CSP	Cysteine string protein
DAB	3,3'-diaminobenzidine
DKO	Double knockout
DMSO	Dimethyl sulfoxide
DTT	Dithiothreitol
EGFP	Enhanced green fluorescent protein
EGTA	Ethylene glycol tetraacetic acid
EDL	*Extensor digitorum longus*
EM	Electron microscopy
EPS	Epidermal growth factor receptor substrate
FACS	Fluorescence-activated cell sorting
FCVI	*Flexor caudalis ventralis inferior*
FCVS	*Flexor caudalis ventralis superior*
FRAP	Fluorescence recovery after photobleaching
FWHM	Full width half maximum
GABA	γ-aminobutyric acid
GAP	GTPase activating protein
GDI	GDP dissociation inhibitor
GDP	Guanosine diphosphate
GEF	Guanine-nucleotide exchange factor
GFP	Green fluorescent protein

GTP	Guanosine triphosphate
HEPES	4-(2-hydroxyethyl)-1-piperazineethanesulfonic acid
HRP	Horseradish-peroxidase
Hsc70	70 kDa heat shock cognate protein
IVM	Inter-vesicular matrix
mEPP	Miniature end-plate potential
NA	Numerical aperture
NHS-ester	N-hydroxysuccinimidyl-ester
NMJ	Neuromuscular junction
NSF	N-ethylmaleimide-sensitive factor
PAGE	Polyacrylamide gel electrophoresis
PBS	Phosphate buffered saline
PFA	Paraformaldehyde
PKA	Protein kinase A
PNS	Peripheral nervous system
PSD	Postsynaptic density
PSF	Point spread function
Rab	Ras-related in brain
RIM	Rab3-interacting molecule
RNAi	RNA interference
ROI	Region of interest
ROS	Reactive oxygen species
RRP	Readily releasable pool
SDS	Sodium dodecyl sulfate
SEM	Standard error of the mean
SM protein	Sec1/Munc18-like protein
SNAP	Soluble NSF-attachment protein
SNAP-25	25-kDa synaptosome-associated protein
SNARE	Soluble N-ethylmaleimide-sensitive factor attachment protein receptor
STED	Stimulated emission depletion
SypHy	Synaptophysin-pHluorin
TDE	2,2'-thiodiethanol
TEMED	Tetramethylethylenediamine
TKO	Triple knockout
TRIS	Tris(hydroxymethyl)aminomethane
TTX	Tetrodotoxin
UAS	Upstream activating sequences

VAMP   Vesicle-associated membrane protein

VGSC   Voltage-gated sodium channel

VNC   Ventral nerve cord

1. Introduction

1.1 Synaptic Function

The human brain is estimated to contain up to 100 billion neurons, with tens of billions of neurons found in the neocortex alone (Pakkenberg and Gundersen, 1997). Each neuron, in turn, is thought to form around 1,000 connections to neighboring neurons. However, knowledge of this cellular structure of the brain could only be gained in the 19th century, after the advent of staining techniques which revolutionized brain histology: the Nissl stain and the Golgi stain. Especially the Golgi stain, which was invented by Camillo Golgi, allowed for the first time the visualization of a typical neuron, with soma, axon and dendrites. Camillo Golgi's investigations resulted in his proposal of the *reticular theory*, stating that neurons in the brain are interconnected via their axons and dendrites and therefore represent an exception to the cell theory (according to which each tissue is made up of single cells as the basic unit). In contrast, Santiago Ramón y Cajal, who also employed the Golgi stain to visualize neuronal circuits, proposed the *neuron doctrine*, claiming that no such cellular continuity exists between individual neurons. Indeed, using high resolution microscopy (such as electron microscopy, EM), unequivocal proof for the neuron doctrine could be obtained - albeit only half a century later (Bear et al., 2006). However, a term for the point of contact and communication between two neurons was already introduced in 1897 by Michael Foster and Sir Charles Scott Sherrington: the synapse (Foster and Sherrington, 1897).

1.1.1 The Morphology and Functional Characteristics of Synapses

To ensure the efficient transmission of the electrical signal between neurons, two different types of synapses have evolved: the electrical and the chemical synapse. These two types of synapses differ not only in their function but also in their morphology.

Electrical synapses were first described for giant motor synapses of the crayfish (Furshpan and Potter, 1959) but have also been demonstrated in vertebrates (for instance Galarreta and Hestrin, 1999; Venance et al., 2000). They are formed by gap junctions and allow for the exchange of ions, small metobolites and second messengers between neurons. In neuronal communication, the arrival of an action potential in the presynaptic cell induces ionic current to flow across the gap junction directly into the postsynaptic neuron; the cells are therefore electrically coupled (Bear et al., 2006). Importantly, the current flow can be bi-directional and sub-threshold potentials can also be transmitted, in striking contrast to conventional chemical synapses (see below). These two features might well constitute the major advantages of transmission via electrical synapses and have been implicated in the

generation of synchronous activity and functional coupling of neurons (refer to Hormuzdi et al., 2004, for further details on the role of electrical synapses in neuronal networks).

A second and more frequently encountered type of synapse is the chemical synapse, which was exclusively investigated in this study. I will therefore focus on chemical synaptic transmission in the next sections. In chemical synapses, the pre- and postsynaptic side are separated by the synaptic cleft, which is about 20-50 nm wide (10 times wider than the gap between electrically coupled cells; Bear et al., 2006). In order to transmit the electrical signal from the presynaptic cell over the synaptic cleft to the postsynaptic side, it needs to be transformed into a chemical signal as follows: upon arrival of an action potential, voltage-gated calcium channels within the presynaptic plasma membrane open. The resulting influx of calcium ions triggers the fusion of small (up to ~50 nm diameter; Bear et al., 2006) membrane-bound organelles, the synaptic vesicles, with the plasma membrane (see Section 1.1.3). This fusion leads to the release of neurotransmitter molecules from the vesicle interior into the synaptic cleft. Neurotransmitter molecules can then diffuse towards their respective postsynaptic receptors, which constitute neurotransmitter-gated ion channels. Binding of neurotransmitter therefore causes the influx of ions into the postsynaptic cell, changes the cell's membrane potential (in either an inhibitory or an excitatory fashion) and thereby transforms the chemical back into an electrical signal. Meanwhile, the vesicle membrane is retrieved from the presynaptic plasma membrane by one of the proposed recycling pathways (see Section 1.1.4) and refilled with neurotransmitter molecules to complete the synaptic vesicle cycle (Katz, 1969; Sudhof, 2004). Importantly, because of its quite complex nature, the vesicle cycle allows for the precise regulation and fine-tuning of synaptic output.

The presynaptic area where neurotransmitter release and thereby the transformation into a chemical signal occurs is termed the active zone. Whereas active zone morphology can differ among synapses and organisms (refer for instance to Zhai and Bellen, 2004), it can generally be readily identified in electron micrographs due to 1) the increased electron-density on both the pre- and postsynaptic side (indicative of proteinaceous structures extending into the presynaptic cytoplasm and involved in vesicle release, or representing the receptors and associated structures of the postsynaptic density, PSD, respectively) and 2) the cluster of synaptic vesicles generally associated with the active zones (Bear et al., 2006).

Although sharing the basic features described above, subtypes of chemical synapses differ substantially in their morphology, depending on their specific requirements. For instance, some synapses which display graded responses to stimulation have developed specialized active zone-anchored structures extending into the cytoplasm: the synaptic ribbons. These proteinaceous structures might function like a „conveyor-belt" to transport vesicles very rapidly to the active zones and are especially common in sensory synapses (examples are the bipolar cells and photoreceptors of the vertebrate retina and the

mechanosensory inner ear hair cells; Lenzi and von Gersdorff, 2001; Parsons and Sterling, 2003).

A second example are the neuromuscular junctions (NMJs) of the peripheral nervous system (PNS), which display structural specializations that are remarkably different from the structure of central nervous system (CNS) synapses. As reliable transmission at an NMJ can be vitally important, a "safety factor" has evolved which ensures that every action potential in the motor axon triggers an action potential in the muscle and which results from the combination of several structural features (Wood and Slater, 2001): for example, NMJs generally contain much more vesicles than many CNS synapses (up to several hundred thousand as compared to 100 to 200 vesicles in hippocampal terminals; Rizzoli and Betz, 2005). They also often have several hundred active zones per terminal (for instance ~200 in human and ~850 in the mouse NMJ; Ruiz et al., 2011; Slater et al., 1992; Slater, 2003), whereas hippocampal boutons display only one active zone (Schikorski and Stevens, 1997). Maybe the most striking specialization, however, are the extensive junctional folds observed in the post-synaptic membrane (motor end-plate; Bear et al., 2006). It has been proposed that the folds might serve to amplify the transmitter effect and to lower the effective threshold for action potential generation in the muscle by two mechanisms: 1) voltage-gated sodium channels (VGSCs) are present at high density within the folds, as shown by EM immunolabelling (Flucher and Daniels, 1989). These VGSCs open in response to depolarization induced by neurotransmitter binding and are responsible for action potential generation. Neurotransmitter receptors, on the other hand, are generally located at the fold rim, directly opposing the active zones (Flucher and Daniels, 1989). Because of the high density of VGSCs in the folds, less depolarisation is required for action potential generation (a principle that is for instance also employed at the nodes of Ranvier and the axon hillock; Catterall, 1992; Wood and Slater, 2001; Slater, 2003). 2) The narrow geometry of the interfold space results in a high resistance path to the flow of current, which is therefore intensified and displays an enhanced depolarising effect on the VGSCs (Vautrin and Mambrini, 1989). This effect has been quantified and discussed in detail (Martin, 1994; Wood and Slater, 2001; Bewick, 2003). Clearly, both pre- and postsynaptic factors contribute to reliable transmission and the balance between the two differs between distinct organisms and synapses (reviewed by Slater, 2003). In addition, junctional folds might also play a role in the removal of neurotransmitter, as they have for instance been proposed to increase the diffusion of glutamate from the synaptic cleft in *Drosophila* NMJs (in contrast to acetylcholine and its respective degrading enzyme acetylcholineesterase, no glutamate-inactivating enzymes exist; Kuromi and Kidokoro, 2003).

1.1.2 Synaptic Vesicle Composition

As stated above, synaptic vesicles are small organelles, with a diameter of up to ~50 nm. Native synaptic vesicle membranes have a lipid composition of 40% phosphatidylcholine, 32% phosphatidylethanolamine, 12% phosphatidylserine, 5% phosphatidylinositol and 10% cholesterol (wt/wt) (Nagy et al., 1976; Benfenati et al., 1989; note that a higher cholesterol content has also been reported; Takamori et al., 2006).

Recently, a quantitative description of the composition of an average synaptic vesicle was presented (Takamori et al., 2006). One of the most striking observations was the high protein density of the membrane, with transmembrane domains representing a quarter of the membrane volume. In addition, many proteins interact only transiently with synaptic vesicles, i.e. only during specific stages of the vesicle cycle. The two major classes of obligatory synaptic vesicle components comprise proteins involved in exo- and endocytosis and in neurotransmitter uptake. To fulfil the second function, vesicles contain a vacuolar type proton-pump, which generates an electrochemical gradient over the vesicle membrane, thereby driving transporter-mediated neurotransmitter uptake (reviewed in Ahnert-Hilger et al., 2003). Interestingly, the proton-pump is present at very low copy numbers (only ~1 copy per vesicle). The number of neurotransmitter transporters per vesicle is in the range of 9 to 14 (Takamori et al., 2006).

By far the most abundant synaptic vesicle protein is the SNARE (soluble N-ethylmaleimide-sensitive factor attachment protein receptor) protein synaptobrevin or VAMP (vesicle-associated membrane protein), of which 70 copies are present per vesicle. SNAREs are involved in mediating membrane fusion events in general (as discussed in Section 1.1.3 and Jahn and Scheller, 2006), and synaptobrevin in particular plays a role in the fusion of synaptic vesicles with the plasma membrane. In addition to synaptobrevin, many more SNARE proteins were identified on vesicles, among them synaptobrevin's cognate SNARE partners syntaxin 1 and SNAP-25 (25-kDa synaptosome-associated protein) (Takamori et al., 2006). Another SNARE protein found on synaptic vesicles is Vti1a-*β*, which is involved in endosomal and trans-Golgi network trafficking events (Antonin et al., 2000; Sudhof, 2004). This indicated that endosomal intermediates might be involved in the synaptic vesicle cycle (see Section 1.1.4). In line with this observation, further endosomal SNARE proteins were also found on synaptic vesicles, namely syntaxin 6 and syntaxin 13 (Rizzoli et al., 2006).

In addition to SNARE proteins, Takamori and colleagues also found a multitude of small Rab (Ras-related in brain; Schwartz et al., 2007) GTPases on synaptic vesicles (Takamori et al., 2006). As discussed in Section 1.1.3, Rab proteins are major players of cellular trafficking events and are generally considered to be specific organelle markers. In agreement with previous studies, synaptic vesicles were found to interact with Rab3a, Rab3b

and Rab3c (Schluter et al., 2002), with 10 Rab3a proteins found on an average vesicle (Takamori et al., 2006), as well as Rab11 (Khvotchev et al., 2003) and the endosomal marker Rab5 (Fischer von Mollard et al., 1994). The distinct Rabs also mediate the interaction of vesicles with Rab effectors such as Rims (Rab3-interacting molecules; Wang et al., 1997; Kaeser, 2011) and rabphilin (Shirataki et al., 1993) (Section 1.1.3).

Other abundant synaptic vesicle proteins quantified by Takamori and colleagues are synaptophysin (32 copies per vesicle), the calcium-sensor synaptotagmin 1 (15 copies) and synapsin (8 copies). Together with the vacuolar proton-pump, neurotransmitter transporters, SNAREs and Rab proteins described above, these molecules are believed to form the basic vesicular machinery for neurotransmitter loading and release.

In the same study, many more proteins were found to interact with synaptic vesicles, among them molecules involved in clathrin-mediated endocytosis (CME; discussed in Section 1.1.4), which is of special importance for the molecular buffer model of vesicle function developed in this thesis (see Section 4.4.2). One should also emphasize that proteins which were found in very small quantities on the average synaptic vesicle (such as the endosomal SNARE Vti1a-β described above; Takamori et al., 2006) could well be strongly enriched on a subpopulation of vesicles, thereby possibly representing molecular tags distinguishing between vesicle populations with distinct properties ("vesicle pools"; refer to Section 1.2).

The proteins described above play distinct roles in the synaptic vesicle cycle of exo- and endocytosis. Since both the participation of vesicles in this cycle and the regulation of the proteins involved were investigated in this study, the relevant molecular mechanisms will be explained in the next two sections.

1.1.3 Mechanism of Synaptic Vesicle Exocytosis

The fusion of synaptic vesicles with the plasma membrane is a complex and highly-regulated process which involves a plethora of presynaptic proteins. Its basic mechanism is however similar to many other intracellular trafficking and membrane fusion events, in that it encompasses a Rab and a SNARE cycle, with the former involved in membrane attachment and the latter mediating fusion (Jahn et al., 2003). In addition, synaptic vesicle exocytosis is regulated by proteins coupling vesicle fusion to calcium influx.

The Rab Cycle and its Role in Vesicle Tethering

Rab proteins exist in an inactive soluble GDP-bound state and an active membrane-attached GTP-bound state. The cytosolic GDP-bound state is stabilized by binding to GDI

5

(GDP dissociation inhibitor; Araki et al., 1990). As mentioned in Section 1.1.2, Rabs are quite specific for their target membranes, to which they are recruited by a poorly understood process involving the exchange of GDP for GTP, catalyzed by GEFs (guanine-nucleotide exchange factors). At steady state, GTP-bound Rabs are found on the donor membrane. They then recruit Rab effectors (often forming large multimeric complexes), which are either directly linked to the acceptor membrane or bind to acceptor membrane components via a secondary interaction. This process therefore brings the two membranes in close proximity and is termed tethering or docking. However, membrane fusion itself is probably mediated by different molecular players, as discussed below. After fusion has been completed, the GTPase activity of the Rabs is triggered by interaction with a GAP (GTPase activating protein), leaving Rab in its inactive GDP-bound state, which is then again bound by GDI and consequently removed from the membrane (Jahn et al., 2003).

As described in Section 1.1.2, many different Rabs are associated with synaptic vesicles, with the most abundant being Rab3a (Takamori et al., 2006). Interestingly, the association and dissociation cycle of Rab3a to and from synaptic vesicles strongly depends on fusion activity, as Rab3a unbinds from the vesicles during exocytosis in a reversible manner (Fischer von Mollard et al., 1991).

One of the effectors of Rab3 is the active zone protein Rim (Wang et al., 1997). This interaction is involved in directing the vesicles to the active zone and mediates their docking (Weimer et al., 2006; Gracheva et al., 2008). In addition, Rim interacts with calcium channels and therefore ensures that the docked vesicles are optimally positioned for calcium-triggered release (Gracheva et al., 2008). Rim also binds Munc13, thereby forming a tripartite complex with Rab3, which is involved in transforming the synaptic vesicles into a readily releasable state ("priming"; Dulubova et al., 2005).

The SNARE Cycle and its Role in Vesicle Fusion

After the membranes have been attached, the next step to fusion is the assembly of the SNARE complex (see also Section 1.1.2). For the well-characterized process of synaptic vesicle fusion, one member of the forming SNARE complex is located on the vesicle (synaptobrevin) and two on the plasma membrane (syntaxin 1 and SNAP-25). As all members of the large superfamily of SNARE proteins, the SNAREs involved in vesicle fusion all share a so-called SNARE motif, which is a 60-70 amino acid stretch arranged in heptad repeats, which are typical for coiled coils (Bock et al., 2001; Jahn et al., 2003; Jahn and Scheller, 2006). SNAREs generally contain a C-terminal transmembrane domain next to the SNARE motif, but SNAP-25 for instance is palmitoylated instead. In addition, many SNAREs have independently folded domains at their N-terminus, although for example the

evolutionarily younger "brevins" lack this structural component (Jahn et al., 2003; Jahn and Scheller, 2006; see also Rossi et al., 2004).

Although unstructured in solution, appropriate SNARE motifs interact spontaneously with each other to form stable coiled coils of four helical-bundles, with all SNARE motifs in parallel orientation. With regard to vesicle fusion, it is likely that the close apposition of two membranes and their respective SNAREs leads to a "zipping-up" mechanism from the N-terminal end of the SNARE motifs to the membrane-anchored C-terminal end of the SNARE proteins, finally resulting in the formation of the fully intertwined SNARE complex. This process will force the membranes into even closer proximity and is thought to largely overcome the energy barrier for membrane fusion (Hanson et al., 1997; Jahn et al., 2003; Jahn and Scheller, 2006). In line with this model, SNARE complexes were found to be very stable, indicating that their formation releases substantial amounts of energy (Fasshauer et al., 2002).

The crystal structure of the neuronal SNARE complex was solved by Sutton and colleagues in 1998 and has been shown to be homologous to SNARE complexes involved in other membrane fusion events, in spite of limited sequence homology (Sutton et al., 1998; Antonin et al., 2002). A highly conserved feature is the presence of an ionic layer within the helix bundle, which consists of one arginine (R) and three glutamine (Q) residues. Accordingly, each SNARE motif which participates in the formation of a core complex can be classified according to its specific position and amino acid contribution as either an R- or a Qa-, Qb-, or Qc-SNARE (Fasshauer et al., 1998), and each functional SNARE core complex displays this composition. For the case of synaptic vesicle fusion, synaptobrevin provides the R-SNARE motif and syntaxin 1 the Qa-motif. SNAP-25 has two SNARE-motifs connected by a linker and can therefore provide both the Qb- and Qc-motifs (Jahn et al., 2003).

As explained above, the different SNAREs are in a *trans*-conformation (on different compartments or organelles) at the beginning of the reaction. However, membrane fusion results in the formation of a *cis*-complex, i.e. all three (or four) SNARE proteins involved in complex formation are now found on the same membrane. As a last step of the SNARE cycle, the core complex therefore needs to be dissociated and the different SNAREs need to be recycled back to their respective compartments (Sollner et al., 1993a; Sollner et al., 1993b). Core complex disassembly is catalyzed by the AAA+ (ATPases associated with diverse cellular activities) protein NSF (N-ethylmaleimide-sensitive factor, from which the SNARE proteins derive their name) and SNAP cofactors (soluble NSF-attachment proteins) (Block et al., 1988; Sollner et al., 1993b; Hanson et al., 1995; Hayashi et al., 1995).

As the SNARE core complex drives membrane fusion, its assembly needs to be tightly regulated. Among others, soluble proteins of the SM family (Sec1/Munc18-like proteins) are involved in this process. Although essential for membrane fusion, their

molecular function is not understood in detail. As reviewed by Jahn and colleagues, they might couple the Rab and SNARE cycles (Jahn et al., 2003). They often bind to syntaxin-like SNAREs. Munc18-1, for instance, binds to a closed conformation of syntaxin 1 (Dulubova et al., 1999) and thereby prevents core complex formation. However, this cannot be a general functional interaction of all SM proteins, as members of the SM protein family have also been proposed to recognize and bind syntaxin SNAREs in the open conformation (as for instance described in Dulubova et al., 2002; see also Sudhof, 2004). The molecular function of SM proteins in fusion therefore remains enigmatic.

The Function of Calcium Sensors in Controlling Vesicle Fusion

The interplay of SNAREs and SM proteins by itself does not cause synaptic vesicle fusion, but results in the formation of a fusion intermediate which is stabilized by the cytoplasmic protein complexin (McMahon et al., 1995; Chen et al., 2002). This interaction is proposed to leave the vesicle in a calcium-responsive state which would explain the fast onset of vesicle exocytosis upon calcium entry (in possibly less than 100 µs; Sabatini and Regehr, 1996). Synchronous and fast vesicle release relies on the calcium-sensor synaptotagmin 1, which is present in high copy numbers on synaptic vesicles (compare Section 1.1.2; Brose et al., 1992; Geppert et al., 1994). Synaptotagmin 1 has two calcium-binding C_2-domains, called C_2A and C_2B. Both domains interact with phospholipids in a calcium-dependent manner, and the respective cooperativity, affinity and cation selectivity correlates with observations of (fast) neurotransmitter release (Brose et al., 1992; Ubach et al., 1998; Schneggenburger and Neher, 2000; Fernandez et al., 2001). The interaction with phospholipids substantially increases the domains' calcium affinity, probably because the negatively charged phospholipid headgroups fill empty coordination sites (Zhang et al., 1998b; Fernandez-Chacon et al., 2001). The calcium-dependent interaction of synaptotagmin with the phospholipids of the plasma membrane might result in the insertion of hydrophobic amino acids from the calcium-sensor and thereby induce mechanical stress on the membrane. This might in turn function to destabilize the above-described fusion intermediate and thereby result in fusion pore opening (as reviewed in Jahn et al., 2003; Sudhof, 2004).

In addition to its interaction with phospholipids, synaptotagmin has also been reported to interact with many other molecular players of vesicle exocytosis, including SNAREs (Bennett et al., 1992; Sollner et al., 1993a; Schiavo et al., 1997) and calcium channels (Leveque et al., 1992). Although being best described, synaptotagmin 1 is probably not the only calcium sensor involved in vesicle release, as other members of the large synaptotagmin gene family might for instance be involved in asynchronous release (Sudhof,

2002; Sugita et al., 2002). Also, a different calcium-sensor for spontaneous (i.e., action potential-independent) fusion has recently been described (Groffen et al., 2010).

Fine-tuning the Vesicle Cycle: the Role of Synapsin

One presynaptic protein of special interest for this thesis due to its function in the regulation of synaptic vesicle release and maintenance of the so-called reserve pool of vesicles (see Section 1.2.1) is synapsin, the first synaptic vesicle protein identified (De Camilli et al., 1983a; De Camilli et al., 1983b; Huttner et al., 1983; see also Greengard et al., 1994; Sudhof, 2004; Cesca et al., 2010). Synapsin might also be involved in the delivery of vesicles to the active zones and even in synchronizing release (as reviewed in Bykhovskaia, 2011). In mammals, different isoforms exist which result from alternative splicing of the three synapsin genes. All synapsins share similar N-terminal and central domains, but the C-terminus is variable (Sudhof et al., 1989; Sudhof, 2004). The N-terminus has three domains, A, B, and C. The A domain contains a highly conserved phosphorylation site for protein kinase A (PKA) and calcium/calmodulin-dependent protein kinase I (CaMKI) (Huttner et al., 1981; Sudhof, 2004; Cesca et al., 2010). Importantly, synapsin interacts with lipids (Benfenati et al., 1989) and particularly with synaptic vesicles in a manner which depends on the phosphorylation status of the A domain, with phosphorylation abolishing the interaction (Hosaka et al., 1999). It should be noted that a multitude of additional phosphorylation pathways and phosphorylation sites affecting vesicle binding have been described, involving for instance CaMKII (see for instance Schiebler et al., 1986; reviewed in Cesca et al., 2010; Bykhovskaia, 2011). Similarly, phosphorylation negatively regulates synapsin's interaction with the actin cytoskeleton (Petrucci and Morrow, 1987). Finally, the C domain mediates synapsin dimerization (Esser et al., 1998), although other domains could also play a role (Monaldi et al., 2010). In summary, these properties of synapsin have resulted in a model according to which synapsin in its dephosphorylated form cross-links synaptic vesicles and tethers them to the cytoskeleton. Upon stimulation, however, synapsin becomes phosphorylated and releases the vesicles, which can then fuse with the plasma membrane (as reviewed in Cesca et al., 2010). This model would also explain why vesicles which are docked at the active zone are devoid of synapsin (in contrast to vesicles more distal from the active zone; Pieribone et al., 1995), as are clathrin-coated endocytic intermediates (Bloom et al., 2003). As will be further discussed in Sections 4.3.1 and 4.4.2, this model is still highly debated, as it was for instance described that vesicle clusters within the synapse do not contain actin (Dunaevsky and Connor, 2000).

As mentioned above, synapsin has also been implicated in the subsequent steps of vesicle release, such as delivery of vesicles to the active zone (Bykhovskaia, 2011), due to

its redistribution from the distal vesicle cluster towards the vesicles proximal to the active zone during synaptic activity (Bloom et al., 2003; Tao-Cheng, 2006). Targeting of vesicles to the active zone via synapsin could involve the Rab3/Rim pathway described above, as synapsin has been shown to interact with Rab3a (Giovedi et al., 2004).

In addition, synapsin might be involved in the synchronization of vesicle release (Hilfiker et al., 1998; Coleman and Bykhovskaia, 2009b; discussed in Bykhovskaia, 2011), possibly by acting in concert with Rab3/Rim to position vesicles in optimal proximity to calcium channels (see above; compare also Schluter et al., 2006; Coleman and Bykhovskaia, 2009a). Finally, increasing evidence is presented for an additional role of synapsin in vesicle endocytosis (Akbergenova and Bykhovskaia, 2010; Bloom et al., 2003), a process that will be discussed in the following section.

1.1.4 Mechanisms of Synaptic Vesicle Endocytosis

Whereas there might be many remaining open questions with regard to vesicle docking, priming and release and the molecules involved, the basic pathway of exocytosis seems rather straightforward. This is however not the case for vesicle reuptake, for which several different recycling pathways are proposed. These recycling modes are kiss-and-run, clathrin-mediated endocytosis (CME), bulk endocytosis and endosomal recycling (Figure 1.1; see also Rizzoli and Jahn, 2007), which will be explained in detail below. It is also conceivable that several recycling pathways exist in parallel, that the choice of the pathway depends on the stimulation conditions, or that distinct subpopulations of vesicles ("pools"; as described in Section 1.2) use different mechanisms of retrieval (see for instance Denker and Rizzoli, 2010).
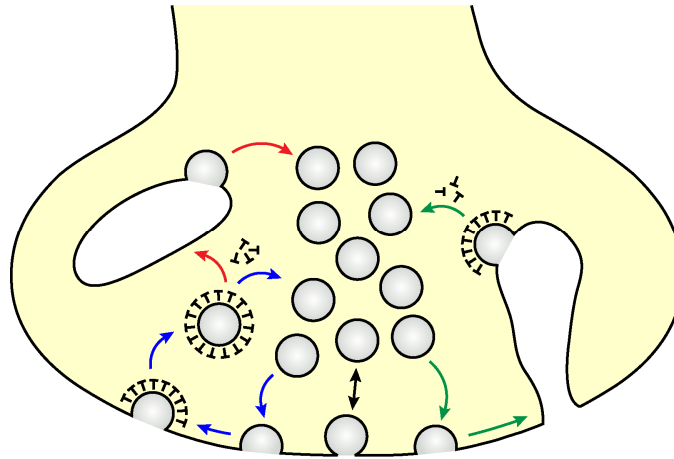
Figure 1.1: Summary of vesicle recycling pathways
Vesicles fuse either by full collapse into the plasma membrane or by forming only a transient fusion pore. In the latter case, the fusion pore is rapidly closed after neurotransmitter release and the vesicle is retrieved (kiss-and-run; black arrow). In the case of full fusion, the vesicle membrane can be retrieved by clathrin-mediated endocytosis (CME; blue arrows), either directly or in combination with endosomal sorting (red arrows). Instead of being retrieved from the membrane by CME, fully fused vesicles can also be recycled through bulk invaginations from the plasma membrane, from which new vesicles are in turn formed by CME (green arrows).

Kiss-and-run

According to the model of kiss-and-run vesicle recycling, the vesicles only fuse transiently via the formation of a short-lived fusion pore, i.e. without full collapse into the plasma membrane (Fesce et al., 1994). This mechanism would allow for fast retrieval of the vesicle membrane (reaching time constants of approximately 100 ms; Sun et al., 2002; Rizzoli and Jahn, 2007; black arrow in Figure 1.1), followed by refilling with neurotransmitter. It would also circumvent the problem of losing vesicle components into the plasma membrane upon fusion, which would result in the requirement of some sort of sorting, either at the plasma membrane (as in CME) or within a specialized intracellular compartment (as in endosomal sorting, see below). The kiss-and-run mechanism is therefore an attractive hypothesis, especially with regard to mammalian CNS synapses, in which only a small fraction of all vesicles seem to be actively releasing neurotransmitter and which might therefore rely on fast recycling modes (examples are hippocampal neurons; Harata et al., 2001a; Harata et al., 2001b; but possibly also the calyx of Held of the auditory pathway; de Lange et al., 2003; vesicle use will be discussed in detail in Section 1.3.1).

However, the model has remained controversial, although the first evidence of a clathrin-independent recycling mode involving small vesicular structures was presented already in one of the first EM studies of vesicle retrieval at the frog NMJ (Ceccarelli et al., 1973).

Several additional pieces of evidence in favor of kiss-and-run recycling have been obtained since the seminal study of Ceccarelli and colleagues. For instance, when frog NMJs were treated with the kinase inhibitor staurosporine, neurotransmitter release was unaffected, whereas vesicles which had taken up the styryl dye FM 1-43 in a previous round of stimulation could not be efficiently destained, consistent with vesicle fusion through pores which are so short-lived that they allow for the escape of small neurotransmitter molecules, but not for equilibration of the substantially larger and membrane-bound dye with the extracellular medium (Henkel and Betz, 1995b). (See Figure 2.1 for a presentation of FM dye function and uptake.)

Retention of a substantial amount of FM dye during (initial) vesicle release was also observed in hippocampal cultures, and was taken as an indication for fast and possibly kiss-and-run recycling (Klingauf et al., 1998). A similar observation was also made in a study which employed the labelling and subsequent destaining of only a single vesicle (Aravanis et al., 2003) and in an investigation in which the uptake of a hydrophilic quencher into recycling vesicles revealed FM dye retention (Harata et al., 2006). Note however that no dye retention but full fusion and complete dye loss were found in a more recent study (Chen et al., 2008).

FM dye labelling represents only one of several techniques which have been used to study (fast) vesicle recycling. One of the most powerful methods has been the visualization of vesicle exo- and endocytosis by the use of pHluorins. PHluorins were introduced in 1998 and are fusion products of a pH-sensitive GFP variant to the lumenal domain of a synaptic vesicle protein, with the classical example being synaptopHluorin (involving fusion to synaptobrevin; Miesenbock et al., 1998; see also Denker and Rizzoli, 2010). The GFP fluorescence is quenched within the acidic lumen of the vesicles (the internal pH is ~5.6), but upon exocytosis and exposure to the more neutral pH of the extracellular fluid, it becomes dequenched and its fluorescence increases by a factor of ~10 (compare Section 3.1.3; Denker et al., 2011a). Subsequent endocytosis and reacidification again result in quenching of the fluorescence (see also Figure 3.12 A for a schematic of pHluorin function). When expressing synaptopHluorin in hippocampal cultures to resolve the recycling of single vesicles, endocytic events with very fast kinetics (again in the range of a few hundred ms, see above) were observed (Gandhi and Stevens, 2003).

Rapid endocytosis with very small time constants was also found in the calyx of Held synapse when using capacitance measurements (Sun et al., 2002; Wu et al., 2005). The major advantage of this method as compared to imaging approaches is its superb time-resolution (Wu et al., 2005). It should be pointed out, however, that at least some of the very fast capacitance transients observed in these measurements could not be related to neurotransmitter release, as these events were still observed when calyceal terminals had

been loaded with botulinum toxin, which blocks vesicle fusion by SNARE cleavage (Yamashita et al., 2005).

Finally, recent evidence in favor of the kiss-and-run recycling mode comes from even another alternative technique, employing quantum dots displaying pH-dependent photoluminescence changes. After loading vesicles of cultured hippocampal neurons with these quantum dots, exocytosis could be monitored by an increase in photoluminescence, but their large size as compared to fusion pores allowed kiss-and-run (quantum dot retention) and full-collapse fusion (loss of quantum dot) to be distinguished (Zhang et al., 2009). Importantly, this study also showed that both kiss-and-run and full-collapse fusion can occur in parallel (in line with the results of many of the works described above)- and both modes may even be used subsequently by the same vesicle. As described in Section 1.2.1, the question on what stimulation conditions trigger which of the two recycling modes has remained as controversial as the existence of kiss-and-run itself (see next section), with some of the above-mentioned studies proposing a preference for fast recycling under low stimulation conditions (for instance Sun et al., 2002; Harata et al., 2006) and others under strong stimulation (for example Wu et al., 2005; Zhang et al., 2009).

Clathrin-mediated Endocytosis (CME)

For clathrin-mediated endocytosis to occur, the vesicle first undergoes full collapse into the plasma membrane, from which it is then retrieved by the formation and pinch-off of a clathrin-coated pit (blue arrows in Figure 1.1). This process is generally believed to be much slower than kiss-and-run, on the scale of many seconds (see for instance Granseth et al., 2006), although this is debatable if preformed clathrin-coated pits exist on the plasma membrane (a "readily retrievable" vesicle pool; see for instance Gandhi and Stevens, 2003; Rizzoli and Jahn, 2007; see also Section 1.2.2). There is also some controversy regarding the behavior of the vesicular proteins after fusion with the plasma membrane: the vesicle components might either remain together or they might disperse and mix with plasma membrane proteins, which would require additional sorting (Fernandez-Alfonso et al., 2006; Wienisch and Klingauf, 2006; Opazo et al., 2010). Alternatively, the sorting step might involve endosomes, as discussed below and illustrated by red arrows in Figure 1.1.

What is the basic mechanism of clathrin-coated endocytosis? The clathrin coat is mainly composed of clathrin triskelia (Kirchhausen et al., 1986) and clathrin adaptor proteins. Coat formation is triggered when the AP2 adaptor recognizes and binds synaptotagmin on the plasma membrane (Zhang et al., 1994; Li et al., 1995). The bound AP2 then serves as a platform for the binding of clathrin triskelia in conjunction with a second adaptor called AP180 (De Camilli and Takei, 1996; Hao et al., 1999; Slepnev and De Camilli, 2000). As reviewed in

Slepnev and De Camilli, 2000, many additional accessory factors are involved in CME, including proteins which might be involved in membrane deformation (amphiphysin and endophilin; Micheva et al., 1997; Itoh and De Camilli, 2006). Amphiphysin also recruits the GTPase dynamin to the clathrin-coated pit (David et al., 1996; Shupliakov et al., 1997), which mediates the pinching-off of the vesicle from the plasma membrane (Hinshaw and Schmid, 1995; Takei et al., 1995a). In addition, amphiphysin also interacts with an inositol-5-phosphatase, synaptojanin, which is involved in the subsequent uncoating reaction and several other processes (De Camilli and Takei, 1996; McPherson et al., 1996; Slepnev and De Camilli, 2000). Other major molecular players in the shedding of the clathrin coat after endocytosis are the uncoating ATPase Hsc70 (Paddenberg et al., 1990; Zinsmaier and Bronk, 2001) and auxilin (Ungewickell et al., 1995). This is then followed by synaptic vesicle refilling with neurotransmitter.

The evidence for CME in synaptic vesicle recycling is strong and its existence is much less controversial than for the kiss-and-run recycling mode. The question here is rather if and under which conditions it is the dominating pathway for endocytosis.

As for kiss-and-run, the first evidence for CME dates back to the 1970s, when Heuser and Reese published their seminal EM study on vesicle recycling pathways in the frog NMJ (Heuser and Reese, 1973). They also proposed that the clathrin-coated vesicles they observed were subsequently recycled via cisternae, from which again new vesicles could bud. This might be indicative of the endosomal recycling pathway described below. Note that relatively high frequency stimulation (10 Hz) was employed in this study.

In line with an important function for CME in vesicle recycling, the molecular players described above are found at high concentration within nerve terminals (note that this observation is of special importance for the concept of vesicles functioning as a molecular buffer, as developed in this thesis; Section 4.4.2). These proteins often form "endocytic zones" surrounding the active zones (for instance at the *Drosophila* NMJ; Roos and Kelly, 1999; see also Brodin et al., 2000). Also, when clathrin-coated vesicles were purified from rat brain, it was shown that most of them displayed a synaptic vesicle-like protein composition, indicating that coated vesicles are mainly used to retrieve synaptic vesicles in the brain (Maycox et al., 1992).

In a series of studies, components of the clathrin-coat assembly machinery were perturbed. For instance, when the function of AP180 was impeded in the giant synapse of the squid, synaptic transmission was blocked and the number of vesicles inside the synapse was reduced, which was interestingly coupled with an increased size of the remaining vesicles (Morgan et al., 1999). Endocytosis was also impaired in a *Drosophila* mutant of the same protein and, again, vesicle sizes were significantly enlarged (Zhang et al., 1998a). These results underscore the importance of CME for vesicle recycling and present an

interesting role for AP180 in regulating vesicle size. The significance of CME was also demonstrated when the interaction of amphiphysin and dynamin was disrupted in the lamprey giant reticulospinal synapse, resulting in a depression of transmission and in distorted synaptic ultrastructure (Shupliakov et al., 1997). Finally, in a more recent study, Granseth and colleagues blocked CME either by RNAi against clathrin itself or by overexpressing a fragment of AP180 in a dominant-negative approach and monitored vesicle endocytosis using synaptophysin-pHluorin (SypHy). The study was performed in hippocampal cultures, in which most of the kiss-and-run results described above were also obtained, and showed that removing CME essentially blocks all endocytosis, indicating that CME is the major recycling mode employed in these synapses (Granseth et al., 2006).

Finally, it should be noted that full fusion has been employed in many studies to label recycling vesicles by bulky markers such as antibodies (Willig et al., 2006) or even quantum dots (see above; Zhang et al., 2009), with especially this last study implicating that kiss-and-run and full fusion can be used subsequently by the same vesicle.

Bulk Endocytosis

As for kiss-and-run and CME, bulk endocytosis was first described in the 1970s in the frog NMJ (Gennaro et al., 1978). As for CME, the existence of bulk endocytosis is widely accepted, but it has only been observed under strong stimulation conditions (as for instance reviewed in Clayton and Cousin, 2009). Massive vesicle exocytosis triggered by high frequency stimulation causes an increase in the amount of membrane at the nerve terminal periphery, which is compensated for by the formation of large invaginations from the plasma membrane (green arrows in Figure 1.1). These invaginations probably bud off from the plasma membrane (not depicted in Figure 1.1), forming endosomal-like intermediates, from which new vesicles can then be formed.

Bulk endocytosis has for instance been observed in neuromuscular preparations of the frog (Gennaro et al., 1978, see above; Miller and Heuser, 1984; Richards et al., 2000; Richards et al., 2003) and the snake (Teng and Wilkinson, 2000). Evidence for this recycling mode has also been obtained from cultured cerebellar granule neurons (Clayton et al., 2008) and the calyx of Held (de Lange et al., 2003; Wu and Wu, 2007).

In contrast to its existence, the speed at which bulk endocytosis proceeds is controversial. It has generally been reported that bulk endocytosis is a slow pathway (with a half-time of about 8 minutes in the frog NMJ for example; Richards et al., 2000), but recent evidence indicated that it might proceed much faster (with a half-time of less than 20 seconds at the calyx of Held; Wu and Wu, 2007).

Importantly, it is questionable whether this recycling mode, which obviously can be used for vesicle retrieval under strong stimulation, is also employed under physiologically more relevant conditions (compare discussion on stimulation frequencies employed in *in vitro* studies as compared to *in vivo*; Section 1.3.1).

Endosomal Recycling

Endosomal recycling in combination with CME (i.e. the retrieval of vesicle membrane from the plasma membrane via clathrin coats which is followed by recycling and presumably sorting of vesicle components via an endosomal intermediate and subsequent budding of new vesicles from the endosome; red arrows in Figure 1.1) has also been proposed already by Heuser and Reese (1973), as described above. However, these cisternae or endosomal-like structures have only been described for strongly stimulated preparations (including the calyx of Held; de Lange et al., 2003) and are generally not observed by EM in resting terminals or at low frequencies of stimulation, which could indicate that they are of a very transient nature.

Strong evidence for a likely participation of endosomes in vesicle recycling at least under some conditions comes from the biochemical composition of vesicles, as described in Section 1.1.2. Molecular markers which are involved in endosomal fusion are found on synaptic vesicles, such as the SNARE proteins Vti1a-*β* (Antonin et al., 2000), syntaxin 6 and syntaxin 13 (Rizzoli et al., 2006), and the small GTPase Rab5 (Fischer von Mollard et al., 1994). The importance of Rab5 for vesicle recycling was demonstrated in NMJs of *Drosophila* Rab5 mutant larvae, where evoked neurotransmitter release was found to be impaired (Wucherpfennig et al., 2003). In the same study, a GFP-tagged endosomal marker was expressed to allow for monitoring of endosomal dynamics in relation to vesicle recycling. Interestingly, vesicle depletion resulted in disappearance of the endosomal signal, and recovery was only observed when vesicles were allowed to reform (this protocol took advantage of the temperature-sensitive dynamin mutant *shibire*, in which vesicle recycling, but not release, is inhibited above 29°C; note that this mutant was also extensively used throughout the study described herein). This observation strongly implies that endosomes are part of the vesicle recycling pathway. Note that cisternal structures could be visualized in this work by performing cryoimmuno-EM.

Similar to the Rab5 *Drosophila* mutant described above, further components of the endosomal recycling pathway were knocked out (σ1B-adaptin as part of the AP1-σ1B complex) or inhibited (AP3) and vesicle recycling was monitored in hippocampal cultures (Glyvuk et al., 2010; Voglmaier et al., 2006). Again, compensatory endocytosis was found to be inhibited upon stimulation.

Finally, endosomal sorting was shown to be essential at least for a subpopulation of synaptic vesicles (the readily releasable vesicle pool, RRP; see next section), as these vesicles were depleted when endosomal sorting was inhibited by a dominant-negative approach, in which soluble syntaxin 13 fragments were expressed (Hoopmann et al., 2010). The recycling of synaptic vesicles via endosomes was also verified by experiments investigating the colocalization of endocytosed vesicles and an endosomal marker, by observing the participation of endosomal proteins in vesicle recycling using pHluorins and by ultrastructural investigations employing photo-oxidation, a technique combining fluorescence and electron microscopy (Hoopmann et al., 2010). In this method, a fluorescent signal is transformed into a signal that can be visualized by EM by taking advantage of the fact that excitation of a fluorescent dye results in the production of reactive oxygen species (ROS), which can then oxidize a substrate such as 3,3'-diaminobenzidine (DAB), causing DAB to polymerize and form an electron-dense precipitate (as detailed in Materials and Methods; Section 2.4). When used in combination with styryl dyes (Section 2.4.1), photo-oxidation provides the advantage of efficient vesicle labelling (due to the extremely fast on-rates, with FM 1-43 for instance presenting a k_{on} of over 10^5 mM^{-1} s^{-1}; Richards et al., 2005) and allows for the ultrastructural investigation of the number (and localization) of recycled vesicles and the morphology of the vesicle recycling process. The same study also demonstrated why endosomal recycling might indeed be necessary during vesicle retrieval: the vesicle composition changed on endocytosis, with vesicles acquiring plasma membrane components, which would explain the need for an additional sorting station to achieve fusion-competent vesicles with the correct protein composition (Hoopmann et al., 2010). Note that the recycling of RRP vesicles via endosomes was also confirmed in a later study (Uytterhoeven et al., 2011), which also identified the GTPase activating protein (GAP) Skywalker as a regulatory factor involved. The implications of these studies for the use of different recycling modes by distinct vesicle populations are discussed in more detail in the next section.

In summary, the controversy on the major pathway for vesicle endocytosis is not yet resolved. Convincing evidence has been presented for each of the four pathways (kiss-and-run, CME, bulk endocytosis and endosomal sorting) and obviously, at least three of these pathways are to some extent related, as vesicles retrieved by CME can then fuse to endosomes to experience further sorting (or they might fuse to each other in homotypic fusion) and large amounts of membrane retrieved by bulk endocytosis can pinch off from the plasma membrane and form endosomal-like compartments. Synapses seem to be able to use several recycling pathways and this is even true on the level of single vesicles (Zhang et al., 2009). This may provide the synapse with the opportunity to optimally respond to different

stimuli and conditions. However, the question on what pathway predominates under which *in vitro* conditions has not been unequivocally answered, and the distinct roles of these recycling modes *in vivo* are virtually unknown. Preferences of distinct vesicle subpopulations for the described recycling pathways also require further investigation, an issue that is further discussed in the next section.

1.2 Synaptic Vesicle Pools

Whereas synaptic vesicles all appear similar at the ultrastructural level, they differ in their release abilities: some vesicles are more eager to be released than others, as was demonstrated by numerous *in vitro* studies and also seems to be the case *in vivo*, as shown by the work presented in this thesis.

The concept that vesicles display different release capacities was introduced by the work of Birks and MacIntosh at the beginning of the 1960s, when they studied acetylcholine release in cat sympathetic ganglia (Birks and MacIntosh, 1961). Similar results were obtained a few years later in human intercostal muscle (Elmqvist and Quastel, 1965). The observation of a few vesicles releasing very quickly, followed by slower and more reluctant release afterwards has by now been extended to virtually all important synaptic preparations, including for instance the *Drosophila* (Delgado et al., 2000) and frog (Richards et al., 2000; Richards et al., 2003) NMJs, the lamprey CNS (Pieribone et al., 1995), the rat calyx of Held (Schneggenburger et al., 1999) and goldfish retinal bipolar cells (Neves and Lagnado, 1999).

In this section, I will first introduce the well-established model of three distinct vesicle pools, discussing also their respective localization within the synapse with regard to the active zones and the distinct recycling modes employed by the different vesicle populations. I will then shortly introduce three new vesicle pool concepts. Finally, I will focus on differences in vesicle mobility between the distinct vesicle pools.

1.2.1 The Traditional Three-Pool Model

According to the three-pool model, vesicles generally belong to one of the following three pools: the readily releasable pool (RRP), the recycling pool and the reserve pool (Rizzoli and Betz, 2005; Denker and Rizzoli, 2010).

The vesicles of the RRP are those vesicles which are docked at the active zone and primed for release (Schikorski and Stevens, 2001), which means that these vesicles are the first to be exocytosed upon arrival of a stimulus. This pool generally contains only ~1-2% of all vesicles within a synapse. The RRP is considered to be a part of the recycling pool, which contains the vesicles which recycle repeatedly upon moderate stimulation, without

involvement of the reserve pool vesicles (see for instance Pyle et al., 2000). The recycling pool contains 10-20% of the vesicles within a synapse, leaving the remaining 80-90% of synaptic vesicles as members of the reserve pool. These vesicles only release under high frequencies of stimulation (10-100 Hz for many seconds or minutes) and only after the recycling pool (and RRP) vesicles have been depleted (Rizzoli and Betz, 2005; Denker and Rizzoli, 2010).

Recruitment of the reserve pool vesicles after recycling pool depletion was for instance demonstrated by Kuromi and Kidokoro, using the *Drosophila shibire* mutant described above (Kuromi and Kidokoro, 1998). Whereas vesicle recycling was restricted to the recycling pool (termed exo/endo cycling pool in this preparation) during high potassium stimulation at room temperature, the reserve pool vesicles were recruited when the recycling pool was depleted by high potassium stimulation at the non-permissive temperature (>29°C), resulting in completely depleted nerve terminals. Similar observations come from the frog NMJ, where release from the reserve pool is only initiated after recycling pool depletion (Richards et al., 2000; Richards et al., 2003).

Interestingly, hippocampal synapses display an "extreme" case of reserve pool vesicles, as at least ~50% of the vesicles do not release even under strong stimulation, thereby forming a "resting" reserve pool (Harata et al., 2001a; Harata et al., 2001b; Fernandez-Alfonso and Ryan, 2008; Opazo et al., 2010). Note, however, that virtually all vesicles of this preparation participated in neurotransmitter release in a recent study employing mild stimulation over several minutes (Ikeda and Bekkers, 2009), an interesting observation that will be further discussed in section 1.3.1 (see also Denker and Rizzoli, 2010).

It was generally assumed that the different release abilities of the distinct vesicle pools were represented by their differential localization with regard to the active zones, with the RRP vesicles being docked at the active zones, the recycling pool vesicles located directly behind them and the reserve pool vesicles positioned even farther away from the active zones, as depicted in Figure 1.2 A. Indications that the reserve and recycling pool vesicles display differential localization within the synapse came for instance from the *Drosophila* larval NMJ, where Kuromi and Kidokoro proposed in a series of studies using fluorescence microscopy and different labelling protocols for the exo/endo cycling (recycling) and reserve vesicle pool that the exo/endo cycling pool is located at the terminal periphery (where the active zones are located), whereas the reserve pool resides in the terminal center (Kuromi and Kidokoro, 1998; Kuromi and Kidokoro, 1999; Kuromi and Kidokoro, 2000; Kuromi and Kidokoro, 2002; reviewed in Kuromi and Kidokoro, 2003; Kuromi and Kidokoro, 2005).
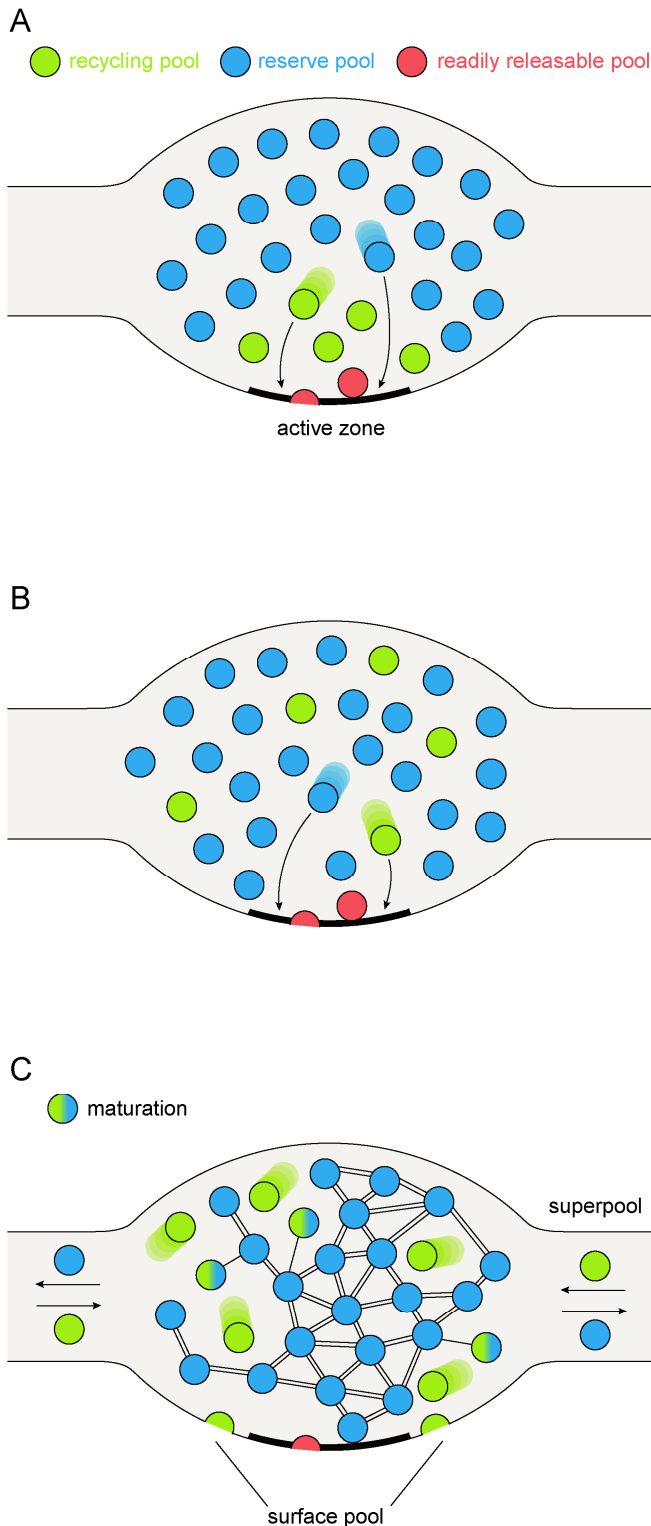
Figure 1.2: Synaptic vesicle pool models
(A) The classical model of vesicle pool organization. The readily releasable pool (RRP) vesicles are the recycling pool vesicles docked at the active zone and primed for release (depicted in red). They are therefore able to undergo fusion immediately upon arrival of an action potential. The recycling pool vesicles (green) are located directly behind them and are recruited subsequently (left arrow). They undergo repeated recycling under moderate stimulation conditions. The reserve pool vesicles (blue) are located even behind the recycling pool vesicles and only come into play during high frequency stimulation and after recycling pool depletion (right arrow). (B) The new model of vesicle pool localization, taking into account ultrastructural evidence pointing to the recycling and reserve pool vesicles being intermixed. As in the classical model, the RRP vesicles consist of recycling pool vesicles which find themselves in a privileged position, docked at the active zone. The recycling and reserve pool vesicles are however spatially intermixed. Nevertheless, the general concept of recycling pool vesicles being eager to be released upon RRP depletion (right arrow) and reserve pool vesicles being only recruited upon recycling pool depletion (left arrow) still holds true. (Refer also to Rizzoli and Betz, 2005, for a discussion of pool localization.) (C) An extension of the pool model implementing recent findings (as suggested in Denker and Rizzoli, 2010). As in (B), the recycling and reserve pool vesicles are intermixed, but they differ in their mobility: whereas the recycling pool vesicles diffuse freely within the synaptic volume, the reserve pool vesicles are immobilized by a cross-linking molecule. As indicated, recycling pool vesicles can "mature" to become reserve pool vesicles by getting bound to the scaffolding molecule (as represented by the green-blue intermediates, which are less strongly cross-linked as indicated by single as compared to double bonds). Also shown are the surface pool, which is considered part of the recycling pool, and the superpool, representing the exchange of recycling and reserve pool vesicles between adjacent boutons. (From Denker and Rizzoli, 2010)

Importantly, however, many recent studies involving selective styryl dye labelling of the recycling pool (i.e. using conditions in which the recycling pool vesicles recycle repeatedly without recruitment from the reserve pool of vesicles) and subsequent photo-oxidation (see above and detailed description in Section 2.4) showed that the recycling pool (which is then found labelled/dark in the EM) is intermixed with the reserve pool (unlabelled) vesicles (reviewed in Rizzoli and Betz, 2005). This has for instance been shown for rat hippocampal cultures (Harata et al., 2001b) and for the rat calyx of Held (de Lange et al., 2003). Similar results were obtained in the frog NMJ: the recycling and reserve pool vesicles were again intermixed, with however the recycling pool vesicles being excluded from the cores of vesicle clusters (Rizzoli and Betz, 2004; see Figure 1.3 A).

A

B
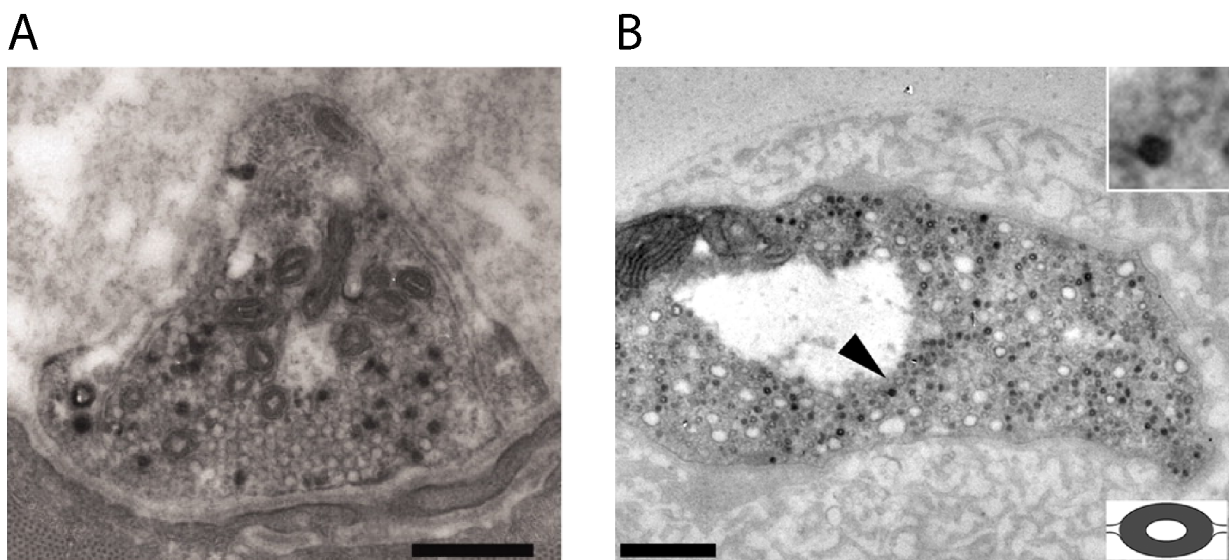
Figure 1.3: Recycling and reserve pool vesicles are spatially intermixed
(A) Frog NMJ stimulated in presence of the styryl dye FM 1-43 for 10 seconds at 30 Hz (resulting in labelling of the recycling pool). Stimulation was followed by a 10 minute resting period and photo-oxidation. (From Rizzoli and Betz, 2004) (B) *Drosophila* NMJ labelled by 5 minute application of 90 mM KCl in presence of FM 1-43, which has been reported to label the exo/endo cycling pool (i.e. the recycling pool; compare Kuromi and Kidokoro, 1998), followed by photo-oxidation. The arrowhead points to the area enlarged in the inset, showing a labelled and an unlabelled vesicle. The cartoon displays the peripheral staining expected if the exo/endo cycling pool was located at the bouton periphery and the reserve pool in the bouton center, as was proposed before. Note that the terminal center is now shown to be devoid of vesicles instead of hosting the reserve pool. (From Denker et al., 2009) Note that recycling (labelled, dark) and reserve pool vesicles (unlabelled) are intermixed for both preparations. Size bars are 500 nm.

Using a very different approach, Paillart and colleagues investigated vesicle recycling at goldfish retinal bipolar cells by decorating the entire cell membrane with an electron-dense marker (cationized ferritin) and directly following the endocytosis process by EM (Paillart et al., 2003). They found that uptake was mainly via relatively large (up to 200 nm) endosomal structures which then slowly budded off vesicles. Again, labelled and unlabelled structures were found to be intermixed.

While it was therefore convincingly shown for nearly all major synaptic preparations that recycling and reserve pool vesicles are spatially intermixed and that therefore release ability cannot be determined by proximity to active zones, this was for many years in striking contrast to the *Drosophila* NMJ, where the above-described concept of distinctly distributed pools according to the studies by Kuromi and Kidokoro was still accepted. This model was however derived from investigations employing fluorescence microscopy, whereas ultrastructural evidence from high-resolution electron microscopy was still lacking. The respective experiments involving vesicle pool labelling by styryl dyes and subsequent photo-oxidation were only performed a few years ago and indicated that the terminal centers are actually devoid of vesicles (instead of being occupied by the reserve pool) and that the recycling and reserve pool vesicles are spatially intermixed at the bouton periphery (Akbergenova and Bykhovskaia, 2009; Denker et al., 2009; see Figure 1.3 B).

With the *Drosophila* larval NMJ thus connected to the spatial vesicle pool organization shown for the other major synaptic preparations, the pool model could recently be revised, as indicated in Figure 1.2 B (see also Denker and Rizzoli, 2010). The RRP vesicles are still considered to be the recycling pool vesicles which find themselves docked at the active zone and primed for release, thereby occupying a privileged position. However, the recycling and reserve pool vesicles do not occupy distinct positions within the terminal but are intermixed with each other. Nevertheless, the reserve pool vesicles are still more reluctant to be released than the recycling pool vesicles and are only recruited upon depletion of the latter. It should be noted, however, that the spatial intermixing of vesicles with distinct release abilities might extend even to the docked vesicles, as some vesicles in close proximity to the active zones did not undergo recycling upon moderate stimulation both in the frog (Rizzoli and Betz, 2004) and in the *Drosophila* NMJ (Denker et al., 2009), indicating that they were not or only reluctantly releasable (see also Denker and Rizzoli, 2010).

An important consequence of this paradigm shift is the conclusion that there must be a molecular difference between recycling and reserve pool vesicles, rendering the first more and the latter less eager to be released, as localization within the terminal obviously cannot account for this functional difference. The question of what molecule(s) might constitute this difference will be further discussed in Sections 1.2.3 and 4.3.

As the distinct vesicle pools show different release kinetics, they might also be endocytosed at different rates. As described in Section 1.1.4, several different recycling mechanisms have been described at presynaptic terminals, but their involvement in the endocytosis of distinct pools has not been unequivocally clarified, although there seems to be a clear tendency in the literature: as detailed below, mild stimulation triggering release from the recycling pool is often reported to drive a fast vesicle recycling mode, whereas high-

frequency stimulation seems to evoke slower vesicle recycling (as also discussed in Rizzoli and Betz, 2005).

This phenomenon is already evident in the electron microscopy studies performed by Heuser and Reese and by Ceccarelli and co-workers in 1973 in the frog NMJ: whereas stimulation at 10 Hz caused vesicle depletion (i.e. the reserve pool of vesicles was involved in neurotransmitter release) and the occurrence of cisternae, stimulation at only 2 Hz did not deplete vesicles (presumably causing repeated release from the recycling vesicle pool) and also did not trigger cisternae formation (Ceccarelli et al., 1973; Heuser and Reese, 1973). Whereas Heuser and Reese interpreted their observation of cisternae as a result of vesicle coalescence, more recent investigations in the same preparation show that they result from invaginations, i.e. the bulk endocytosis pathway described in Section 1.1.4 (Richards et al., 2000; Richards et al., 2003). As mentioned above, vesicle recycling via invaginations from the plasma membrane was found to be rather slow in these studies (with a half-time of about 8 minutes). This slow recycling pathway is reported to refill the reserve pool of vesicles, whereas the retrieval of the recycling pool is much more rapid, refilling the pool within about one minute (probably by direct retrieval from the plasma membrane). Therefore, two recycling routes exist in the frog NMJ which selectively refill the recycling and reserve vesicle pools.

Similarly, two different recycling pathways were described in ultrastructural investigations of the *Drosophila* NMJ, with a rapid pathway involving no intermediate structures and a slower pathway involving pinching off of endosomal-like intermediates from the plasma membrane (Koenig and Ikeda, 1996; in agreement with the results obtained in the frog). Interestingly, whereas the first pathway was described to emanate from the active zone, the second pathway was observed to take place further away from the active zone. Koenig and Ikeda also suggested that the two distinct recycling routes selectively refill different vesicle pools, i.e. the recycling (within about 1 minute) and reserve pool (within about 30 minutes), respectively. Importantly, rapid endocytosis of recycling pool vesicles as compared to slow retrieval of the reserve pool was not restricted to the NMJs, but seemed to represent a more general phenomenon, as it was also observed in synapses of the mammalian CNS (Pyle et al., 2000; see also de Lange et al., 2003).

Whereas the studies mentioned above used imaging approaches to investigate vesicle endocytosis, Sun and colleagues took advantage of the increased time-resolution of capacitance measurements at the calyx of Held (see above; Sun et al., 2002). Whereas the time constants of endocytosis were very fast after single vesicle fusion or stimulation at low frequency (<2 Hz) (in the range of ~100 ms; see above), they slowed down dramatically when stimulation frequency was increased, reaching tens of seconds (presumably associated with the recruitment of release-reluctant vesicles). It could be shown that this was

due to the accumulation of fused and unretrieved vesicles in the plasma membrane (also discussed in Sudhof, 2004).

It should be noted that the rapid endocytosis mode generally associated with low frequency stimulation and thereby with release from the recycling pool or even just the RRP would not necessarily imply kiss-and-run: CME might be able to achieve similar speeds (as reviewed in Rizzoli and Jahn, 2007) and recent evidence surprisingly shows that endosomal recycling might be the pathway of choice for the RRP and is about as fast as kiss-and-run and CME, i.e. about 30 seconds for one whole vesicle cycle (Hoopmann et al., 2010; Uytterhoeven et al., 2011). Note, however, that a propensity of RRP vesicles for kiss-and-run has also been reported (Zhang et al., 2009).

In summary, the synapse could achieve the rapid recycling speed involved in maintaining reliable release from the recycling pool during moderate stimulation by several mechanisms, including kiss-and-run, CME and endosomal sorting. Under high frequency stimulation, synapses resort to bulk endocytosis, possibly due to changes in membrane tension resulting from massive vesicle exocytosis (see also Sudhof, 2004). Bulk endocytosis therefore likely represents an emergency route of compensatory membrane retrieval. In agreement with its described role in retrieval of the reserve pool vesicles, both events (release from the reserve pool and bulk endocytosis) only occur after strong, probably non-physiological stimulation, raising the question on whether they play a role under *in vivo* conditions.

1.2.2 Extension of the Traditional Model: The New Vesicle Pools

In the recent years, three new vesicle pool concepts have been introduced, namely the surface pool, the "super-pool" and the spontaneously releasing pool, which shall only shortly be introduced here and are described in detail in Denker and Rizzoli, 2010. These new pools should not be regarded as replacing but rather as complementing the former model.

The surface pool consists of vesicles stranded at the plasma membrane, which may undergo endocytosis upon stimulation (Figure 1.2 C). It was first observed when vesicle recycling was monitored in hippocampal neurons by using synaptopHluorin (Gandhi and Stevens, 2003). Its existence was confirmed in several recent studies, showing exchange of vesicle-resident and surface-resident vesicle components upon stimulation, with the two populations being distinguished either by bleaching (Fernandez-Alfonso et al., 2006) or proteolytic cleavage of surface-resident pHluorins (Wienisch and Klingauf, 2006). Interestingly, the stranded pool was preferentially endocytosed during stimulation (Wienisch and Klingauf, 2006), in line with the hypothesis of a "readily retrievable pool", consisting of

pre-assembled endocytic structures at resting synapses, which can be rapidly endocytosed upon stimulation (Rizzoli and Jahn, 2007; Hua et al., 2011a). It should also be pointed out that uptake of the surface pool has been used for years to label synaptic vesicles (Willig et al., 2006; Westphal et al., 2008), further confirming this new concept.

The second recently introduced pool is the "super-pool": according to this concept, vesicles are not spatially restricted to their original bouton, but are instead exchanged between boutons at high rate (reviewed in Denker and Rizzoli, 2010; Staras and Branco, 2010). This was shown by labelling vesicles in hippocampal cultures with styryl dyes, followed by fluorescence recovery after photobleaching (FRAP), during which single terminals were photobleached and the recovery of fluorescence was monitored (Darcy et al., 2006). This recovery reflected the entrance of labelled vesicles from non-bleached boutons and was found to be substantial. Note that the exchanged vesicles could be released from the host synapse upon stimulation (see also Staras et al., 2010). Importantly, both recycling and reserve pool vesicles were exchanged (Darcy et al., 2006; Figure 1.2 C), as was confirmed by two recent studies (Fernandez-Alfonso and Ryan, 2008; Kamin et al., 2010). In addition, STED (stimulated emission depletion) microscopy (a high-resolution microscopy technique breaking the diffraction limit of light by de-excitation of fluorescent dyes; explained in Section 2.13.2), allowed for the investigation of single vesicle movements, again confirming the existence of a highly mobile superpool (Westphal et al., 2008; Kamin et al., 2010). Note that this vesicle sharing between boutons could have important functional implications in terms of synaptic plasticity (Staras and Branco, 2010).

The third and most controversial of the new pool concepts is the model of a distinct spontaneously releasing vesicle pool (reviewed in Denker and Rizzoli, 2010). Small spontaneous postsynaptic potentials were already described in the 1950s. These unitary potentials were termed quanta and result from single vesicle fusion (Fatt and Katz, 1952; Del Castillo and Katz, 1954; Ceccarelli and Hurlbut, 1980; Katz, 2003). According to the quantal theory, these potentials are identical to the basic building blocks of the stimulated release response (Fatt and Katz, 1952; Del Castillo and Katz, 1954). However, whether these two modes of release indeed originate from the same vesicle pool remains controversial: on the one hand, they share common regulatory mechanisms, with for instance both release modes enhanced by calcium (Angleson and Betz, 2001; Sara et al., 2005). There is also evidence from the frog NMJ that virtually all vesicles can undergo spontaneous fusion (Henkel and Betz, 1995a; Rizzoli and Betz, 2002). On the other hand, spontaneously recycling vesicles were reluctantly rereleased under activity in hippocampal cultures, but preferentially underwent a second round of spontaneous release, arguing in favor of a distinct spontaneously releasing pool (Sara et al., 2005). This result was however contested by two further studies comparing dye uptake and subsequent release under different recycling

paradigms (Groemer and Klingauf, 2007; Wilhelm et al., 2010). While this discrepancy could possibly be due to problems associated with the different styryl dyes employed (Zhu and Stevens, 2008; Chung et al., 2010; discussed in Denker and Rizzoli, 2010), styryl dye-independent approaches also provided ambiguous evidence: a recent study employing labelling of biotinylated synaptobrevin by colored streptavidin again indicated that the two release modes rely on distinct vesicle pools (Fredj and Burrone, 2009). Also, these pools displayed a differential dependency on dynamin (Chung et al., 2010). On the other hand, a common pool of origin was recently reported by two studies using several styryl dye-independent techniques (i.e. a sequential labelling protocol, synaptopHluorin and a novel pH-sensitive dye; Hua et al., 2010; Wilhelm et al., 2010).

In summary, the controversy on the existence of the spontaneously releasing vesicle pool is still not resolved. The evidence for the surface pool and superpool is more conclusive and they can therefore be integrated into an extended three-pool model (Figure 1.2 C).

1.2.3 Synaptic Vesicle Mobility versus Synaptic Vesicle Pools

As described in Denker and Rizzoli, 2010, when envisioning the vesicle cycle, it is generally assumed that vesicles are stably integrated into the synaptic vesicle cluster at rest, but that stimulation triggers their transport to the active zone, enabling vesicle fusion and neurotransmitter release. Indeed, styryl dye labelled vesicle clusters were shown to be largely stable at rest as shown by FRAP studies both in the frog NMJ (Henkel et al., 1996b) and in cultured hippocampal neurons (Shtrahman et al., 2005). Surprisingly however, vesicle mobility remained restricted during stimulation (Henkel et al., 1996b; see also Betz et al., 1992a; Lemke and Klingauf, 2005), indicating that vesicles do not move towards the active zone before fusion.

Another FRAP study of styryl dye labelled vesicles in the frog NMJ showed that vesicles in the recycling pool (which makes up only ~10-20% of the total vesicle population as described in Section 1.2.1; Rizzoli and Betz, 2005) are mobile at rest, whereas the reserve pool vesicles are immobile (Gaffield et al., 2006). Nerve stimulation caused mobilization of reserve pool vesicles, whereas the mobility of the recycling pool did not increase.

Finally, vesicle mobility was shown to be temperature-dependent at least in the mouse NMJ in a similar FRAP study employing again vesicles labelled with a styryl dye: room temperature rendered vesicles largely immobile, whereas raising the temperature to physiological levels increased vesicle mobility (Gaffield and Betz, 2007). As most *in vitro* studies are generally performed at room temperature, this is an important observation whose impact will be further discussed in Section 1.3.2.

With the advent of high-resolution and especially live STED microscopy, mobility could be investigated on a single vesicle level, as mentioned above and discussed in Denker and Rizzoli, 2010. A small fraction (up to ~10-20%) of all vesicles was stained by labelling of the surface pool of synaptotagmin in hippocampal cultures, followed by endocytosis (Westphal et al., 2008; see also Section 1.2.2 for details on the surface pool). Vesicle mobility was then investigated by real-time STED microscopy, indicating that vesicle movement was quite substantial, especially outside boutons. Vesicles typically moved in a random fashion within synaptic boutons, but directional movement was also observed, in particular along axonal tracts. Interestingly, vesicles sometimes got stuck in "hot spots" of vesicle localization. These areas of low mobility might reflect pockets within the vesicle cluster and are in agreement with the "stick-and-diffuse" model according to which vesicles diffuse freely but become occasionally transiently stuck by binding to intraterminal structures (Shtrahman et al., 2005).

These results were further confirmed by a subsequent study, which additionally demonstrated that whereas recently recycled vesicles are highly mobile, they lose their mobility over time, presumably in conjunction with integration into the vesicle cluster (Kamin et al., 2010). The mobile vesicles might therefore well represent the recycling pool, whereas the immobile vesicles could be equivalent to the reserve pool. Neither the mobility of the mobile recently endocytosed nor of the more "mature" (compare also Figure 1.2 C and Figure 1.4 B) cluster-integrated and immobile vesicles increased under physiological stimulation, in agreement with several studies cited above. On the other hand, incubation with tetrodotoxin (TTX, which blocks voltage-gated sodium channels and thereby action potential generation), resulted in faster "maturation" of recently endocytosed vesicles, i.e. faster integration into the vesicle cluster, strongly indicating that activity maintains the recycling vesicles in the mobile state.

As summarized in Figure 1.2 C and discussed in Denker and Rizzoli, 2010, and Kamin et al., 2010, a model of vesicle mobility in relation to release abilities of distinct pools can be derived: synapses contain clusters of immobile, presumably reserve pool vesicles, and a minor fraction of mobile, actively recycling vesicles (i.e. the recycling pool). As their mobility does not increase upon physiological stimulation (Kamin et al., 2010), they seem to be mobile enough to reach the active zones and undergo fusion without a further need to increase their speed (with stimulation only increasing their potential to fuse). Constant fusion with the plasma membrane and recycling seems to keep these vesicles in an active state, possibly by preventing their association with some cross-linking or scaffolding molecule (the identity of which was investigated in this study; see Section 3.2). Over time, however, the recycling pool vesicles acquire some properties of the reserve pool vesicles, lose their mobility and release ability and integrate into the vesicle cluster (as indicated by the green-

blue intermediates in Figure 1.2 C). It is important to point out that such loss of release capacity has been described before in FM dye release studies in the frog NMJ (Rizzoli and Betz, 2004; see also experiments by Pyle and colleagues in hippocampal cultures; Pyle et al., 2000). Therefore, some turnover between the recycling and reserve pool vesicles takes place. Of course, to prevent depletion of the recycling pool of vesicles, a comparable change of identity needs to occur for the reserve pool vesicles. How could these release-resistant vesicles turn into recycling pool vesicles and release neurotransmitter without an increase in mobility under stimulation, as reported above? And why has it been so difficult to monitor such a change from reserve to recycling pool vesicles? A possible answer for the first question comes from EM studies employing FM dye labelling followed by photo-oxidation in the frog (Rizzoli and Betz, 2004) and *Drosophila* NMJ (Denker et al., 2009), as indicated in Section 1.2.1: some of the vesicles that were found to be docked at the active zone did not undergo recycling under moderate stimulation and were obviously reluctant to be released, indicating that they might belong to the reserve pool of vesicles. This is also in agreement with the fact that substantially more vesicles are found docked at active zones (Schikorski and Stevens, 2001) than are released per action potential (Murthy et al., 1997; Gandhi and Stevens, 2003), at least in hippocampal cultures. Possibly, occasionally one of these docked reserve pool vesicles fuses with the plasma membrane and enters the recycling pool upon endocytosis to repopulate it (see also Figure 1.4 B). This would explain why no increase in mobility is observed before fusion. However, one would expect to observe an increase in mobility after vesicle recycling and change of the reserve into a recycling pool vesicle. One possible reason why this is often not observed might lie in the FM dye destaining technique, which by definition only follows vesicles up to their fusion, upon which they become invisible and undetectable. Consequently, destaining of styryl-dye loaded preparations by stimulation results in gradual dimming as dye is released, but no increase in mobility (Henkel et al., 1996b), as the releasing reserve pool vesicles are already docked at the active zone (or are transported to the active zones in an occasional manner, in agreement with their mobility associated with exchange across boutons; Darcy et al., 2006; Fernandez-Alfonso and Ryan, 2008; Kamin et al., 2010). Upon endocytosis, they experience an increase in mobility, which cannot be observed by FM dye destaining, but has been shown by antibody labelling (Kraszewski et al., 1996).

This model still leaves the question on what restricts the mobility of the reserve pool vesicles unanswered. Possible candidates (especially synapsin) will be further elaborated upon in the Discussion (Section 4.3).

1.3 Synaptic Function *in Vitro* versus *in Vivo*

Nearly all of the models concerning synaptic function described above have been gained from *in vitro* preparations, such as cultured neurons, brain slices or muscle preparations. Obviously, the importance of the afore-mentioned investigations for our understanding of synaptic function cannot be over-emphasized, as these studies demonstrated how synapses can behave under certain conditions and how they respond to defined stimuli. These investigations have laid the basis for virtually all of the described concepts, especially for our understanding of synaptic vesicle recycling modes, vesicle mobility and vesicle pools. However, it is not known whether the results obtained *in vitro* are representative of the *in vivo* situation, although some of the preparations might be closer to the physiological conditions than others (i.e. acute slices as compared to cultured neurons).

1.3.1 Synaptic Vesicle Use and Pools under Different Stimulation Conditions *in Vitro*

One of the very basic questions on which *in vitro* studies provide extremely conflicting results is the problem of how many of the vesicles are actually involved in recycling. In accordance with the concept of a relatively small recycling pool of vesicles, one would expect that under physiologically relevant stimulation conditions, only a small percentage of vesicles undergo recycling. Strong stimulation should result in the recruitment of vesicles from the reserve pool. As will be further discussed in Section 1.3.2, this model obviously depends on the knowledge of what stimulation frequencies are actually physiologically relevant, i.e. what stimulation conditions occur in a living animal. However, whereas some knowledge has been gathered for synapses which allow for electrophysiological measurements in *vivo*, the physiological stimulation frequencies for many of the frequently studied *in vitro* preparations have not been conclusively identified. Therefore, the various stimulation protocols presented below and used for testing vesicle use *in vitro* need to be viewed with caution.

One of the techniques which have been extensively used to study the amount of vesicles recycling under defined stimulation conditions is photo-oxidation, as described above and in more detail in Materials and Methods, Section 2.4. The percentage of labelled (i.e. recycling) vesicles was found to be quite small for most preparations tested, even under relatively high frequency stimulation (i.e. above a few Hz, refer to Section 1.3.2 for a further discussion on stimulation frequencies). For instance, Harata and colleagues found only 10-20% of the vesicles in hippocampal neurons labelled after 10 Hz stimulation for 2 minutes or after high potassium application for 90 seconds (note that such stimulation had been reported to cause the complete turnover of the functional vesicle population; Harata et al., 2001a; Harata et al., 2001b). Similar numbers of labelled vesicles were found in the frog NMJ

after 30 Hz stimulation for 10 seconds (Rizzoli and Betz, 2004). For the rat calyx of Held synapse in the auditory pathway, only ~5% of the vesicles were found labelled after stimulation at 5 Hz for 20 minutes or at 20 Hz for 5 minutes. Interestingly, high potassium stimulation for 15 minutes resulted in the recruitment of many more vesicles (~40%; i.e. involving the reserve pool; de Lange et al., 2003).

In the *Drosophila* NMJ, in principal virtually all vesicles could be forced to be released under 30 Hz stimulation for 5 minutes (Denker et al., 2009; see also Figure 3.7), but some (the reserve pool) vesicles are much more reluctantly released than others, with for instance high potassium stimulation leaving at least 50% of the vesicles unused (Kuromi and Kidokoro, 1998; Kuromi and Kidokoro, 1999; Kuromi and Kidokoro, 2000; Kuromi and Kidokoro, 2002).

In studies employing conventional or high-resolution fluorescence microscopy (without subsequent photo-oxidation) in hippocampal cultures, a maximum of around half of all vesicles could be released, even when applying 600 action potentials at 20 Hz (Opazo et al., 2010; see also Fernandez-Alfonso and Ryan, 2008, and Section 1.2.1).

These examples show that the amount of vesicles which are triggered to be released depends to a large extent on the specific preparation and on the stimulation paradigms. With detailed knowledge about the physiological stimulation conditions lacking for many preparations (see Section 1.3.2), the choice of stimulation protocols depends largely on the investigators and a general agreement on how a mild or strong stimulus is defined is lacking, with for instance high potassium stimulation being used either as a mild (Kuromi and Kidokoro, 1998; Kuromi and Kidokoro, 1999; Kuromi and Kidokoro, 2000; Kuromi and Kidokoro, 2002) or a strong stimulus (for instance de Lange et al., 2003).

It is important to note that most experiments on synaptic function not only comprise high frequencies of stimulation, but are generally also performed over very short time intervals, on the scale of a few minutes. As reviewed in Denker and Rizzoli, 2010, low frequencies of stimulation applied over many minutes or hours could possibly represent the *in vivo* situation more closely, at least for some preparations. For example, when frog NMJs were stimulated at 2 Hz (generally regarded to be a quite low and possibly physiologically relevant stimulation protocol) for 6 to 8 hours, nearly all vesicles had undergone recycling at least once (Ceccarelli et al., 1972). Interestingly, at low frequencies of stimulation (0.2 Hz), the majority of synaptic vesicles were released over ten minutes even in hippocampal cultures (Ikeda and Bekkers, 2009), which had been introduced before as having an extremely release-resistant reserve vesicle pool (Harata et al., 2001a; Harata et al., 2001b; Fernandez-Alfonso and Ryan, 2008; Opazo et al., 2010; see above and Section 1.2.1). Note that this result is also in agreement with an earlier study monitoring single quantal events in hippocampal cultures (Ryan et al., 1997).

These observations clearly indicate that a distinction between the different vesicle pools, in particular the recycling and reserve pool vesicles, is not as evident under mild as under strong stimulation conditions (although the preferential localization of the RRP at the active zone will still leave these vesicles with the fastest release kinetics). A comparison between the observation of vesicle release and its implications for the vesicle pool model under these different conditions is provided in Figure 1.4. As discussed in Denker and Rizzoli, 2010, the turnover between the recycling and reserve pool vesicles, as described in Section 1.2.3, seems to be too fast to allow the pools to be distinguished in long-lasting protocols employing mild stimulation, whereas it is slow enough to allow for differentiation when protocols are short.

In summary, a plethora of data has been presented on the number of vesicles which recycle in different preparations under various stimulation conditions, ranging from mild to very strong levels of stimulation. Contradictory results on the amount of releasable vesicles within a synapse come especially from the well-studied hippocampal neurons (for example Harata et al., 2001a; Harata et al., 2001b; as compared to Ryan et al., 1997; Ikeda and Bekkers, 2009), the preparation for which this question is possibly most important, as hippocampal boutons contain only a few hundred synaptic vesicles (Rizzoli and Betz, 2005). The discrepancy between this limited resource and the results on a large, release-resistant vesicle pool in the same preparation has actually strongly supported the kiss-and-run model of vesicle release, which could explain how these small synapses can still sustain long trains of stimulation. This example shows that there is obviously a strong need to consolidate these results, especially with regard to the *in vivo* situation, to further promote our understanding of synaptic function.
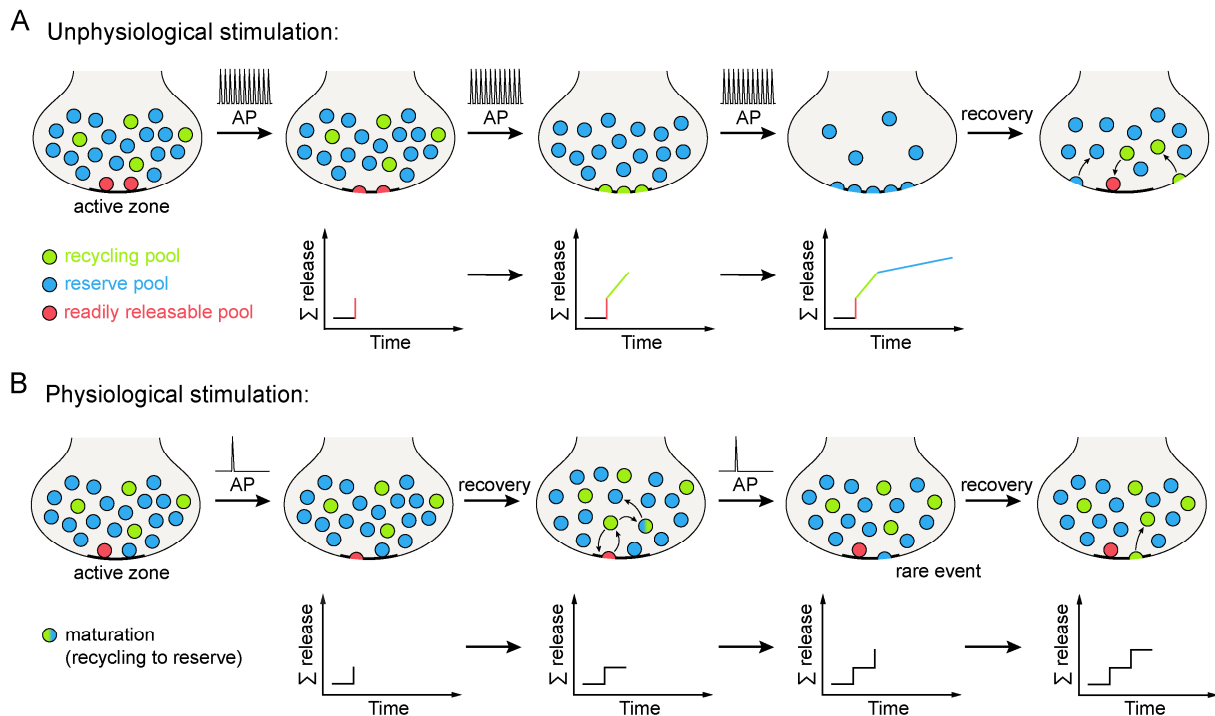
Figure 1.4: Vesicle release under physiological and unphysiological stimulation
(A) Depicted is a synapse with the recycling and reserve pool vesicles intermixed, as in Figure 1.2 B and C. The graphs below indicate summed release. The arrival of a train of action potentials (as generally used for high frequency stimulation protocols) first triggers release of the RRP (red) with very fast kinetics. Further stimulation causes the recycling pool vesicles (green) to fuse, but their release kinetics are somewhat slower, as they still need to reach the active zone and become docked and primed before they can undergo fusion. Even further stimulation triggers the release of the reserve pool of vesicles (blue) with even slower release kinetics. This tri-phasic release process is therefore in agreement with the three-pool model as described in Section 1.2.1. The pools are reformed during recovery, with some of the recycling pool vesicles repopulating the RRP. (B) Upon physiological levels of stimulation, vesicles of the RRP fuse with the active zone. However, the low stimulation frequency allows these vesicles to be recovered after exocytosis, replenishing the recycling pool. These new recycling pool vesicles can then either maintain their recycling pool status and eventually dock again at the active zone to be released in a subsequent stimulus, or they can "mature" to become reserve pool vesicles (indicated by the green-blue intermediate). Rarely, a reserve pool vesicle docked at the active zone will also undergo fusion and repopulate the recycling pool after endocytosis, as described in Section 1.2.3. Note that for physiological stimulation, no differences in release kinetics indicative of distinct vesicle pools can be observed (as shown in the graphs of summed release). (From Denker and Rizzoli, 2010)

1.3.2 Synaptic Function *in Vivo*

One of the major caveats when relating conclusions drawn from *in vitro* studies to the *in vivo* situation is the problem of temperature: most studies on synaptic vesicle pools, recycling pathways and mobility have been performed at room temperature. However, synaptic function has probably evolved to work (more or less) optimally at the animal's own body temperature. One example comes from the antarctic fish *Pagothenia borchgrevinki*, with quantal release (measured from the extraocular muscles) maximal at 5°C, but declining substantially above 10°C and ceasing at about 18°C (Pockett and Macdonald, 1986).

Whereas this example shows that synaptic function has been adapted to its normal working temperature in the course of evolution, many of the major synaptic preparations described above come from warm-blooded animals, which can have body temperatures well above 35°C. Therefore, conducting experiments on synaptic function at room temperature means that these preparations are investigated at least 10°C below the physiological body temperature (although room temperature might represent the physiological temperature at least for some invertebrate species; see also Introduction of Micheva and Smith, 2005).

What effects could the cooling of such preparations have? Importantly, studies published more than 20 to 25 years ago already stated that cooling (even by only 5-10°C) caused a depolarizing shift in the membrane potential of hippocampal neurons and an increase in resting input resistance (Thompson et al., 1985; Shen and Schwartzkroin, 1988). Consequently, moderately cooled neurons were brought closer to the spiking threshold and displayed increased excitability, as confirmed in later studies in the rat visual cortex (Volgushev et al., 2000a; Volgushev et al., 2000b). Pyott and Rosenmund found that low temperatures (25°C as compared to 35°C) resulted in increased synaptic depression during high frequency stimulation in hippocampal neurons, whereas higher temperatures resulted in an increased rate of refilling of the RRP and a decrease in the number of quanta released per action potential (a decreased release probability) and therefore a reduction in synaptic depression, which was also accompanied by increased maintenance of synchronous release (Pyott and Rosenmund, 2002). Further differences in synaptic function between room temperature and physiological temperature were presented by Micheva and Smith (again in hippocampal neurons), who showed that the size of the recycling pool was twofold larger at 37°C than at 23°C and that the rates of both exo-and endocytosis were increased at the higher temperature (Micheva and Smith, 2005). As mentioned in Section 1.2.3, vesicle mobility was also found to be temperature-dependent, with mobility being substantially higher at physiological than at room temperature in the mouse NMJ (Gaffield and Betz, 2007).

Intriguingly, hypothermia was even shown to influence synaptic morphology, with dendritic spines disappearing in a reversible manner upon cooling as investigated in hippocampal neurons *in vitro* (Kirov et al., 2004; Roelandse and Matus, 2004). In agreement with these results, significant loss of dendritic spines has also been reported in hibernating animals (Popov et al., 1992).

In summary, these studies clearly demonstrate that results obtained at room temperature cannot easily be extrapolated to higher temperatures. To understand synaptic function *in vivo*, further studies at physiologically relevant temperatures are needed. Even when performed at the appropriate temperature, however, *in vitro* experiments can only approximate the physiological situation, as for instance buffer composition and oxygen supply will not perfectly mimic the *in vivo* conditions.

In addition, and as mentioned in Section 1.3.1, investigators are challenged with choosing the right stimulation protocol for their respective preparations and questions. As described above, *in vitro* experiments often involve high stimulation frequencies, up to 100 Hz (for instance Gaffield et al., 2009), which might not be relevant for the *in vivo* situation. Unfortunately, it has been very difficult to measure stimulation frequencies in a living animal, mostly due to problems of accessibility and stability.

However, some investigators succeeded in determining normal firing frequencies. For example, Koenig and Ikeda recorded frequencies of 5 to 10 Hz from the *Drosophila* dorsal longitudinal flight muscle in stationary flight (Koenig and Ikeda, 1980). (Interestingly, they also reported in a later study that these frequencies and even stimulation at up to 20 Hz could be sustained by a small vesicle subpopulation, which presumably corresponds to the recycling pool, and that stimulation above 20 Hz resulted in muscle damage (Koenig and Ikeda, 1999).) Recently, electrophysiological recordings were also obtained from the brains of freely moving rats, both from the motor cortex and the hippocampus (Lee et al., 2006). Firing rates were found to be generally very low (<1 Hz).

In vivo recordings from mammalian NMJs have for example been obtained from the hindlimbs of freely moving rats and cats. Hennig and Lømo investigated firing patterns from the fast-twitching *extensor digitorum longus* (EDL) and the slow-twitching *soleus* muscle (Hennig and Lømo, 1985), which flex the ankle and extend the toes or extend the ankle, respectively (as described in Bewick, 2003). Whereas the slow-twitching *soleus* muscle was stimulated at 10-20 Hz for tens of minutes, much higher frequencies (~100 Hz) were recorded for the EDL. However, stimulation of the EDL occurred in bursts of 5-10 impulses, with the motor neurons remaining quiescent for tens of minutes in between (see also Gorassini et al., 2000). Therefore, the average firing rate of the EDL muscle is actually quite low. Similarly, recordings from the cat hindlimb showed that firing frequencies of up to ~27 Hz were reached when the cat was running on a treadmill at speeds of more than 1 m/s, but these high firing frequencies again occurred in short bursts of activity (Hoffer et al., 1987).

What do these results imply for synaptic function and vesicle use *in vivo*? Do the reserve pool vesicles actually get involved in vesicle recycling under physiological conditions? One important observation in this context is that there seems to be a postsynaptic upper limit to the usefulness of stimulation, at least for the NMJ, as the muscle will eventually cease to respond. For example, as reviewed in Slater, 2003, evidence has been presented that, at least in humans, failure of transmission at the NMJ cannot be evoked by voluntary activity, meaning that the muscle will at some point fail to respond, whereas the presynapse can still fire (Bigland-Ritchie et al., 1982).

Some reasonable estimates can be made for vesicle use *in vivo* for some of the major synaptic preparations introduced above when combining data from different studies (refer

also to the Introduction of Denker et al., 2011a): for instance, in the frog NMJ, one action potential is enough to cause muscle contraction. Therefore, firing frequencies of 1 or 2 Hz appear reasonable. When also considering that one action potential causes the release of only about 100 vesicles (or up to ~400; Katz and Miledi, 1979) and using a recycling time of about 1 minute (Betz and Bewick, 1992), 5-10% of the vesicles should be sufficient to sustain synaptic transmission.

One could argue that smaller synapses in the CNS might use a larger percentage of their vesicles (at least as compared to the large NMJs; Rizzoli and Betz, 2005), but their release probability is generally very low (Murthy et al., 1997; Gandhi and Stevens, 2003), so vesicle use could again be limited.

Similarly, more vesicles might be used at one of the most active synapses described, the calyx of Held. The calyx is normally active *in vivo* at ~30 Hz, but it can also sustain firing rates of ~600 Hz or even higher (Kopp-Scheinpflug et al., 2008). At the same time, the calyx is a huge synapse containing hundreds of thousands of vesicles (de Lange et al., 2003) and ~550 active zones (Satzler et al., 2002). However, as the release probability and quantal content of this synapse are quite low (fewer than 20 vesicles are released per action potential; Lorteije et al., 2009; indicating that only few of the active zones release a vesicle at any one time point and therefore effectively act like independent conventional synapses; see Sudhof, 2004; Denker and Rizzoli, 2010), ~20% of the vesicles should still be sufficient to maintain transmission at 30 Hz, when assuming a recycling time of 1 minute, as above (albeit 600 Hz firing would probably require more vesicles).

In summary, although firing frequencies can be quite substantial *in vivo*, they often result in the release of only few vesicles per active zone at any one time point, due to low release probabilities (this is also the case for the rat hindlimb muscles described above; Hennig and Lømo, 1985; where any given active zone will release a quantum on average only once every second in both slow and fast motor units, as discussed in Slater, 2003). It is therefore conceivable that vesicle use *in vivo* is actually quite limited, but experimental evidence for this hypothesis has been lacking.

1.4 Scope of the Project

The first and major aim of this project was therefore to determine the amount of vesicles involved in vesicle recycling *in vivo* and to provide a point of reference for previous *in vitro* studies. The approach of studying synaptic function under physiological conditions was defined as cellular ethology (i.e. the investigation of the natural behavior of cells). Importantly, to allow for interpretation of the results in an evolutionary context, I wanted to employ a variety of model organisms, ranging from nematodes and insects over fish,

amphibians and birds to mammals. In addition, I intended to study both adult and developing animals and to include synapses from both the central and peripheral nervous system.

To monitor the number of vesicles which undergo recycling in a living and behaving animal, I planned to inject the styryl dye FM 1-43 into the respective animal, which should then be allowed to behave freely for a defined amount of time before dissection of the muscle or organ of interest. In contrast to previous studies investigating presynaptic activity *in vivo* by optical approaches (Svoboda et al., 1997; Petzold et al., 2008), I wanted to determine the exact number and intrasynaptic localization of vesicles which had been used for neurotransmission by the living animal. Therefore, the FM dye injection should be combined with photo-oxidation, which would allow me to subsequently visualize the actively recycling and possibly non-recycling vesicles by electron microscopy.

The results obtained by this method should then be consolidated by the use of pHluorin *Drosophila* larvae in combination with bafilomycin injection and by investigating vesicle use in both larvae and adult flies of the temperature-sensitive *Drosophila* dynamin mutant *shibire*.

A further goal of this project was to gain insight into the molecular mechanism distinguishing between different vesicle pools *in vivo* (if distinct populations of actively recycling and non-recycling vesicles were found in the experiments described above). As a first approach to this question, I intended to study vesicle mobility and vesicle use in a third *Drosophila* mutant, a synapsin knockout strain.

If recycling as well as inactive vesicle populations were to be found *in vivo*, a further aim of this work would be the investigation of the synaptic function of the release-reluctant vesicle population. I therefore planned to investigate the spatial colocalization and functional relationship between synaptic vesicles and several well-described proteins involved in vesicle recycling by both conventional and high resolution (STED) microscopy. The results obtained from these experiments should then be further verified and extended by biochemical investigations of purified synaptic vesicles.

Therefore, this study should improve our understanding of synaptic function *in vivo*, thereby also placing concepts derived from previous *in vitro* studies into perspective of the requirements of a living animal. It might also lay the ground-work for further studies in accordance with the cellular ethology approach.

2. Materials and Methods

All materials and methods described herein are also explained in detail in Denker et al., 2011a, and Denker et al., 2011b.

2.1 Animals

All animals were obtained either from commercial suppliers or from laboratories specialized in their use. *Drosophila* wildtype strains used here were w[1] and w[1118] and were kindly provided by Dr. Carolin Wichmann, Free University of Berlin. *shibire*[ts1] mutant flies (Grigliatti et al., 1973) were provided by Prof. Stephan Sigrist, Free University of Berlin, and contained a bar-eye and GFP balancer for recognition of homozygous mutants (*shibire*[ts1]/FM7-Actin GFP). "Cantonized" homozygous Syn[97CS] flies were used for synapsin null mutant experiments. These were kindly provided by Prof. Erich Buchner, University of Würzburg (Godenschwege et al., 2004). To obtain pHluorin flies expressing synaptobrevin-pHluorin in motoneurons, males from the D42-GAL4 driver line (obtained from Prof. Andre Fiala, University of Göttingen) were crossed to UAS-synaptopHluorin III females (obtained from Prof. Stephan Sigrist, Free University of Berlin; note that UAS stands for upstream activating sequences; Duffy, 2002). Generally, third instar larvae were used for all experiments, with adult flies being used in addition in the *shibire* paralysis experiments (Section 2.11). Flies were generally maintained at 21°C; pHluorin flies were kept at 25°C with a 12 hour day/night rhythm, but experiments were performed at 21°C. Wildtype Bristol N2 *C. elegans* worms were kept at 20°C according to standard methods (Brenner, 1974) and were kindly provided by Dr. Ling Luo and Dr. Stefan Eimer, European Neuroscience Institute. Locusts were maintained in a terrarium at room temperature and were fed on grass and special locust food (Nekton, Pforzheim, Germany). They were provided by Dr. Andrea Wirmer and Dr. Ralf Heinrich, University of Göttingen. Zebrafish were obtained from a commercial supplier and were kept in an aquarium at 24°C. Frogs were also obtained from a commercial supplier and were maintained at 16°C and fed on live prey at least once per week. Wildtype (female CD-1, B6/N and B6/J and male B6/N and B6/J) mice were maintained in standard cages and were obtained from the animal facility of the European Neuroscience Institute. Chicken embryos were kindly provided by Alexandra Klusowski and Dr. Till Marquardt, European Neuroscience Institute. Fertilized eggs (wildtype, LSL white eggs, Geflügelzucht Horstmann, Germany) were maintained at 37.8°C until embryonic day (E) 11-12. Crickets were obtained from a commercial supplier, and were kept on commercial pellet food, according to the supplier's instructions. All animals were treated according to the

regulations of the University of Göttingen and of the State Niedersachsen (Landesamt für Verbraucherschutz, LAVES, Braunschweig, Germany).

2.2 Chemicals

All chemicals were purchased from Sigma (Taufkirchen, Germany), Merck (Darmstadt, Germany) or VWR (Hannover, Germany), unless otherwise stated. FM 1-43 (SynaptoGreen) was obtained from Biotrend (Cologne, Germany).

2.3 Buffers and Solutions

The buffers and solutions employed in this study are summarized in Table 2.1. For all injected animals, dissections were performed in a mixture of ice-cold/frozen Ca^{2+}-free buffer ($CaCl_2$ was replaced with $MgCl_2$ and 1 mM EGTA was added).

Table 2.1: Buffers and solutions

Buffer or Solution	Composition
Anode buffer (10×)	2 M TRIS (pH 8.9)
ATP source	100 mM ATP, 800 mM creatine phosphate, 800 u/mg creatine kinase
Blotto buffer	PBS + 5% milk powder + 0.1% Tween 20
Cathode buffer (10×)	1 M TRIS, 1 M Tricin, 1% SDS
C. elegans buffer	150 mM NaCl, 5 mM KCl, 5 mM $CaCl_2$, 4 mM $MgCl_2$, 10 mM glucose, 5 mM sucrose, 15 mM HEPES (pH 7.3) (Sumakovic et al., 2009)
Chicken Ringer	150 mM NaCl, 3 mM KCl, 2.5 mM $CaCl_2$, 1.2 mM $MgCl_2$, 17 mM glucose, 10 mM HEPES (pH 7.2) (modified from Nguyen and Sargent, 2002)
DHM mix	10 mM DTT, 625 mM HEPES, 75 mM Mg acetate (pH 7.3)
Drosophila HL3 buffer (for injection)	70 mM NaCl, 5 mM KCl, 1.5 mM $CaCl_2$, 20 mM $MgCl_2$, 10 mM $NaHCO_3$, 5 mM trehalose, 115 mM sucrose, 5 mM HEPES (pH 7.2) (Reist et al., 1998)
Frog Ringer	115 mM NaCl, 2 mM KCl, 1.8 mM $CaCl_2$, 5 mM HEPES (pH 7.2) (Rizzoli and Betz, 2004)
Gel buffer	3 M TRIS, 0.3% SDS (pH 8.45)
Hexokinase system	1500 u/ml hexokinase (Roche, Mannheim, Germany) in 250 mM D-glucose
High salt PBS	500 mM NaCl, 20 mM Na_2HPO_4 (pH 7.4)
Homogenization buffer	250 mM sucrose, 3 mM imidazole (pH 7.5)
Locust high potassium saline (also used for crickets)	100 mM NaCl, 50 mM KCl, 4 mM NaH_2PO_4, 6 mM Na_2HPO_4, 2 mM $CaCl_2$, 90 mM sucrose (pH 6.8)
Locust standard saline (also used for crickets)	140 mM NaCl, 10 mM KCl, 4 mM NaH_2PO_4, 6 mM Na_2HPO_4, 2 mM $CaCl_2$, 90 mM sucrose (pH 6.8) (Clements and May, 1974)
M9 buffer for *C. elegans* rescue	22 mM KH_2PO_4, 22 mM Na_2HPO_4, 85 mM NaCl, 1 mM $MgSO_4$ (Brenner, 1974)
Mouse Ringer	154 mM NaCl, 5 mM KCl, 2 mM $CaCl_2$, 1 mM $MgCl_2$, 11 mM glucose, 5 mM HEPES (pH 7.3) (Angaut-Petit et al., 1987)
Mowiol	6 g glycerol AR, 2.4 g Mowiol 4-88 (Calbiochem, Darmstadt, Germany), 6 ml H_2O, 12 ml 0.2 M TRIS (pH 7.2) (Willig et al., 2006)
Phosphate buffered saline (PBS)	150 mM NaCl, 20 mM Na_2HPO_4 (pH 7.4)
Sample buffer	50 mM TRIS, 4% SDS, 0.01% Serva Blue G, 12% glycerol, 2% β-mercaptoethanol (pH 6.8)
Sodium buffer	140 mM NaCl, 5 mM KCl, 10 mM glucose, 5 mM $NaHCO_3$, 1.2 mM Na_2HPO_4, 1 mM $MgCl_2$, 20 mM HEPES (pH 7.4)
Standard *Drosophila* buffer (for stimulation)	130 mM NaCl, 36 mM sucrose, 5 mM KCl, 2 mM $CaCl_2$, 2 mM $MgCl_2$, 5 mM HEPES (pH 7.3) (Jan and Jan, 1976; Kuromi and Kidokoro, 1998)
Stripping buffer	2% SDS , 62.5 mM TRIS (pH 6.8), 0.8% β-mercaptoethanol
Sucrose/cytosol buffer	320 mM sucrose, 5 mM HEPES (pH 7.4)
Transfer buffer	200 mM glycin, 25 mM TRIS, 20% MeOH, 0.04% SDS
Wash buffer	PBS + 0.05% Tween 20
Zebrafish Ringer	116 mM NaCl, 2.9 mM KCl, 1.8 mM $CaCl_2$, 5 mM HEPES (pH 7.2) (Redenti and Chappell, 2003)

2.4 FM Dye Injection and Photo-oxidation

To investigate vesicle recycling and use *in vivo*, I injected the styryl dye FM 1-43 into living animals, either into the body cavity or subcutaneously, as indicated in Figure 2.1 for a *Drosophila* larva. After injection, the animal was allowed to behave freely (i.e. move around, communicate with other animals, eat and rest) for a defined amount of time. As explained in Section 2.4.1, the FM dye reaches the synapses and is taken up into recycling vesicles, thereby monitoring vesicle use after injection. After a specified time (10 minutes to 4 hours), the animal was sacrificed and the organ of interest was dissected. This was followed by fixation and photo-oxidation, involving the illumination of the preparation in presence of di-amino-benzidine (DAB). Illumination causes the production of reactive oxygen species (ROS) by the FM dye and subsequent oxidation of the membrane-permeant DAB, which then polymerizes and forms an electron-dense precipitate selectively within the dye-labelled vesicles. After photo-oxidation, the preparations were processed for electron microscopy, which allowed for the quantification of the number of vesicles used in the time from injection to dissection and also for the visualization of the exact localization of these vesicles within the synapse.
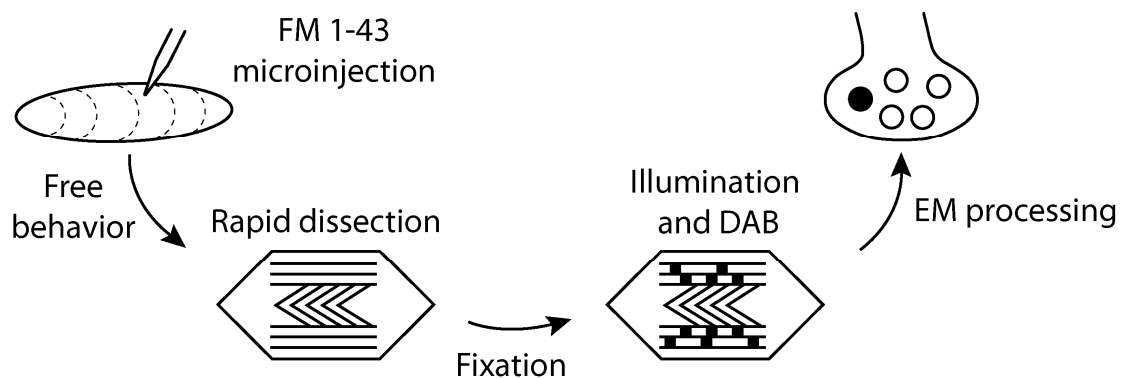
Figure 2.1: The general experimental procedure for studying vesicle use *in vivo*
FM 1-43 is injected into a living animal, which is then allowed to behave freely for a defined amount of time, during which recycling vesicles will take up the dye and therefore become labelled. The organ of interest is then dissected and fixed, followed by illumination in the presence of di-amino-benzidine (DAB) (photo-oxidation). This causes DAB to form an electron-dense precipitate within the dye-labelled vesicles and allows for subsequent counting of labelled vesicles in EM. (From Denker et al., 2011a)

2.4.1 Monitoring Synaptic Vesicle Recycling With FM Dyes- General Remarks

Styryl dyes are sensitive markers for membrane retrieval. FM dyes share a general structure which is shown in Figure 2.2 A for the widely used FM 1-43. A hydrophobic part, which usually consists of two aliphatic chains, allows the reversible insertion into membranes. The length of these chains determines the hydrophobicity of the dye, and thus its affinity for membranes. The dye molecule also contains a hydrophilic head group (with two positive charges) which prevents penetration through the membranes. These two moieties are connected by aromatic rings and one or more double bonds, which determine the dye's spectral properties. Importantly, the dyes are several-hundred fold more fluorescent in the lipid environment of the membrane than in water, which renders the dye molecules essentially invisible in solution.

Figure 2.2 B displays a typical FM dye labelling experiment as traditionally performed for monitoring vesicle recycling in a presynaptic terminal *in vitro*. Upon dissecting the preparation of interest (for instance an NMJ), dye-containing buffer is added. The dye diffuses into the preparation and inserts into the presynaptic plasma membrane, where its fluorescence increases substantially. When vesicles fuse with the plasma membrane (for instance triggered by electrical stimulation) and undergo recycling, they will take up the dye. After vesicle reformation, the vesicles remain labelled, while the extracellular space can be washed to remove excess dye. Furthermore, the labelled vesicles can be unlabelled, if a second round of stimulation is triggered in absence of the dye, resulting in destaining of the preparation.

In the case of *in vivo* injection of the styryl dye, as performed in this project, the process of vesicle labelling is essentially the same as depicted in Figure 2.2 B (2-4). Washout of the dye from the plasma membrane and the extracellular fluid (Figure 2.2 B (5)) only occurs during dissection of the organ of interest. The destaining process described above (Figure 2.2 B (6)) is not performed in this protocol.

Example images of synapses stained with FM dyes either by *in vivo* injection or by electrical stimulation *in vitro* are displayed in Figure 2.2 C and D. Of course, many alternative types of imaging experiments can be devised, with various combinations of staining/destaining, testing various synaptic characteristics such as vesicle pool properties.
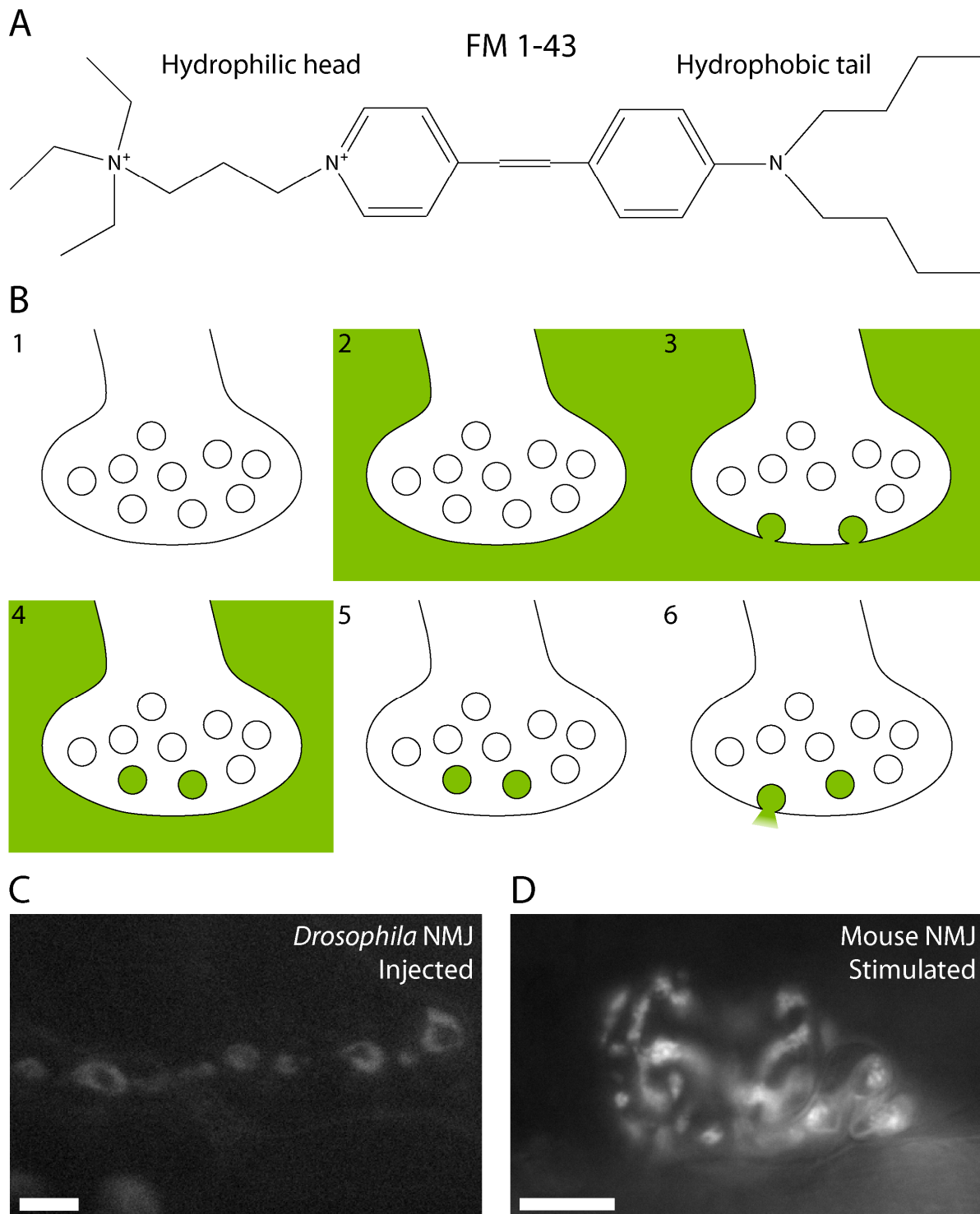
Figure 2.2: FM dye characteristics and staining procedure
(A) The structure of FM 1-43. As each FM dye, the molecule contains a hydrophilic head group and a hydrophobic tail group connected via aromatic rings and double bonds. (B) 1) A presynaptic terminal filled with synaptic vesicles. 2) The FM dye is added to the preparation and inserts into the terminal membrane. 3) Vesicle fusion is stimulated, resulting in 4) dye uptake into the recycling vesicles. 5) The preparation may then be washed to remove excess dye. 6) Further stimulation in the absence of FM dye triggers a new round of vesicle recycling and destaining of previously labelled vesicles. (C) Fluorescence image of a *Drosophila* NMJ nerve terminal at 5 minutes after FM dye injection. Note the dim but discernible fluorescence, following the well-known labelling pattern of this preparation (see for example Denker et al., 2009). Size bar is 5 μm. (D) Mouse NMJ labelled by 30 Hz stimulation for 1 minute in presence of FM 1-43. Size bar is 10 μm. Note that the images in (C) and (D) are not scaled identically and that the experiment presented in (D) was performed by Ingrid-Cristiana Vreja, MSc/PhD program Molecular Biology, Göttingen.

2.4.2 Injection of FM 1-43

All injections were performed to achieve a final concentration of about 10 µM FM 1-43 in the animal (see also Meyers et al., 2003). After dilution of FM 1-43 in the respective buffer, the solution was filtered (Millipore Ultrafree®- MC Sterile centrifugal filter units, 0.22 µm, Millipore, Billerica, USA). A FemtoJet express microinjecting device (Eppendorf, Hamburg, Germany) was employed for microinjection into *Drosophila* third instar larvae, using glass micropipettes prepared from glass tubes (thin wall, 3 inches, 1 mm diameter; World Precision Instruments, Berlin, Germany) with a P-97 pipette puller (Sutter Instrument Co., Novato, USA). A dissection microscope was used to monitor injection (Leica MZ6; Leica, Wetzlar, Germany). Generally, about 20 to 50 nl of FM 1-43 solution were injected into the body cavity and the volume was subsequently checked by injection with the same settings and tip into oil (Halocarbon oil 700, Sigma). A Leica MZ10F fluorescence stereomicroscope equipped with a GFP Plant filter set (Leica) was used to monitor successful microinjection. Young adult *C. elegans* worms were injected into the pseudocoelom using Femtotips (Eppendorf) on a FemtoJet express microinjecting device (Eppendorf). A Zeiss Axiovert 200 microscope (Zeiss, Oberkochen, Germany) equipped with a 40x 0.5 NA objective from Olympus (Hamburg, Germany) was used to monitor successful injection. For all the other animals, injection was performed using 1 ml syringes (Terumo, Somerset, USA) and 0.3 × 20 mm needles (catalogue number 13.201-09, Unimed, Lausanne, Switzerland). In case of locusts, 10 to 20 µl of FM 1-43 solution were injected into the abdominal coelom. For zebrafish, 20 µl were injected subcutaneously near the caudal fin. For frogs, about 20 to 100 µl (depending on the size of the respective frog) were injected subcutaneously into the ventral part of the thorax. In case of mice, 300 µl were injected subcutaneously into the neck. For chicken embryos (E11-E12; stages 37-38) (Hamburger and Hamilton, 1951), a 1.5 x 1.5 cm window was cut in the egg shell and about 50 µl were injected subcutaneously into the upper region of the thigh. After injection, the window was sealed with Parafilm (VWR) to prevent dehydration. Finally, for crickets, 50 to 100 µl of FM 1-43 solution were injected into the first segments of the abdomen or the thorax.

Note that for the quantification of spontaneous vesicle release (presented in Figure 3.19), *Drosophila* third instar larvae were simultaneously injected with FM 1-43 (as described above) and tetrodotoxin (TTX; calculated to result in a final concentration of 5 µM in the animal).

2.4.3 Maintenance after Injection

Upon injection, animals were generally kept in an environment that allowed them to move, eat and rest. Third instar *Drosophila* larvae were maintained on standard cornmeal medium. *C. elegans* were rescued with M9 buffer after injection and kept on Nematode Growth Medium (NGM; 16 g Agar, 3 g NaCl, 3 g peptone ad 1 L ddH$_2$O; autoclaved). Locusts and crickets were kept on fresh grass; zebrafish were kept in normal aquarium water; frogs were maintained in a terrarium with sufficient water, and occasionally fed with live prey; mice were maintained in standard cages provided with food and water. Chicken eggs were kept in an incubator at ~38°C. All animals survived injection and behaved normally afterwards (i.e. moved, communicated/interacted with other animals, ate, or slept, in ways that were indistinguishable from uninjected control animals).

2.4.4 Dissections

At the specified time after injection, dissections of the respective muscles and organs (Figures 3.1 to 3.3) were performed rapidly in sylgard-coated culture dishes in a mixture of frozen/ice-cold Ca^{2+}-free buffer. The dissection of *Drosophila* larvae was performed according to Jan and Jan, 1976. Note that the ventral longitudinal muscles 6 and 7 were employed. In case of adult flies (*shibire* paralysis experiment; Section 2.11), the thorax was cut longitudinally, leaving the ventral side with legs and coxa intact and the femur was removed. *C. elegans* were cut vertically into three pieces. Locusts were sacrificed by decapitation and the third pair of legs was removed. The femurs were then opened, and the *tibial flexor* muscle was spread out. In case of zebrafish, animals were sacrificed and skin and superficial tail muscles were removed to expose the *adductor caudalis ventralis*, *flexor caudalis ventralis inferior* and *superior* muscles. The dissection of the frog *cutaneous pectoris* muscle was performed as described in Blioch et al., 1968. Dissection of the mouse *levator auris longus* muscle was done according to Angaut-Petit et al., 1987. Chicken embryos (Hamburger and Hamilton, 1951) were sacrificed by decapitation, the legs were removed and the *gastrocnemius pars interna* and *externa* muscles were exposed. For crickets, the animals were sacrificed by decapitation and the eye and associated optic lobe with lamina and medulla were removed (see Honegger and Schurmann, 1975; Honegger, 1977).

In some instances, the fluorescence of the preparations was checked after injection and dissection and before proceeding to photo-oxidation, as for example presented in Figure 2.2 C. For this, a Zeiss Axioskop 2 FS plus microscope equipped with a 63× 1.0 NA objective from Zeiss, a 100 W mercury lamp (Osram, Augsburg, Germany) and a back mirror (to

collect back-scattered light) was used. An EGFP Long Pass filter set (AHF, Tübingen; 470/40 nm excitation filter; 495 nm dichroic mirror; 500 nm long pass emission filter) was employed.

2.4.5 Photo-oxidation

A detailed video protocol of the photo-oxidation procedure is provided in Opazo and Rizzoli, 2010.

a) After dissection, the preparations were fixed. I generally employed 2.5% glutaraldehyde fixation (in phosphate buffered saline, PBS), as formaldehyde has been reported to increase spontaneous release frequency (Smith and Reese, 1980). The temperature for fixation also required careful consideration: whereas the fixation procedure is faster at room temperature, fixation on ice decreases the amount of vesicles fusing spontaneously while fixation is not yet complete. I therefore generally combined the two approaches by first fixing on ice for ~30 minutes, followed by further fixation at room temperature to speed up the process for an additional 30 to 60 minutes.

b) Fixation was followed by thorough washing in PBS. As all subsequent steps, until fluorescence illumination, this washing was performed at 4°C.

c) Samples were then removed from the dissection dish (they are relatively robust after glutaraldehyde fixation) and washed for ~20 minutes in 100 mM NH$_4$Cl (in PBS). This step neutralizes free aldehyde groups of the remaining glutaraldehyde and it also decreases glutaraldehyde autofluorescence. If this step is omitted or shortened, residual free glutaraldehyde will later react with DAB and form a transparent crystalline precipitate which is easily observed by visual inspection. In my hands, samples which display such precipitate formation should be discarded, as photo-oxidation is rarely successful in this case. Should precipitate formation be observed, it is advisable to prolong the NH$_4$Cl washing or to add an additional step of washing with 100 mM glycine.

d) The samples were transferred to PBS and washed thoroughly. They were then pinned into a new dish and exposed to a second round of PBS washing. These washing steps should eliminate all residual free fixative.

e) The samples were incubated for 30 to 60 minutes (not much longer) at 4°C with (filtered) 1.5 mg/ml DAB (in PBS). The DAB solution should either be prepared fresh or stored for not more than a few hours at 4°C.

f) Before illumination, the DAB solution used for the incubation of the preparations was replaced with fresh solution. The samples were then individually placed under the microscope objective. I used a 20× 0.5 NA objective from Olympus, which provided a good compromise between the size of the illumination field (and thereby also the photo-oxidation spot) and the illumination time (which increases with lower magnification). I used a dry objective (not immersed in the solution on upright microscope setups) to avoid contamination with DAB. The same microscope and filter set was used as for the FM imaging described above.

The photo-oxidation reaction, as depicted in Figure 2.3, begins upon the start of illumination. The FM dye is excited and emits photons; at the same time, it produces ROS. As the DAB is membrane-permeant and can penetrate into the preparation, it will reach the labelled vesicles and become oxidized, resulting in its precipitation, as described above. Importantly, this reaction only takes place in the immediate proximity of the dye (here the vesicular lumen) as the ROS are highly reactive and have a very short life-time.

The progress of the photo-oxidation reaction should be carefully monitored. As indicated in Figure 2.3 B, the illumination first resulted in the bleaching of the FM dye fluorescence. A few minutes after bleaching was complete, the preparations assumed a brown color. I generally continued the reaction for another 5 to 10 minutes to ensure complete photo-oxidation. At this time, the nerve terminals had turned completely dark brown (clearly visible on top of the residual glutaraldehyde autofluorescence of the background) and some photo-oxidation product could also be observed on neighboring tissues such as the muscle surface. This was probably due to DAB precipitation induced by the tissue or fixative autofluorescence. Successful precipitate formation could also be easily observed by transmission light.

As will be discussed below, the exact time point of stopping the reaction (by simply switching the lamp off) needed to be chosen carefully and depended to a large extent on light intensity and on properties of the respective preparation. In my hands, illumination between 30 to 45 minutes often gave optimal results (using a 20× objective). When photo-oxidation was not complete after one hour, the sample could generally be discarded – no further oxidation was to be expected. This could be due to poor DAB penetration, but was often caused by using fluorescence lamps which were too old and therefore not intense enough (also refer to Section 2.4.8 for a discussion of low light intensity).
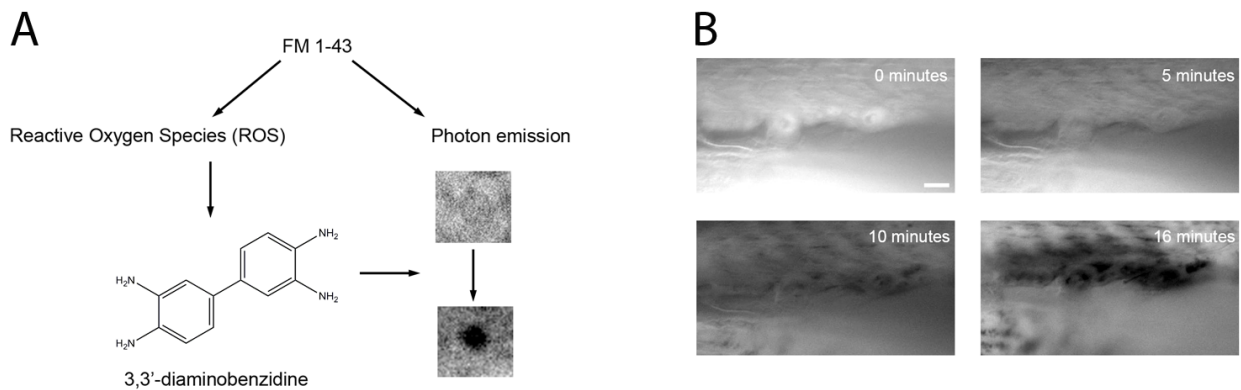
Figure 2.3: The photo-oxidation reaction
(A) The principle of the photo-oxidation reaction. Illumination results in photon emission and in the production of reactive oxygen species (ROS). When preparations are simultaneously incubated with DAB, the ROS will oxidize the DAB, causing it to form an electron-dense precipitate which can be visualized by EM. As the ROS are highly reactive and short-lived, this reaction only occurs in the immediate proximity of the labelled structures (synaptic vesicles in this case). (B) The progress of the photo-oxidation reaction in a *Drosophila* NMJ. At the beginning of the reaction, the FM fluorescence is bleached. Shortly afterwards, the brown DAB precipitate appears, marking the beginning of successful photo-oxidation. The reaction should not be stopped at this point but be continued for another 5 to 10 minutes to ensure successful and complete DAB oxidation. At this point, synapses have turned dark brown and some photo-oxidation is observed on neighboring tissues such as the muscle surface (for instance due to glutaraldehyde autofluorescence). Note that these images were taken with a 63× objective to better visualize the process (I generally employed a 20× objective). Size bar is 2 μm. (From Denker et al., 2009)

2.4.6 Processing of Photo-oxidized Preparations for Electron Microscopy

a) When photo-oxidation was complete, the DAB was washed off and replaced with PBS. The photo-oxidation spot was cut from the rest of the preparation (this ensured that photo-oxidized synapses were quickly found in electron microscopy). The cut tissue could be stored at 4°C in PBS for up to two days.

b) The samples were then post-fixed and stained with 1% osmium tetroxide (Fluka, Sigma, Taufkirchen, Germany; in filtered PBS). Generally, about 150 to 200 μl per sample were sufficient. Incubation in osmium tetroxide was performed at room temperature for 45 to 60 minutes. For *C. elegans*, adult flies (*shibire* experiment) and crickets, the procedure was slightly modified to prevent poor penetration of osmium. For *C. elegans*, incubation in 2% osmium tetroxide was performed for 1 hour at room temperature and for an additional hour at 4°C. For flies and crickets, treatment with 1% osmium tetroxide at room temperature was extended to 1.5 hours.

c) The osmium was removed by thorough washing with filtered PBS (at least three times; at room temperature, as all subsequent steps).

d) The samples were dehydrated according to the following scheme:

	30% ethanol	5 min
	50% ethanol	5 min
	70% ethanol	5 min
	90% ethanol	10 min
	95% ethanol	10 min
3×	100% ethanol	10 min
1:1	ethanol:propylene oxide	10 min
3×	propylene oxide	10 min
1:1	propylene oxide:epon	12-18 hours (under constant agitation)

For samples which were easily penetrated (such as the *Drosophila* NMJ) the last three steps involving propylene oxide (Electron Microscopy Sciences, Hatfield, USA) were omitted. Instead, samples were transferred into a 1:1 mixture of ethanol:epon resin (Plano, Wetzlar, Germany) and incubated for 12 to 18 hours under constant agitation.

e) The propylene oxide:epon or ethanol:epon mixture was removed and replaced with fresh 100% epon resin. The samples were kept in open vials for ~8 hours to allow for complete evaporation of the organic solvent. For *C. elegans*, two additional incubation steps with 100% epon resin for 6 hours under continuous agitation were added before evaporation of propylene oxide.

f) The samples were then incubated in moulds in fresh resin for 24 to 48 hours at 60°C, to allow for epon polymerization.

g) The samples were cut into 90-100 nm thick sections on a Leica EM UC 6 microtome. Generally, no further staining was necessary, i.e. no uranyl acetate or lead citrate stains, as they would reduce the signal-to-noise ratio and diminish the recognition of the DAB product in EM. I found the use of the osmium stain alone to be sufficient for visualizing the sample's ultrastructure, at the same time allowing for reliable identification of the photo-oxidation product.

For the investigation of frog Schwann cells and for the *shibire* samples (larvae and adults), sections were post-stained with 2% uranyl acetate (Plano) in 50% ethanol for 2 minutes.

2.4.7 Electron Microscopy and Data Analysis

A Zeiss EM 902A microscope, equipped with a 1024 × 1024 CCD detector (Proscan CCD HSS 512/1024; Proscan Electronic Systems, Scheuring, Germany), was used for the acquisition of electron micrographs.

Image analysis was performed using custom-written MATLAB routines (The Mathworks, Natick, USA), as previously described (Rizzoli and Betz, 2004). Briefly, the plasma membrane, active zones, vacuoles (labelled and unlabelled), and vesicles (labelled and unlabelled) were drawn manually, using a Wacom PL 720 LCD tablet monitor (Wacom, Krefeld, Germany). Distances from the centers of labelled and unlabelled vesicles to the nearest active zone and plasma membrane were calculated (Figure 3.6). The 3D reconstructions were obtained from serial sections, with the reconstructions made from individual synapses being several micrometer-long (resulting in reconstruction volumes of up to several μm^3).

As the photo-oxidation reaction proceeds in an all-or-none manner, labelled and unlabelled vesicles can generally be readily distinguished by visual inspection. In addition, a more objective criterion is provided by the relative density concept, which is explained in Figure 2.4 A: whereas unlabelled vesicles display a higher density at the vesicle membrane than in the clear core when visualized by EM, labelled vesicles have a dark electron-dense core, which displays a higher density than the surrounding membrane. Consequently, the relative density (the ratio between the lumenal and membrane density) should be lower than 1 for unlabelled, but larger than 1 for labelled vesicles.

The reliability of distinguishing labelled and unlabelled vesicles from each other in the different preparations by visual inspection was tested by calculating the relative density for vesicles which had been designated as labelled or unlabelled by the user. To calculate the relative density, a region of interest (ROI) was chosen within the vesicle lumen and the average density was measured. This was divided by the average density of the synaptic vesicle membrane, which was obtained by drawing a line scan along the outer edge of the vesicle. The relative density distributions of the labelled and unlabelled vesicles (Figure 2.4 B) show that these two vesicle populations can indeed by reliably distinguished by visual inspection, as the error rates were very low, only ~1.5% for the labelled and ~3% for the unlabelled vesicles.
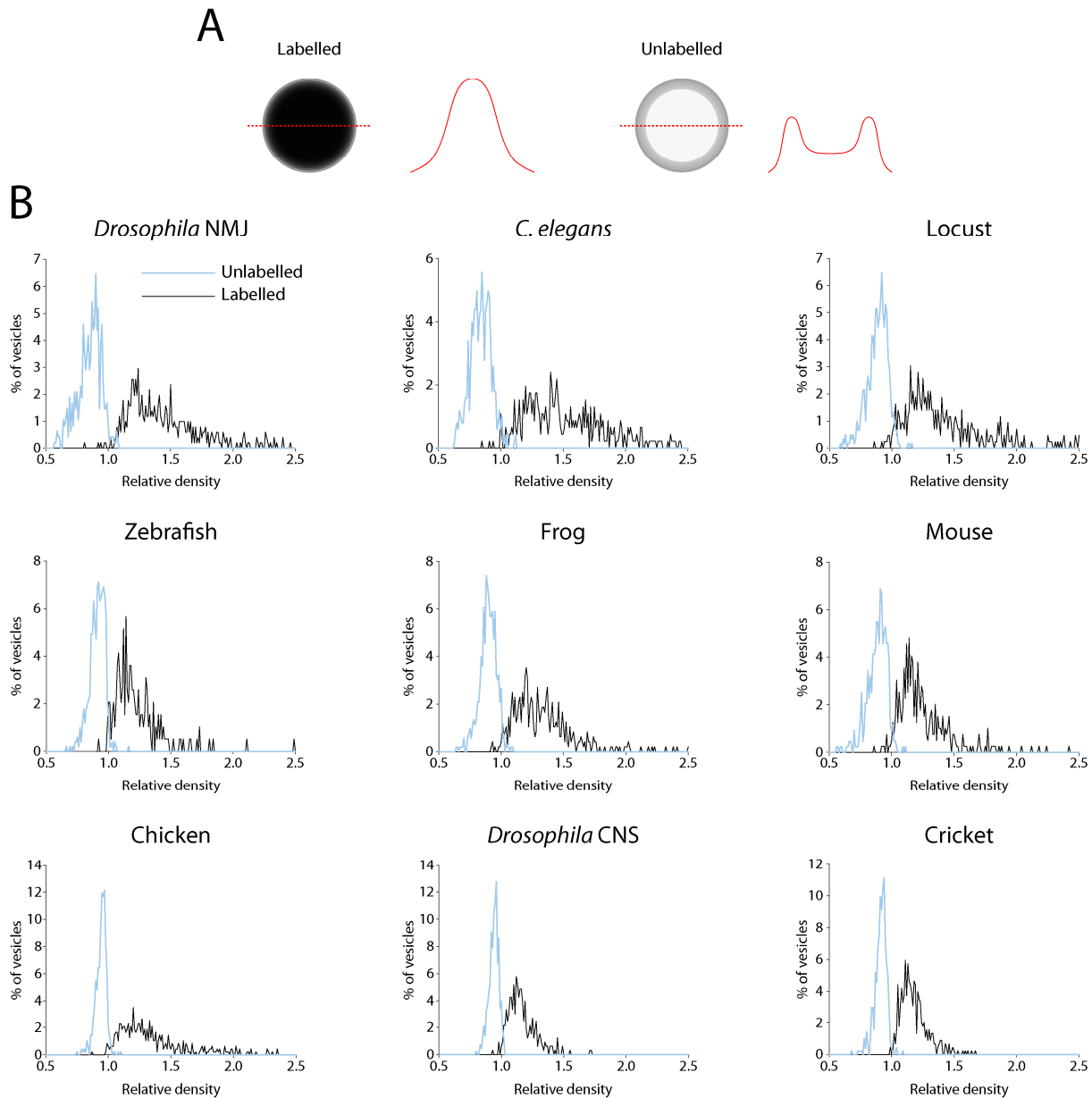
Figure 2.4: Labelled and unlabelled vesicles can be reliably distinguished
(A) The concept of relative density. Whereas control (unlabelled) synaptic vesicles contain a clear core which is less dense than the surrounding membrane, photo-oxidized (labelled) vesicles have a dark (filled) core. This density difference can be expressed as the relative density - the ratio between lumenal and membrane density. Theoretically, this value should be larger than 1 for the labelled vesicles, and lower than 1 for the unlabelled vesicles (see also Rizzoli and Betz, 2004; Denker et al., 2009).
(B) Relative density measurements were performed for each of the preparations investigated. Vesicles were manually designated as "labelled" (black) or "unlabelled" (cyan) by the user. Subsequently, the relative density was calculated as follows: the average density of an ROI (region of interest) within the vesicle lumen was measured and divided by the average membrane density, which was obtained by drawing line scans along the vesicle membrane. Importantly, it has been shown that the relative density distributions of vesicles designated as unlabelled are indistinguishable from the relative density distributions of vesicles which were not photo-oxidized (Rizzoli and Betz, 2004). Note that the distributions hardly overlap, indicating that labelled and unlabelled vesicles can be reliably distinguished. The error rate was ~1.5% for the labelled and ~3% for the unlabelled vesicles. For each data set, approximately 200 to 600 vesicles were analyzed, for each labelled and unlabelled vesicles. (From Denker et al., 2011a)

In a second approach, the relative density distributions of the labelled and unlabelled vesicles were pooled (i.e. without prior judgement on the labelling status of the vesicle) and fit with two-peak Gaussian curves (as shown in Figure 2.5 for distributions obtained from *C. elegans*). The equation for this double Gaussian curve (i.e. the sum of two Gaussians) is:

$$y = \frac{1}{\sqrt{2\pi\sigma_1^2}} e^{-\frac{(x-\mu_1)^2}{2\sigma_1^2}} + \frac{1}{\sqrt{2\pi\sigma_2^2}} e^{-\frac{(x-\mu_2)^2}{2\sigma_2^2}}$$

Instead of the theoretical cut-off of 1, the inflexion point was now used as the cut-off, which resulted in a change in error rates to ~7% for the labelled vesicles and to ~0.5% for the unlabelled vesicles. This means that the labelling status of only a small minority of the vesicles was wrongly judged and that the chance of counting an unlabelled vesicle erringly as labelled was larger than making an error in the opposite direction.
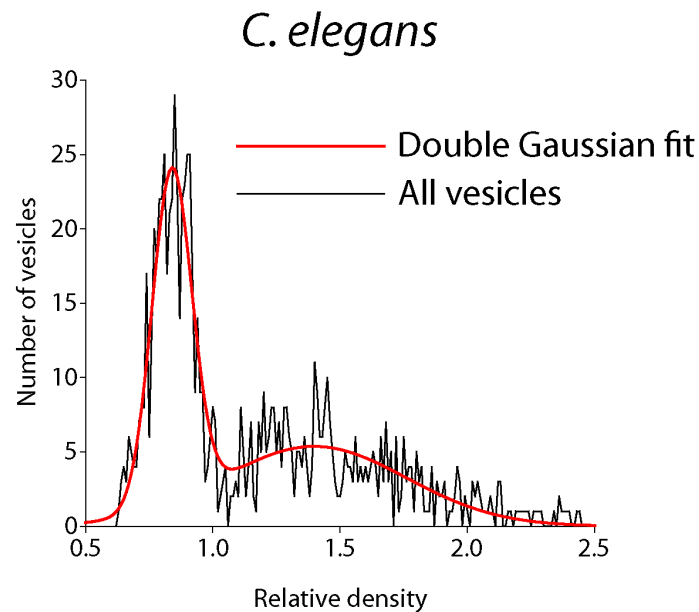
Figure 2.5: Alternative analysis of relative density graphs by double Gaussian fit
As shown here for the example of the *C. elegans* data, relative density graphs can also be analyzed by combining the vesicle populations and then fitting a two-peak Gaussian curve to the distribution. Instead of the theoretical cut-off of 1, the inflexion point of the curve now provides the cut-off for the labelled and unlabelled vesicle populations. Using this value, the error rate changes to ~7% for the labelled vesicles and to ~0.5% for the unlabelled vesicles (compare values obtained in Figure 2.4). (From Denker et al., 2011a)

As mentioned in Section 2.4.6, reliable differentiation between labelled and unlabelled vesicles can be supported by using a relatively low contrast enhancement of the samples – meaning relatively low post-staining of the EM grids (i.e. by not using lead citrate staining,

and as little as possible uranium acetate, thus relying mostly on osmium staining for contrast), albeit at the cost of image quality.

2.4.8 Photo-oxidation: Troubleshooting

As the photo-oxidation technique is associated with several caveats, this section will describe some of the difficulties encountered when optimizing this method for the different preparations employed in this study.

The major difficulty of the photo-oxidation technique was the occurrence of under- or over-oxidized terminals, as displayed in Figure 2.6 A and B, respectively. Note that under- and over-oxidized preparations were generally excluded from analysis.

In under-oxidized synapses, no reaction product was observed. This could be due to several factors, such as limited DAB penetration, too low light intensity, and too short illumination times (i.e. the reaction was stopped too early). The limited penetration of DAB into the preparation was especially evident for very thick samples: for these tissues, I often observed successful photo-oxidation in surface layers (on both sides of the preparation), but more central structures did not reveal precipitate formation. For most muscle preparations, where the terminals are found on the muscle surface, the limited DAB penetration was generally not a major drawback of the technique. Photo-oxidation efficiency could however also be limited by too low light intensity, which could be increased by using a high intensity mercury lamp (combined with a back mirror to collect back-scattered light, see above). The illumination spot should be well focused on the structure of interest. The most common error resulting in under-oxidized synapses was the choice of too short illumination times. Importantly, completely oxidized synapses were generally not found immediately after the disappearance of the FM fluorescence, and not even after the initial appearance of the dark DAB precipitate, but ~5 to 10 minutes later.

On the other hand, illuminating the samples for too long was also not an option, as this easily caused over-oxidation. Over-oxidized terminals displayed a "negative" image of what one would expect to find in a well-oxidized sample (compare for example Figure 1.3 and Figure 2.6 B): the cytosol was dark, due to DAB precipitate spilling out of damaged organelles, and unlabelled organelles (which exclude the dark cytosol) appeared clear. In this case, all potentially labelled structures were obscured by the very dark staining of the cytosol. Furthermore, over-oxidized samples often displayed a heavily distorted ultrastructure, with many vacuolar structures. As described below, these problems were mainly caused by the photo-oxidation of mitochondria.

In summary, the time window in which to stop the photo-oxidation reaction was found to be quite narrow. It is also important to mention that experience with illumination times from

one specific preparation could not necessarily be directly applied to another preparation. For instance, I found mouse NMJs to be much more susceptible to over-oxidation than all other preparations investigated.

Interestingly, FM labelled structures were generally not the first to oxidize DAB. Instead, mitochondria often started to precipitate DAB even in synapses which were obviously illuminated for too short time intervals to observe any labelled synaptic vesicles (note for instance mitochondrion in Figure 2.6 A). This precipitation was in my hands dependent on illumination and was not observed outside the photo-oxidation spot, but it did not depend on the presence of the dye. Whereas the photo-oxidation of the mitochondria could be used as an indication for successful DAB penetration and sufficient light intensity, it also represented the main cause for the deleterious effects of over-oxidation: when the mitochondria accumulated too high amounts of DAB precipitate, they started to swell, distorting the synaptic ultrastructure. When illumination was continued further, the mitochondria eventually burst and spilled their dark DAB precipitate content, resulting in the electron-dense cytoplasm described above. The process is displayed in Figure 2.6 C-F for the mouse NMJ.

Different mechanisms have been proposed to account for the high susceptibility of mitochondria to over-oxidation, and in both scenarios the mitochondrial respiratory chain plays a central role: first, cytochromes display strong autofluorescence and will therefore also produce ROS and oxidize the DAB under illumination. Second, respiratory enzymes may display residual enzymatic activity even after fixation, also resulting in the production of ROS. In line with the second hypothesis, addition of potassium cyanide, which is an inhibitor of the mitochondrial respiratory chain, reduces background DAB precipitation in the mitochondria (Deerinck et al., 1994; Monosov et al., 1996; Grabenbauer et al., 2005). The fact that illumination is required for the appearance of precipitate in the mitochondria (see above) argues for a combination of the two mechanisms.

If illumination times were chosen carefully, spilling of mitochondrial contents could generally be avoided for most synapses. Therefore, and because of its high toxicity, I refrained from using potassium cyanide to prevent over-oxidation.
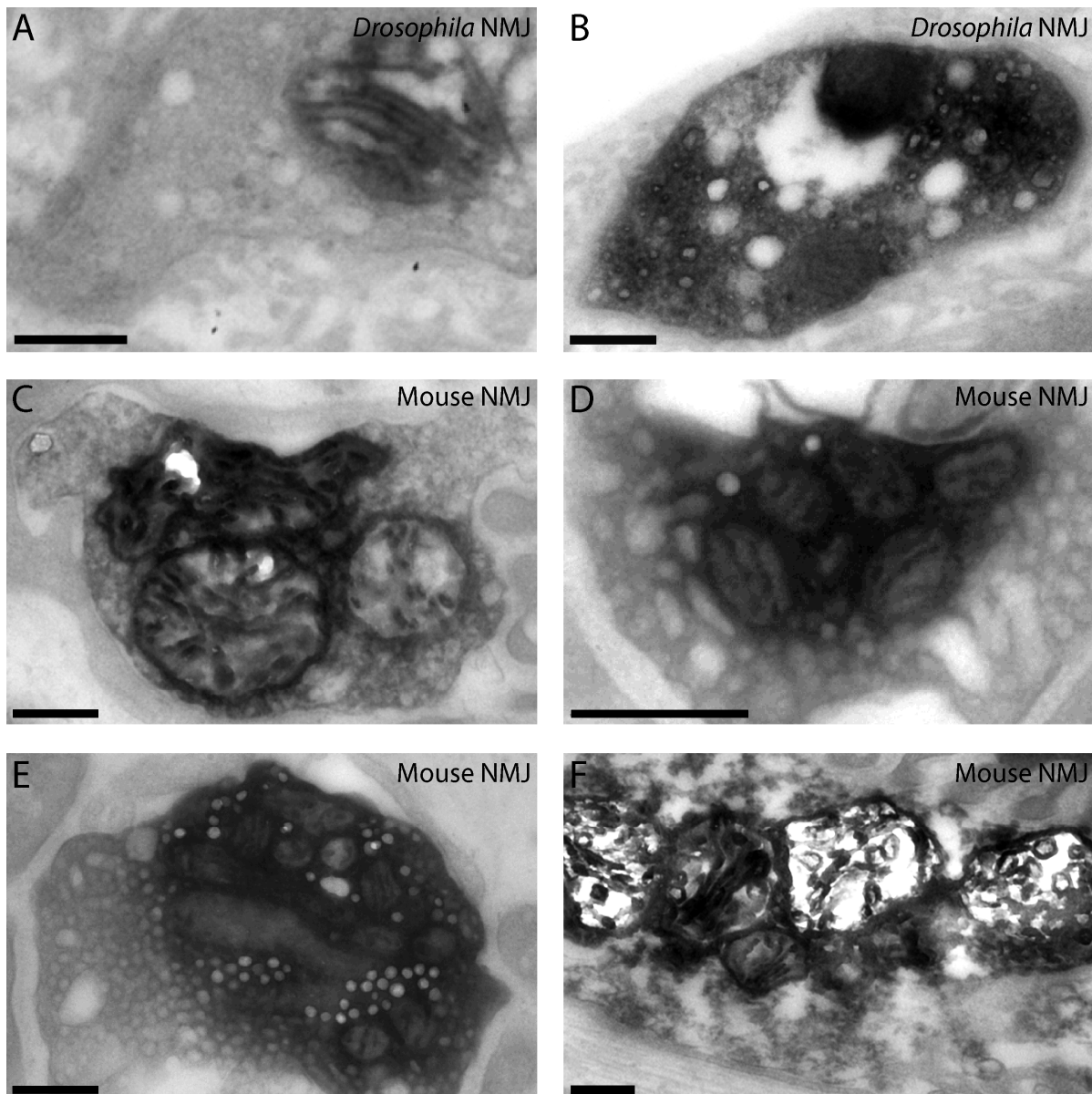
Figure 2.6: Photo-oxidation troubleshooting
(A) Under-oxidized nerve terminal from the *Drosophila* NMJ. (B) Over-oxidized nerve terminal from the *Drosophila* NMJ. Note dark cytosol. (C-F) Different stages of mitochondrial distortions due to accumulation of DAB precipitate, as observed in the mouse NMJ. Mitochondria first start to swell (C), and then burst, releasing the DAB content into the cytosol (D). This results in the "negative" image of dark cytosol and clear vesicles typical for over-oxidized samples (E) (compare also (B)). Finally, mitochondria having spilled most of their contents can even appear "empty", while the morphology of the entire synapse is extremely poor (F). Size bars are 300 nm for all images. Note that some of the images were taken by Katharina Kröhnert and Benjamin Wilhelm, European Neuroscience Institute, Göttingen.

2.5 Electrical Stimulation

Electrical stimulation was performed essentially as described in Denker et al., 2009: preparations were mounted in a chamber equipped with a platinum plate electrode (the electrodes were 8 mm apart; the device was custom-made in the workshop of the Max Planck Institute for Biophysical Chemistry, Göttingen, Germany). Generally, 100 mA shocks

were delivered at 30 Hz for 5 minutes (10 seconds for the FRAP experiment, Figure 3.17; 1 minute for testing the effect of ionomycin on exocytosis; Figure 3.29), using an A385 stimulus isolator and an A310 Accupulser™ stimulator (both World Precision Instruments).

For dye loading, stimulation was performed in the presence of 10 µM FM 1-43 in the respective (Ca^{2+}-containing) buffer. Upon stimulation, preparations were allowed to recover in presence of the dye for 5-10 minutes to allow for complete vesicle recycling. In case of locust and cricket, stimulation was performed by depolarization in high potassium saline (50 mM KCl, with 10 µM FM 1-43) for 5 minutes to avoid mounting these fragile preparations in the stimulation chamber. Typically, stimulation protocols were followed by brief washing in Ca^{2+}-free buffer (at 4°C), before fixation and photo-oxidation.

2.6 Predator/Prey Experiment

Locusts were injected with FM 1-43 solution as described above. Two hours later, the locusts were placed individually into a terrarium (29.5 × 32 × 19 cm) with three frogs. After the locust had been caught and ingested, the respective frog was immediately sacrificed, the locust was retrieved from its stomach, dissected in a mixture of frozen/ice-cold Ca^{2+}-free buffer, fixed, photo-oxidized and processed for EM as described above.

2.7 Testing Dye Availability in Body Fluids after Injection

Per cricket, 50-100 µl of 180 µM FM 1-43 in standard *Drosophila* buffer were injected, resulting in a final concentration of ~10 µM in the animals (see also Section 2.4.2). *Drosophila* buffer was employed because the body fluids collected afterwards were later used for labelling of *Drosophila* larvae *in vitro*. Two hours after injection, body fluids were retrieved from the injected crickets by compressing the skull. All fluids were pooled, followed by centrifugation at maximal speed (25,000× g) for 10 minutes in an Eppendorf 5417R cooled centrifuge. After centrifugation, the supernatant was collected and diluted 1:1 in standard *Drosophila* buffer. The diluted cricket body fluids were then used to stimulate four *Drosophila* third instar larvae (30 Hz, 5 minutes; same stimulation device as described above). This was followed by washing in standard *Drosophila* buffer for 5 minutes at 4°C and imaging on a Zeiss Axio Examiner.Z1 microscope equipped with a 63× 1.0 NA objective (Zeiss) and a 100 W mercury lamp (Osram), using a 470/40 nm excitation filter, a 495 nm beamsplitter and a 525/50 nm emission filter (Zeiss). Images were acquired using a QuantEM:512 SC camera (Photometrics, Tucson, USA) and Axiovision software (Zeiss). As a control, four additional *Drosophila* larvae were stimulated in a solution of 10 µM FM 1-43, diluted 1:1 in standard *Drosophila* buffer, as described for the body fluids. Images were

analyzed by calculating the average intensity of the nerve terminals (signal) in a manually chosen ROI and subtracting the background intensity, which was similarly measured in the neighboring muscle area.

2.8 Fluorescence Spectrophotometry

Crickets were injected and body fluids were retrieved two hours after injection as described above. Body fluids were then snap-frozen with liquid nitrogen and stored overnight at -20°C. The samples were then centrifuged at maximal speed (25,000× g) for 60 minutes in an Eppendorf 5417R cooled centrifuge and supernatants were collected. In addition, a dilution series of FM 1-43 in standard *Drosophila* buffer was prepared and diluted 1:1 in 20% CHAPS (Henkel et al., 1996a). Similarly, the cricket supernatants were also diluted 1:1 in 20% CHAPS. All solutions were measured in a Fluoromax-2 fluorescence spectrophotometer (Jobin Yvon, Horiba Scientific Instruments, North Edison, USA) at an excitation of 488 nm (2 nm bandwidth) and an emission of 538 nm (3 nm bandwidth), using quartz cuvettes (1.5 mm width). Whereas duplicate readings were obtained and averaged for the FM 1-43 dilution series, the small volume of the experimental samples allowed for only one reading per sample. Linear interpolation from the FM 1-43 dilution series was used to obtain the concentration of FM in the cricket fluid.

Similarly, *Drosophila* larvae were injected with FM dye (in HL3 buffer) as described above and were cut in segments of less than ~0.3 mm two hours after injection. Per tube, the material from three larvae was collected, diluted with 7 µl buffer and mixed 1:1 with 20% CHAPS. This was followed by sonification for 20 minutes in an ice-water bath (Bandelin Sonorex, Bandelin electronic, Berlin) and centrifugation for 15 minutes (same conditions as above). The resulting solution was measured using a Fluoromax-2 fluorescence spectrophotometer, as described above.

2.9 Comparing the Quantities of Released and Photo-oxidized Vesicles

To compare the number of vesicles which release neurotransmitter to the number of vesicles found labelled in EM after photo-oxidation, spontaneous synaptic release was electrophysiologically recorded in *Drosophila* larvae *in vitro*, while simultaneously labelling the recycling vesicles by FM 1-43 uptake. After ~10 minutes of recording, the preparations were fixed, photo-oxidized and processed for EM as described above. For each synapse, on average ~8% of the volume was reconstructed (the total volume of the synapses was estimated from fluorescence imaging, as described below). The number of recycled (labelled) vesicles found in the 3D reconstructions was scaled to the total volume of the

synapses and compared to the number of vesicles released (as recorded electrophysiologically).

Spontaneous release (miniature end-plate potentials; mEPPs) was measured from the ventral longitudinal muscles 6 and 7 of third instar *Drosophila* larvae. Electrophysiology recordings were performed as described in Jan and Jan, 1976 (see also Rizzoli and Betz, 2002). Before the measurements, the nerves connecting the muscles of interest to the upstream ventral ganglia were severed. A P-97 pipette puller (Sutter Instrument Co.) was used to prepare glass micropipettes (25-30 MΩ resistance) from glass tubes (thin wall, 3 inches, 1.5 mm diameter; World Precision Instruments). The filling solution employed was 3 M potassium acetate. An ELC-03 XS amplifier (npi electronic GmbH, Tamm, Germany) was used, which was digitized with an INT-20X interface (npi electronic) using the CellWorks software (version 6.0b1; npi electronic). The number of spontaneous events was determined manually using custom-written MATLAB routines (Rizzoli and Betz, 2002; Rizzoli and Betz, 2004). During the brief time frame (~1 minute) when the preparation was handled before fixation, no measurements could be obtained; for this time period, the same release rate was assumed as for the rest of the recorded trace.

While electrophysiological recordings were performed to monitor vesicle release, FM 1-43 (10 µM) was present in the buffer to detect vesicle recycling. A Zeiss Axio Examiner.Z1 microscope equipped with a 20× 1.0 NA objective (Zeiss) and a 100 W mercury lamp (Osram) was employed to visualize the fluorescence of the *Drosophila* subsynaptic reticulum on the unfixed preparation. A 470/40 nm excitation filter, a 495 nm beamsplitter and a 525/50 nm emission filter (Zeiss) were used, and images were acquired employing a QuantEM:512 SC camera (Photometrics, Tucson, USA) and Axiovision software (Zeiss). Z-stacks were performed (400 nm interval between the images) to allow for visualization of the complete terminal, and were subsequently deconvolved using AxioVision 4 deconvolution software (Zeiss). To determine the volume of the fluorescently labelled preparations, two different methods were employed: in the first approach, the outline of the preparations was drawn for each individual deconvolved stack section and the corresponding volume was calculated. In the second approach, all stack sections were summed and each bouton area in the resulting image was filled with ellipses. Both methods rendered nearly identical volume estimates (with the second method calculating the volume to 97 ± 8 % of the values obtained by the first method; n = 7 synaptic volume reconstructions).

To determine the number of recycled vesicles, preparations were then washed with ice-cold PBS, fixed, photo-oxidized and processed for EM, as described above. For each synapse, the quantity of labelled vesicles was determined for reconstructions of 1 to 4 NMJ segments. The volume of the surrounding subsynaptic reticulum was calculated from its outline, which was manually drawn in each EM section, and the corresponding section

thickness. The shrinking in volume produced by glutaraldehyde fixation and plastic-embedding (as determined before; Gaffield et al., 2006) was accounted for. The number of labelled vesicles found in the reconstructed NMJ segments was then scaled to the total volume of the synapse (as determined by fluorescence microscopy).

2.10 pHluorin Experiments

Drosophila larvae expressing pHluorin in motoneurons were obtained as described in Section 2.1. Images were acquired using a Zeiss Axioskop 2 FS plus microscope equipped with a 63x 1.0 NA objective (Zeiss), using the same filters as for the FM dye imaging (Section 2.4.4). Bafilomycin A1 was injected to obtain a final concentration of ~1 µM in the larvae (0.5 µM were used for the stimulation experiments). For data analysis, custom-written MATLAB routines were employed. Briefly, synaptic regions of interest were manually chosen, the average fluorescence within the terminals was determined and the average background fluorescence from regions in immediate proximity to the synapses was subtracted.

Note that the values presented in Figure 3.12 C were corrected for the fluorescence of the pHluorin surface pool (representing ~70% of the fluorescence of control synapses, 4 independent experiments). Surface fluorescence was determined by measuring synaptic fluorescence at pH 7.2 and subtracting from this value the fluorescence observed at pH 5.5 (i.e. when the surface pool is quenched) (see also Sankaranarayanan et al., 2000). In addition, to obtain a more accurate estimate of the recycling vesicle pool, the values were further corrected for the fluorescence of the quenched vesicles (derived from the increase of fluorescence obtained upon NH_4Cl treatment, which neutralizes the vesicular pH; a quenched vesicle is in my hands 10-fold less fluorescent than a de-quenched one; 4 independent experiments).

2.11 Vesicle Use in Paralyzed *Shibire* Larvae

S*hibire* or control larvae (with at least one wildtype copy of dynamin) were placed in standard *Drosophila* buffer in a water bath at 32°C and were monitored using a stereomicroscope (MZ6, Leica). In an analogous experiment, adult *shibire* or control flies were placed in a tube inside a waterbath at 32°C, allowing for monitoring of paralysis, which caused the animals to "drop" to the bottom of the tube. When paralysis had occurred (~15 seconds after the switch to the non-permissive temperature), the animals were either immediately dissected in ice-cold Ca^{2+}-free buffer or kept at the non-permissive temperature for further 10 minutes. After dissection, the animals were fixed and processed for EM, as described above.

Importantly, no loss of vesicles was observed for control larvae and flies after 10 minutes at the non-permissive temperature.

2.12 Fluorescence Recovery After Photobleaching (FRAP)

Synapses of *Drosophila* larvae were labelled by stimulation at 30 Hz for 10 seconds in the presence of FM 1-43. To allow for optimal imaging using oil immersion, the larvae were then mounted ventral side-down on glass coverslips. Imaging was performed using a Leica SP5 STED laser-scanning confocal microscope equipped with a 63x 1.4 NA oil-immersion objective (Leica), and excitation was provided by an Argon laser (488 nm line, at 20% of the current). Whereas 100% of the laser light transmission was used for bleaching, 10% was used for image acquisition. Images (512 x 512 pixels, 32 nm pixel width) were acquired every 5.24 seconds, and the laser dwell time was 20 µs/pixel. For bleaching, the laser was applied to a selected point of interest within the terminal for 150 ms. To be able to image different terminals at a similar dynamic range, detector gains needed to be adjusted; detector gain does not influence the recovery (Gaffield et al., 2006).

Self-written MATLAB routines were used for data analysis. Fluorescence was measured not only within the bleached spot, but also within the bouton containing the bleached spot, within the neighboring boutons, and within the background area outside boutons. The latter value was subtracted from all other values. The quantification of fluorescence in the neighboring boutons was used to correct for the photobleaching induced by image acquisition. The fluorescence within the bleached spot was expressed as percentage of the total loss during bleaching. As it was assumed that vesicles could only enter into the bleached spot from the bouton containing it, the fraction of the total fluorescence lost by this bouton during bleaching was determined and provided the maximal possible recovery (100%; see details also in Gaffield et al., 2006).

2.13 Immunostaining- Colocalization Experiment

2.13.1 Immunostaining

Mouse *levator auris longus* muscles were dissected in standard mouse saline. Muscles were fixed in 4% paraformaldehyde (PFA; in PBS) for 60 minutes and subsequently quenched with 100 mM NH_4Cl (in PBS) for 30 minutes. Muscles were then washed in PBS and permeabilized (3 × 15 minutes PBS + 0.5% Triton X100 + 2.5% BSA (AppliChem, Darmstadt, Germany)). Subsequently, muscles were incubated for 2 hours at room

temperature with the primary antibodies presented in Table 2.2 (typically 1:100 or 1:200 dilution in PBS + 0.5% Triton X100 + 2.5% BSA, from 1 mg/ml stocks in PBS).

Table 2.2: Primary antibodies used for immunostaining (colocalization and synaptic perturbation experiments) and Western Blotting

Antibody target	Antibody type	Source
Amphiphysin 1	rabbit polyclonal	Synaptic Systems, Göttingen, Germany
AP180	rabbit polyclonal	Synaptic Systems, Göttingen, Germany
Bassoon	mouse monoclonal	Stressgen, Assay Designs, Ann Arbor, USA
Caveolin	rabbit polyclonal	Synaptic Systems, Göttingen, Germany
Clathrin heavy chain	mouse monoclonal	BD Biosciences, San Jose, USA
Complexin 1/2	rabbit polyclonal	Synaptic Systems, Göttingen, Germany
Cortactin	mouse monoclonal	Synaptic Systems, Göttingen, Germany
CSP	rabbit polyclonal	Synaptic Systems, Göttingen, Germany
Dynamin 1/2/3	rabbit polyclonal	Synaptic Systems, Göttingen, Germany
Endophilin	rabbit polyclonal	Synaptic Systems, Göttingen, Germany
Hsc70	mouse monoclonal; B-6	Santa Cruz Biotechnology, Heidelberg, Germany
NSF	rabbit polyclonal	Synaptic Systems, Göttingen, Germany
Rab3	rabbit polyclonal	Synaptic Systems, Göttingen, Germany
Rabphilin	rabbit polyclonal; R44	Kindly provided by Prof. Reinhard Jahn, Max Planck Institute for Biophysical Chemistry, Göttingen, Germany
RIM2	rabbit polyclonal	Synaptic Systems, Göttingen, Germany
Synapsin 1/2	rabbit polyclonal	Synaptic Systems, Göttingen, Germany
Synaptobrevin	mouse monoclonal; 69.1	Synaptic Systems, Göttingen, Germany
Synaptojanin 1 C-terminus	rabbit polyclonal	Synaptic Systems, Göttingen, Germany
Synaptophysin	rabbit polyclonal; G96	Kindly provided by Prof. Reinhard Jahn
Synaptophysin 1	guinea pig polyclonal	Synaptic Systems, Göttingen, Germany
Synaptotagmin	mouse monoclonal; 41.1	Synaptic Systems, Göttingen, Germany
Tubulin	rabbit polyclonal	Synaptic Systems, Göttingen, Germany

Following incubation with primary antibodies, the muscles were washed with PBS + 0.5% Triton X100 + 2.5% BSA and incubated for 1 hour at room temperature with the following secondary antibodies (1:100 dilution in PBS + 0.5% Triton X100 + 2.5% BSA, from 0.5 mg/ml stocks in 50% glycerol): anti-guinea pig donkey polyclonal conjugated to Cy2 (Dianova, Hamburg, Germany), anti-rabbit goat polyclonal conjugated to Atto647N (the

antibody was obtained from Dianova, the dye was obtained from Atto-tec, Siegen, Germany; the dye was coupled to the antibody via its N-hydroxysuccinimidyl (NHS)-ester, as described in Willig et al., 2006), and anti-mouse goat polyclonal conjugated to Atto647N (Synaptic Systems). After incubation with secondary antibodies, the muscles were washed overnight in high-salt PBS + 2.5% BSA. Subsequently, the muscles were once more washed with high salt and normal PBS and then embedded in TDE (2,2'-thiodiethanol; Sigma) via a TDE dilution series (30, 50, 70, and 90% in ddH$_2$O, 10 minutes each, followed by 3× 100%, 10 minutes each).

2.13.2 Imaging of Colocalization Experiment- STED Microscopy

To be able to visualize the colocalization of synaptic vesicles with a plethora of synaptic proteins, we employed stimulated emission depletion (STED) microscopy. STED microscopy is one of several new imaging techniques which can overcome the diffraction barrier of light (Hell, 2007). The diffraction limit was formulated nearly 150 years ago and states that the minimal distance between two objects which can still be resolved depends both on the light's wavelength (to which it is directly proportional) and the angular distribution of the light (to which it is inversely proportional) (Abbe, 1873). This results in a diffraction limit of at least ~200 nm in practice when using conventional light microscopes. As depicted in Figure 2.7, STED microscopy breaks the diffraction barrier by overlaying a normal diffraction-limited excitation beam with a so-called depletion beam, which deexcites the fluorescent molecules by stimulated emission (Hell and Wichmann, 1994). This depletion beam is phase-modulated and generally toroidal/doughnut-shaped. Consequently, it only depletes the fluorophores in the periphery but not in the center of the excitation spot. This results in an effective fluorescent spot of subdiffraction size (with resolution as low as 30 nm; Donnert et al., 2006; or even less; Rittweger et al., 2009; note that the X-Y resolution for the setup used herein was in the range of ~70-80 nm).

Image acquisition of the mouse muscles was performed using a Leica TCS SP5 STED confocal microscope (Leica) equipped with a 100× 1.4 NA HCX PL APO CS oil objective (Leica). The green staining (synaptophysin as vesicle marker, Cy2) was excited using the 488 nm line of an Argon laser. When imaged in confocal mode, Atto647N (labelling the protein of interest) was excited using a Helium-Neon laser (633 nm wavelength). When imaged in STED mode, excitation of Atto647N was achieved using a pulsed diode laser (635 nm) and depletion was performed with a Spectra-Physics MaiTai tunable laser (Newport Spectra-Physics GmbH, Darmstadt, Germany) at 750 nm. An AOTF filter (Leica) was used to select appropriate emission intervals. Photomultiplier tubes were used for signal detection in confocal mode and an avalanche photodiode was employed in STED mode. Images were

generally first acquired in the green (synaptophysin) and Atto647N (protein of interest) channels in confocal mode, followed by subsequent acquisition of the corresponding STED image (Atto647N).

In addition to the one-color STED approach described above, two-color STED microscopy was also performed. This two-color STED setup was custom-built in the Department for NanoBiophotonics at the Max Planck Institute for Biophysical Chemistry and is described in Buckers et al., 2011. For two-color STED microscopy, a donkey anti-guinea pig polyclonal antibody labelled with Atto590 (for synaptophysin) and a goat anti-rabbit polyclonal antibody conjugated to Atto647N or a goat anti-mouse polyclonal antibody conjugated to Atto647N (for all other proteins) were used. Images were processed using deconvolution filtering for viewing purposes.
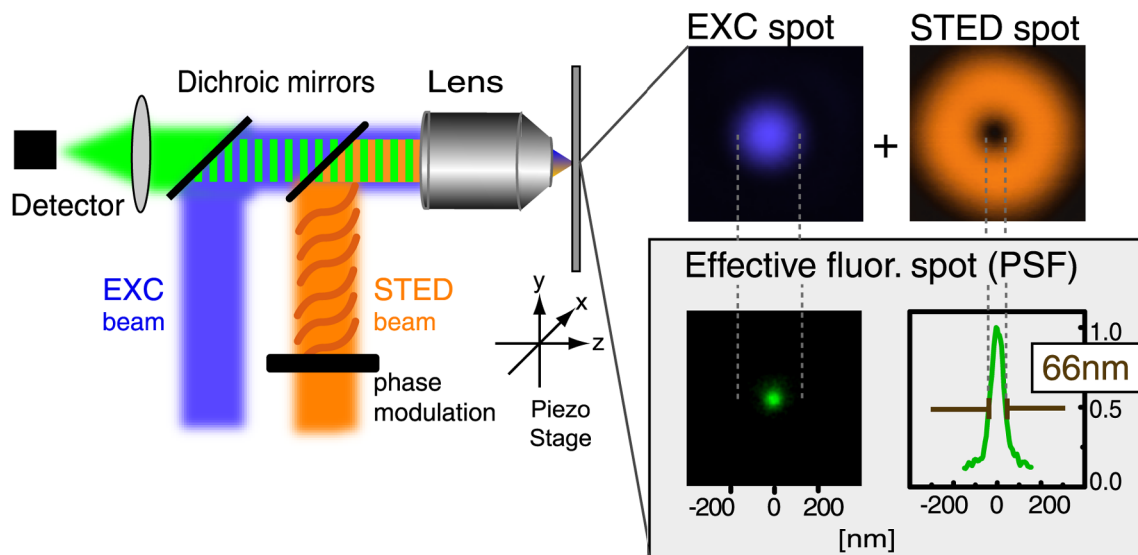
Figure 2.7: The principle of STED microscopy
The diffraction-limited excitation beam (blue) is overlaid with a phase-modulated depletion beam (orange), which is generally doughnut-shaped. This depletion beam de-excites the fluorophores in the periphery of the excitation spot. As the depletion beam has an intensity close to zero in the center, the central fluorophores remain excited. This procedure results in an effective fluorescent spot of subdiffraction size. Note that the full width half maximum (FWHM) of the profile of the resulting fluorescent spot is reduced in this example to 66 nm. PSF: point spread function. (From Willig et al., 2006)

2.13.3 Data Analysis of Colocalization Experiment

Data analysis was performed using custom-written MATLAB routines. Briefly, the STED and corresponding confocal images (Atto647N) were aligned, and ROIs (encompassing a synaptic area of several micrometers in length and at least ~2 µm in width) were manually selected in the images. For each ROI, Pearson's correlation coefficient was determined for the intensities of the green (synaptophysin) and STED (protein of interest) channels.

To better interpret the obtained correlation coefficients, a mathematical model was generated to investigate the influence of different protein affinities for the vesicles on the correlation coefficients. This *in silico* modelling approach is explained in detail in Figure 3.23. Briefly, the mouse 3D reconstruction shown in Figure 3.1 F was used to obtain the distribution of the synaptic volume and of the vesicles therein. A fluorescent label (convolved with a confocal "spot") was placed in each vesicle position and, in addition, virtual proteins were placed in the synaptic volume (these were convolved with a STED "spot"). These proteins were assigned different affinities for the vesicle cluster. To simulate the STED experiments described above, virtual sections through the preparation were performed (with the same Z-resolution as in the real STED experiments), and the correlation coefficient between the confocal (vesicle) and STED (protein) images was calculated.

2.14 Immunostaining- Protein Loss into the Axon upon Synaptic Perturbation

2.14.1 Synaptic Perturbation and Immunostaining

Several different approaches were used to disrupt the vesicle cluster or cause protein diffusion from the synapse into the axon.

In a first approach, mouse muscles were treated with black widow spider venom (BWSV) according to the protocol of Henkel and Betz (Henkel and Betz, 1995a). BWSV was obtained by homogenizing two venom glands from *Latrodectus mactans* in 1 ml Ca^{2+}-free mouse Ringer using a 1 ml teflon glass homogenizer (10 strokes at 700 rpm). The solution was cleared by centrifugation at 20,000× g in a cooled table-top centrifuge for 5 minutes (at 4°C), and the supernatant was kept on ice. From each mouse investigated, one *levator auris longus* muscle was dissected and was cut longitudinally in two halves, which were pinned in independent dishes – one to be used for BWSV incubation, and one to be used as control (note that the halves will be referred to as "muscles" below for simplicity). After dissection, either BWSV-containing mouse Ringer or normal mouse Ringer (containing Ca^{2+}) were added to the muscles and the dishes were incubated at 37°C for two hours. This was followed by a brief wash in Ca^{2+}-free mouse Ringer. The muscles were then fixed, quenched and permeabilized as described in Section 2.13.1. The muscles were then incubated for 2 hours at room temperature with the primary antibodies (refer to Table 2.2 for details on the antibodies employed; typically 1:100 dilution in PBS + 0.5% Triton X100 + 2.5% BSA, from 1 mg/ml stocks in PBS). After incubation with primary antibodies, the muscles were washed thoroughly in PBS + 0.5% Triton X100 + 2.5% BSA. This was followed by incubation for 1 hour at room temperature with the following secondary antibodies (1:100 in PBS + 0.5% Triton X100 + 2.5% BSA, from 0.5 mg/ml stocks in 50% glycerol): anti-guinea pig donkey

polyclonal coupled to Cy2, anti-rabbit goat polyclonal coupled to Cy3 and anti-mouse goat polyclonal coupled to Cy5 (all from Dianova). After incubation with secondary antibodies, the muscles were washed thoroughly first with high salt PBS + 2.5% BSA and subsequently with normal PBS. Finally, the muscles were mounted in Mowiol (prepared as described in Table 2.1) between coverslips (Menzel Gläser, Braunschweig, Germany) and Superfrost slides (Thermo Scientific, Waltham, USA).

The same immunostaining protocol was used for investigating the effects of α-latrotoxin (incubation for two hours at 37°C at a concentration of 2 µg/ml in Ca^{2+}-free mouse Ringer), electrical stimulation (30 Hz, 5 minutes) and ionomycin (which was applied for 60 minutes at room temperature at a concentration of 10 µM in normal mouse buffer; control muscles were treated with solvent alone (0.2% DMSO)). To investigate recovery of synaptic protein localization in the ionomycin experiments, samples were incubated with 5 mM EGTA in the presence of 10 µM ionomycin for 60 minutes at room temperature (with Ca^{2+} replaced by Mg^{2+}).

2.14.2 Imaging the Effects of Synaptic Perturbation

Images of mouse muscles treated with BWSV, α-latrotoxin or ionomycin or electrically stimulated were acquired using an Olympus IX71 microscope equipped with a 20× 0.5 NA objective (Olympus) and an F-View II CCD camera (Olympus, 1376 × 1032 pixels). Illumination was provided by a 100 W mercury lamp (Olympus). The 480/40 HQ excitation filter, the 505 LP Q beamsplitter and the 527/30 HQ emission filter were used for detection of green fluorescence (Cy2). For detection of orange fluorescence (Cy3), the 545/30 HQ excitation filter, the 570 LP Q beamsplitter and the 610/75 HQ emission filter were employed. Finally, red fluorescence (Cy5) was detected using the 620/60 HQ excitation filter, the 660 LP Q beamsplitter and the 700/75 HQ emission filter (all filters were from Chroma, Rockingham, USA).

2.14.3 Data Analysis- Protein Loss into the Axon

Data analysis was performed in a semi-automated fashion using custom-written MATLAB routines. In the first step, lines were drawn along the synapse and onto the axon. Only synapses for which both the terminal and the axon were well focused were taken into account. For each analyzed synapse, the border between the synapse and axon was manually determined. For each channel, the respective intensity was calculated, subtracting the background (selected manually in a region adjacent to the synapse).

Note that on average, BWSV treatment resulted in an increase in terminal diameter by ~50% (n = 12 experiments, p<0.0001, t-test), corresponding to the exocytosis of ~600 vesicles per µm of nerve terminal (or about 50% of the vesicles present within one µm).

2.15 Biochemical Experiments

2.15.1 Composition of Highly Purified Synaptic Vesicles

To obtain highly purified synaptic vesicles from rat brain, a protocol employing sucrose density gradient centrifugation followed by size exclusion chromatography was employed, which ensures that 95% of the organelles obtained carry major synaptic vesicle proteins (Takamori et al., 2006; see also Nagy et al., 1976; Huttner et al., 1983; note that this purification was performed by Dr. Silvio Rizzoli at the Department of Neurobiology, Max Planck Institute for Biophysical Chemistry, Göttingen).

The composition of the synaptic vesicles as compared to brain homogenate was then determined by SDS-PAGE/Western Blotting, according to standard procedures. All buffers employed are presented in Table 2.1 (i.e. sample buffer, gel buffer, cathode and anode buffer for SDS-PAGE; transfer buffer, Blotto buffer, wash buffer and stripping buffer for Western Blotting).

The samples were run on Schägger gels, which were prepared according to the recipe presented in Table 2.3.

Table 2.3: Schägger gel recipe

	Stacking Gel (4×)	Separation Gel (4×)
Gel buffer	1.5 ml	6.7 ml
H_2O	3.7 ml	2.28 ml
50% Glycerol	--	4.24 ml
TEMED	8 µl	12 µl
10% APS	40 µl	100 µl
Acrylamide	800 µl	6.64 ml

Samples were diluted in sample buffer, incubated for 5-10 minutes at 95°C (together with the protein ladder), and 7 µg were loaded per lane.

Western Blotting was performed according to standard procedures. If not stated otherwise, all incubation and washing steps were performed at room temperature. Blots were washed thoroughly in Blotto buffer and incubated overnight at 4°C in a 1:2000-1:10000 dilution of primary antibody in Blotto buffer (refer to Table 2.2 for detailed information on the

antibodies employed). Subsequently, blots were again thoroughly washed in Blotto buffer and incubated for 60 minutes in a 1:4000 dilution of the following HRP (horseradish-peroxidase)-coupled secondary antibodies in Blotto buffer: anti-rabbit goat polyclonal; anti-mouse goat polyclonal (both Dianova). Blots were then thoroughly washed in wash buffer, shortly incubated with 1:1 luminol and oxidant reagent (Pierce, Thermo Fisher Scientific Inc., Rockford, USA) and imaged on a Fujifilm LAS-3000 device.

If desired, blots were stripped to allow for a second round of immunostaining: blots were incubated in stripping buffer at 50°C for 45 minutes in a waterbath. This was followed by thorough washing for 60 minutes in wash buffer and incubation for 30 to 60 minutes with Blotto buffer. The blots could subsequently be used for the next round of immunostaining, washing and imaging, as described above.

2.15.2 Vesicle Pelleting Experiments

For the vesicle pelleting experiments, crude synaptic vesicles (LS1 fraction) were used and subjected to incubation with rat brain cytosol, in the presence or absence of ATP, calcium and EGTA. Refer to Barysch et al., 2010, for further information on the use and storage conditions of the described reagents.

The LS1 fraction was obtained from rat brain as described in Rizzoli et al., 2006 (see also Huttner et al., 1983). Note that retrieval of the LS1 fraction was performed by Dr. Silvio Rizzoli at the Department of Neurobiology, Max Planck Institute for Biophysical Chemistry, Göttingen, and that all steps were generally performed at 4°C. Briefly, the hemispheres and cerebellum were retrieved from rat brain. Homogenization was performed with a glass teflon homogenizer at 900 rpm (10 strokes) in 12 ml sucrose buffer per brain (refer to Table 2.1 for buffer recipes). The homogenate was spun at 5000 rpm for 2 minutes, using a SS34 rotor from a Sorvall centrifuge, and the nuclear pellet was discarded. The supernatant was subjected to high speed centrifugation (same rotor, 11,000 rpm, for 12 minutes). The upper portion of the pellet, which consisted of myelin, synaptosomes, and mitochondria, was retrieved and resuspended in 2 ml sucrose buffer per brain.

The synaptosomes were purified by means of a Ficoll gradient (3 ml of 13% + 1 ml of 9% + 3 ml of 6% + ~3 ml of the resuspended pellet; see also Nicholls, 1978) and centrifugation for 35 minutes at 22,500 rpm (SW41 rotor, Beckman centrifuge), resulting in two bands (~70% purity for synaptosomes). The two bands were pooled, solubilized in 30-36 ml sodium buffer and centrifuged for 12 minutes at 11,000 rpm to remove any remnants of Ficoll (SS34 rotor). The resulting pellet was osmotically lysed by adding 9 volumes of ddH$_2$O and applying 20 strokes at 2000 rpm. Finally, the sample was centrifuged at 70,000 rpm for

20 minutes (Beckman TLA 100.3 rotor), the pellet was discarded and the supernatant of crude vesicles (LS1) was collected. Aliquots were stored at -80°C.

For the vesicle pelleting experiments, assays of 50 μl (for BCA measurements) or 100 μl (for immunoblotting) were prepared. The crude vesicles (35 μg per 100 μl assay) were incubated with a cocktail containing rat brain cytosol (1 mg/ml, prepared as described in Barysch et al., 2010), 45 mM potassium acetate, the DHM mix (to obtain a concentration of 1.35 mM magnesium acetate, 0.18 mM di-thio-threitol, 11.25 mM HEPES buffer, pH ~7.3, in the assay) and either an ATP source system (resulting in 26.7 mM creatine phosphate, 3.3 mM ATP and 13.4 μg creatine kinase, for a 100 μl assay) or an ATP-depletion system (to obtain 25 mM D-glucose and 15 units hexokinase in a 100 μl assay). 1 mM $CaCl_2$ or 5 mM EGTA were added for some experiments. Incubation was performed in a water bath under low agitation at 37°C for 30-45 minutes. The final volume was adjusted to 500 μl with ddH_2O, and samples were centrifuged at 4°C at 90,000 rpm in a Sorvall S120AT2 rotor for 30 minutes.

For BCA measurements, the pellets were taken up in 0.5% Triton X-100 in PBS and protein amounts were measured by adding 1 ml BCA reagent (Novagen) to 100 μl sample, incubating samples in a waterbath at 37°C for 30 minutes and measuring protein amounts with an Eppendorf BioPhotometer in 1.5 ml semi-micro disposable cuvettes (Plastibrand, Wertheim, Germany)

For immunoblotting, two pellets were combined and removed in 100 μl sample buffer. SDS-PAGE was performed as described in Section 2.15.1, with 10 μl of sample loaded per lane. Western Blotting was done exactly as explained in Section 2.15.1.

Custom-written MATLAB routines were employed to measure band density. Values were corrected for variations in vesicle membrane amounts in the pellets (obtained by immunoblotting for the vesicle transmembrane proteins synaptophysin, synaptobrevin and synaptotagmin).

2.16 Statistics

Unless otherwise noted, all values indicate mean ± standard error of the mean (SEM) and numbers (n) refer to the number of independent preparations. P values are derived from student t-tests.

3. Results

The majority of the results described herein have been published in Denker et al., 2011a; Denker et al., 2011b.

3.1 Limited Synaptic Vesicle Use *in Vivo*

3.1.1 Monitoring Vesicle Use *in Vivo* by FM Dye Injection and Photo-Oxidation

As described in Section 1.4, the major aim of this study was to determine the amount of vesicles used by a behaving animal. My first general approach was to inject the fluorescent styryl dye FM 1-43 into several different animal species, ranging from insects and worms over fish, frogs and chicken to mice. Injection was performed either into the body cavity or subcutaneously (as described in Section 2.4.2). Upon injection, the animals were allowed to move around freely for a defined amount of time (from ten minutes to four hours). During this time, vesicle recycling was monitored by dye uptake into recycling vesicles, as described in Section 2.4.1. After the specified time, the organs were dissected, fixed and photo-oxidized, which allowed the dye-labelled (i.e. actively recycling) vesicles to be distinguished in EM from vesicles which had not taken up the dye (i.e. had not been recycling) during the time from dye injection to dissection (refer to Section 2.4 for details on the photo-oxidation reaction; see also Henkel et al., 1996a; Denker et al., 2009; Opazo and Rizzoli, 2010). The general scheme of the injection and photo-oxidation approach is also depicted in Figure 2.1.

I first studied several NMJ preparations, due to their ease of use for both labelling and photo-oxidation. I focused on body motion muscles in *Drosophila* larvae (Figure 3.1 A) and the nematode worm *Caenorhabditis elegans* (Figure 3.1 B), leg motion muscles in locust (*Chorthippus biguttulus*, Figure 3.1 C), tail movement muscles in zebrafish (*Danio rerio*, Figure 3.1 D), the *cutaneous pectoris* chest muscle in frog (*Rana kl. esculenta*, Figure 3.1 E) and the ear-lifting muscle *levator auris longus* in mouse (*Mus musculus*, Figure 3.1 F). Note that all of the animals described herein survived the injection and behaved normally thereafter.

Surprisingly, for all NMJs investigated, the proportion of vesicles labelled *in vivo* during an observation period (i.e. the time from dye injection to dissection) of two hours was always in the range of only 1-4% (see also Figure 3.4). Note that this was also the case for the zebrafish tail muscle, a posture muscle which is continually used by the animal.
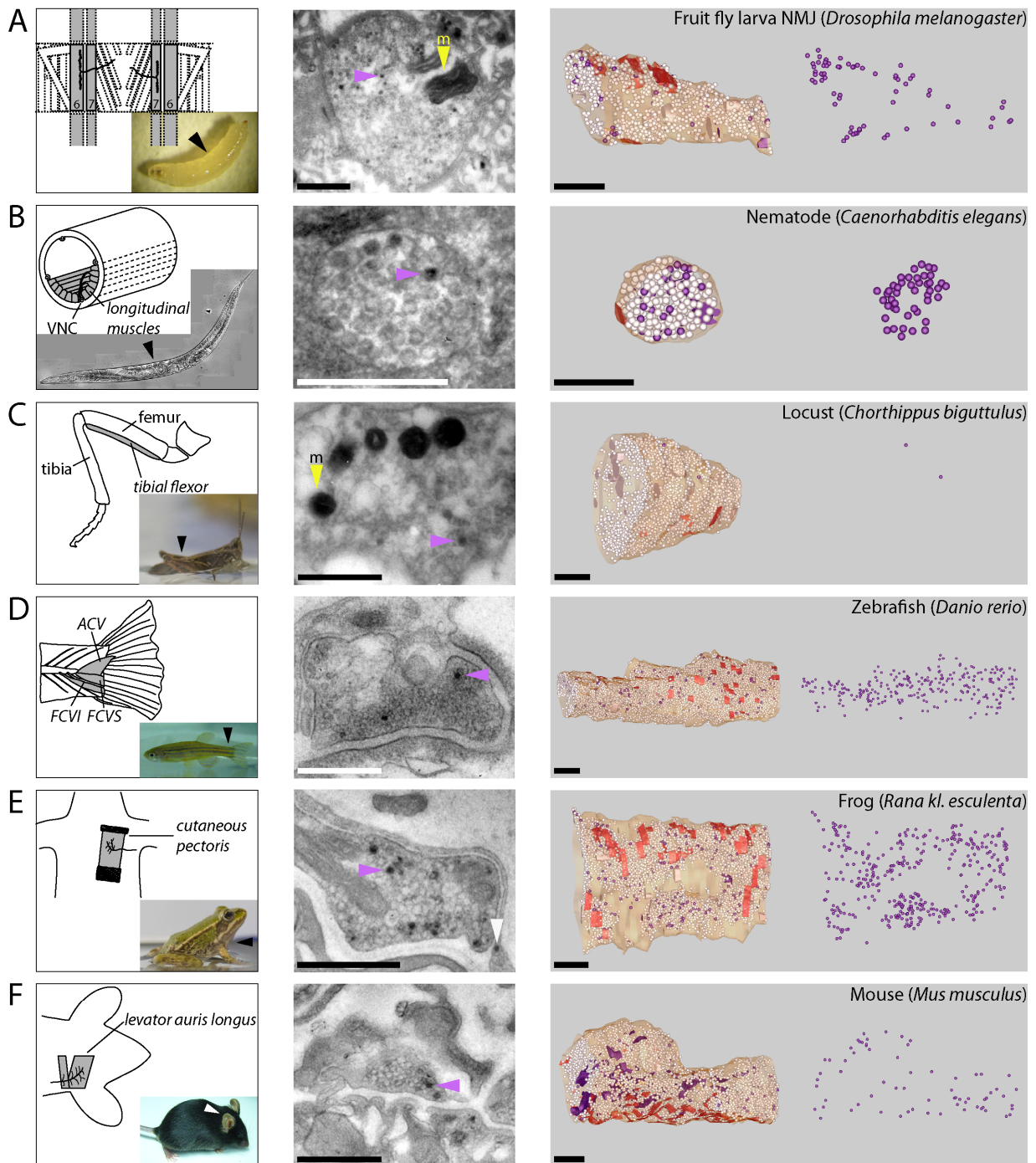
Figure 3.1: Only a few vesicles are recycled *in vivo* in NMJs
Vesicle recycling was monitored by FM dye injection and subsequent photo-oxidation (see main text) for NMJs from distantly related organisms. The left panel displays the muscles of interest (grey) and the approximate position within the animal (arrowheads). The middle panel depicts exemplary electron micrographs. The purple arrowheads indicate exemplary labelled vesicles. The yellow arrowheads indicate mitochondria, which are generally dark in photo-oxidized preparations (especially for insects; see also Section 2.4.8 and Grabenbauer et al., 2005). The white arrowhead in the frog panel (E) indicates a labelled vacuole in the Schwann cell (compare also Figure 3.11). The right panels indicate 3D reconstructions obtained from serial sections. The plasma membrane is shown in yellow, active zones are red, labelled vesicles and vacuoles are purple and unlabelled vesicles and vacuoles are shown in white. The right-most panel depicts only labelled vesicles. Note the low number of labelled vesicles for all preparations. Species names are indicated in the upper right corner. VNC= ventral nerve cord; ACV= *adductor caudalis ventralis*; FCVI= *flexor caudalis ventralis inferior*; FCVS= *flexor caudalis ventralis superior*. Size bars are 500 nm. Zebrafish scheme was drawn after Schneider and Sulner, 2006. (From Denker et al., 2011a)

69

To determine whether more vesicles are used in developing synapses, I tested leg muscles in chicken embryos (*Gallus gallus*; E11-12; stages 37-38; Hamburger and Hamilton, 1951) (Figure 3.2). Chicken embryos were injected with FM 1-43 through a small window in the egg shell and were placed for two hours in an incubator at about 38°C. Upon dissection, fixation and photo-oxidation, only 3-4% of the vesicles were found labelled (and had therefore undergone recycling; see also Figure 3.4). However, I often observed labelled vacuoles or invaginations from the plasma membrane (see electron micrograph and 3D reconstruction in Figure 3.2), which are indicative of the massive membrane trafficking associated with the formation of the NMJ at this point of development.
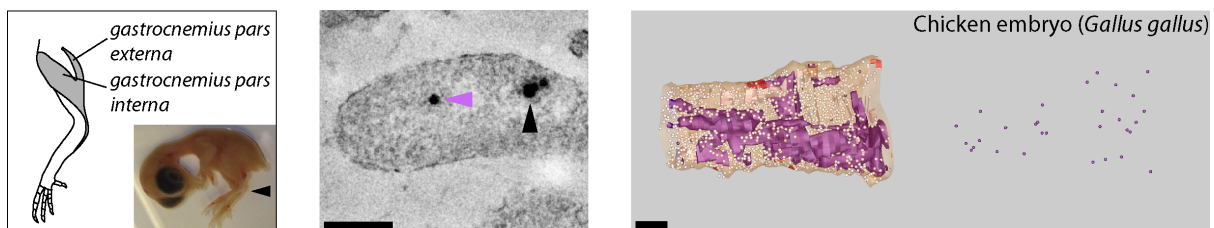
Figure 3.2: Vesicle use *in vivo* in a developing synapse
Chicken embryos (E11-E12) were injected through a small window cut in the egg shell and were then kept in an incubator at about 38°C for two hours. The *gastrocnemius pars externa* and *interna* muscles (shown in grey in the left panel, with the approximate position within the animal indicated by the black arrowhead) were then dissected, fixed and photo-oxidized. The middle panel shows a representative electron micrograph. The purple arrowhead indicates a labelled vesicle; the black arrowhead indicates a labelled vacuole. The right panels show a 3D reconstruction obtained from serial sections, as explained for Figure 3.1. The right-most panel shows only labelled vesicles. Note the low number of labelled vesicles and the huge labelled (purple) vacuole in the 3D reconstruction. Size bars are 500 nm. (From Denker et al., 2011a)

Finally, I investigated vesicle use in CNS synapses, which are generally much smaller than the huge NMJs (Rizzoli and Betz, 2005) and might therefore need to use a higher percentage of their vesicles to maintain their normal *in vivo* function. I studied synapses in the *Drosophila* larva ventral ganglia, a structure controlling body movement (Figure 3.3 A), where only ~1% of the vesicles were used (see Figure 3.4), and in the optic lobe of the cricket (*Gryllus assimilis*), a structure involved in vision (and therefore forming part of a sensory pathway, rather than a motor one), where 3-4% of the vesicles were used (again over two hours, Figure 3.3 B; Figure 3.4).
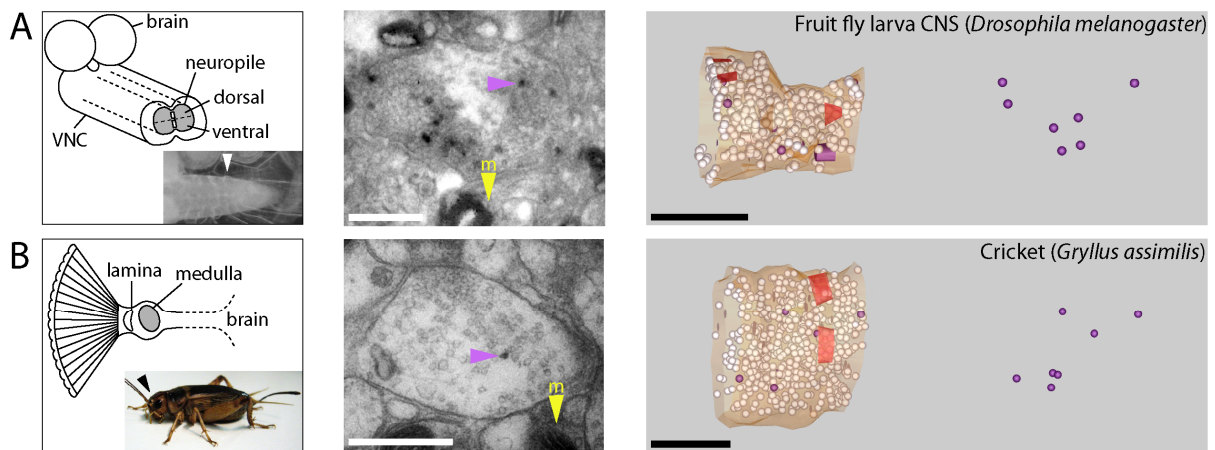
Figure 3.3: Vesicle use *in vivo* in insect CNS synapses
Vesicle use was tested by FM dye injection and photo-oxidation in the *Drosophila* larva ventral ganglia (A), a structure controlling body movement of the animal, and in synapses of the optic lobe of the cricket (B). Left panels indicate the organs of interest (grey) and the approximate position within the animal (arrowhead). The middle panels show exemplary electron micrographs, with the purple arrowheads indicating example labelled vesicles and the yellow arrowheads indicating mitochondria (see also Figure 3.1, Section 2.4.8 and Grabenbauer et al., 2005). Right panels show 3D reconstructions as explained for Figure 3.1, with the right-most panels showing only labelled vesicles. Note the low number of recycled (purple) vesicles. Species names are indicated in the upper right corner. VNC= ventral nerve cord. Size bars are 500 nm. (From Denker et al., 2011a)

Importantly, the low vesicle use in CNS synapses seemed to be as evolutionarily conserved as for the NMJs, as shown by our collaborators Christoph Körber, Heinz Horstmann and Professor Thomas Kuner from the University of Heidelberg, who studied vesicle use *in vivo* in the rat calyx of Held, a highly active synapse of the auditory pathway as described in Section 1.3.2. Anaesthetized rats were stereotaxically injected with horse-radish peroxidase (HRP) into the brain, were allowed to recover from anaesthesia and were then exposed to normal sound levels (i.e. radio music) for 30 minutes. During this time, HRP was taken up by recycling vesicles (see for instance Heuser and Reese, 1973), similar to the FM dye experiments described above. The rats were then transcardially perfused with 4% PFA and brain slices were retrieved. When these were incubated with DAB, the HRP catalyzed the transfer of two electrons from the DAB to hydrogen peroxide, again causing DAB polymerization and precipitation (as in the photo-oxidation experiments; see Denker et al., 2011a, for further details on the HRP injection experiment). Again, only ~3-4% of the vesicles were found to be labelled, in spite of the high activity levels of the calyx of Held. Similar results were obtained for an observation time of 60 minutes.

Therefore, as summarized in Figure 3.4, vesicle use *in vivo* was limited for all preparations investigated. This was true for all NMJs studied -involved in body or limb movement (in *Drosophila*, *C. elegans*, locust, frog, mouse) and body posture (zebrafish)-, as well as CNS synapses involved in motor (*Drosophila*) or sensory (cricket) pathways. Importantly, the investigated synapses were both cholinergic (vertebrate NMJs and *C. elegans*) and glutamatergic (insects), and included both mature and developing organs

(chicken). I therefore conclude that only a small subpopulation of vesicles is involved in release *in vivo* (as will be discussed later, these vesicles presumably recycle repeatedly).
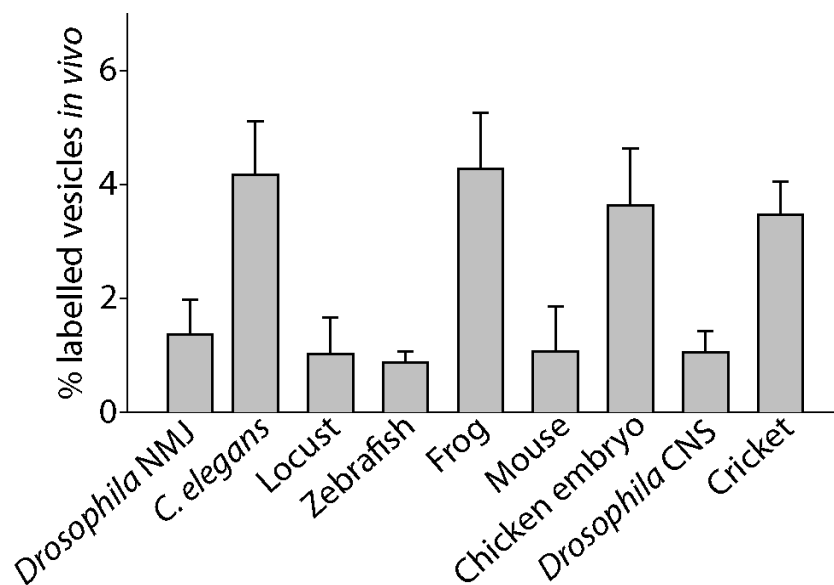
Figure 3.4: Quantification of vesicle use *in vivo* as determined by FM dye injection
Percentage of vesicles found labelled in EM at two hours after injection of the dye. Graph shows mean ± SEM from at least 4 independent preparations from each species. Representative electron micrographs are shown in Figure 3.1 for the NMJs (*Drosophila* to mouse), in Figure 3.2 for the chicken embryo and in Figure 3.3 for the CNS synapses (*Drosophila* and cricket). (From Denker et al., 2011a)

To investigate whether the fraction of actively recycling vesicles is stable over time, I performed two time course experiments, with observation times (between FM 1-43 injection and dissection) of 10 minutes, 2 hours and 4 hours (for *Drosophila* larvae) and 2 hours and 4 hours for frogs (Figure 3.5). Whereas the percentage of labelled vesicles remained quite stable from 10 minutes to 2 hours observation time (*Drosophila* NMJ), an increase from about 1% at 2 hours to about 5-6% at 4 hours after injection or from about 4% at 2 hours to about 8% at 4 hours was observed for the *Drosophila* larva and frog, respectively. Note however that the change for the frog NMJ was not statistically significant (p>0.08, t-test); in contrast to the change observed in *Drosophila* (p<0.0001, t-test). This observation indicates that there might be a very slow rate of intermixing between the actively recycling and inactive vesicle populations. Note that I tried to extend the observation time overnight for the *Drosophila* larvae, however, the majority of the larvae started to pupate during this time period. Whereas this rendered long-term experiments impossible, it also demonstrated that the presence of the FM dye did not cause serious harm to the animals (at least in terms of development).
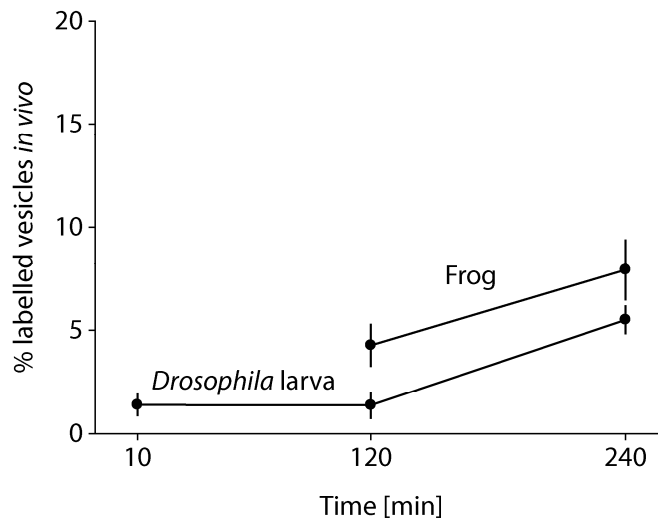
Figure 3.5: Changes in the percentage of labelled vesicles over time
The fraction of actively recycling vesicles (found labelled in EM) increased with longer time periods between injection and dissection for both the *Drosophila* larval and frog NMJ, indicating slow intermixing of actively recycling and inactive vesicles. Graph depicts means ± SEM from 3 to 6 independent preparations. (From Denker et al., 2011a)

The slow intermixing between the actively recycling and inactive vesicles could represent the exchange of a non-permanent molecular tag between the two populations. As described in the Introduction in Section 1.2.1, a molecular difference between the recycling and non-recycling or reserve pool vesicles has been proposed, especially due to the fact that the two vesicle populations were shown to be spatially intermixed *in vitro*. It was therefore of interest to investigate whether the labelled (actively recycling) and unlabelled vesicles displayed a differential localization in our *in vivo* experiments. For all preparations investigated, the distance of the labelled and unlabelled vesicles to the plasma membrane and nearest active zone was calculated from the 3D reconstructions depicted in Figures 3.1, 3.2 and 3.3. No difference between the spatial distributions of labelled and unlabelled vesicles was observed (Figure 3.6). This result is in agreement with previous *in vitro* observations and argues in favor of a molecular difference between the active and inactive vesicle populations.
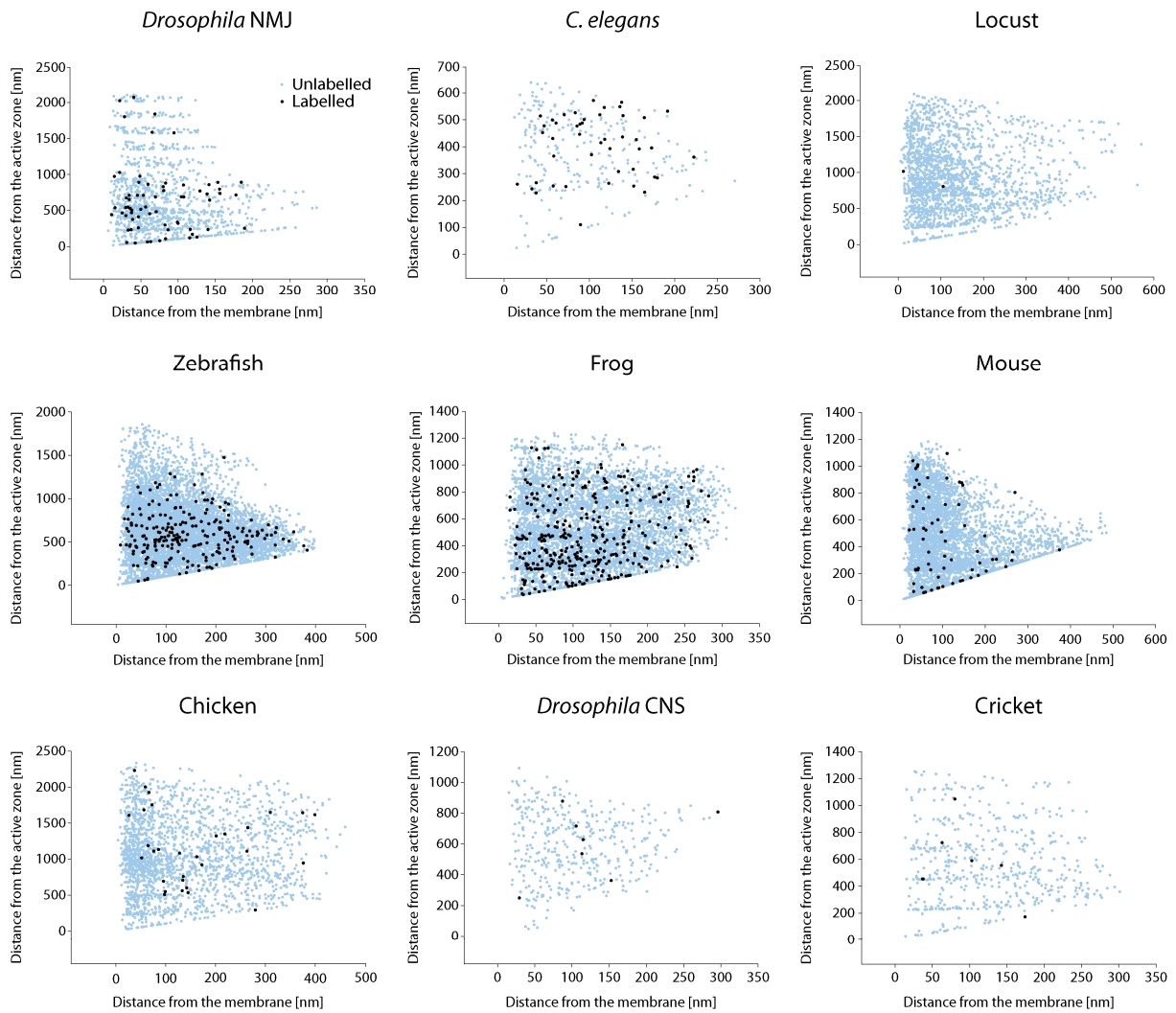
Figure 3.6: Labelled and unlabelled vesicles are intermixed for all preparations investigated
For all preparations investigated, positions of labelled (black) and unlabelled (cyan) vesicles with regard to the nearest active zone and to the plasma membrane are depicted. All distances were calculated from the respective 3D reconstructions shown in Figures 3.1, 3.2 and 3.3.

3.1.2 The Reliability of FM Dye Injection and Photo-Oxidation to Monitor Vesicle Use

Labelling of only a small proportion of vesicles could result from the technique malfunctioning, either due to vesicle fusion through pores which do not allow dye entry (possibly kiss-and-run; Stevens and Williams, 2000) or to imperfect photo-oxidation of dye-labelled vesicles. As a first control, I wanted to test whether more vesicles could in principle be labelled by dye uptake and photo-oxidation in the investigated preparations, or whether the small percentage of labelled vesicles found *in vivo* was somehow due to a saturation of the technique. Therefore, for all preparations studied, high frequency (30 Hz, 5 minutes) or high potassium stimulation in presence of FM 1-43 *in vitro* was also performed, followed by photo-oxidation. Importantly, many more vesicles could generally be labelled by this method

74

(Figure 3.7). This result not only demonstrates that the small number of labelled vesicles *in vivo* is not simply due to an upper limit imposed by the technique, but it also shows that more vesicles can be forced to undergo recycling *in vitro*, although they do not seem to do so *in vivo*.
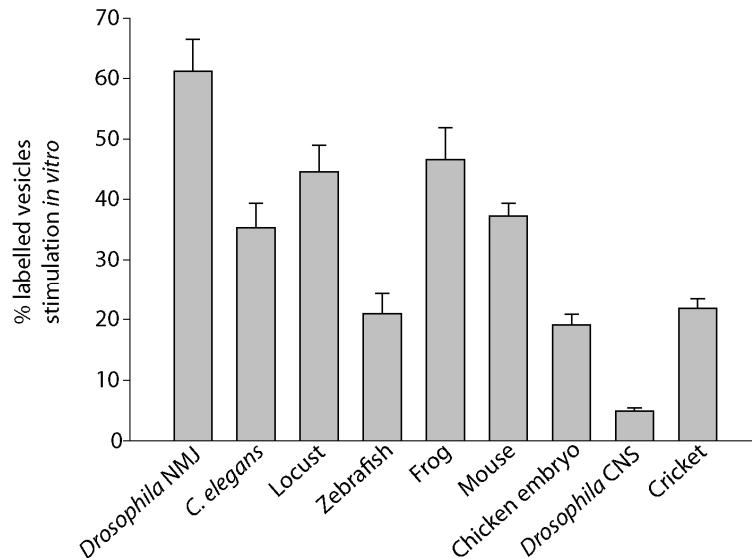
Figure 3.7: A substantial amount of vesicles is labelled by *in vitro* stimulation
Preparations were either labelled by high potassium application (50 mM potassium for 5 minutes; locust and cricket) or by high frequency stimulation (30 Hz, 5 minutes; all other preparations) in presence of FM 1-43 and were subsequently fixed and photo-oxidized. Bars show means ± SEM of at least 10 synapses from 2 to 9 independent preparations. (From Denker et al., 2011a)

But although dye uptake and the photo-oxidation technique *per se* might not be the limiting factors for vesicle labelling, several other problems of the method could be envisioned which might explain the low amount of vesicles labelled *in vivo*.

For instance, it is conceivable that the animals excrete the dye after a short period of time, with the dye therefore not present in the body fluids for the whole observation time. To test for this, body fluids were retrieved from injected crickets and *Drosophila* larvae two hours after injection and fluorescence was measured by spectrophotometry (Figure 3.8 A and B). Whereas the amount of dye injected was initially calculated to result in a concentration of 10 µM in the animal, on average about 8 µM were still present in the body fluids two hours after injection and no preparation displayed a concentration of less than 4.5 µM. Importantly, reliable photo-oxidation can be achieved using FM concentrations a low as 1.2 µM (Rizzoli and Betz, 2004). In addition, the FM dye was fully available for synaptic uptake, as the body fluids obtained from crickets two hours after injection could be used to label *Drosophila* preparations by *in vitro* stimulation; the fluorescence was comparable to that of preparations labelled with 10 µM FM 1-43 in conventional *Drosophila* buffer (Figure 3.8 C and D). I therefore conclude that the FM dye is still available for uptake even hours after injection.
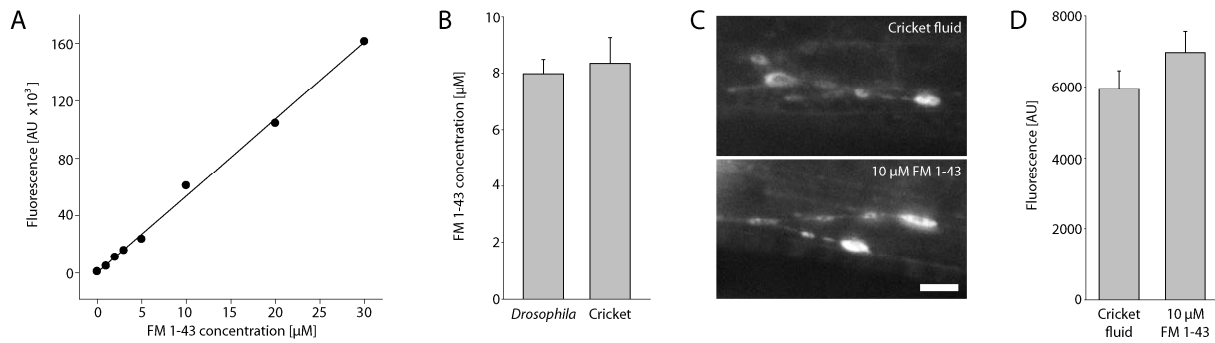
Figure 3.8: FM dye persists in the body fluids for hours after injection
To test for loss of FM dye from body fluids after injection (for instance by dye excretion), body fluids were retrieved from injected crickets and *Drosophila* larvae two hours after injection and dye availability was determined by fluorescence spectrophotometry (A,B) and imaging (C,D).
(A) Fluorescence of FM 1-43 dilutions in 10% CHAPS was measured employing a Fluoromax-2 fluorescence spectrophotometer. The line indicates a linear fit to the data. (B) Linear interpolation from graphs such as the one shown in panel (A) was used to determine the FM concentration in body fluids collected from animals 2 hours after injection. Bars show means ± SEM from 13 crickets and 3 measurements of *Drosophila* larvae (for each measurement, the fluids from 3 larvae were pooled, as the volume obtained from a single larva was too small to be measured). Note that the amount of dye injected was originally calculated to result in a final concentration of ~10 µM in the animal's body. Two hours after injection, dye concentration was ~8 µM on average and above 4.5 µM for all preparations measured. Note that optimal photo-oxidation was obtained in the past with FM 1-43 concentrations as low as 1.2 µM (Rizzoli and Betz, 2004). (C) Upper panel: Representative fluorescence image of *Drosophila* NMJ stimulated for 5 minutes at 30 Hz in body fluids obtained from crickets which had been injected with FM 1-43 2 hours earlier (body fluids were diluted 1:1 in normal *Drosophila* buffer). Lower panel: Representative fluorescence image of *Drosophila* NMJ stimulated for 5 minutes at 30 Hz in conventional *Drosophila* buffer (10 µM FM 1-43, diluted 1:1 in normal *Drosophila* buffer). Size bar is 10 µm. (D) Comparison of fluorescence intensity of *Drosophila* nerve terminals stimulated in body fluids obtained from injected crickets and in conventional *Drosophila* buffer. The fluorescence intensity is not significantly different (p>0.19, t-test). Graph shows means ± SEM from at least 29 different synapses from 4 larvae. (From Denker et al., 2011a)

Although the photo-oxidation technique can in principle label more than only a handful of vesicles (Figure 3.7) and the FM dye was present in the body fluids and available for uptake for hours after injection (Figure 3.8), it was desirable to test whether the number of vesicles released was indeed identical to the number of labelled vesicles observed in EM to further verify the reliability of the method employed. Therefore, spontaneous neurotransmitter release was measured electrophysiologically from *Drosophila* NMJs *in vitro* over ten minutes, while the recycling vesicles were simultaneously labelled with FM 1-43 (Figure 3.9 A and B), followed by photo-oxidation (Figure 3.9 C). The number of recycled (labelled) vesicles was obtained from 3D reconstructions and scaled to the total volume of the synapse, which was calculated from fluorescence images. This number correlated well with the number of vesicles released, as obtained from the cumulative release of the electrophysiological measurements (Figure 3.9 D), indicating that the efficiency of FM dye uptake and photo-oxidation are quite high.
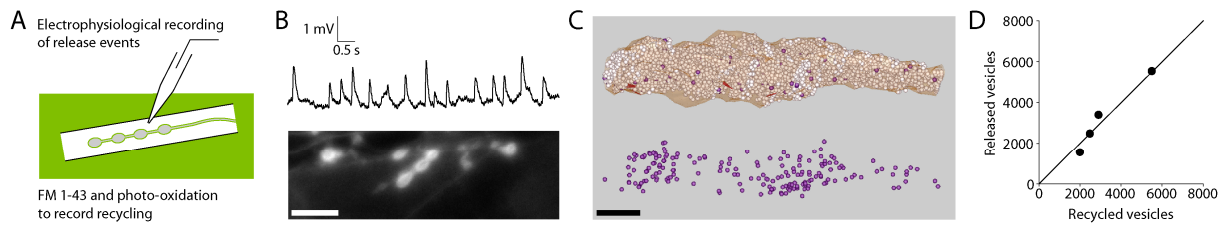
Figure 3.9: Correlation between the numbers of vesicles released and found labelled in EM
To test whether FM dye uptake and photo-oxidation provide a reliable measure of vesicle release, spontaneous release events were measured electrophysiologically from *Drosophila* larva NMJs *in vitro*. At the same time, vesicle recycling was monitored by FM dye photo-oxidation. Indeed, the number of vesicles released over a few minutes was found to be identical, within experimental error, to the number of vesicles recycled (detected as labelled in EM; see also Figure 3.19 C).
(A) Schematic of the experimental setup: comparison of the numbers of vesicles released and recycled. Spontaneous neurotransmitter release was recorded for about 10 minutes from the *Drosophila* larva NMJ. Simultaneously, vesicle recycling was recorded by FM dye uptake and subsequent photo-oxidation. (B) Top, representative spontaneous end-plate potential recordings. Each peak corresponds to an individual released vesicle. Bottom, projection of stack of fluorescence frames of a nerve terminal bathed in FM 1-43. The frames were taken at different heights and span the entire synaptic volume. Size bar is 20 µm. (C) 3D reconstruction obtained from serial sections of a nerve terminal labelled as described in (A,B). As for Figures 3.1-3.3, the plasma membrane is depicted in yellow, active zones are depicted in red, and labelled intraterminal membranes (vesicles and vacuoles) are shown in purple, whereas unlabelled vesicles and vacuoles are shown in white. The lower panel depicts only labelled vesicles. Size bar is 500 nm. (D) Comparison of the number of vesicles released/recycled. The number of labelled vesicles obtained from the 3D reconstructions was scaled to the total volume of the preparation (calculated from the fluorescence images as shown in the lower panel of (B)) and correlated to the number of released vesicles recorded electrophysiologically. For comparison, the identity line is shown. Note that these experiments were performed by Dr. Ioanna Bethani, European Neuroscience Institute, Göttingen. (From Denker et al., 2011a)

Although I was therefore confident that the dye persisted in the body fluids of the animals (Figure 3.8) and would allow to quantitatively monitor vesicle use when combined with photo-oxidation (Figure 3.9), it needed to be demonstrated that the dye was available for uptake at the level of the synapses after injection. This was tested by injecting FM 1-43 into the temperature-sensitive *Drosophila* dynamin mutant *shibire*. As described in Section 1.1.4 of the Introduction, vesicle reformation is blocked in this mutant at the non-permissive temperature (above 29°C), but vesicle release remains intact (Koenig et al., 1983). When a living *shibire* larva is placed at the non-permissive temperature, ~60% of the synaptic vesicles are depleted within 10 minutes (see Figure 3.14). The vesicles are subsequently retrieved when the temperature is lowered. In combination with FM dye injection, this treatment should therefore result in substantial vesicle labelling. The FM dye was injected in *shibire* larvae and allowed to distribute within the animal for 5 minutes. The animals were then placed for 5 minutes at non-permissive temperature, followed by a 10-minute recovery period at permissive temperature. Note that the larvae were kept at the non-permissive temperature for only 5 minutes, as compared to the 10-minute treatment mentioned above, as this ensured complete recovery of movement, whereas the longer treatment seemed to be more harmful. As 60% of the vesicles are lost within 10 minutes at the non-permissive temperature, the 5 minute-treatment should have released about 30% of the vesicles

(assuming a more or less constant release rate); this was indeed confirmed by photo-oxidation: on average ~37% of the vesicles were labelled (Figure 3.10 A and C). Importantly, when the preparations were fixed directly after exposure to the non-permissive temperature for 10 minutes (i.e. without a recovery period), few or no FM-labelled vesicles were observed (Figure 3.10 B and C). I therefore conclude that the dye is fully available for synaptic uptake after injection and that the labelled organelles observed in EM after photo-oxidation represent dynamin-dependent endocytic structures (i.e. vesicles or vacuoles).
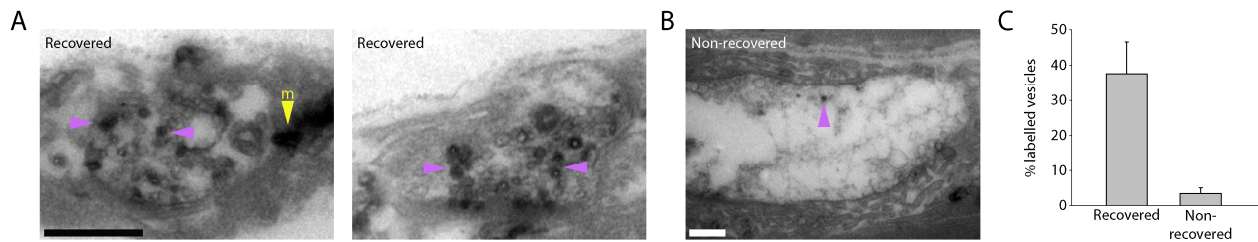
Figure 3.10: FM dye is fully available for uptake at the synapses after injection
To test whether the dye reaches the synapses after injection and is available for vesicular uptake, *shibire* larvae were injected and then placed at the non-permissive temperature, which resulted in vesicle release (due to the physiological activity of the living animal) without subsequent recycling (Koenig et al., 1983). Therefore, vesicles were depleted from the synapses. Returning to the permissive (room) temperature triggered retrieval of the fused vesicles from the plasma membrane (recovery) and should therefore result in a high number of labelled vesicles. Indeed, the percentage of labelled vesicles was found to be substantial in recovered animals (A), whereas non-recovered larvae displayed vesicle depletion and few or no labelled vesicles (B). Purple arrowheads indicate example labelled vesicles, yellow arrowhead indicates a dark mitochondrion (compare Figures 3.1 and 3.3).
(A) FM 1-43 was injected in *shibire* larvae. The dye was allowed to distribute within the animals for 5 minutes, before the larvae were placed for 5 minutes at non-permissive temperature, followed by 10 minutes of recovery at normal (room) temperature, which resulted in complete recovery of movement. Note that many labelled vesicles were observed after this treatment. Note also that keeping the larvae for longer times at the non-permissive temperature (i.e. for 10 minutes, as in (B) and in Figure 3.14) resulted in incomplete recovery of movement. Size bar is 300 nm. (B) FM 1-43 was injected in *shibire* larvae as above. After 5 minutes, the animals were placed for 10 minutes at the non-permissive temperature, followed by immediate dissection (without recovery). Note vesicle depletion and the low number of labelled vesicles. Size bar is 300 nm. (C) Quantification of the percentage of labelled vesicles in injected *shibire* larvae allowed to recover (as explained for (A), left) or dissected immediately after the non-permissive temperature treatment (as explained for (B), right). Note that the percentage of vesicles found labelled in recovered animals is in good agreement with the expected vesicle depletion during 5 minutes at the non-permissive temperature: as about 60% of the vesicles are released during 10 minutes above 29°C (Figure 3.14), 30% vesicle depletion is expected after 5 minutes (assuming a constant release rate). Indeed, about 37% of the vesicles were found labelled in the recovered *shibire* larvae. On the other hand, hardly any labelled vesicles were observed in non-recovered animals and the synapses were largely depleted of vesicles (after 10 minutes at the non-permissive temperature). Graph shows means ± SEM from 3 to 15 different synapses from 4 independent preparations. (From Denker et al., 2011a)

In view of the control experiments described above (Figures 3.7 to 3.10), the results obtained by FM dye injection *in vivo* and subsequent photo-oxidation should reliably reflect the amount of vesicles used by the living animal. However, the low percentage of labelled vesicles generally observed in our preparations required an independent criterion to choose the synapses to be analyzed: if no labelled vesicle was observed in a section, this section could only be analyzed if a) the FM dye indeed reached this specific synapse (although this

should likely be the case in view of the experiments presented in Figure 3.10) and if b) the photo-oxidation technique worked. Consequently, synaptic cross-sections containing no obviously labelled vesicle were only analyzed if the dye was found photo-oxidized in surrounding structures, either in the muscle itself or in the Schwann cells (for vertebrates). Uptake of dye and successful photo-oxidation was of special interest in the Schwann cells, as they are known to undergo substantial membrane trafficking (for instance in the frog; Betz et al., 1992b). In line with efficient photo-oxidation, about 60% of all endosome-like organelles in Schwann cells were found labelled in EM two hours after FM injection into living frogs (Figure 3.11).

Note that analyzing only cross-sections in which obvious FM dye photo-oxidation within surrounding cells was observed would probably rather cause an over- than an underestimation of the percentage of labelled vesicles (and thereby of vesicle use *in vivo*). The error introduced by judging vesicles as labelled or unlabelled by visual inspection also influences the result in the same direction (Figure 2.5). Therefore, and in view of the control experiments presented in this section, I conclude that indeed only a small pool of vesicles participates in the synaptic vesicle cycle *in vivo*.
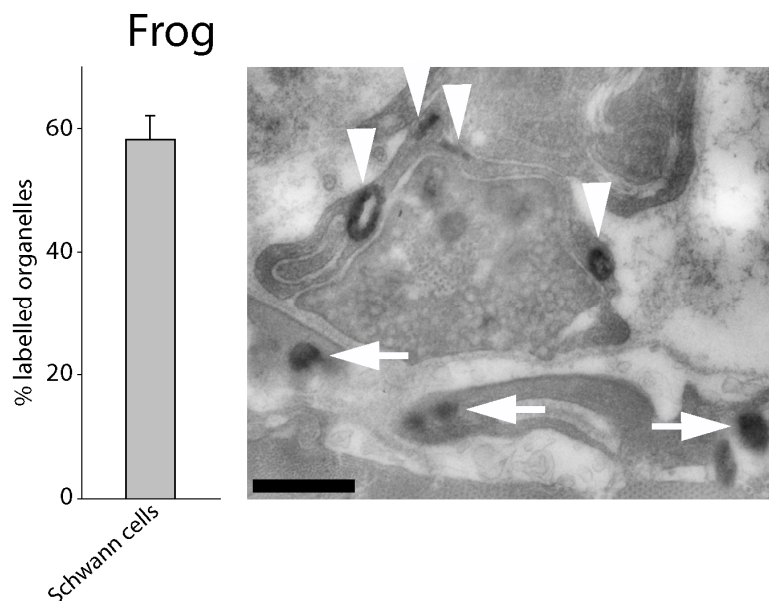
Figure 3.11: Successful FM 1-43 uptake and photo-oxidation in frog Schwann cells
Left panel: percentage of labelled endosome-like organelles (± SEM) in Schwann cells from frogs dissected at two hours after FM 1-43 injection (48 synapses, 3 independent preparations). Note that whereas the majority of the endosome-like organelles in these cells are labelled, only a low percentage of the synaptic vesicles are labelled (compare Figures 3.1 E and 3.4). Right panel: exemplary micrograph of frog nerve terminal surrounded by labelled cells. Arrows indicate labelled organelles within the muscle fiber. Arrowheads point to labelled organelles within the Schwann cell. Note that FM dye uptake in non-neuronal cells can be much higher than in the synapses. Size bar is 400 nm. (From Denker et al., 2011a)

3.1.3 Monitoring Vesicle Use *in Vivo* by pHluorin Imaging

In spite of the control experiments presented in the last section, one major caveat was still associated with the FM dye injection and photo-oxidation technique: it was still conceivable that vesicle recycling *in vivo* might rely mainly on the kiss-and-run mode and that the short-lived fusion pore would prevent efficient FM dye entry (Stevens and Williams, 2000; although this did not seem to be a major problem of the technique *in vitro*, where the numbers of vesicles released and detected as labelled in EM were virtually identical; see Figure 3.9). I therefore wanted to verify the low vesicle use *in vivo* by an independent technique, which did not depend on the uptake of FM 1-43 into recycling vesicles. To achieve this, I employed fluorescence imaging of *Drosophila* larvae expressing pHluorin (i.e. synaptobrevin fused at its intravesicular end to a pH-sensitive GFP moiety; Miesenböck et al., 1998; Reiff et al., 2005). As described in Section 1.1.4 and shown schematically in Figure 3.12 A, pHluorins serve as reporters for synaptic activity, as the GFP is quenched within the acidic lumen of the vesicles, but its fluorescence increases substantially (~10-fold in my hands) after vesicle fusion to the plasma membrane.
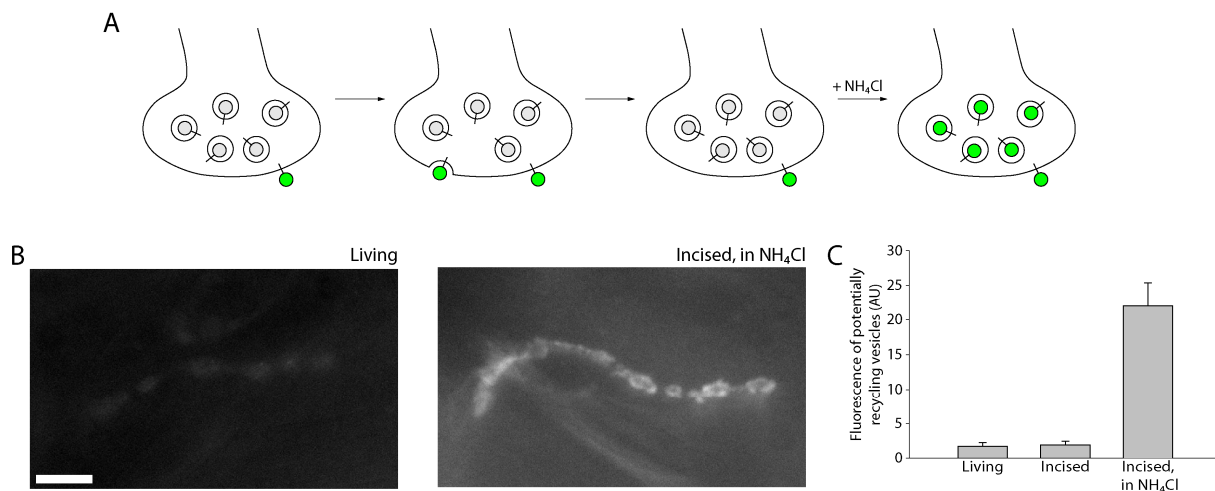
Figure 3.12: pHluorin imaging shows limited vesicle use at any one time *in vivo*
(A) Schematic of pHluorin function as a reporter of synaptic activity. The pH-sensitive GFP moiety is quenched within the acidic lumen of the vesicles (left panel). Upon fusion of a vesicle with the plasma membrane and exposure of the GFP to the more neutral extracellular medium, its fluorescence increases substantially (second panel from left). Subsequent endocytosis and reacidification of the vesicle result again in quenching of the GFP fluorescence (third panel). The fourth panel depicts the result of NH$_4$Cl application, which neutralizes the pH within the vesicles and therefore dequenches the total synaptic vesicle pool. (B) Living pHluorin *Drosophila* larvae were pinned ventral side up and the fluorescence of individual synapses was then imaged through the cuticula (left). To detect the fluorescence of the non-recycling (quenched) vesicles, the cuticula was incised laterally, the synapses were imaged, 100 mM NH$_4$Cl were added to the buffer, and the synapses were imaged again after 1 minute (right). Size bar is 10 µm. (C) Quantification of pHluorin fluorescence in the living larvae. Note that only a small amount of fluorescence is detectable in the living larvae, which does not increase upon incision. NH$_4$Cl treatment reveals a large pool of resting vesicles. Graph shows means ± SEM from 5 experiments. Note that the values were corrected for the fluorescence of the surface pool of pHluorin and for the fluorescence of the quenched vesicles, as described in Section 2.10. (From Denker et al., 2011a)

80

As a first experiment, I investigated vesicle activity in living *Drosophila* larvae expressing pHluorin in their motoneurons. The larvae were pinned in Sylgard dishes (with the ventral side with the muscles of interest up) and were imaged through the cuticula. As shown in the left panel of Figure 3.12 B, the synapses were barely distinguishable under this condition. However, the fluorescence increased strongly when the cuticula was laterally incised and NH_4Cl was added to the buffer, which neutralizes the vesicular pH (Roos and Boron, 1981), revealing a large resting (quenched) pool of vesicles (Figure 3.12 B and C). From these experiments, I conclude that only few vesicles are recycling *in vivo* at any one time, even in these pinned larvae which obviously experience a certain degree of stress.

However, this experiment does not give any evidence on how many vesicles are involved in neurotransmitter release and recycling during a longer period of time. To count the number of vesicles recycling over such a period, we turned to an inhibitor of vesicle acidification, bafilomycin (Fernandez-Alfonso and Ryan, 2004; Poskanzer and Davis, 2004). In presence of bafilomycin, vesicles retrieved from the plasma membrane cannot be re-acidified and therefore remain fluorescent. In a first experiment, the effects of bafilomycin on the NMJs of *Drosophila* pHluorin larvae were investigated. For this purpose, NMJs were stimulated for 5 minutes at 30 Hz in the presence of bafilomycin, which resulted in a substantial increase in synapse fluorescence, as observed in the past for cultured hippocampal nerve terminals (Fernandez-Alfonso and Ryan, 2004). The validity of both bafilomycin treatment in pHluorin larvae and FM photo-oxidation to monitor vesicle use was confirmed by the fact that both methods reported similar fractions of recycling vesicles (about 60%) under these stimulation conditions (Figure 3.13 A; compare also Figure 3.7).

With the functionality of bafilomycin thus confirmed for the pHluorin larvae used herein, the proton pump inhibitor was injected into living larvae (calculated to obtain a final concentration of ~ 1 µM within the animal). The injected larvae were then allowed to behave freely for 10 to 120 minutes. Due to the inhibition of vesicle reacidification, this treatment should provide a cumulative measurement of vesicle use *in vivo*, with every vesicle undergoing recycling at least once during the observation period remaining fluorescent and unused vesicles remaining dark (see schematic of experimental design in Figure 3.13 B). After this defined time period, the larvae were dissected and investigated by fluorescence microscopy.

Note that bafilomycin injection resulted in rapid loss of coordinated movement (within ~2 minutes after injection). However, although the larvae were largely paralyzed, some occasional movement was still observed. This was especially evident during the added stress of pinning and dissection, indicating that the upstream neurons could still fire and evoke occasional muscle responses. This is likely due to the fact that the low amount of bafilomycin we employed (albeit sufficient to block pHluorin quenching; Poskanzer and

Davis, 2004) penetrates more easily into the NMJs (which are bathed by the hemolymph into which bafilomycin is injected) than into the more compact structure of the brain.
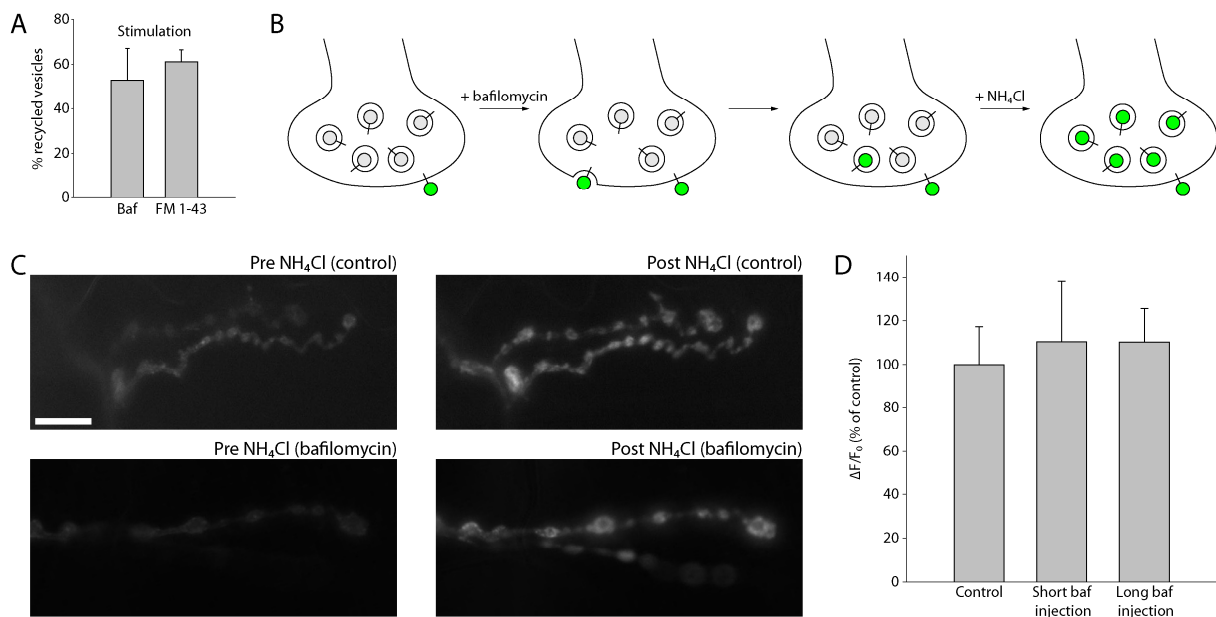
Figure 3.13: pHluorin imaging confirms the use of only few synaptic vesicles *in vivo*
(A) To test the function of bafilomycin in the *Drosophila* NMJ, dissected pHluorin larvae were stimulated at 30 Hz for 5 minutes in its presence. To obtain the percentage of vesicles recycling upon stimulation, the fluorescence increase obtained when stimulating in presence of bafilomycin was expressed as percentage of the fluorescence increase caused by application of NH_4Cl (which reveals the total vesicle pool; left bar; graph shows mean ± SEM from 5 independent experiments). The right bar indicates the percentage of vesicles labelled under identical stimulation conditions by FM dye photo-oxidation (reproduced from Figure 3.7). Note that the monitored percentage of recycled vesicles is very similar for the two approaches. (B) Schematic of the experimental design to determine the amount of vesicles recycling over a specified time period *in vivo*. To obtain a cumulative measure of vesicle recycling, bafilomycin was injected into pHluorin larvae. As described in the main text, bafilomycin inhibits vesicle re-acidification after retrieval, therefore rendering every vesicle undergoing exo- and endocytosis in presence of bafilomycin fluorescent (middle panels). After the observation period, the larvae were dissected and imaged. Subsequently, NH_4Cl was applied to reveal the pool of vesicles which had not undergone recycling. (C) Typical fluorescence images showing the effects of bafilomycin injection and NH_4Cl application. Synaptic fluorescence is not substantially brighter in larvae which had been injected with bafilomycin (11 minutes before dissection for the example depicted in the lower row) as compared to non-injected animals (upper row). Non-injected larvae displayed a substantial increase in synaptic fluorescence upon NH_4Cl application (see also Figure 3.12). However, a similar effect was also observed in bafilomycin-injected animals, indicative of a large unused (quenched) vesicle pool. Size bar is 10 μm. (D) Quantitative comparison of the size of the non-recycling vesicle pool in bafilomycin-injected versus control (uninjected) pHluorin larvae. The fractional fluorescence increase induced by NH_4Cl application is expressed as percentage of the fractional increase observed in control larvae. Graph shows means ± SEM from 4 to 9 independent experiments. Short baf injection: dissection at 10 to 30 minutes after bafilomycin injection. Long baf injection: dissection at 120 minutes after bafilomycin injection. (From Denker et al., 2011a)

Importantly, the fluorescence of the preparations was not significantly increased after bafilomycin injection as compared to non-injected larvae ($p > 0.1$, t-test, 4 to 9 experiments), supporting my previous result of limited vesicle use *in vivo*. To avoid problems associated with variations in fluorescence intensity among different preparations due to variable levels of pHluorin expression, the fractional fluorescence increase upon NH_4Cl application was also

determined. As described above, NH₄Cl application neutralizes the vesicular pH and therefore reports the size of the vesicle pool remaining inactive during bafilomycin treatment. Importantly, the size of the resting vesicle pool observed after bafilomycin injection was indistinguishable from that of control (non-injected) preparations (Figure 3.13 C and D).

Therefore, the results obtained for pHluorin *Drosophila* larvae are in good agreement with my photo-oxidation data, indicating that only a minor fraction of the vesicles are involved in recycling *in vivo*. As explained above, confirmation of the results obtained by uptake of FM 1-43 (or HRP, for the calyx of Held) and subsequent photo-oxidation by employing pHluorin imaging was of special importance in view of the ongoing debate on the incidence of kiss-and-run recycling (see Section 1.1.4). Whereas the small and transient fusion pore of this recycling mode might impede efficient FM dye uptake, this is not likely a major limitation for pHluorin experiments, which rely only on the release of protons. In summary, the good agreement of the pHluorin data with the results presented in Section 3.1.1 not only confirms once more the reliability of the photo-oxidation method to report vesicle use but also the surprisingly low number of recycling vesicles *in vivo*.

3.1.4 Limited Vesicle Use *in Vivo* is Supported by Electron Microscopy in *Shibire*

In spite of the good agreement of the photo-oxidation (Section 3.1.1) and pHluorin data (Section 3.1.3), it might still be argued that the injection procedure itself (of either FM dye or bafilomycin) might somehow affect synaptic physiology- in spite of the fact that all animals behaved normally after FM 1-43 injection (see Section 3.1.1). Therefore, I resorted to an assay to monitor the amount of vesicles used *in vivo* without the need for any injection of dye or drugs. I took advantage of the fact that recycled vesicles cannot be retrieved at the non-permissive temperature (above 29°C) in the *Drosophila* dynamin mutant *shibire*, as explained above (see also Figure 3.10).

These animals are known to paralyze at the non-permissive temperature, which is thought to be a result of synaptic vesicle depletion (Koenig et al., 1983). Interestingly, however, I observed paralysis of *shibire* larvae already at 10-15 seconds after exposure to the non-permissive temperature (see Figure 3.14 A). When larvae were dissected immediately after the onset of paralysis and then investigated by electron microscopy, the NMJs still contained numerous vesicles – indistinguishable from control *shibire* larvae kept at the permissive temperature (Figure 3.14 B and C). Therefore, the animals seemed to paralyze although a large reservoir of vesicles was still available. This result is compatible with the hypothesis of limited vesicle use *in vivo* as derived from the photo-oxidation and pHluorin data, since efficient neurotransmission in the living animal could be maintained by a small vesicle population, with the other vesicles releasing less efficiently or in a less

synchronous manner, thereby not reaching the action potential threshold of the muscle. In line with this argument, the remaining vesicles could eventually be triggered to be released when the larvae were maintained at the non-permissive temperature for 10 minutes (Figure 3.14 B and C), but the animals still remained paralyzed, possibly because these vesicles are not normally destined for release.
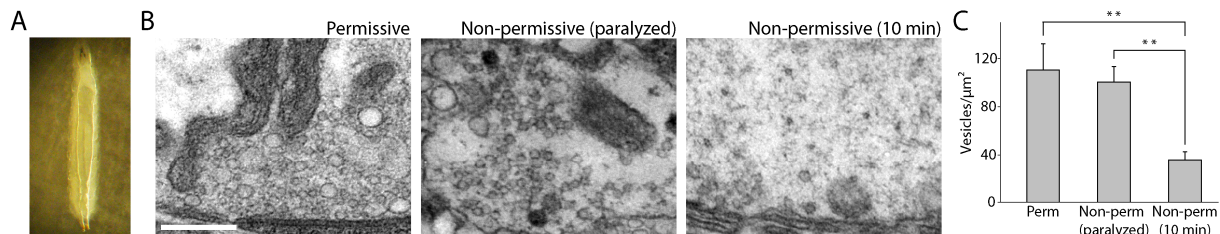
Figure 3.14: Electron microscopy of *Drosophila shibire* larvae
(A) *Shibire* larvae become paralyzed after ~15 seconds at non-permissive temperature (above 29°C). Note rigid posture of the paralyzed animals as compared to a control larva (Figure 3.1 A). (B) Exemplary electron micrographs of *shibire* larva NMJ at permissive temperature (room temperature, left), at non-permissive temperature for 15 seconds (immediately after the onset of paralysis, center) and after 10 minutes at non-permissive temperature (right). Size bar is 300 nm. Note the presence of numerous vesicles after 15 seconds as compared to the depleted nerve terminal after 10 minutes from the switch to non-permissive temperature. (C) Vesicle amounts in *shibire* larvae at non-permissive temperature are not significantly lower at onset of paralysis as compared to larvae at permissive temperature, but decrease significantly after 10 minutes at non-permissive temperature ($p < 0.001$, t-test). Graph shows means ± SEM from at least 11 synapses from 3 to 5 preparations. (From Denker et al., 2011a)

The substantial vesicle depletion during prolonged exposure to the non-permissive temperature might also serve as an argument against an alternative explanation for the early onset of paralysis without significant vesicle loss: it could be argued that the remaining vesicles cannot fuse as the release sites are blocked by fused vesicle components (Kawasaki et al., 2000; see also Neher, 2010, and Section 4). Note, however, that this second explanation can also not be excluded on the basis of my results. I therefore tentatively conclude that the observed paralysis in spite of the presence of a large vesicle reservoir is at least in agreement with the use of only a small vesicle pool to maintain synaptic transmission *in vivo*.

In addition, the vesicle depletion observed after 10 minutes at the non-permissive temperature also allows three further conclusions: first, the upstream neurons were obviously still firing at least to some degree in the paralyzed *shibire* larvae, as they still triggered vesicle release from the NMJ. Second, this observation further supports the results obtained when monitoring vesicle recycling under strong stimulation (Figure 3.7): obviously, the resting vesicles can be forced to be released by depletion of the active vesicle pool, although they do not participate in recycling *in vivo*. The molecular mechanism mediating this switch from a resting to an actively recycling vesicle is currently unknown. This issue will be further explored in Section 4.1.2. Third, and most importantly, the fact that substantial vesicle depletion is observed within 10 minutes under physiological activity in *shibire* larvae at the

non-permissive temperature indicates that synaptic activity *in vivo* is quite substantial. As I however also observed that only few vesicles participate in synaptic vesicle recycling in the same time period *in vivo* (by FM dye injection and photo-oxidation, Figure 3.1, and by bafilomycin injection in pHluorin larvae, Figure 3.13), these vesicles must be recycling repeatedly to sustain normal levels of activity.

Note that the observations presented above seemed to reflect a general phenotype of the *shibire* mutant, as they were not restricted to the larvae, but were also found in adult flies (Figure 3.15).
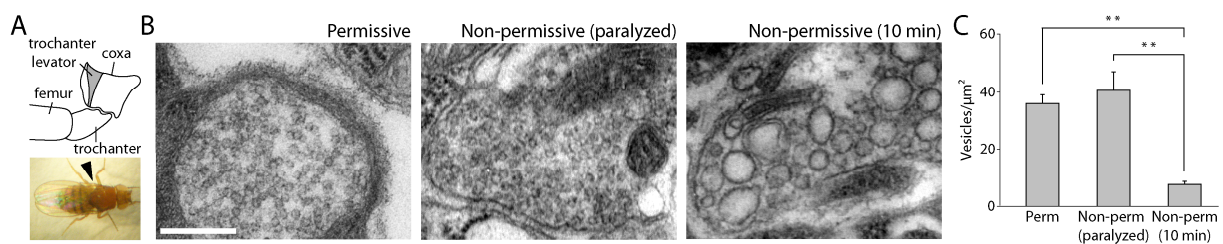
Figure 3.15: Electron microscopy of *Drosophila shibire* adults
(A) *Intracoxal trochanter levator* muscle (grey) and its position within the adult fly (arrowhead). (B) Representative nerve terminals of *shibire* adult NMJ at permissive temperature (room temperature, left), at non-permissive temperature for 15 seconds (immediately after the onset of paralysis, center) and at 10 minutes after the switch to non-permissive temperature (right). Size bar is 300 nm. Note the presence of abundant synaptic vesicles after 15 seconds as compared to the depleted nerve terminal after 10 minutes at non-permissive temperature. The large membranes observed after 10 minutes likely represent plasma membrane infoldings. (C) When paralysis sets in after ~15 seconds at the non-permissive temperature, no significant effects can be seen on the number of vesicles present in the synapse. However, after 10 minutes at the non-permissive temperature, synapses of *shibire* adults contain significantly fewer vesicles (p<0.001, t-test) than at permissive temperature. Graph shows means ± SEM from at least 62 different synapses from 3 independent preparations. (From Denker et al., 2011a)

3.1.5 Few Synaptic Vesicles Participate In Neurotransmission Even Under Stress

The limited vesicle use observed could be explained by the relatively low stress levels experienced by the experimental animals under laboratory settings: except for the injection and dissection, the animals were maintained in a low-stress environment with reduced stimuli as compared to the natural environment, where the animals face extreme life situations associated with high stress levels. It was therefore conceivable that such a situation associated with higher *in vivo* activity would trigger the release and use of more vesicles. Therefore, I reproduced a physiologically relevant setting in which an animal is exposed to maximal stress.

For this experiment, the *tibial flexor* muscle of the third pair of legs of the locust was investigated, as this is the main muscle involved in the animal's escape mechanism (jumping). Locusts were injected with FM 1-43 exactly as described above (see also Figure 3.1) and were placed individually in a terrarium occupied by several frogs two hours later.

Note that frogs represent natural predators of locusts. As depicted in Figure 3.16 A, the locusts tried to escape from the frogs, with frequent jumping. Generally, several failed capture attempts were observed (lasting approximately 5 to 10 minutes), before each locust was eventually caught and ingested (Figure 3.16 A, right panels). The respective frog was then immediately sacrificed, the locust was retrieved from its stomach and the *tibial flexor* muscle was photo-oxidized. Surprisingly, however, even this life-or-death situation only triggered the release of about 5% of all synaptic vesicles, increasing significantly from about 1% in the non-stressed animal (Figure 3.16 B-D). Note that the restricted movement within the terrarium might actually impose even higher stress levels on the locust than experienced in the natural habitat, where it would either be caught in the first capture attempt, or else would escape from its predator after the first jumps (as the distance covered by a locust jump is substantially beyond the jumping range of the frogs).
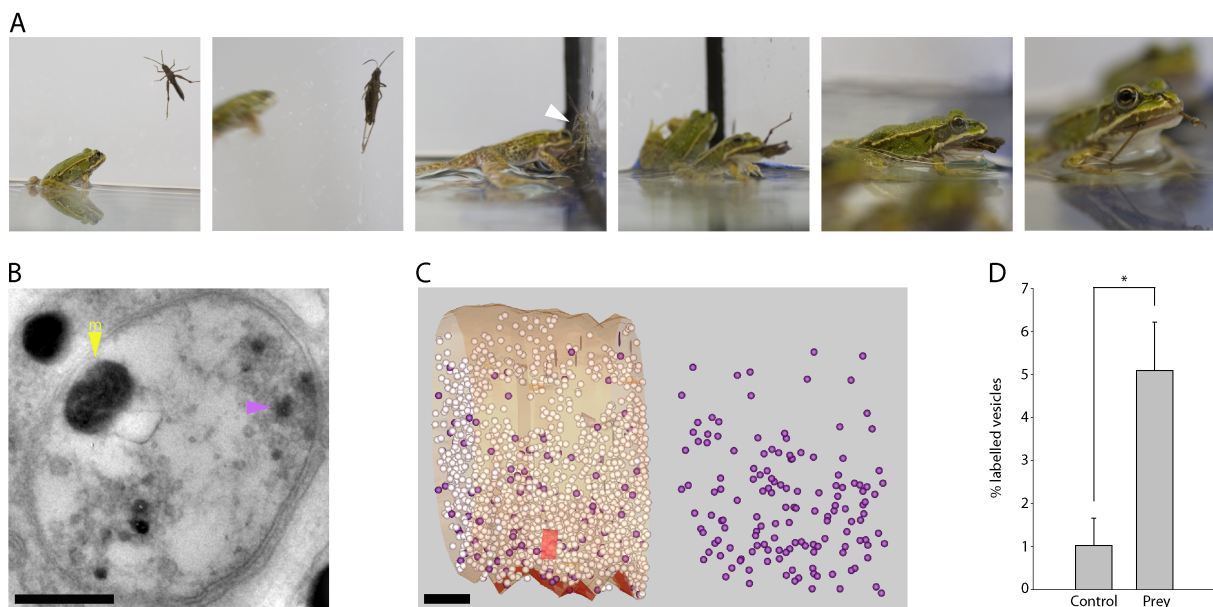
Figure 3.16: Limited vesicle use persists under extreme physiological stimulation
(A) Representative images of the hunted locust experiment. Two hours after FM 1-43 injection, a single locust was placed into a terrarium with several frogs. The locust actively tried to avoid the frogs. The arrowhead in the third panel points to the position of the locust immediately after it escaped from a capture attempt (note that the head of the frog is behind the locust). After about 5 to 10 minutes, each locust was caught and eventually ingested (right panels). The frog was dissected immediately afterwards, and the *tibial flexor* muscle of the third pair of legs of the locust was fixed and photo-oxidized. (B) Electron micrograph of hunted locust NMJ. The purple arrowhead indicates two closely apposed labelled vesicles; yellow arrowhead indicates a mitochondrion. Size bar is 400 nm. (C) 3D reconstruction of a nerve terminal from a hunted locust. As in Figures 3.1, 3.2, 3.3 and 3.9, the plasma membrane is depicted in yellow, active zones are red, and intraterminal membranes (vesicles and vacuoles) are purple if labelled and white if unlabelled. Size bar is 300 nm. (D) Percentage of labelled vesicles for locusts kept in a normal terrarium for 2 hours after injection (control) and for locusts which after 2 hours served as prey for the frogs (4 to 8 independent preparations, with typically 5 to 10 synapses per preparation; means ± SEM are shown; $p < 0.05$, t-test; note that the control value is the same as in Figure 3.4). (From Denker et al., 2011a)

I therefore conclude that the limited vesicle use observed *in vivo* in non-stressed animals persists even under extreme physiological stress, with 95% of the vesicles not undergoing recycling in the described life-or-death situation. It should however be emphasized that the number of labelled vesicles was significantly increased as compared to the control animals, indicating that the *tibial flexor* muscle was indeed more active when the locust was threatened by predators, as expected. Of course, this experiment does not exclude the possibility that there might be a natural situation triggering higher vesicle use. However, this seems rather unlikely, although not impossible, in view of the fact that the presented experiment resulted in the death of all locusts employed, rendering it difficult to envision a situation encompassing a stronger need for movement (and therefore vesicle recycling).

3.2 Synapsin as a Molecular Marker to Differentiate Between the Pools

From the experiments presented in Section 3.1, I conclude that the majority of synaptic vesicles do not fuse with the plasma membrane and release neurotransmitter *in vivo* (even under high stress levels; see Figure 3.16). This could for instance be due to a physical barrier which lowers the mobility of the inactive vesicle population as compared to the actively recycling vesicles. The immobilized inactive vesicles would therefore not be able to compete with the much more mobile active vesicles for release sites (see also Section 4.1.2). As described in Sections 1.1.3 and 4.3.1, one of the post promising candidates to fulfil such a role in the synapse is synapsin, which has been reported to bind to synaptic vesicles and/or to the cytoskeleton and might act as a "glue" keeping vesicles in a clustered (possibly inactive) form (see for instance Cesca et al., 2010). I therefore next tested the role of synapsin in vesicle clustering and mobility and its influence on vesicle use *in vivo*, using synapsin-null *Drosophila* larvae (Godenschwege et al., 2004).

Vesicle clustering was first investigated by electron microscopy in synapsin-null NMJs, however, no obvious morphological deficiencies could be observed (in agreement with the previous study, Godenschwege et al., 2004). However, the mobility of the synaptic vesicles was significantly increased as compared to wildtype animals, as shown by fluorescence recovery after photobleaching (FRAP) experiments: nerve terminals of the NMJs of third instar larvae were first labelled by *in vitro* stimulation at 30 Hz for 10 seconds in presence of FM 1-43. Subsequently, spots were bleached within the synaptic boutons and the recovery of fluorescence within the bleached areas was monitored over time (Figure 3.17 A). Fluorescence recovery is proportional to vesicle mobility (Gaffield et al., 2006). Recovery was significantly higher in the synapsin-null *Drosophila* larvae as compared to wildtype larvae (Figure 3.17 B). Note that the substantial recovery observed also in the wildtype is due

to 1) the fact that many of the labelled vesicles likely belong to the mobile and active vesicle population (since FM labelling was performed with a short stimulation pulse), and 2) recovery of the background fluorescence. The background fluorescence represents FM dye bound to the pre- and post-synaptic plasma membranes; it has been reported that such fluorescence recovers after bleaching to ~50% of the initial levels in similar experiments in the frog NMJ (Gaffield et al., 2006).
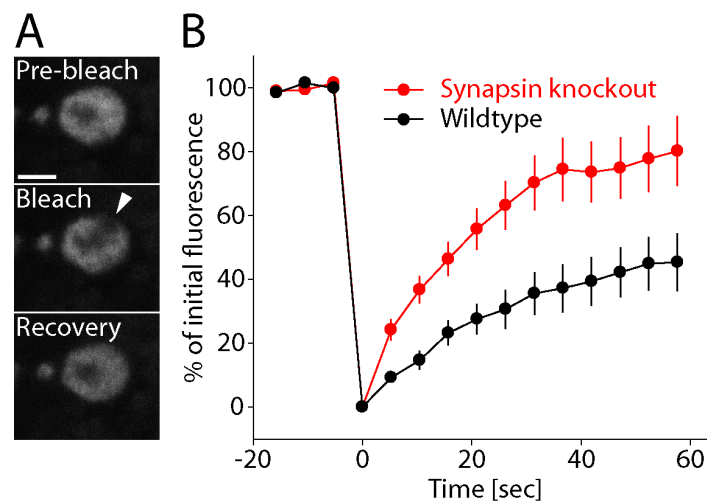
Figure 3.17: Vesicle mobility is increased in synapsin knockout *Drosophila* larvae
(A) Fluorescence recovery after photobleaching (FRAP) experiments were performed on wildtype and synapsin knockout *Drosophila* larva NMJs. After dissection, larvae were stimulated at 30 Hz for 10 seconds in presence of 10 µM FM 1-43. This relatively brief stimulus resulted in measurable FM dye loading for both wildtype and synapsin knockout larvae. The panels depict a typical FRAP experiment in a synapsin knockout bouton. A small region was bleached (middle panel, arrowhead); the fluorescence of the bleached area recovered largely within ~40 seconds (lower panel). Size bar is 2 µm. (B) Quantification of the recovery of fluorescence within the bleached area. Means ± SEM of 35 (wildtype) and 49 (synapsin knockout) recovery curves are depicted, from 6 independent experiments each. Note that the fluorescence recovery is significantly higher in the synapsin knockout as compared to the wildtype boutons (p<0.005, Kolmogorov-Smirnov test), indicating that vesicle mobility is higher in these preparations. (From Denker et al., 2011a)

To test whether the observed increase in vesicle mobility (i.e. the decrease in the vesicles' ability to cross-link to each other) correlates with an increase in the number of actively recycling vesicles *in vivo*, synapsin-null larvae were injected with FM 1-43 and subsequently photo-oxidized as described in Section 3.1.1. Indeed, about a third of the vesicles were labelled at 2 to 4 hours after FM dye injection, indicating much higher vesicle use than in the wildtype (Figure 3.18). I therefore conclude that synapsin serves as a molecular marker for the resting vesicle population.

However, these results also clearly show that synapsin cannot be the only molecular player involved in inhibiting mobility and limiting release of the inactive vesicles, as a large pool of vesicles still did not participate in recycling in the synapsin-null larvae. This is not surprising in view of the fact that filaments cross-linking vesicles have been observed in synapsin knockout mice by electron tomography (Siksou et al., 2007). It should also be noted

that the soluble nature of synapsin implies a non-permanent vesicle tag, which might be exchanged between members of the two populations, allowing for intermixing of the pools. A slow intermixing (on the time scale of hours) is in agreement with the time courses obtained in the FM dye injection and photo-oxidation experiments (Figure 3.5).
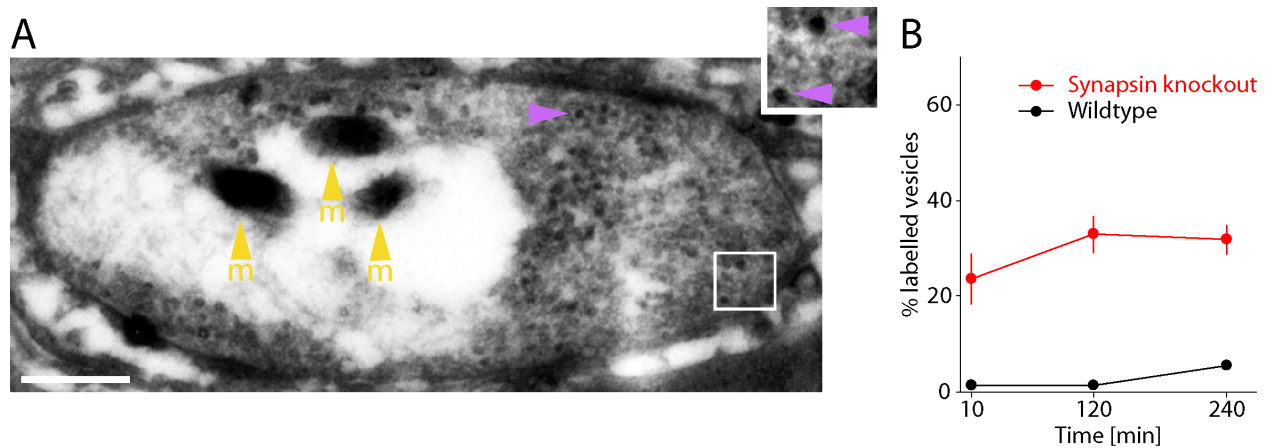
Figure 3.18: More vesicles undergo recycling *in vivo* in synapsin knockout *Drosophila* larvae
(A) Representative electron micrograph of a nerve terminal of a synapsin knockout larva at 4 hours after injection of FM 1-43. Purple arrowhead indicates a labelled vesicle; yellow arrowheads point to three mitochondria. The inset displays a zoom-up of the region indicated by the white square, showing two further labelled vesicles. Size bar is 400 nm. Note that vesicle density/vesicle numbers were not significantly different from wildtype (as reported before; Godenschwege et al., 2004). (B) Percentage of labelled vesicles in synapsin knockout as compared to wildtype larvae at different time points after injection. Note that the wildtype time course is reproduced from Figure 3.5 for comparison. Graph shows averages ± SEM from 3 to 6 independent preparations (typically ~10 synapses were used for each preparation). Note that the error bars are occasionally smaller than the symbol size. (From Denker et al., 2011a)

To investigate whether the increased amount of vesicle labelling observed in synapsin-null larvae was due to a higher rate of spontaneous vesicle fusion or to increased vesicle use during activity, the size of the recycling vesicle pool under spontaneous (action potential-independent) conditions was determined. To prevent action potential generation, wildtype or synapsin-null larvae were injected simultaneously with FM 1-43 and tetrodotoxin (TTX), which blocks sodium channels. The larvae paralyzed within a few seconds, and were fixed and photo-oxidized at 10 minutes after injection. In both wildtype and synapsin-null larvae, about 1-2% of the vesicles were labelled (Figure 3.19), indicating that synapsin removal specifically increased the amount of vesicles used during activity, and not spontaneous vesicle use.
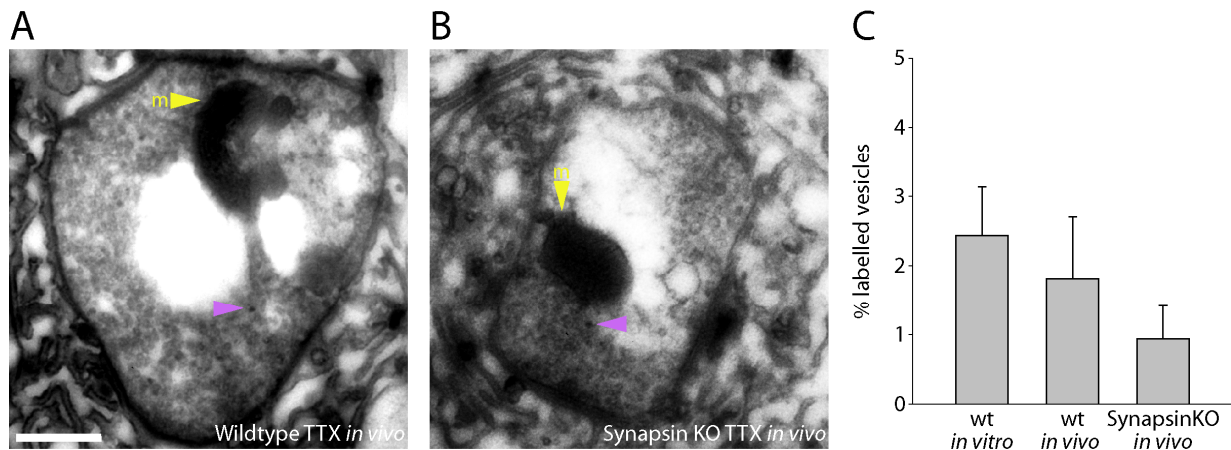
Figure 3.19: Spontaneous vesicle release in wildtype and synapsin knockout larvae
Spontaneous release *in vivo* was determined by fixation and photo-oxidation 10 minutes after simultaneous injection of FM 1-43 and tetrodotoxin (TTX). (A) Representative electron micrograph of wildtype nerve terminal. Yellow arrowheads indicate mitochondria; purple arrowheads point to exemplary labelled vesicles. Size bar applies to (A) and (B) and is 400 nm. (B) Representative electron micrograph of synapsin knockout terminal. (C) Quantification of spontaneous vesicle recycling. The wildtype *in vitro* data are derived from the experiment depicted in Figure 3.9 and are added for comparison. Graph shows means ± SEM from 4 independent preparations each.

3.3 The Resting Vesicles Serve As a Molecular Buffer

With limited vesicle use thus well established in evolutionarily distant organisms and at least one of the molecular players identified, one major unresolved question concerns the function of the non-recycling vesicles. As will be discussed in Section 4.4.1 of the Discussion, several hypotheses have been put forth for the function of the huge number of synaptic vesicles, including a role under high activity (although the hunted locust experiment presented in Section 3.1.5 would argue against this), in spontaneous release (Fredj and Burrone, 2009; albeit in this case these vesicles should also have been labelled), or in neurotransmitter storage (although neurotransmitter flux over the vesicle membrane seems to be rather limited; Van der Kloot, 2003). As these hypotheses can be rejected in view of the arguments presented above and in Section 4.4.1, an alternative model for the function of the non-recycling vesicles was developed:

To ensure the efficiency of the synaptic vesicle cycle, synapses need to contain a high concentration of the soluble accessory molecules involved (such as synapsins, Rab proteins, or the proteins involved in the formation of the clathrin coat; Sudhof, 2004; Shupliakov, 2009; note that these proteins shuttle between the cytosol and membranes). As it would not be economical for the neuron to fill the whole axon, which generally has a substantially larger volume than the synapse itself, with these proteins, the surplus vesicles might serve as a molecular buffer to retain them inside the nerve terminal, preventing their diffusion into the axonal space. At the same time, the buffer should be able to provide these

proteins upon demand to a recycling vesicle, i.e. its affinity for these proteins should not be higher than the protein affinity for a fused vesicle.

What are the basic requirements the vesicle cluster near the active zone needs to fulfil to serve as a molecular buffer? First, it has to enrich the aforementioned soluble proteins and second, it needs to release them in a regulated (probably stimulation-dependent) fashion. These requirements were tested in the experiments presented below.

3.3.1 Synaptic Vesicle Clusters Bind a Plethora of Soluble Proteins

It was first tested whether the vesicle cluster, which largely consists of vesicles which do not undergo vesicle recycling, as described in the previous sections, indeed binds and concentrates soluble accessory molecules. Note that these proteins, while critical for the progress of the vesicle cycle, generally do not function on the (resting) vesicle cluster and are therefore not necessarily expected to be bound to it, but could well be diffused into the synaptic space (except for synapsin, which functions by cross-linking vesicles to each other or to the cytoskeleton; Cesca et al., 2010). Colocalization of the accessory molecules with the vesicle cluster was investigated by fixation and immunostaining of mouse NMJs (*levator auris longus* muscle, depicted in Figure 3.1 F). Note that the mouse NMJ was chosen due to the availability of high-quality antibodies against many synaptic proteins. The immunostainings were monitored by stimulated emission depletion (STED) microscopy, a technique allowing for sub-diffraction resolution and introduced in Section 2.13.2 (see also Willig et al., 2006). This enabled the investigation of the synaptic distribution of the proteins of interest within the confined space of the NMJs.

As expected from the literature and my results, synapsin was found in the vesicle clusters (Figure 3.20; see also Section 1.1.3).
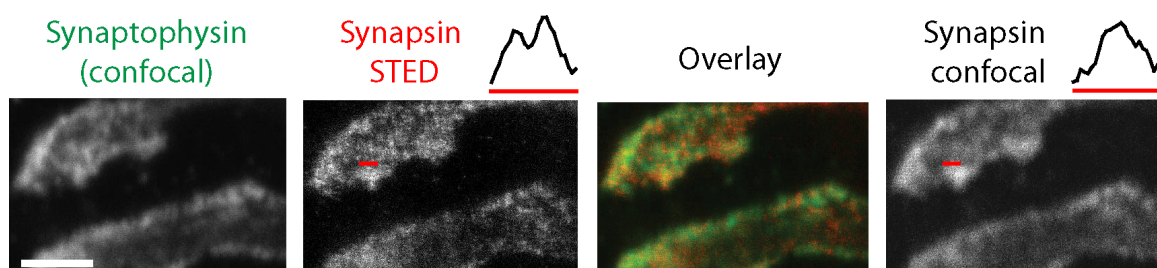
Figure 3.20: Colocalization of synaptic vesicle clusters and synapsin
The *levator auris longus* muscle from the mouse was dissected, fixed and immunostained for the protein of interest (here synapsin) and synaptophysin (an integral synaptic vesicle protein). While the vesicles were visualized in confocal mode (left panel), the protein of interest was visualized in STED mode (second panel from left; Willig et al., 2006). Note that the resolution achieved by STED microscopy was ~70-80 nm in the X-Y plane. The third panel depicts the overlay of the synaptophysin (confocal mode, green) and synapsin (STED mode, red) channels. The fourth panel is added for comparison and indicates that individual protein clusters are better resolved by STED than by confocal microscopy (see line scans). Size bar is 2 μm. Note that this experiment was performed by Katharina Kröhnert, European Neuroscience Institute, Göttingen. (From Denker et al., 2011b)

In agreement with the molecular buffer model, similar results were obtained for most of the other soluble synaptic proteins investigated (Figure 3.21), including proteins which function in exocytosis, either directly by modulating the SNARE fusion proteins (complexin, NSF) or indirectly (Rab3, rabphilin, CSP (cysteine string protein; Evans et al., 2003)), proteins which are involved in endocytosis (clathrin, dynamin, endophilin, synaptojanin, amphiphysin, AP180, Hsc70), or proteins associated with the active zone (Rim2).
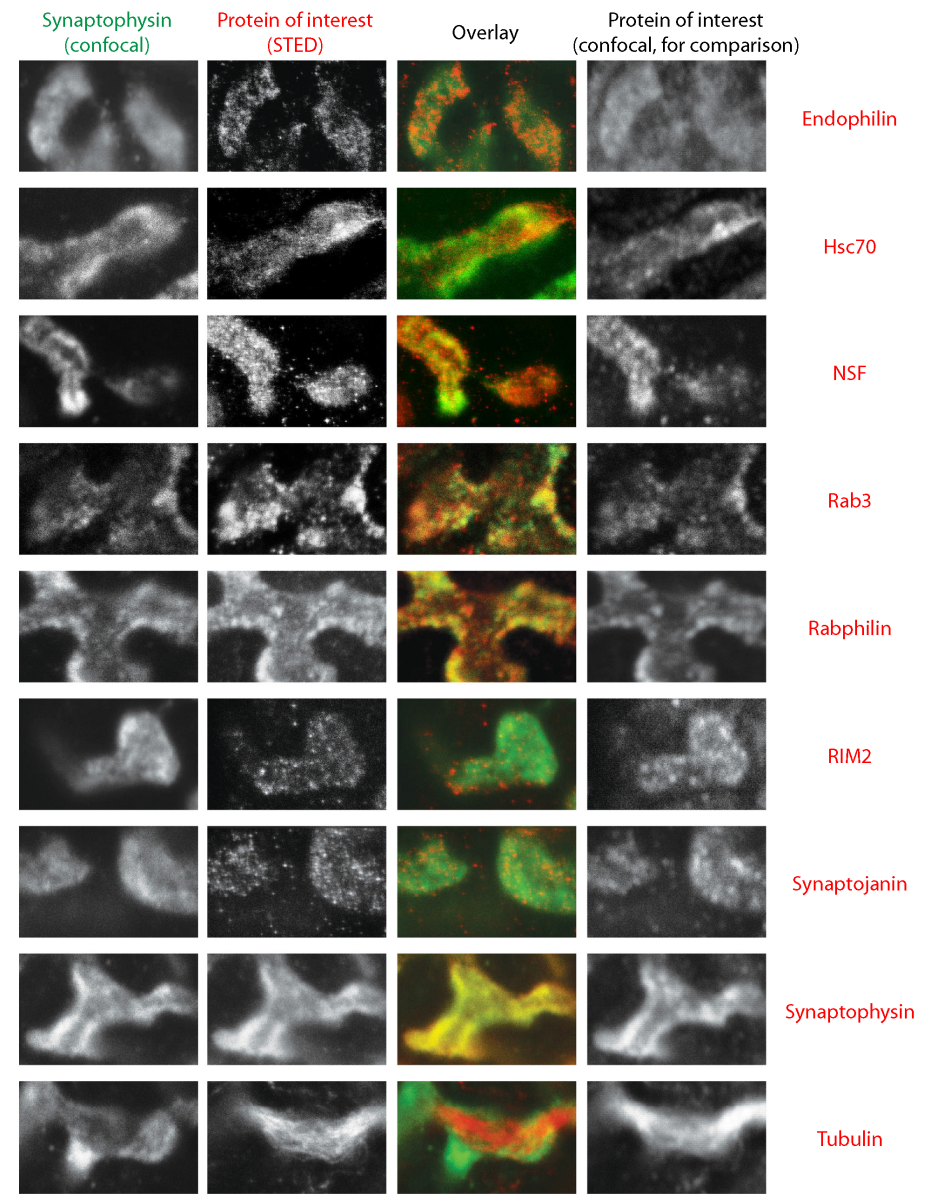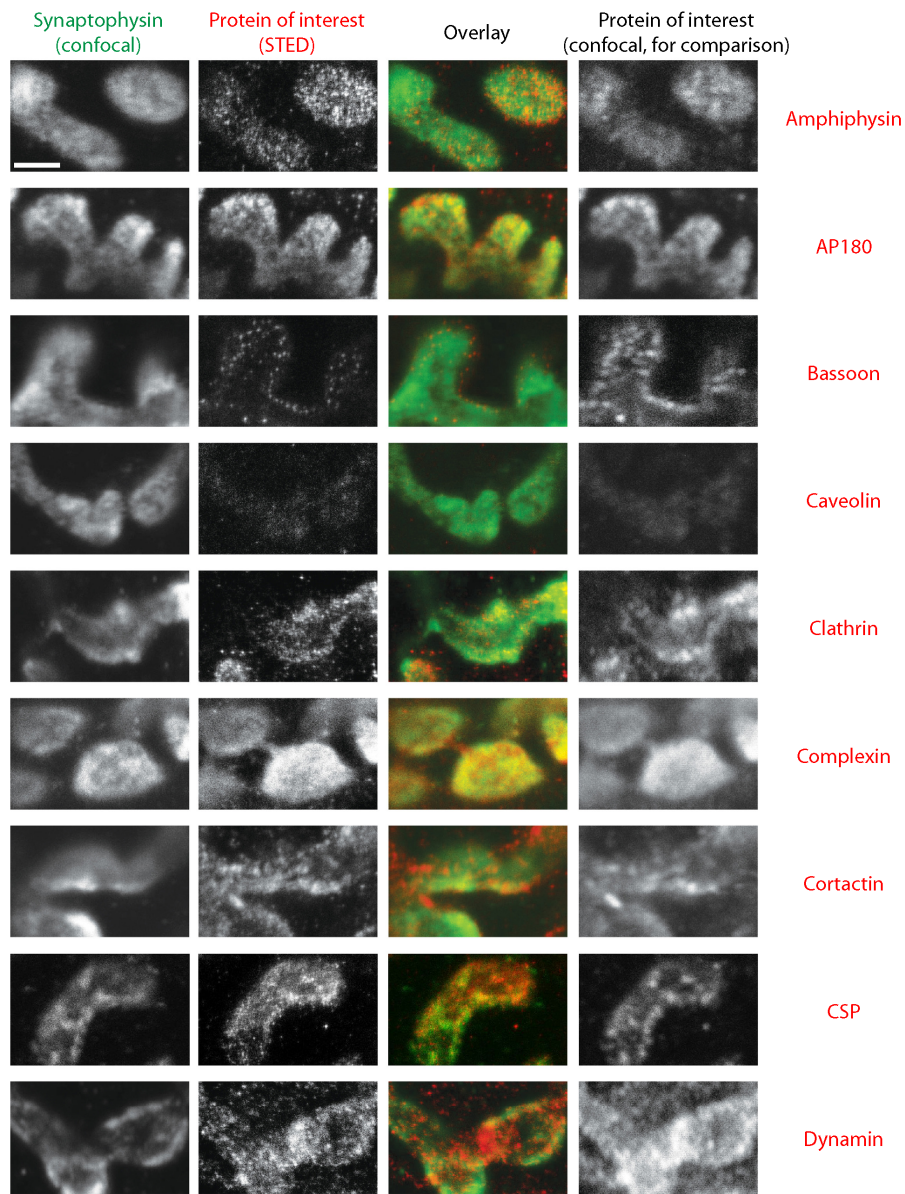
Figure 3.21: Colocalization of synaptic vesicle clusters and soluble accessory proteins
Exemplary immunostainings for the vesicle marker synaptophysin (confocal mode, left panels) and the protein of interest (STED mode, second panel from left; confocal mode, fourth panel from left). The third panel shows the overlay of the synaptophysin (confocal mode, green) and protein of interest (STED mode, red) images. Size bar is 2 µm. The proteins of interest are alphabetically ordered. Most soluble proteins investigated were found to colocalize to different degrees with synaptophysin (i.e., amphiphysin, AP180, clathrin, complexin, CSP, dynamin, endophilin, Hsc70, NSF, Rab3, rabphilin, RIM2, synaptojanin). Exceptions are tubulin and the active zone protein Bassoon, which show a lower correlation, and caveolin and cortactin, which might even avoid the vesicle clusters. Note that these experiments were performed by Katharina Kröhnert, European Neuroscience Institute, Göttingen. (From Denker et al., 2011b)

The degree of correlation of the investigated soluble molecules with the vesicle clusters was then quantified, as depicted in Figure 3.22. Note however that a certain degree of correlation is expected even if the two would not interact, as they share the same confined synaptic space.
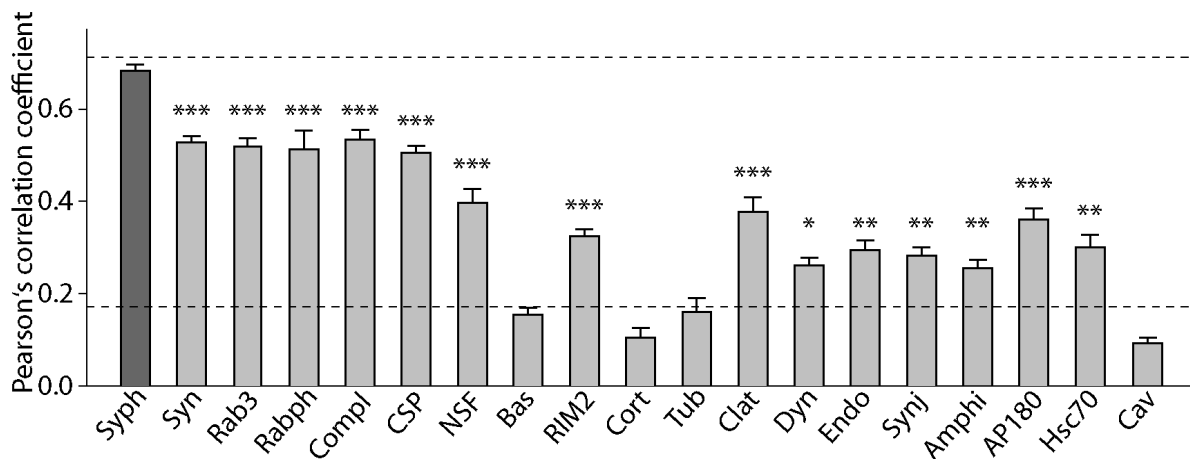
Figure 3.22: Quantification of colocalization of the vesicle clusters and the proteins of interest
Pearson's correlation coefficient was calculated for the proteins of interest and synaptophysin as a vesicle marker. In the positive control (dark grey), the correlation of synaptophysin (Syph) with itself was determined by staining with two different antibodies (see Table 2.2) and visualizing in confocal and STED mode, respectively. The investigated proteins may me grouped in vesicle-associated proteins (synapsin, Syn), proteins involved in exocytosis (Rab3; rabphilin, Rabph; complexin, Compl; CSP; NSF), active zone proteins (Bassoon, Bas; RIM2), cytoskeletal proteins (cortactin, Cort; tubulin, Tub), clathrin machinery components (clathrin, Clat ; dynamin, Dyn; endophilin, Endo; synaptojanin, Synj; amphiphysin, Amphi; AP180; Hsc70) and proteins not associated with vesicles (caveolin, Cav). Graph shows means ± SEM of 24 to 162 synaptic areas. The dotted lines indicate the expected correlation coefficients for a protein showing no affinity for the vesicle clusters and therefore distributing randomly in the synaptic volume (0.17) and for a protein fully bound to vesicles (0.71) and were calculated from the *in silico* model presented in Figure 3.23. Asterisks indicate significant colocalization of the respective protein with synaptic vesicles (*** $p < 0.0001$, ** $p < 0.01$, * $p < 0.05$, t-test). (From Denker et al., 2011b)

To better interpret the obtained correlation coefficients and their dependence on vesicle/protein affinities, an *in silico* model was generated, as depicted in Figure 3.23. The mouse 3D reconstruction shown in Figure 3.1 F was used to provide the architecture of the synaptic volume and the vesicle positions therein. In addition, soluble proteins were placed within the synapse and were convoluted with a STED "spot" (point spread function, PSF),

whereas the vesicles were convoluted with a confocal "spot". The protein distribution was simulated for different affinities for the vesicle clusters. Virtual sections were performed to obtain pseudo-fluorescence images of both vesicles and proteins (employing the same resolution, Z-drift, etc. as in the experimental setting), and the correlation coefficients between the images were calculated.
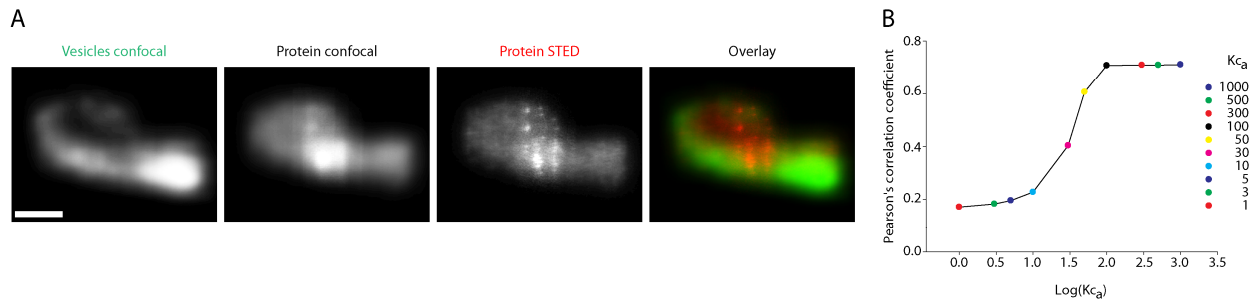
Figure 3.23: *In silico* **modelling of the correlation of vesicle clusters and synaptic proteins**
To better evaluate the results obtained in the immunostaining experiments presented in Figures 3.20 to 3.22, an *in silico* model was generated as also described in Section 2.13.3. The mouse 3D reconstruction shown in Figure 3.1 F was used to provide the architectural framework of the modelled synapse, rendering the distribution of the synaptic volume and of the vesicles therein. The number of vesicles in the reconstructed volume was 4447. In addition, 4500 virtual proteins were placed within the synapse. Whereas these protein spots were then convoluted with measured STED "spots" (point spread function, PSF), each vesicle position was convoluted with a confocal "spot" (note that these "spots" were obtained by measuring dye-coupled single antibodies, using the microscope setup described in Section 2.13.2 and used for the experiments presented in Figures 3.20 and 3.21). In a next step, virtual sections were made through the reconstruction, employing the same Z-resolution as provided by the microscope setting. Subsequently, the correlation coefficient between the vesicle and protein images was calculated. To simulate the real experiment as closely as possible, a small Z-drift was allowed between the images. Note that for each of the different affinities of the proteins for the vesicle clusters (Kc_a) simulated, protein positions were modelled 800 times, with the graph in (B) showing the mean correlation coefficient.
(A) Pseudo-fluorescence images for a simulation of a Kc_a of 1, i.e. of no special affinity of the proteins for the vesicle clusters. As for Figures 3.20 and 3.21, a confocal image of the distribution of the proteins of interest is also shown, which only serves for comparison, and was not used to calculate the correlation coefficient. Size bar is 1 µm. (B) Pearson's correlation coefficient calculated for different affinities of the proteins for the vesicle clusters (ranging from a Kc_a of 1 to 1000). Note that a Kc_a of 1 (indicating random positioning of the proteins within the synapse) does not result in a correlation coefficient of 0, as would normally be expected, but of ~0.17. This is due to the fact that, although the molecules are randomly distributed, they still share the same volume with the vesicles, which, in conjunction with the confocal Z-resolution (also of the STED images) results in some overlap of the respective PSFs and consequently in correlation. Therefore, proteins displaying an even lower correlation than 0.17, such as cortactin and caveolin (Figure 3.22) even avoid the vesicle clusters. Similarly, the maximal correlation coefficient achievable in this system is not 1, as would normally be expected for Pearson's correlation coefficient, but ~0.71 (when all proteins are bound to vesicles; see synaptophysin in Figure 3.22). This can be explained by the differences in confocal and STED imaging and by the fact that the positions of the simulated fluorophores on the vesicles are not identical (as would be the case in the real experiment). Note that modelling was performed by Dr. Silvio Rizzoli, European Neuroscience Institute, Göttingen. (From Denker et al., 2011b)

This modelling approach provided two important pieces of information: first, the maximal Pearson's correlation coefficient which can be obtained in this system is not 1, as would be normally expected, but about 0.71 (upper dotted line in Figure 3.22), due to differences between confocal and STED microscopy and to differences in fluorophore

positions. Second, molecules not binding to the vesicle clusters with any special affinity and therefore distributing randomly within the synaptic space, do not provide a correlation coefficient of 0, as expected, but of about 0.17 (lower dotted line in figure 3.22). This can be explained by the fact that vesicles and proteins share the same restricted synaptic volume (see legend of Figure 3.23 for further details on modelling the correlation coefficients). Importantly, the validity of the model is confirmed by the fact that the calculated correlation coefficients are in good agreement with the experimentally determined values as shown in Figure 3.22: the correlation coefficient of the positive control synaptophysin is close to the maximally possible value, and proteins known not to bind to vesicles (tubulin and Bassoon) are in the range calculated for randomly distributing proteins. As indicated by the asterisks in Figure 3.22, the correlation coefficients of the vast majority of the proteins investigated were significantly higher than for tubulin and Bassoon, indicating that they bind to and interact with the vesicle clusters. Interestingly, two of the proteins investigated (cortactin and caveolin) provided an even lower correlation than tubulin and Bassoon, indicating that they avoid the vesicle clusters.

As shown in Figure 3.24, the colocalization of several synaptic proteins with the vesicle clusters could also be confirmed by two-color STED microscopy.
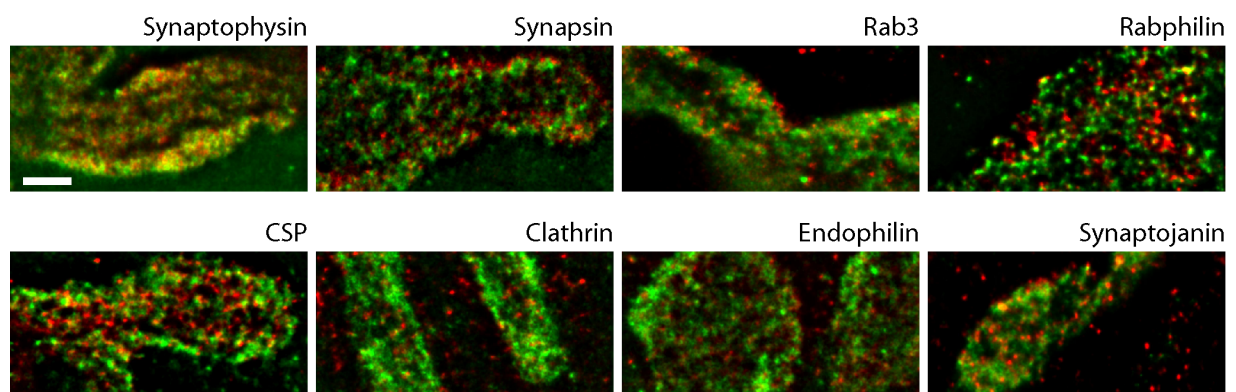
Figure 3.24: Two-color STED microscopy confirms correlation of soluble proteins and vesicles
Two-color STED images depicting the vesicle marker synaptophysin in green and the proteins of interest in red. The upper left panel shows the positive control (double staining for synaptophysin; see also Figure 3.22). Note that the basic observations are the same as for Figures 3.20 and 3.21, with the vesicle clusters colocalizing to different degrees with the proteins of interest. Size bar is 1 μm. These experiments were performed by Katharina Kröhnert, European Neuroscience Institute, Göttingen, and Johanna Bückers, Max Planck Institute for Biophysical Chemistry, Göttingen. (From Denker et al., 2011b)

Whereas many soluble proteins involved in synaptic vesicle recycling were thus shown to colocalize with the vesicle clusters, this does not necessarily imply that there is a direct interaction between the two. Therefore, the complement of soluble proteins bound to highly purified synaptic vesicles was analyzed by Western Blotting and compared to the composition of brain homogenate (Figure 3.25; highly purified vesicles were prepared by Dr.

Silvio Rizzoli at the Department of Neurobiology, Max Planck Institute for Biophysical Chemistry, Göttingen, according to protocols presented in Nagy et al., 1976; Huttner et al., 1983; Takamori et al., 2006; see Section 2.15.1). In agreement with a previous study (Takamori et al., 2006), several soluble proteins were found to be enriched on the purified synaptic vesicles, including CSP, Rab3, rabphilin and at lower levels synapsin. In addition, members of the clathrin pathway were also present at low amounts. Note that the vesicle purification protocol employed is quite lengthy (lasting more than 30 to 36 hours) and one might therefore expect that the majority of loosely associated proteins would be lost from the vesicles- rendering the observed presence of many soluble molecules on these vesicles all the more remarkable. In agreement with this statement, vesicles were shown to readily pick up higher quantities of most of these molecules from cytosol (see Section 3.3.3), further illustrating that the non-recycling vesicles could indeed function as a molecular buffer.
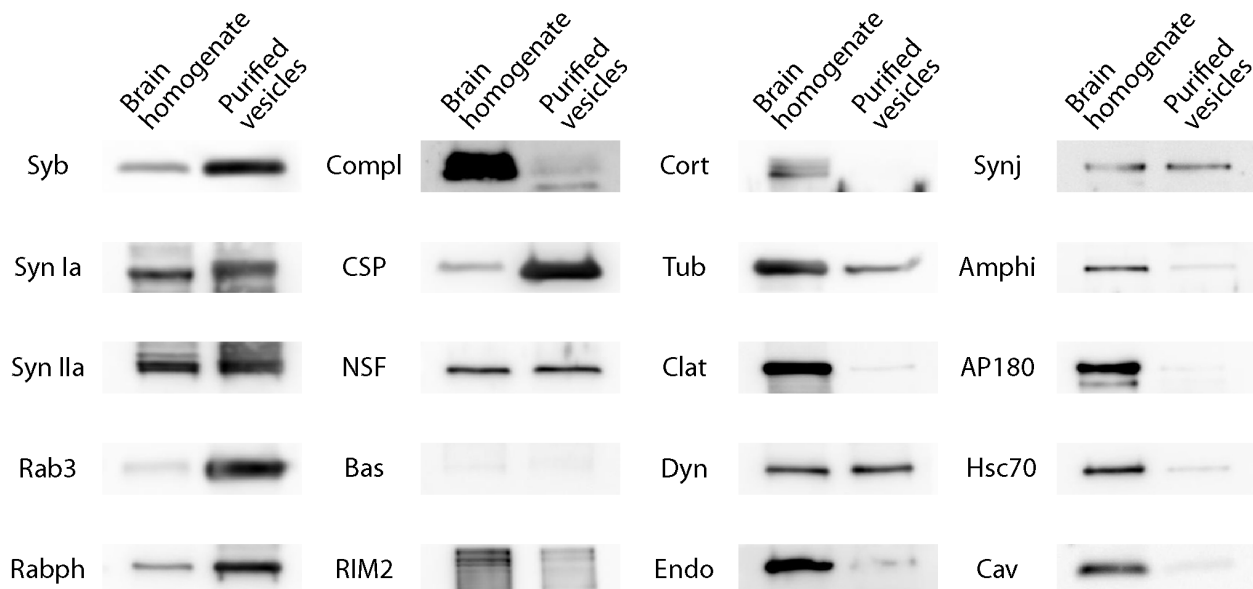
Figure 3.25: A multitude of soluble proteins bind to synaptic vesicles
Synaptic vesicles were purified from rat brain according to Takamori et al., 2006 (note that this protocol results in 95% purity in terms of synaptic vesicles). Western Blotting was performed to compare the protein composition of brain homogenate (left) as compared to the purified vesicles (right). Note that integral synaptic vesicle proteins are expected to be enriched in the purified vesicles, as shown in the upper left for synaptobrevin (Syb). Several soluble proteins show similar enrichment, namely Rab3, rabphilin (Rabph), and CSP. The two synapsin isoforms are enriched to a lesser extent. Dynamin (Dyn) and synaptojanin (Synj) are also found (albeit not enriched) on the purified vesicles, in agreement with the presence of members of the clathrin pathway on purified synaptic vesicles reported by Takamori and colleagues (Takamori et al., 2006). Similarly, NSF was also found in the vesicle preparation. In addition, several other molecules are detected on synaptic vesicles at lower levels, including for instance complexin (which is present only in trace amounts). (From Denker et al., 2011b)

3.3.2 The Effect of Synaptic Perturbations on Synaptic Protein Localization

If the vesicle clusters serve as a molecular buffer for the soluble factors involved in synaptic vesicle recycling, as proposed above, they should not only bind and enrich these proteins, as shown in the last section, but their disruption should also cause loss of these proteins from the synapse into the axon. This was achieved by treating the mouse *levator auris longus* muscle with black widow spider venom (BWSV), which in the absence of calcium triggers massive vesicle exocytosis without subsequent recycling (Henkel and Betz, 1995a). When vesicles were thus depleted from the NMJs, most of the soluble synaptic proteins indicated indeed diffused into the axon, as shown by immunostaining (Figure 3.26; see also Table 4.1).

BWSV encompasses a mixture of several different toxins, and it was therefore of interest to confirm that the effects on synaptic protein distribution evoked by BWSV could be reproduced by its main component, α-latrotoxin. Indeed, as shown in Figure 3.27, when the experiment was repeated using purified α-latrotoxin, the effects on the localization of synapsin, Rab3 and rabphilin were virtually identical to the effects of the full venom.

The significant loss of vesicle associated proteins into the axon upon triggering of massive vesicle fusion is to some level surprising, as the vesicle membrane itself is not lost from the synapse. Indeed, many of the molecules involved in the clathrin-mediated endocytosis (CME) pathway were retained in the synapse, in agreement with their role in vesicle retrieval from the plasma membrane (Figure 3.26 C). For many other proteins, however, their binding to the vesicle membrane was obviously weakened by integration of the vesicle into the plasma membrane. Different explanations for such a reduced affinity could be envisioned: first, the lipid composition of the vesicle membrane differs from the composition of the plasma membrane, especially with regard to phosphoinositides (Di Paolo and De Camilli, 2006); and second, the membrane curvature (which is sensed by many membrane binding proteins) would be altered by integration into the plasma membrane.
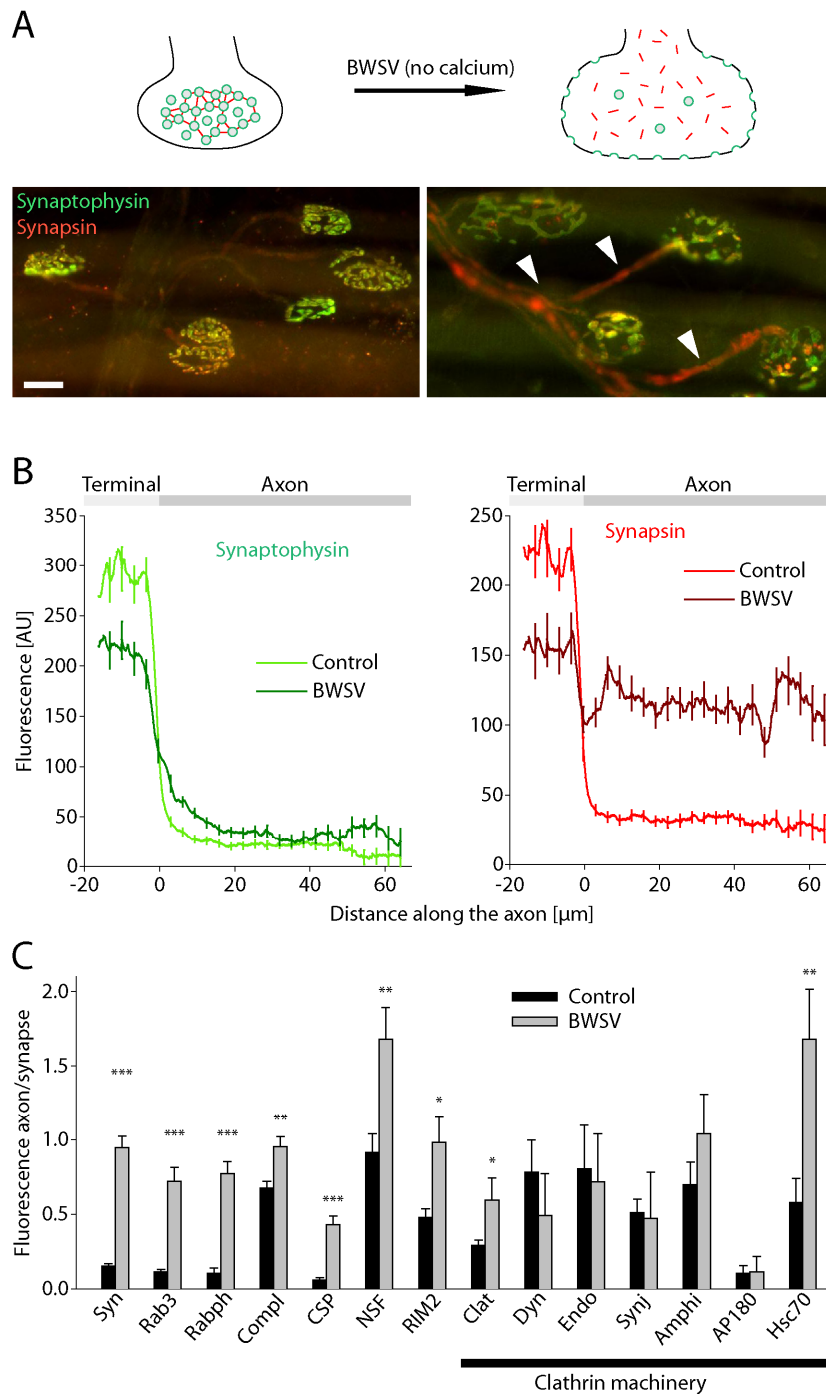
Figure 3.26: BWSV-induced vesicle cluster disruption causes protein loss from the synapse
(A) BWSV incubation in the absence of calcium results in massive vesicle exocytosis without subsequent endocytosis (Henkel and Betz, 1995a), as shown by the scheme. Whereas the integral synaptic vesicle protein synaptophysin (green) remains largely in the synapses of the mouse NMJ, synapsin (red) diffuses into the axons (arrowheads). Size bar is 20 µm. (B) The signal intensity within the nerve terminal and axon was quantified for synaptophysin (left) and synapsin (right). Note the decrease of synapsin signal in the terminal and associated increase in the axon after BWSV treatment. Graphs show means ± SEM of at least 99 synapses from 3 to 4 independent preparations. (C) BWSV-induced changes of protein localization in the mouse NMJ. Bar graph shows the mean ratio of fluorescence within the axon to synaptic fluorescence (± SEM) for control (black) and BWSV-treated preparations (grey). 21 to 112 synapses from 2 to 4 independent preparations were analyzed. Note that asterisks indicate significant protein diffusion into the axons (*** $p<0.0001$, ** $p<0.01$, * $p<0.05$, t-test), and that the members of the clathrin pathway are not expected to leave the synapse upon BWSV-incubation, as they would bind to the fused vesicles. (From Denker et al., 2011b)
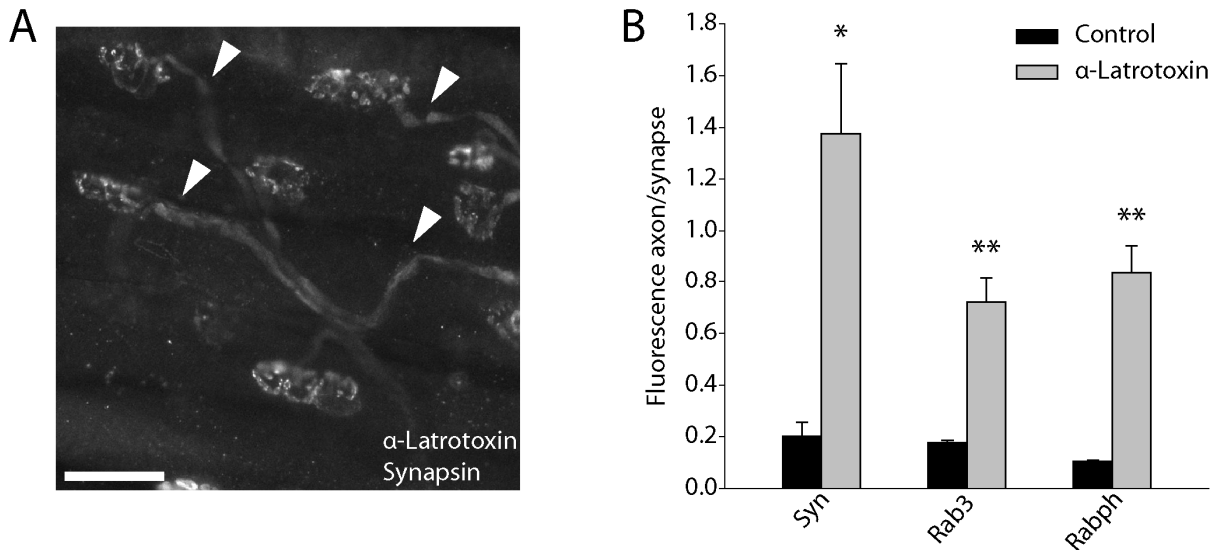
Figure 3.27: The effects of BWSV treatment are reproduced by α-latrotoxin
(A) To investigate whether the effects of BWSV on synaptic protein distribution are mediated by the venom's main component α-latrotoxin, the above described experiment was repeated under the same conditions, replacing the full venom by 2 μg/ml purified α-latrotoxin. Arrowheads indicate high levels of synapsin in the axons after α-latrotoxin treatment. Size bar is 50 μm. (B) α-latrotoxin-induced changes in protein distribution. Graph shows the mean ratio of fluorescence within the axon to synaptic fluorescence (3 experiments; ± SEM) for control (black) and latrotoxin-treated preparations (grey). Note that asterisks indicate significant protein diffusion into the axons (** $p<0.01$, * $p<0.05$, t-test), and that the values obtained are very similar to those obtained with BWSV (Figure 3.26 C). (From Denker et al., 2011b)

Of course, the loss of soluble proteins into the axon could also be a secondary effect of the BWSV/α-latrotoxin treatment. Therefore, as a next step, the effect of prolonged *in vitro* stimulation (which should trigger substantial vesicle recycling) on protein distribution in mouse NMJs was investigated. As synapsin, Rab3 and rabphilin provided easily measurable changes upon BWSV or α-latrotoxin treatment, they were chosen as representative markers of the distribution of accessory molecules. Indeed, as shown in Figure 3.28, all three proteins diffused into the axon upon 5 minutes stimulation at 30 Hz and returned into the synapse during a subsequent recovery phase, although recovery for rabphilin was not perfect (note that axonal fluorescence might also be decreased due to diffusion out of the field of view instead of return to the synapse). Imperfect recovery may be explained by the fact that the employed stimulation paradigm is well beyond the physiological range of this mouse muscle. Note that diffusion of synapsin into axons upon synaptic activity and subsequent recovery have been reported before for cultured hippocampal neurons (Chi et al., 2001). I therefore conclude that strong stimulation results in (partly reversible) protein loss from the synapse into the axon, as observed before for BWSV/α-latrotoxin treatment.

In summary, the experiments presented in this and the previous section are in good agreement with the hypothesis that the vesicle cluster functions as a molecular buffer, in that the vesicles 1) bind and concentrate at least some soluble factors involved in vesicle recycling and 2) release them upon synaptic perturbation or stimulation. However, the

experiments presented so far cannot explain how the buffering (i.e. the binding and unbinding) of these very diverse synaptic proteins could be regulated and how this might be related to synaptic activity, a problem that was addressed by the experiments described in the next section.
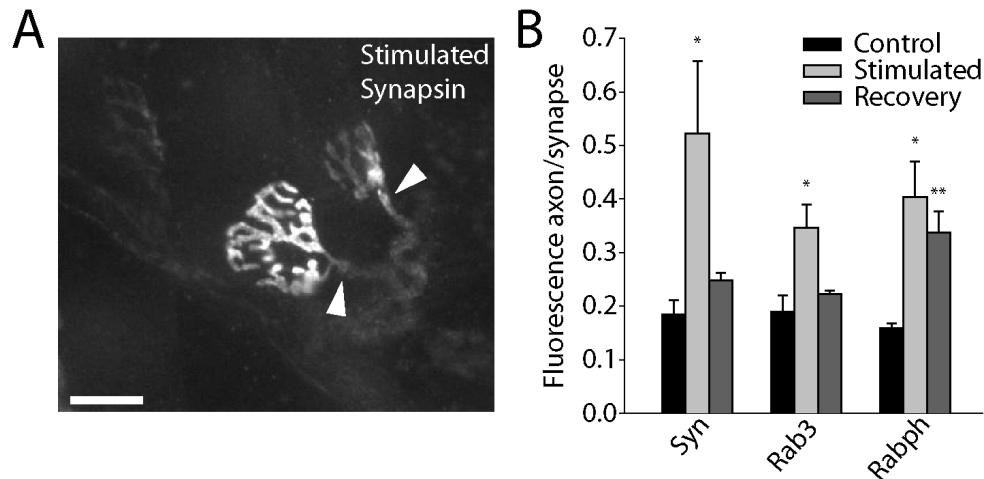
Figure 3.28: Soluble proteins are lost from the synapse upon strong stimulation
(A) Mouse *levator auris longus* muscles were stimulated for 5 minutes at 30 Hz and the effects on protein localization within the NMJ were investigated by immunostaining. Stimulation results in diffusion of synapsin from the synapse into the axons (arrowheads), as observed before for BWSV and α-latrotoxin treatment. Size bar is 20 μm. (B) Quantification of stimulation-induced changes in protein distribution. Graph shows the mean ratio of axonal as compared to synaptic fluorescence (3 to 4 experiments; ± SEM) for non-stimulated (control, black), strongly stimulated (5 minutes, 30 Hz, light grey) and recovered preparations (recovery lasted for 20 minutes after stimulation, dark grey). Note that all proteins investigated were lost into the axon upon stimulation and returned into the synapses during a 20-minute recovery period, although recovery was not always perfect, especially for rabphilin. Significant protein diffusion into axons is indicated by asterisks (** $p < 0.01$, * $p < 0.05$, t-test). Note that these experiments were performed by Katharina Kröhnert, European Neuroscience Institute, Göttingen. (From Denker et al., 2011b)

3.3.3 The Molecular Buffer is Controlled by Calcium

The observed protein loss into the axon upon stimulation could be explained by two different mechanisms: either the unbinding of proteins from the vesicle cluster is triggered by the induction of vesicle recycling, or it is simply mediated by the calcium influx during stimulation, independent of vesicle fusion. To distinguish between these two possibilities, I resorted to ionomycin, an ionophore whose application causes an increase in intracellular calcium levels, but which has been reported to increase exocytosis only mildly at the frog NMJ (Rizzoli and Betz, 2002; note however that a concentration of only 0.5 μM ionomycin was employed in this study, whereas 10 μM ionomycin were used in the experiments described below). When mouse muscles were treated with ionomycin for 60 minutes, synapsin, Rab3 and rabphilin were again lost from the synapse (Figure 3.29 A and B), and they returned upon replacement of calcium in the extracellular buffer by EGTA (which in the presence of ionomycin reduces intracellular calcium levels; Figure 3.29 B). Note that

ionomycin did not trigger a measurable increase in vesicle exocytosis in my hands, despite the high concentration employed (Figure 3.29 C). This experiment demonstrates that the binding and unbinding of several soluble synaptic proteins to vesicles is regulated by calcium.
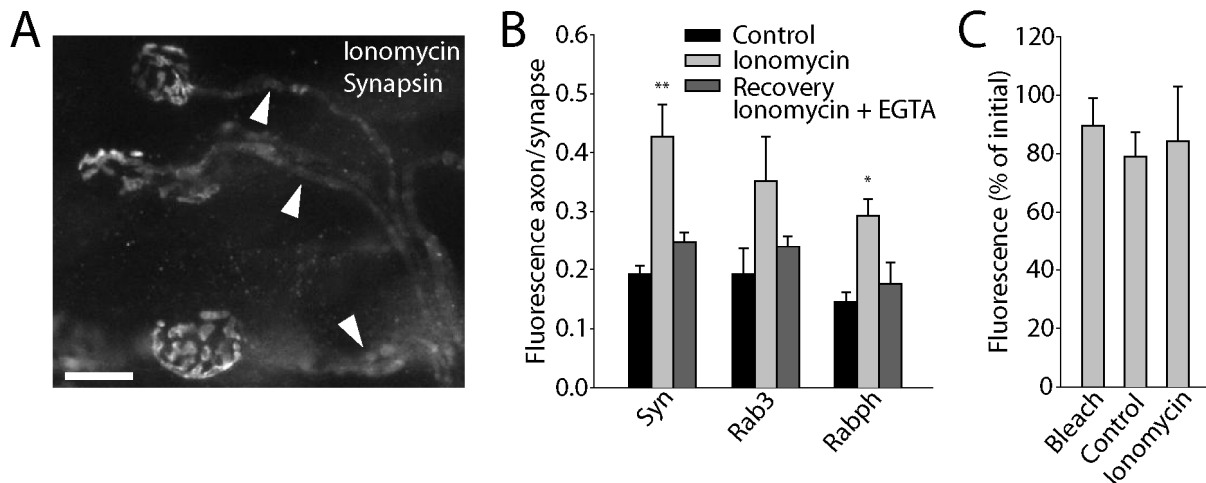
Figure 3.29: Increased intracellular calcium levels are sufficient to evoke protein loss
(A) Protein distribution was investigated in mouse NMJs, which had been incubated with 10 µM ionomycin in normal mouse buffer for 60 minutes. As indicated by the arrowheads, the increased intracellular calcium concentration induced by ionomycin triggers loss of soluble proteins from the synapse into the axon (depicted here for synapsin). Size bar is 20 µm. (B) Quantification of the effect of ionomycin on protein distribution. Graph shows the mean ratio of axonal and synaptic fluorescence (3 to 4 experiments; ± SEM) for control preparations (incubated only with mouse buffer + 0.2% DMSO, black), for ionomycin-treated preparations (light grey) and for recovered preparations (preparations were allowed to recover in calcium-free, 5 mM EGTA-supplemented buffer in presence of ionomycin for 60 minutes, dark grey). Note that proteins were generally lost into the axon upon ionomycin incubation and returned to the synapse during the recovery period. Significant protein diffusion into the axons is indicated by asterisks (** $p < 0.01$, * $p < 0.05$, t-test). (C) Quantification of the effect of ionomycin on vesicle exocytosis. Mouse NMJs were loaded with FM 1-43 by stimulation for 60 seconds at 30 Hz and then incubated for 60 minutes at room temperature in normal mouse buffer (with or without ionomycin). The residual fluorescence was then measured. Note that the remaining fluorescence for both ionomycin-treated and untreated preparations does not differ significantly from the photobleaching control (preparations imaged twice within ~1 to 5 minutes), indicating that ionomycin does not trigger a measurable increase in vesicle exocytosis. Graph shows means ± SEM from 4 to 5 experiments. (From Denker et al., 2011b)

This finding was then verified by an independent assay, using again isolated synaptic vesicles. If the vesicles indeed act as a buffer for soluble recycling factors, then they should accumulate these molecules when placed in contact with a source of such proteins, such as purified cytosol. On the other hand, an increase in calcium concentration should remove these proteins from the vesicles. This was tested by incubating isolated synaptic vesicles *in vitro* with rat brain cytosol, in presence or absence of calcium, as described in Section 2.15.2. In addition, the effects of ATP on protein binding were investigated. After incubation for 30 to 45 minutes, the vesicles were collected from solution by ultracentrifugation and the protein amount in the resulting pellets was analyzed by a standard BCA assay. As depicted in Figure 3.30, whereas cytosol addition caused a significant enrichment of proteins on the

vesicles, the further addition of calcium resulted in a significant reduction of protein levels in the vesicle pellets.
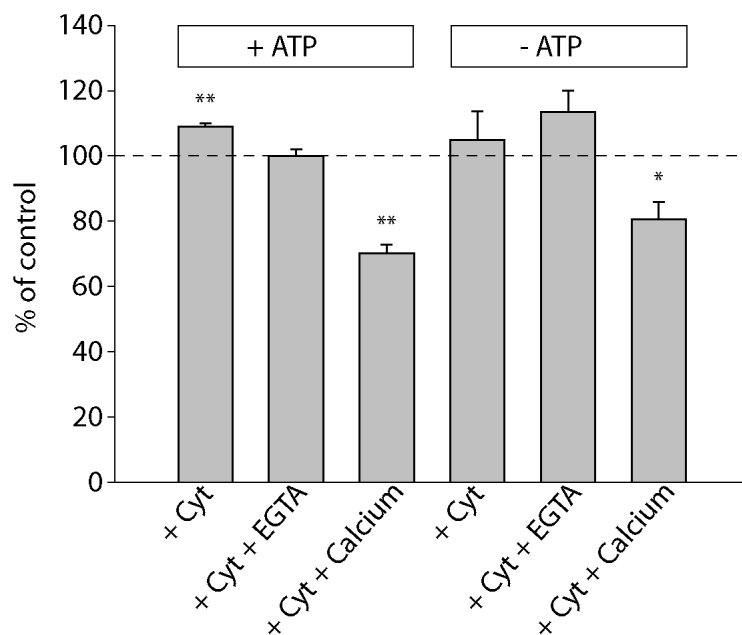
Figure 3.30: Effects of cytosol, calcium and ATP on molecular buffering
Isolated synaptic vesicles were incubated for 30 minutes at 37°C with rat brain cytosol and different combinations of an ATP-regenerating system (+ATP), an ATP-depleting system (-ATP), calcium (1 mM) or EGTA (5 mM). After incubation, the mixtures were ultracentrifuged, and the protein amount in the vesicle pellets was analyzed by a standard BCA protocol. Note that cytosol addition resulted in a significant increase in protein amounts as compared to the control (vesicles without cytosol addition; $p < 0.01$, t-test). Calcium addition, on the other hand, resulted in substantial protein loss from the pellet, independent of ATP (** $p < 0.01$, * $p < 0.05$, t-test). Graph shows means ± SEM from 3 independent experiments.

To determine the identity of the proteins gained or lost from the vesicle pellet upon cytosol or calcium addition, Western Blotting was performed. Note that blotting against the synaptic vesicle transmembrane proteins synaptobrevin, synaptophysin and synaptotagmin was performed to correct for any changes in vesicle amount within the pellets (representative blots are shown in Figure 3.31 A). Depending on their role in the synaptic vesicle cycle and on their buffering behavior, the proteins investigated could be sorted into five groups: the soluble synaptic vesicle proteins (Figure 3.31 B), the CME effector proteins (Figure 3.32), the CME adaptor proteins (Figure 3.33), the accumulators (Figure 3.34) and the trace proteins (Figure 3.35).

The influence of cytosol and calcium addition on vesicle binding of the soluble synaptic vesicle proteins synapsin, Rab3, rabphilin, and CSP is depicted in Figure 3.31 B. Upon incubation of the vesicles with cytosol, the levels of these proteins increased by about 60 to 360% and decreased to initial or slightly higher levels upon calcium addition.
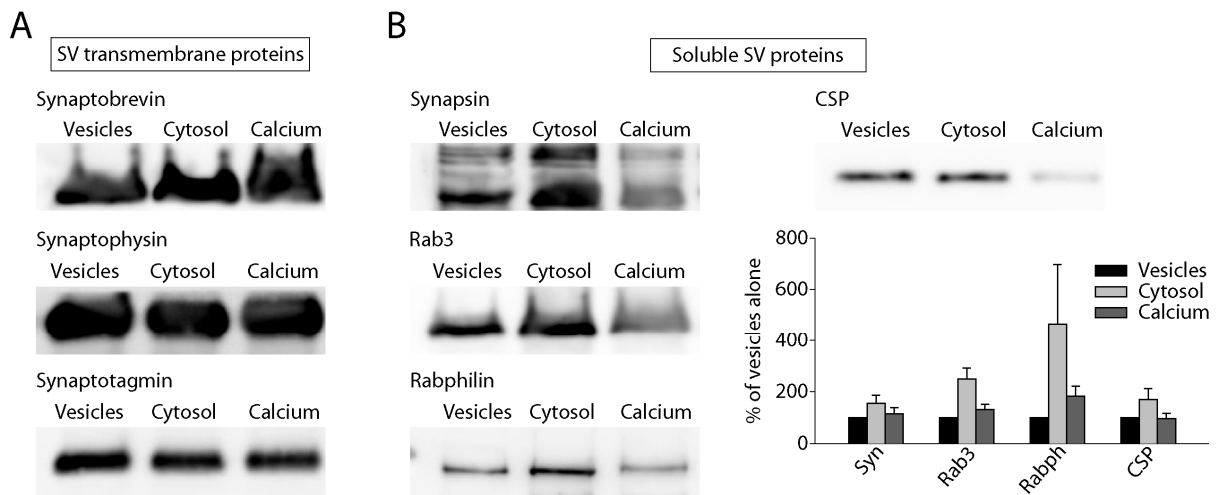
Figure 3.31: Calcium-dependent buffering of soluble synaptic vesicle proteins
Vesicle pelleting experiments were performed as described in the legend of Figure 3.30 and the nature of the proteins binding and unbinding from the vesicles was investigated by SDS-PAGE and Western Blotting. Note that only the conditions "vesicles" (vesicles without cytosol addition, i.e. the control of Figure 3.30), "cytosol" (vesicles plus cytosol; first bar in Figure 3.30) and "calcium" (vesicles plus cytosol plus 1 mM calcium; third bar in Figure 3.30) were tested, with all mixtures containing the ATP-regenerating system. (A) Representative blots for the vesicle transmembrane proteins synaptobrevin, synaptophysin, and synaptotagmin, used to correct for any variations in the amount of vesicles in the pellet (note that no change is expected upon cytosol or calcium addition). (B) Representative blots and quantification of buffering behavior for the soluble synaptic vesicle proteins synapsin, Rab3, rabphilin and CSP. Note that the levels of these proteins generally increase upon cytosol addition and return to the initial value upon calcium addition. The two bands observed in the synapsin blot represent synapsin Ia and IIa. Graph shows means ± SEM from 3 to 6 measurements from 3 to 4 experiments. (From Denker et al., 2011b)

The effector proteins of the clathrin-mediated endocytosis pathway (clathrin, dynamin and endophilin) behaved similarly, enriching on the vesicle pellets by about 70 to 140% after cytosol addition and being removed again by calcium addition (Figure 3.32).

An interesting observation was made for adaptors or accessory factors of the clathrin-mediated endocytic pathway, namely synaptojanin, amphiphysin, and AP180. These were enriched on the vesicles when cytosol was added (by about 30 to 90%), as described above for the soluble synaptic vesicle proteins and CME effector proteins, but calcium addition caused a striking loss even below initial levels (with for instance synaptojanin being lost to about 12% of its initial abundance; Figure 3.33).
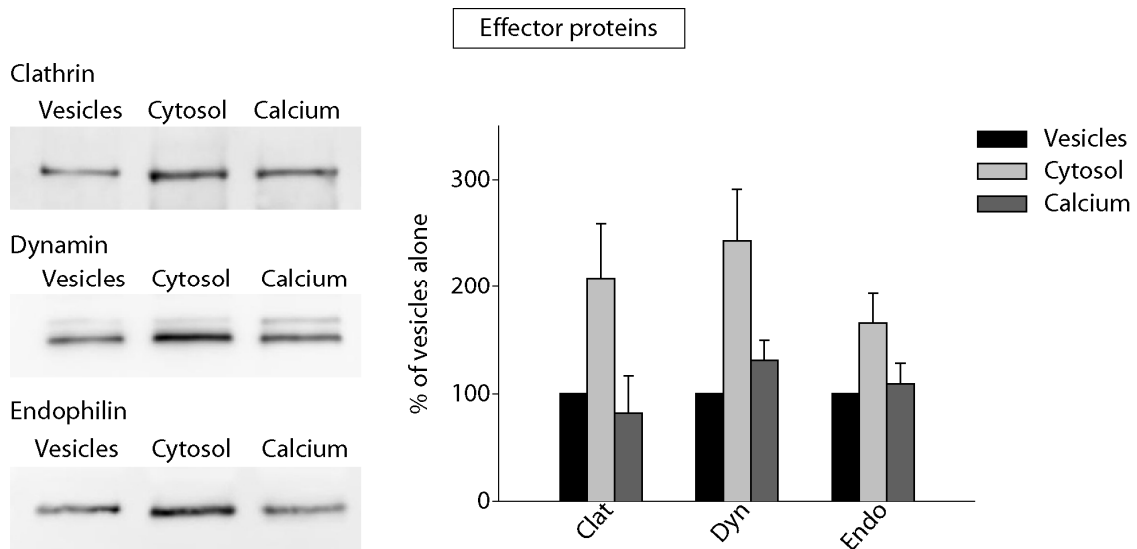
Figure 3.32: Calcium-dependent buffering of CME effector proteins
Exemplary blots and quantification of vesicle pelleting experiments for clathrin, dynamin and endophilin, which are directly involved in endocytosis. These proteins behave in a similar fashion as the soluble synaptic vesicle proteins presented in Figure 3.31, in that they accumulate on the vesicles upon cytosol addition and are released upon calcium addition. Values were corrected for variations in vesicle amounts in the pellets (see Figure 3.31 A). Graph shows means ± SEM from 4 to 5 measurements from 3 to 4 experiments. (From Denker et al., 2011b)
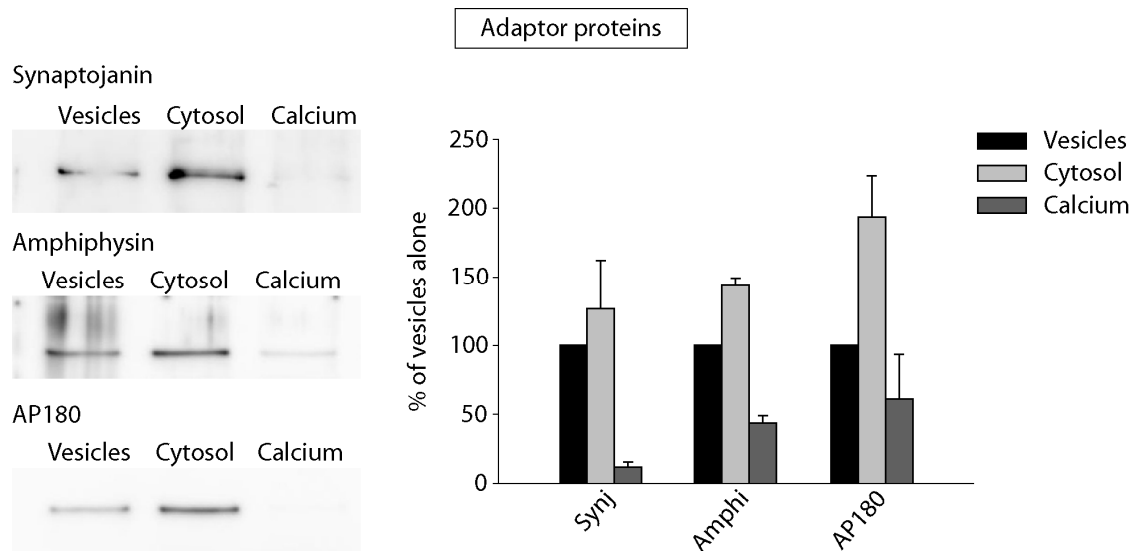
Figure 3.33: Calcium-dependent buffering of CME adaptor proteins
Representative blots and quantification of the vesicle binding behavior of synaptojanin, amphiphysin and AP180, which serve accessory functions during clathrin mediated endocytosis. Note that these factors accumulate on the vesicles upon cytosol addition and are strongly removed by calcium, even below initial levels. All values were corrected for variations in the amount of vesicle membrane in the pellets (see Figure 3.31 A). Graph shows means ± SEM from 3 to 4 measurements from at least 2 independent experiments. (From Denker et al., 2011b)

Another interesting finding was obtained for NSF, Hsc70 and RIM2, as these three proteins enriched on the vesicles at very high levels upon cytosol addition (reaching up to about 1500% of initial levels; this group was therefore named "accumulators"; Figure 3.34). Whereas calcium addition caused a decrease in the levels of these proteins on the vesicles, their amount was still several folds above the initial values.
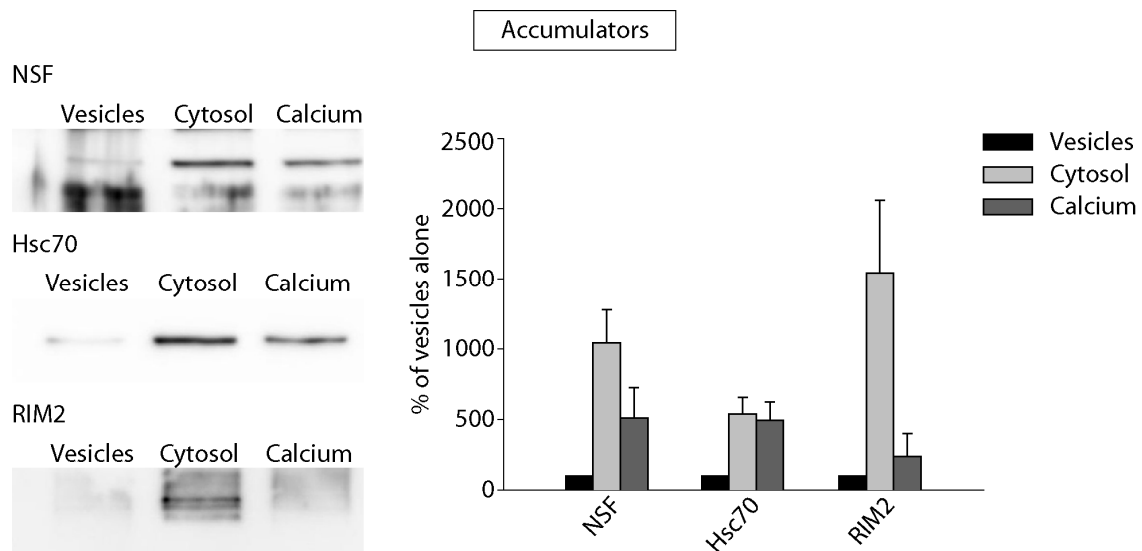
Figure 3.34: Calcium-dependent buffering of NSF, Hsc70 and RIM2 ("accumulators")
As shown in the representative blots and the quantification of protein amounts, NSF, Hsc70 and RIM2 accumulate to high levels on vesicles upon cytosol addition. Whereas calcium triggers release of these proteins from the vesicles, as for the other proteins described above, the "accumulators" do not reach initial levels. Note that the lower bands in the NSF blot represent nonspecific binding of the polyclonal antibody (possibly to human keratin bands). Values were corrected for variations in the amount of vesicles (see Figure 3.31 A). Graph shows means ± SEM from 3 to 4 measurements from at least 2 independent experiments. Note that the Y-axis reaches 2500%. (From Denker et al., 2011b)

An exception from the generally observed accumulation on vesicles upon cytosol addition and calcium-induced release from the vesicles was found to be complexin, where no substantial changes were observed (Figure 3.35 A). Interestingly, complexin was found on purified synaptic vesicles only in trace amounts (Figure 3.25), and, in line with this argument, was found at higher levels in the axons under normal conditions than any of the other proteins tested (Figure 3.35 B). It is therefore conceivable that complexin relies less on the vesicular buffer than the other factors which are strongly enriched in the synapse (see also Table 4.1).
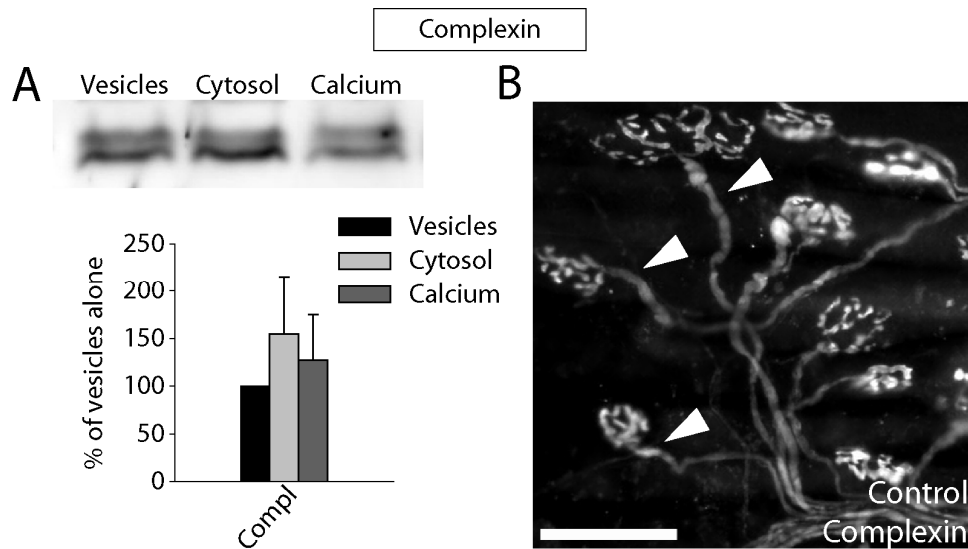
Figure 3.35: Cytosol and calcium addition do not substantially alter vesicular complexin levels
(A) Upper panel: representative complexin blot showing that complexin levels on the isolated vesicles are hardly changed upon incubation with cytosol, both in presence and absence of calcium. Lower panel: quantification showing means ± SEM from 5 measurements from 3 experiments. Values were corrected for variations in the amount of vesicles (see Figure 3.31 A). (B) Immunostaining of the mouse NMJ showing that complexin is present at high levels in the axons under normal conditions (arrowheads) and might therefore be less dependent on buffering than the afore-presented proteins. Size bar is 50 µm. (From Denker et al., 2011b)

However, in general these vesicle pelleting experiments showed that cytosol addition results in protein accumulation on the vesicles (mostly by about 50 to 300%; p<0.05, paired t-test; n=14 proteins), and that calcium addition removes these proteins from the cytosol-treated vesicles (mostly to initial levels; p<0.05, paired t-test; n=14 proteins). In conjunction with the observations made in the mouse NMJ after ionomycin application (Figure 3.29), these results argue for a role of calcium in regulating binding and unbinding of several soluble proteins to and from the vesicle clusters. I therefore conclude that the vesicle cluster fulfils the basic requirements for the hypothesized molecular buffer, in that it concentrates accessory factors required for synaptic vesicle recycling and can release them upon demand (probably triggered by the calcium influx associated with stimulation).

4. Discussion

The initial question to be addressed in this project was the amount of vesicles used by a living organism. This *in vivo* result would then serve as a point of reference for the numerous *in vitro* studies on vesicle use introduced in Section 1. My investigation of the amount of vesicles recycling in a behaving animal was extended to 11 different preparations (with the calyx of Held study performed by our collaborators Christoph Körber, Heinz Horstmann and Professor Thomas Kuner from the University of Heidelberg), ranging from insects (*Drosophila* larva NMJ and CNS, *Drosophila* adult, locust, cricket) and nematodes (*C. elegans*) over fish (zebrafish), amphibians (frog) and birds (chicken embryo) to mammals (mouse, rat).

Using injection of FM 1-43 into the living animals and subsequent photo-oxidation, I found that only about 1 to 5% of the synaptic vesicles had undergone recycling during a time period of a few hours (note that HRP injection followed by DAB incubation was performed for the rat calyx of Held, with similar results). As will be discussed in Section 4.2, the investigated synapses experience different activity levels under physiological conditions. The preparations also spanned glutamatergic (insects) and cholinergic (vertebrate NMJs and *C. elegans*) synapses and both developing and adult stages. Interestingly, the actively recycling vesicles were found to be utterly intermixed with the non-recycling vesicle population, indicating that they need to be highly mobile to quickly reach the active zones.

In view of this surprisingly low number of labelled vesicles, as visualized by EM, several control experiments were performed to test the validity of the dye injection and photo-oxidation approach: first, it was conceivable that the animals excrete the dye after injection, thereby effectively reducing the observation time. However, using fluorescence spectrophotometry, it was shown that the dye remains present in the body fluids of the injected animals for hours. Second, it could be imagined that the dye is not taken up by every vesicle undergoing recycling (possibly due to kiss-and-run fusion; Stevens and Williams, 2000). It should however be noted that the fast k_{on} of FM 1-43 (see Section 1.1.4) renders it probably the most reliable of the vesicle recycling markers generally employed, as HRP uptake or application of antibodies targeted against the lumenal domain of synaptic vesicle proteins is substantially less efficient. Nevertheless, limited FM dye uptake was a concern associated with the technique and, in addition, the photo-oxidation might not reliably transform every fluorescently labelled vesicle into the electron-dense organelle expected in EM. This was tested by directly comparing the electrophysiologically determined number of vesicles releasing spontaneously in presence of FM 1-43 in the *Drosophila* NMJ *in vitro* with the number of labelled vesicles found afterwards in EM. This experiment showed that every vesicle releasing neurotransmitter and recycling in presence of FM 1-43 was found labelled

in EM after the photo-oxidation reaction. As this experiment was performed *in vitro*, it could still be argued that the dye did not reach the synapses efficiently after injection into the living animal. Therefore, a third control experiment was performed to show dye availability at the level of the synapses by injecting FM 1-43 into *shibire* larvae and placing them subsequently for 5 minutes at non-permissive and then for 10 minutes at permissive temperature. As expected, this treatment resulted in substantial vesicle labelling, demonstrating that the dye reaches the nerve terminals upon injection.

As one could still argue that dye uptake into recycling vesicles, albeit not limiting *in vitro*, might be a limiting factor *in vivo*, I also used pHluorin *Drosophila* larvae in combination with bafilomycin injection to monitor vesicle use in the living animal. The signal in these experiments did not depend on uptake of a fluorescent marker, but on proton release, which is too fast to be restricted by the short and transient opening of a small fusion pore. The results obtained in this system were in good agreement with the photo-oxidation data, as only few vesicles seemed to be involved in recycling over hours.

This result was also in line with the observation of vesicle use in the temperature-sensitive *Drosophila* dynamin mutant *shibire*, which was chosen as an experimental system to circumvent the need for any injection. *Shibire* larvae and flies paralyzed very quickly at the non-permissive temperature (after about 10 to 15 seconds), although many vesicles were still present in the synapses at this time point. Depletion only occurred when the animals were maintained at the non-permissive temperature for 10 minutes. This experiment provided several important insights: the massive depletion after 10 minutes at the non-permissive temperature indicated 1) that the majority of synaptic vesicles are in principle release-competent, which was also in line with the results obtained after strong stimulation in presence of FM 1-43 and subsequent photo-oxidation and 2) that activity *in vivo* can be substantial, i.e. that the few vesicles undergoing recycling in the injection/photo-oxidation and pHluorin experiments must do so repeatedly. The rapid paralysis of the *shibire* larvae and adult flies in spite of the presence of a large vesicle reservoir was compatible with the use of only few vesicles *in vivo*, as the majority of the vesicles were not able to support efficient neurotransmission and consequently larval movement- possibly because they are not destined for release *in vivo*.

On the other hand, the *shibire* system might have a few caveats, which complicates the interpretation of this result: first, as discussed for instance in Chung et al., 2010, *shibire* is a dominant-negative mutant, and secondary effects on other trafficking pathways cannot be excluded. Second, the onset of paralysis was extremely quick, especially in view of the fact that vesicle recycling generally proceeds much slower, on the scale of tens of seconds to a minute (Betz and Wu, 1995). At least two different explanations for this phenomenon are conceivable: one possibility is that vesicle recycling at the *Drosophila* larval NMJ might

involve a readily retrievable vesicle pool (see for instance Hua et al., 2011a; see also Section 1.1.4 and 1.2.2), which would effectively reduce the recycling time (Rizzoli and Jahn, 2007). This scenario is compatible with the depletion of the actively recycling vesicles after a few seconds, causing paralysis of the animal. A second option would be that exocytosis itself is somehow impeded by the inhibition of endocytosis. Indeed and as reviewed in Neher, 2010, rapid onset of synaptic fatigue during stimulation under recycling inhibition is a well-documented phenomenon: Kawasaki and colleagues observed a significant reduction in synaptic current in *shibire* flies at non-permissive temperature after only 20 ms of repetitive stimulation (i.e. already for the second stimulus of 50 Hz stimulation; Kawasaki et al., 2000). No vesicle depletion could be observed at this time point. Similarly, fast synaptic depression upon interference with endocytosis has also been described for the lamprey giant reticulospinal synapse (Shupliakov et al., 1997), mouse cortical neurons (Ferguson et al., 2007) and the rat calyx of Held (Hosoi et al., 2009; Wu et al., 2009). Therefore, endocytosis seems to retrogradely regulate exocytosis. One possible explanation for this phenomenon in a role of the endocytic machinery in the clearing of release sites: as described in Section 1.1.3 and discussed in Neher, 2010, the components of the docked vesicles of the readily releasable pool (RRP) undergo multiple interactions with active zone proteins (including the binding of Rab3 and RIM and the formation of the SNARE complex). Upon exocytosis, these interactions need to be resolved quickly and the vesicle components need to be translocated from the release sites to the endocytic hotspots of the "periactive zone" (Roos and Kelly, 1999). This process might be triggered by components of the endocytic machinery, which might therefore play an additional role in release site clearing and consequently in the replenishment of the RRP (Kawasaki et al., 2000; Hosoi et al., 2009; Wu et al., 2009). Consequently, inhibition of endocytosis could result in an accumulation of fused vesicle components at the release sites and might therefore inhibit subsequent exocytosis (Neher, 2010), possibly explaining the rapid onset of paralysis observed in the *shibire* experiment presented in Figures 3.14 and 3.15 (which might therefore not necessarily be associated with loss of the small actively recycling vesicle population). However, paralysis of the *shibire* flies and larvae, albeit quite fast as compared to the general endocytic time course, was much slower than the rapid synaptic depression observed in the above-described studies. The massive vesicle depletion observed when maintaining the animals for 10 minutes at the non-permissive temperature also argues against release site block. In summary, the *shibire* EM data are not easily interpreted, but they are at least in agreement with the limited vesicle use observed in the photo-oxidation and pHluorin experiments.

Importantly, the use of a small vesicle population was not only conserved among distantly related organisms, but it also persisted under extreme physiological stress, as observed when exposing locusts after FM 1-43 injection to several frogs in a small terrarium.

Although a significant increase in vesicle use (from 1% in the non-stressed to 5% in the stressed locusts) was observed, 95% of the vesicles were still not involved in neurotransmitter release under this condition.

The general observation of limited vesicle use *in vivo* for all the animals, experiments and conditions tested raised (at least) two further questions: 1) what is the molecular difference between the actively recycling and inactive vesicles? 2) What is the function of the non-recycling vesicles?

To address the first question, I turned to synapsin-null *Drosophila* larvae, as synapsin is the best described candidate as a marker for the reserve vesicle pool (this will be further discussed in Section 4.3.1). As mentioned above, the actively recycling vesicles were found to be utterly intermixed with the non-releasing vesicles in EM, and it was therefore argued that the active vesicles need to be highly mobile, while the non-recycling vesicles might be immobilized in clusters, possibly by synapsin. Indeed, vesicle mobility was found to be increased in synapsin-null larvae, as was the percentage of vesicles undergoing recycling *in vivo* (with about a third of the vesicles labelled after 2 to 4 hours; note that this was not due to increased spontaneous vesicle release). It was therefore concluded that synapsin is one of the major factors differentiating between the active and inactive vesicle pools, but it was also evident that additional molecular players are also involved, which still await identification.

Finally, I addressed the question of the function of the non-recycling vesicle population. As discussed in Section 4.4.1, in addition to neurotransmitter release, several alternative functions have been proposed for synaptic vesicles. However, many of these hypotheses seemed unlikely to represent the function of the majority of the vesicles in view of my results and the results from other groups. Therefore, I explored the alternative possibility that the surplus vesicles might serve as a molecular buffer for molecules involved in synaptic vesicle recycling, retaining them in the synapse and preventing their diffusion into the axon. The two basic requirements which would need to be fulfilled for the vesicle cluster to serve as a molecular buffer are 1) that the vesicles concentrate the molecules to be buffered and 2) that they release these molecules upon demand, i.e. that the buffer is controlled, probably in a stimulation-dependent manner. Indeed, immunostainings of a vesicle marker and candidate proteins in the mouse NMJ combined with stimulated emission depletion (STED) microscopy revealed a significant colocalization between the two. The (surprisingly stable) interaction between the vesicles and the accessory molecules was further shown by Western Blotting of highly purified vesicles. Perturbation of synaptic organization by application of BWSV (or α-latrotoxin) in the absence of calcium resulted in massive vesicle exocytosis and protein diffusion from the synapse into the large volume of the axon, as demonstrated by immunostaining. To test whether such protein release from the vesicle cluster could be regulated in a stimulation-dependent manner, as might be expected

if the vesicles buffered molecules involved in vesicle recycling, mouse NMJs were tetanically stimulated and the effect on protein localization was investigated. Indeed, this treatment also resulted in protein loss into the axon. Importantly, application of ionomycin, which increases intracellular calcium concentration without triggering an observable increase in exocytosis, had the same effect, indicating that calcium influx is sufficient to trigger the release of protein from the buffer. This effect of calcium on the buffering properties was further tested by incubating purified synaptic vesicles either with cytosol alone (which should, according to the buffering hypothesis, result in protein accumulation on the vesicles) or with cytosol and calcium (which should prevent protein accumulation or should even induce protein loss below initial levels). Notably, the results were again in agreement with a (calcium-regulated) buffering function of the non-recycling vesicles, as the vesicles displayed the expected protein binding behavior. Interesting differences in vesicle binding were observed between different accessory factors by Western Blotting analysis, with for instance some proteins, such as synaptojanin, being highly responsive to calcium treatment (i.e. being deeply depleted from the vesicles upon calcium application) and others, such as RIM2, being accumulated to a very high extent from the cytoplasm.

In summary, this project proposes a new function for the majority of synaptic vesicles, which do not directly participate in neurotransmitter release *in vivo*. These vesicles are likely cross-linked by synapsin and probably other factors and are thereby kept immobile. However, they support neurotransmission indirectly by enriching vesicle recycling factors and providing them to (actively) recycling vesicles upon stimulation-induced calcium influx, thereby coupling exo- and endocytosis and ensuring reliable recycling.

4.1 A New Model of Synaptic Function *in Vivo*

From the *in vivo* investigations of synaptic function presented in this thesis and from previous studies performed *in vitro*, a new model of vesicle pools, vesicle recycling and vesicle mobility under physiologically relevant conditions can be deduced, as depicted in Figure 4.1. This model will be discussed in detail below.

Briefly, synapses contain a large inactive and a small active vesicle population, which are spatially intermixed. Whereas the actively recycling vesicles are highly mobile, the inactive vesicles are clustered and immobilized by cross-linking proteins. The latter support neurotransmission indirectly, by concentrating soluble recycling factors in the synapse and by providing them to recycling vesicles on demand. The distinct functions of these two vesicle populations are possibly not only reflected in their differential mobilities, but also in the recycling modes employed upon fusion (triggered under physiologically relevant

conditions for the active vesicles and by strong unphysiological stimulation for the buffer vesicles).
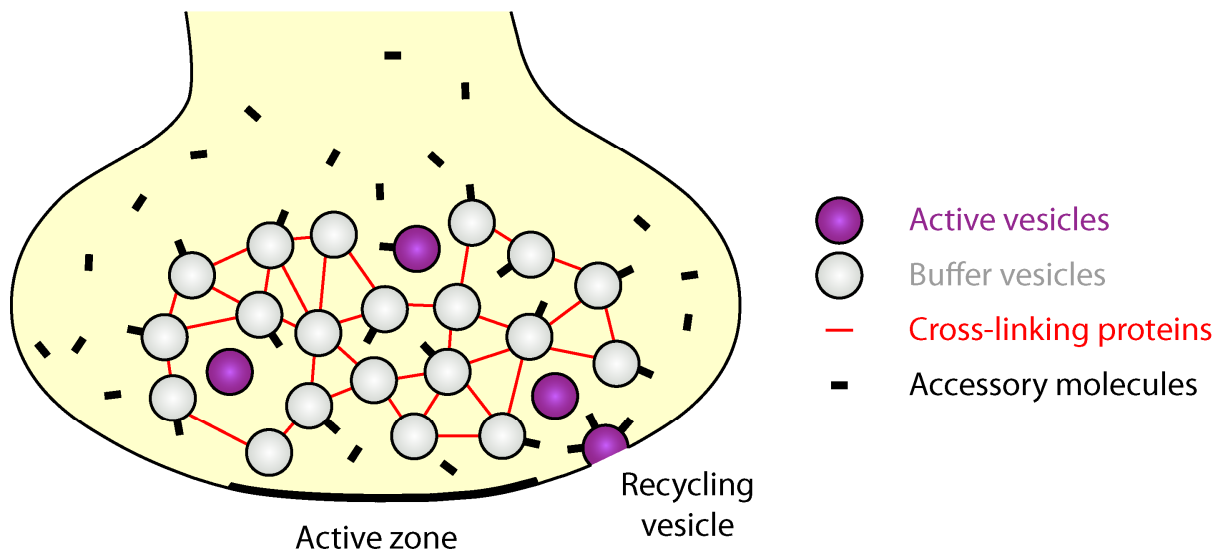
Figure 4.1: The new model of synaptic function
According to the new model of vesicle function *in vivo* developed herein, only few vesicles (purple) are actively participating in neurotransmitter release, meaning that they undergo cycles of repetitive release and recycling upon stimulation. These vesicles are likely highly mobile. The majority of the vesicles (grey) do not undergo recycling and instead serve as a molecular buffer for soluble molecules involved in the vesicle cycle (black), preventing their diffusion into the axon. These buffer vesicles are kept in place by cross-linking proteins such as synapsin (red). (Adapted from Denker et al., 2011b)

4.1.1 Vesicle Recycling *in Vivo*: Relation to Vesicle Pools

The results on vesicle use *in vivo* presented in this study clearly indicate that the previously proposed idea of distinct vesicle populations with different release properties ("pools") holds true *in vivo* and does not simply constitute an *in vitro* artifact. However, previous *in vitro* estimates of the relative sizes of the recycling and release-resistant vesicle pools differ substantially from the results presented herein: as described in Sections 1.2.1 and 1.3.1, different percentages of releasable vesicles have been reported for different preparations and stimulation paradigms. In short, several studies have indicated that at least in the NMJs, all vesicles can be forced to undergo recycling, although the release from the reserve pool requires strong and prolonged stimulation (for instance Rizzoli and Betz, 2004; Denker et al., 2009). However, the resting vesicle pool was very reluctant to be released in hippocampal neurons (Harata et al., 2001a; Harata et al., 2001b). From these different observations in the established *in vitro* systems, the well-accepted three-pool model as introduced in Section 1.2.1 and discussed in Rizzoli and Betz, 2005, was derived, stating that generally 1-2% of the vesicles belong to the RRP, 10-20% compose the recycling vesicle pool and the remaining 80-90% belong to the reserve vesicle pool. However, when vesicle

113

use was monitored *in vivo* by FM dye injection, followed by dissection and photo-oxidation two hours later, the percentage of recycling (labelled) vesicles was consistently extremely low, in the range of only 1-5%. Also, no significant vesicle loss was observed in the paralyzed *shibire* larvae, which would again argue for a very small number of actively recycling vesicles. To my knowledge, such a small recycling pool (including the RRP) of only a few percent of the vesicles has not been described before. Also, according to my data, the non-recycling vesicles do not constitute a vesicle reserve and are not even destined for release *in vivo*, but function as a molecular buffer (see also Section 4.4).

In addition to the mere numbers, another important observation with regard to vesicle pools *in vivo* is the very slow intermixing (on the timescale of hours) taking place between the actively recycling and inactive vesicle populations. This result supports the idea of a non-permanent vesicle tag, such as synapsin (see Sections 4.1.2 and 4.3.1), which can be exchanged between the vesicle pools. Therefore, and in agreement with previous *in vitro* observations of vesicles changing their release abilities (Betz and Henkel, 1994; Pyle et al., 2000; Rizzoli and Betz, 2004) and the model of pool intermixing due to changes in vesicle mobility and vesicle "maturation" (Section 1.2.3), the distinction between recycling and buffer vesicles is only relatively, but not absolutely, stable over time, meaning that vesicles can change their identity and release (and possibly recycling) characteristics by binding or unbinding of one or several specific pool tags. It is therefore conceivable that over a very long time, all vesicles would eventually participate in neurotransmitter release, although I cannot rule out that some vesicles never recycle *in vivo*. Also, it is possible that the rate of intermixing can be increased under certain conditions, such as at higher temperatures (note that the time course experiments presented in Figure 3.5 were performed for the *Drosophila* larva and the frog, both of which could well adapt synaptic function to changes in the environmental temperature). However, at any point in time only a small fraction of the total vesicle complement within a synapse releases neurotransmitter, and this population recycles repeatedly.

4.1.2 Vesicle Recycling *in Vivo*: Integrating Known Mobility Parameters

The finding that only a small fraction of the synaptic vesicles are destined for neurotransmitter release is also in agreement with two recent studies on vesicle mobility and vesicle recycling, which will be discussed in this and the following section. As the new results on vesicle mobility have already been described in Section 1.2.3, they shall only be shortly repeated here and put into perspective of the data on vesicle use *in vivo* presented above.

The analysis of the spatial distribution of actively recycling and inactive vesicles showed that they are utterly intermixed (Figure 3.6). This observation is in accordance with

several previous *in vitro* studies, indicating that vesicle pools with distinct release abilities are not spatially segregated (Harata et al., 2001b; de Lange et al., 2003; Paillart et al., 2003; Rizzoli and Betz, 2004; Akbergenova and Bykhovskaia, 2009; Denker et al., 2009; Section 1.2.1). This result however also implies that one of the distinctions between the active and inactive vesicles might be their mobility, as the recycling vesicles need to be highly mobile to quickly reach the active zone (which is necessary as the active vesicle pool is quite small and recycles repeatedly *in vivo*). The non-recycling vesicles on the other hand could be cross-linked and immobilized, preventing them from reaching the active zone and undergoing fusion. In this project, synapsin was found to be a good candidate for retaining the inactive vesicles, as its deletion increased vesicle mobility and vesicle use *in vivo* (note however that several other factors might also be involved in distinguishing actively recycling and inactive vesicles and that mobility might not be the only factor limiting release of non-recycling vesicles; see also Section 4.3.2).

This model is in good agreement with the fact that only few recently endocytosed vesicles were found to be mobile in hippocampal neurons *in vitro*, with all other vesicles essentially immobile (Kamin et al., 2010; Section 1.2.3). Importantly, vesicle mobility of neither of the two vesicle populations increased significantly upon physiological stimulation, which fits well with the hypothesis that the actively recycling vesicles are already mobile enough to reach the active zone (probably by simple diffusion), with stimulation only increasing their fusion ability, and that the resting vesicles are not meant to be released during physiological activity. Also, slow intermixing between the two vesicle pools was observed, which was even on a very similar time scale (of a few hours) to the slow turnover found *in vivo* (Figure 3.5). This slow intermixing was due to the integration of the mobile and actively recycling vesicle population into the immobile vesicle cluster. Interestingly, this "maturation" process (Denker and Rizzoli, 2010; Kamin et al., 2010) was accelerated when synaptic activity was inhibited by TTX application, indicating that activity maintains the recycling vesicles in a mobile state.

The maturation of mobile actively recycling to cluster-integrated immobile inactive vesicles might be explained by "capture" of the active vesicles by synapsin. As long as synaptic activity is high, the actively recycling vesicles will be quickly rereleased upon endocytosis. However, over time and especially when a synapse remains silent for an extended period of time (as under TTX application), the freely diffusing vesicles might start to accumulate synapsin, being eventually cross-linked to other vesicles and to the cytoskeleton and thereby integrating into the vesicle cluster (note that synaptic vesicles contain on average about 8 synapsin molecules; Takamori et al., 2006). As described in Section 1.2.3, this loss of actively recycling vesicles could be compensated for by the occasional fusion of

reserve pool vesicles docked at the active zone (as have for instance been observed in the frog and *Drosophila* NMJs; Rizzoli and Betz, 2004; Denker et al., 2009).

As shown by tetanic stimulation and in the *shibire* experiments, the non-recycling vesicles can eventually be forced to release. For tetanic stimulation, this could be explained by increased calcium levels, which induce the phosphorylation of synapsin and possibly other vesicle cross-linking molecules (Section 4.3) by calcium-dependent kinases (such as for instance CaMKI and CaMKII; Section 1.1.3) and thereby trigger the release of vesicles from the cluster. For *shibire* (as well as for strong stimulation), the resting vesicle population only seems to undergo recycling after the active vesicle pool has been depleted (as also shown for the frog NMJ; Richards et al., 2000). Again, this could be explained by the differences in mobility between actively recycling and non-recycling vesicles (Gaffield et al., 2006; Kamin et al., 2010): as non-recycling vesicles are much less mobile than the presumably freely diffusing actively recycling vesicles, they do not have a good chance to reach an empty release site at an active zone- these would be immediately occupied by another highly mobile recycling vesicle. Only after elimination of this competition by recycling pool depletion (which is unlikely to ever occur *in vivo*) does the chance of docking of a resting vesicle increase (although this remains an inefficient process, as indicated by the persistent paralysis of *shibire* flies and larvae, suggesting that these vesicles are not meant to be released).

4.1.3 Vesicle Recycling *in Vivo*: Potential Recycling Mechanisms

With efficient neurotransmission maintained by only a small vesicle pool, the reliable retrieval of these vesicles after fusion and their rapid recycling would be essential. Therefore, a specialized recycling mode might have evolved to ensure optimal sorting of the vesicle components of the actively recycling vesicles. Indeed, it has recently been demonstrated in hippocampal neurons *in vitro* that the vesicles displaying the highest release ability, i.e. the vesicles of the RRP, are optimally sorted via endosomes (Hoopmann et al., 2010; see also Uytterhoeven et al., 2011; as also discussed in Sections 1.1.4 and 1.2.1). This observation is at first sight surprising, as the RRP should be recycling quite rapidly (see Section 1.2.1). However, Hoopmann and colleagues could show that endosomal recycling is surprisingly fast, requiring about 30 seconds for a complete vesicle cycle, which is on the time scale of vesicle rerelease for the kiss-and-run recycling mode (Aravanis et al., 2003; see Section 1.1.4).

Why would the recycling vesicle need to pass through an endosome before being reused? Hoopmann and colleagues found that upon endocytosis, vesicles become contaminated with plasma membrane components, such as the SNAREs syntaxin 1 and

SNAP-25. Therefore, the few (mobile) vesicles responsible for maintaining neurotransmission actively would need to be reliably sorted. On the other hand, when recycling of the reluctantly releasable vesicle population was triggered by prolonged high frequency stimulation, they seemed to employ a different recycling route, without passing through an endosome. This observation is in agreement with the results presented in this project: these resting vesicles are not involved in neurotransmission *in vivo* and are therefore not meant to fuse. As they do not ensure efficient neurotransmission directly, there is no need for them to have an optimally regulated composition- they only need to display a certain affinity for accessory molecules to serve their buffering purpose, as discussed in Section 4.4.

Finally, such endosomal intermediates were hardly observed in the electron micrographs of injected animals (see Figures 3.1 to 3.3). This can well be explained by the transient nature of the endosomal intermediates. Indeed, the endosomes themselves might be relatively small (possibly on the scale of vesicles) and only increase in size upon fusion with vesicles. Alternatively, vesicles could fuse with each other (homotypic fusion) and somehow form a sorting station. Note that I defined the small membrane-bound organelles observed in the electron micrographs as vesicles using only the criterion of size. It might be interesting (although possibly technically challenging) to combine the photo-oxidation technique with immunogold-labelling for an endosomal marker, such as Rab5.

It should also be noted that small vesicular structures were nearly exclusively observed, with no strong evidence for bulk endocytosis. As discussed in Section 1.1.4, bulk endocytosis is often associated with high levels of stimulation, which in view of my data probably do not reflect the physiological activity levels. An exception was the chicken embryo, where bulk endocytosis and labelled vacuoles were often observed (Figure 3.2), probably due to the fact that the NMJ is still in the process of formation at this developmental stage (E11-E12). Therefore, I tentatively conclude that the major recycling modes employed *in vivo* are mainly characterized by small vesicular structures (as would be expected for CME and kiss-and-run), possibly involving transient fusion with endosomes (Hoopmann et al., 2010).

4.2 Synaptic Activity and Vesicle Use *in Vivo*

The consistency in the low percentage of labelled vesicles after FM dye injection and photo-oxidation in the different preparations employed is striking, with the small pool of actively recycling vesicles probably reflecting a general concept of synaptic function. As will be discussed in this section, I cannot exclude the existence of conditions or preparations in which vesicle use would be substantially higher. However, at least for several of the synapses investigated herein, such a scenario is highly unlikely.

For instance, I observed low vesicle use in NMJs controlling body movement, as for the ventral muscles of *Drosophila* larvae and *C. elegans*. When observing the behavior of these animals, it is clear that these muscles are frequently used. On the other hand, the movement of larvae is inherently slow, on the scale of about 1 mm/sec (on agarose; Caldwell et al., 2003), which is in the same range as the speed of *C. elegans* (Park et al., 2008; note however that *C. elegans* is only about 1 mm in length, which is about a fourth of the third instar larva, with the worm therefore being substantially faster than the larva with respect to its body size). It is difficult to envision a physiologically relevant situation which could trigger much faster movement and therefore synaptic activity.

Of course, the need for movement is substantially increased in the extreme (physiologically relevant) situation of predation. Nevertheless, a very high speed and synaptic activity could not be attained in larvae (and probably also worms) even under these conditions. In line with this argument, whereas synaptic activity and vesicle use were significantly increased upon predation of locusts by frogs (Figure 3.16), the jumping behavior of the escaping locusts was still infrequent and 95% of the vesicles still did not recycle (although a stronger need for movement than in this life-or-death struggle can hardly occur). It should also be noted that the usefulness of presynaptic firing at the NMJs is limited by the fatigue of the muscle (Bigland-Ritchie et al., 1982; reviewed in Slater, 2003), as described in Section 1.3.2. Therefore, extremely high firing frequencies leading to muscle cramps would even be counterproductive for successful escape from a predator.

In the absence of a predator, the third pair of legs of the locust was used much less frequently, either for occasional jumps or during communication (singing). Infrequent use was for example also characteristic for the *levator auris longus* muscle of the mouse, which is responsible for adjusting the ear position. On the other hand, higher demands for vesicle use could have been imagined for the tail muscle of the zebrafish, which is a continually used muscle involved in body posture, can beat several times per second (Thomas and Janz, 2011) and supports swimming speeds of half a meter per second, rendering the zebrafish one of the fastest swimming fish ever measured (Plaut, 2000). Nevertheless, only about 1% of the synaptic vesicles had participated in neurotransmitter release in this preparation at two hours after FM dye injection (Figure 3.4). A high number of recycling vesicles might also have been expected for the calyx of Held, which fires at very high frequencies of about 30 or up to several hundred Hz *in vivo* (Kopp-Scheinpflug et al., 2008). However, as explained in Section 1.3.2, the low quantal content (Lorteije et al., 2009) as compared to the large total vesicle pool (de Lange et al., 2003), indicates that the calyx could sustain firing at these rates using only a minority of its vesicles- albeit the actually observed percentage of labelled vesicles (about 3.5%) was much lower than was originally estimated (20% for 30 Hz firing,

see Section 1.3.2). This could possibly be explained by the use of very fast recycling modes, as have indeed been observed at this synapse (Sun et al., 2002).

Could there be synapses which use a much higher percentage of the vesicles? As alluded to above, it is difficult to envision an NMJ which would experience such high activity levels, especially as these generally result in muscle fatigue. One interesting counterexample might possibly be the pectoral muscle of hummingbirds, which moves the wing. Hummingbirds beat their wings about 35 to 45 times per second, both in hovering and locomotive flight (Hagiwara et al., 1968). This is driven by burst discharges of the same frequency, with up to five impulses at 300 to 500 Hz per burst and wing beat. The investigation of vesicle use in these NMJs would therefore be an interesting follow-up experiment of the project presented here.

Another system in which vesicle use could be substantially higher than for the synapses investigated in this project are ribbon synapses. Ribbon synapses are glutamatergic synapses which respond to graded depolarization and display very high rates of release (see also Sterling and Matthews, 2005, and Section 1.1.1). The properties of the three distinct vesicle pools also differ from conventional synapses (compare Section 1.2.1), as although three populations with different release kinetics are observed (reflecting the RRP, the recycling pool attached to the synaptic ribbon and the cytoplasmic reserve pool; reviewed in Rizzoli and Betz, 2005), the recycling pool does not seem to be refilled mainly by retrieved vesicles, but by cytoplasmic vesicles binding to the ribbon in goldfish retinal bipolar cells (Holt et al., 2004; note that different observations have been reported for cone photoreceptors; Rea et al., 2004).   In addition, the reserve pool vesicles are highly mobile in ribbon synapses (Holt et al., 2004; Rea et al., 2004), which fits the model of vesicle mobility introduced above (Section 4.1.2), as these synapses also lack synapsin (Mandell et al., 1990; Von Kriegstein et al., 1999). Rapid intermixing between the recycling and reserve pool vesicles, in combination with the high rates of release sustained by ribbon synapses (e.g. about 20 vesicles per second per active zone at cone-bipolar contacts of the turtle under light stimulation; Ashmore and Copenhagen, 1983), could therefore result in the use of a high percentage of vesicles in these synapses. As will be further discussed in Section 4.4.2, the special morphology of ribbon synapses might allow them to take advantage of the full complement of vesicles for neurotransmission, instead of maintaining the majority as a molecular buffer. A further interesting follow-up experiment of the study presented here would therefore also be the investigation of vesicle use *in vivo* in ribbon synapses, for instance by injection of FM dye into the goldfish eye. However, I want to emphasize that I refrained from such experiments because they would be ethically problematic.

4.3 Vesicle Pool Tags

As discussed in Section 4.1.2, the actively recycling and non-recycling vesicles are not spatially separated *in vivo* but intermixed (Figure 3.6), in agreement with previous *in vitro* studies of vesicle pool localization (Section 1.2.1). Therefore, their release abilities do not differ due to differential localization relative to the active zones. Instead, there seems to be a molecular difference between the actively recycling and resting/buffer vesicles, and this molecular tag (or tags) can be exchanged between vesicle populations, as shown by the time courses (Figure 3.5). One of the possible candidates for distinguishing recycling and inactive vesicles has already been introduced above: synapsin. In the following section, I will discuss results on the role of synapsin in maintaining and controlling the reserve or non-recycling (buffer) vesicles. In Section 4.3.2, I will discuss further candidate molecules which could also be involved in distinguishing actively recycling and release-reluctant vesicle pools, possibly in addition to synapsin.

4.3.1 Synapsin As a Vesicle Pool Marker

When nerve terminals were investigated by quick-freeze deep-etch electron microscopy, a meshwork of filaments cross-linking vesicles and possibly also connecting vesicles to the cytoskeleton was observed (Landis et al., 1988; Hirokawa et al., 1989; see also Pechstein and Shupliakov, 2010). These were proposed to be synapsin mono- or multimers, due to matching molecular dimensions and immunoreactivity (Landis et al., 1988; Hirokawa et al., 1989). As discussed in Section 1.1.3, synapsin was found to be preferentially localized to a vesicle pool distant from the active zone (Pieribone et al., 1995) and was not found on clathrin-coated intermediates (Bloom et al., 2003), possibly indicating a role on reserve pool vesicles. Synapsin's role in vesicle clustering could well be mediated by synapsin dimers (Esser et al., 1998; Monaldi et al., 2010) and seems to be controlled by phosophorylation (see Section 1.1.3 and Cesca et al., 2010). According to the current working model, stimulation-induced calcium influx triggers synapsin phosphorylation by CAMKI and CAMKII which causes it to unbind from the vesicles and disperse, allowing for vesicle pool turnover (compare Huttner et al., 1983; Hirokawa et al., 1989; Chi et al., 2001). This is in line with early observations of vesicle cluster disruption and increased vesicle mobility upon application of the phosphatase inhibitor okadaic acid (Betz and Henkel, 1994; Kraszewski et al., 1995).

In agreement with a role of synapsin in the maintenance of the reserve or reluctantly-releasable vesicle pool (Hilfiker et al., 1999), knockout mice lacking one of the three mammalian synapsin genes displayed a reduction of vesicle numbers. This vesicle loss was

more evident for areas distal from the active zone (Takei et al., 1995b). A similar observation was made after injection of synapsin antibodies into lamprey reticulospinal axons, which not only depleted the distal vesicle pool, but also depressed neurotransmitter release under high frequency stimulation (18-20 Hz), whereas release under mild stimulation (0.2 Hz) could still be sustained, again supporting a role of synapsin as a regulator and molecular tag for the reserve vesicle pool (Pieribone et al., 1995).

As mammals possess three synapsin genes with possibly redundant functions (see above), the investigation of synaptic morphology and function in synapsin triple knockout (TKO) mice was desirable. As presented by Gitler and colleagues, these mice were surprisingly found to be viable and also displayed normal brain anatomy, albeit displaying mild abnormalities in balance and coordination (Gitler et al., 2004). However, the hypothesis of synapsin regulating the reluctantly-recycling vesicle population was supported by an increased rate of synaptic depression and a decrease in vesicle numbers distal from the active zones at excitatory (glutamatergic) synapses of cultured hippocampal neurons obtained from these mice. Basal transmission was not affected. However, the results obtained in the synapsin triple knockout mice were complicated by the observation that an opposite phenotype was observed at inhibitory (GABAergic) synapses, where the reduction in vesicle numbers was not restricted to areas distal from the active zones and where basal transmission was reduced, whereas the rate of depression was not affected. The authors therefore concluded that synapsin regulates the reserve vesicle pool in excitatory and the RRP in inhibitory synapses. Note that opposite effects on glutamatergic and GABAergic neurotransmission have also been reported for isolated nerve terminals obtained from the neocortex of synapsin I and II double knockout (DKO) mice (Lonart and Simsek-Duran, 2006).

Interestingly, when NMJs of synapsin-null *Drosophila* larvae (which have only one synapsin gene; the same stock as used in this project, Figures 3.17 to 3.19) were studied, no differences in synaptic ultrastructure were observed, shedding doubt on synapsin as the sole molecular player in vesicle clustering (Godenschwege et al., 2004; in agreement with Siksou et al., 2007, indicating that cross-linking filaments other than synapsin are involved in vesicle clustering, and my results presented in Section 3.2, showing that synapsin is not the only factor limiting mobility and release ability of the non-recycling vesicles). Synaptic transmission was also found to be normal at this synapse up to stimulation frequencies of 5 Hz. Similarly, synapsin-null flies displayed no changes in brain morphology. The only differences observed were in complex behavior, such as defects in learning and memory (Godenschwege et al., 2004; Michels et al., 2005). These results could indicate that synapsin, while not necessary for maintaining synaptic transmission, is involved in the fine-tuning of synaptic function.

Reduced vesicle mobility upon synapsin binding lies at the core of the synapsin hypothesis. However, when vesicle mobility was monitored by FRAP in triple knockout mice, it was found to be indistinguishable from wildtype mice, as was synaptic transmission, although vesicle numbers were reduced (Gaffield and Betz, 2007). It should be noted that the lack of an effect on synaptic transmission, which is in striking contrast to the results obtained by Gitler and colleagues (Gitler et al., 2004), could be explained by the investigation of CNS synapses in the latter study, whereas Gaffield and Betz studied the NMJ, which has many more vesicles (Rizzoli and Betz, 2005) and might therefore be less susceptible to vesicle loss (Gaffield and Betz, 2007). Importantly, the study by Gaffield and Betz supported the well-described concept of regulation of vesicle mobility by phosphorylation, indicating that another phospho-protein than synapsin might be involved.

On the other hand, a role of synapsin in controlling vesicle mobility is supported by the observation that mobility is substantially increased in ribbon synapses (Holt et al., 2004; Rea et al., 2004), which lack synapsin (Mandell et al., 1990; see also Section 4.2). Also, the FRAP experiments on synapsin-null *Drosophila* larvae presented in this study (Figure 3.17) clearly indicate a function of synapsin in regulating vesicle mobility. I therefore tentatively conclude that synapsin plays some role in immobilizing the non-recycling vesicle population and might therefore serve as a molecular tag for this vesicle pool. The model on the differential regulation of the mobility and thereby release-capacity of the distinct pools developed above (Sections 1.2.3 and 4.1.2; see also Denker and Rizzoli, 2010, and discussion of Kamin et al., 2010) might therefore still hold true: the non-recycling vesicles are immobilized by a molecular "glue", whereas the actively recycling vesicles are mobile (in agreement with Gaffield et al., 2006). Over time (and especially when synaptic activity and consequently vesicle recycling are low), these active vesicles might start binding to the "glue" and become immobilized, whereas resting vesicles could either fuse at the active zone (if already docked) or else unbind with a low probability from the cluster, thereby turning into actively recycling vesicles (note that there is no current experimental evidence for the second possibility that I am aware of; Denker and Rizzoli, 2010). However, other molecular players than synapsin also seem to be involved in differentiating between the active and inactive/buffer vesicles. Possible candidates for this function will be presented in the next section.

4.3.2 Alternative Candidates for Vesicle Pool Markers

As described above, the ambiguous results obtained when investigating synapsin knockout animals (with the importance of synapsin for maintaining neurotransmission possibly also differing among organisms) and the fact that cross-linking of vesicles seems to

be mediated also by other molecules, in addition to synapsin (Siksou et al., 2007), renders the existence of additional or alternative pool tags very likely. Importantly, these tags might not necessarily occur in an all-or-none manner, but could also display a graded distribution with a certain threshold of molecules present on or absent from a vesicle endowing it with certain release abilities.

In view of the recently clarified molecular composition of an "average" synaptic vesicle (Takamori et al., 2006), several candidate proteins can be excluded, as they are present in so high amounts on the "average" vesicle that they likely represent a common vesicle complement found on each vesicle (see Section 1.1.2). These proteins include synaptobrevin (70 copies per vesicle), synaptophysin (32 copies per vesicle) and synaptotagmin 1 (15 copies per vesicle). On the other hand, some proteins were found at very low numbers, such as the endosomal SNARE proteins. In view of the fact that the actively recycling vesicle pool was consistently small for all preparations presented in the project described here, making up only a few percent of all vesicles, these proteins could well be enriched on the active vesicle population, serving as a molecular tag. In case of the endosomal SNAREs, this would be in agreement with a selective recycling of the active vesicles via endosomes (see Section 4.1.3; note that these would represent a permanent tag and their mode of exchange between the vesicle pools remains unknown).

A promising approach to identify alternative (reserve) pool markers is finding proteins which 1) are regulated in a phosphorylation-dependent manner and 2) are lacking in ribbon synapses, where vesicle mobility and pool intermixing are much higher (Holt et al., 2004; Rea et al., 2004) and pool affiliation might be mainly reflected by ribbon attachment (note that in ribbon synapses, vesicle mobility might be regulated in an opposite manner to conventional synapses, with the application of the phosphatase inhibitor okadaic acid disrupting rather than enhancing mobility; Guatimosim et al., 2002; Rea et al., 2004; further indicating that a suitable reserve pool tag for conventional synapses might be lacking in ribbon synapses). In addition to synapsin, which other proteins display these characteristics? As described in Bykhovskaia, 2011, and in the discussion of Gaffield and Betz, 2007, a likely candidate is rabphilin (Von Kriegstein et al., 1999). Rabphilin is phosphorylated after okadaic acid application, as is synapsin (Lonart and Sudhof, 1998). Interestingly, in a synapsin I and II double knockout (DKO), rabphilin phosphorylation was increased, possibly indicating a regulatory function of synapsin (Lonart and Simsek-Duran, 2006). If rabphilin would function as a (reserve) vesicle pool tag, one would expect to observe an effect on synaptic transmission in rabphilin knockout mice. In a first study, such an effect was not observed (Schluter et al., 1999), but when transmission was investigated more closely, rabphilin deletion was found to significantly accelerate recovery from synaptic depression, which argues in favor of increased vesicle recruitment (Deak et al., 2006). Note, however, that the

authors of the second study concluded that rabphilin is involved in vesicle priming, as an interaction of rabphilin with SNAP-25 was found to be required.

As explained above and in the discussion of Gaffield and Betz, 2007, a molecular vesicle tag functioning similarly to synapsin would probably be regulated in a phosphorylation-dependent manner and would likely display changes in phosphorylation pattern upon okadaic acid application (in line with the changes in vesicle mobility triggered by this treatment, see above). This rules out at least a few candidates, namely amphiphysin 1, dynamin 1, and synaptojanin 1 (Bauerfeind et al., 1997).

Another possibility for vesicle pool markers would be a differential distribution of calcium sensors and calcium sensor isoforms among the different vesicle populations. In this scenario, the resting vesicle population would require much higher calcium levels to be triggered to fuse at the active zones (explaining why high frequency stimulation is required to recruit these vesicles; note that this hypothesis in some sense overlaps with the synapsin theory, as synapsin phosphorylation is calcium-dependent, with synapsin binding thereby acting as an indirect calcium sensor). Indeed, release abilities could for instance be controlled by differential distribution of synaptotagmin isoforms, which display distinct calcium affinities (Sugita et al., 2002).

Several other proteins which could distinguish between actively recycling and non-recycling vesicle populations have been proposed: for instance, a differential distribution of the SNARE tetanus toxin-insensitive vesicle-associated membrane protein (VAMP7) has recently been described, with VAMP7 preferentially targeted to the resting vesicle pool in hippocampal neurons (Hua et al., 2011b). Interestingly, the vesicle-associated protein α-synuclein, mutations of which have been implicated in Parkinson's disease, might also function as a molecular tag of the reserve vesicle pool, as synapses of α-synuclein knockout mice display reduced numbers of undocked vesicles and a significant impairment in sustaining prolonged stimulation trains (Cabin et al., 2002; also discussed in Murthy and De Camilli, 2003).

In summary, the question of the relevant molecular tags distinguishing between the distinct vesicle pools is still unresolved, although for instance synapsin is likely to play a role. Although beyond the scope of this PhD project, it would be interesting to investigate the molecular composition of the two vesicle populations in more detail. This could involve FM dye injection into a living animal to label the vesicles undergoing recycling *in vivo*, followed by vesicle purification and vesicle FACS (fluorescence-activated cell sorting) to separate the vesicle populations. Instead, one could also separate the populations by taking advantage of the fact that the dye-containing vesicles display a shift in equilibrium density in density gradients after photo-oxidation (Courtoy et al., 1984). Vesicle composition could subsequently be investigated either by immunoblotting or mass spectrometry.

4.4 The Function of the Non-Recycling Vesicle Pool: The Buffer Pool Model

The observation that only a minority of all synaptic vesicles participate in neurotransmission not only raises the question on how these actively recycling vesicles might differ from the non-recycling vesicles, but also on the function of the "surplus" vesicles. In view of the fact that a large non-recycling vesicle pool (of quite consistent size as compared to the active vesicle pool) was found to be conserved in all preparations investigated in this study, it seems probable that these vesicles fulfil an important function. As described above, several experiments (Figures 3.20 to 3.35) indicate that the resting vesicles might serve as a molecular buffer for proteins involved in vesicle recycling, which I therefore consider their most probable physiological function. In this section, I will first introduce previous theories on the function of the non- or reluctantly-recycling vesicle population. I will then discuss the buffer pool model in more detail and will finally concentrate on the role of calcium in controlling the molecular buffer.

4.4.1 Previous Hypotheses for the Function of the Reluctantly-recycling Vesicles

The fact that some synapses, such as the NMJs or the calyx of Held, contain a multitude of vesicles has been known for decades (see also Rizzoli and Betz, 2005). As all vesicles appear to be filled with neurotransmitter (enabling experiments such as the one described in Ikeda and Bekkers, 2009), a logical assumption has been that these vesicles are also involved in releasing neurotransmitter, possibly functioning as a vesicle reserve. However, as described in Section 1.2.1, releasing these vesicles required prolonged high frequency stimulation in many preparations, with a large percentage of the vesicles in hippocampal neurons not even releasing under these conditions (Harata et al., 2001a; Harata et al., 2001b; Rizzoli and Betz, 2005; Denker and Rizzoli, 2010). Also, the "reserve" pool only became involved in recycling after the depletion of the recycling pool (Richards et al., 2000). In view of my *in vivo* data on vesicle use, such a scenario is highly unlikely to ever occur in the living animal, indicating that such a vesicle reserve is not necessary to sustain transmission *in vivo* (which is instead maintained by the few actively recycling vesicles).

Recently, it has been proposed that the resting vesicles in cultured hippocampal neurons drive spontaneous vesicle fusion, again in line with the original understanding that these vesicles are destined for fusion (Fredj and Burrone, 2009; see Section 1.2.2). However, if this was the case, I would have detected these vesicles in my FM 1-43 injection and photo-oxidation and pHluorin experiments. I therefore conclude that the reserve or resting vesicle population does not undergo fusion *in vivo* and therefore serves another function than neurotransmitter release.

Another possibility would be that the majority of vesicles serve to store neurotransmitter at the site of use, although the necessity of such a store is questionable at least for synapses employing amino acid neurotransmitters. The major argument against a function of vesicles in neurotransmitter storage is however the fact that vesicles seem to be relatively inert in terms of neurotransmitter exchange, at least as discussed in Van der Kloot, 2003, for acetylcholine. This tight containment of acetylcholine is for instance demonstrated by the substantial amount still present in the vesicles after vesicle isolation (Van der Kloot, 2003). Also, when slices of resting *Torpedo* electric organs were exposed to labelled choline, the cytoplasmic acetylcholine fraction became rapidly labelled, due to the fact that acetylcholine constantly leaks from the terminal and is then hydrolyzed in the synaptic cleft by acetylcholineesterase into choline and acetate. These components are then taken up again into the synapse and new acetylcholine is synthesized by the enzyme choline acetyltransferase, with the whole cycle being termed "futile recycling" (Whittaker, 1987). Isolated synaptic vesicles from such preparations did however not incorporate labelled acetylcholine, indicating that vesicles in resting preparations do not exchange much neurotransmitter with the cytoplasm (and might therefore not constitute a suitable neurotransmitter store). From such experiments, the percentage of acetylcholine in the cytoplasm could be calculated to be about 22% in the *Torpedo* electric organ (Weiler et al., 1982; Whittaker, 1987). Note that this fraction could be much higher in other preparations, with less than 20% of the total acetylcholine reported to be in vesicles in the rat diaphragm (Potter, 1970), casting further doubts on the usefulness of a vesicular acetylcholine store in the synaptic terminal (see also Van der Kloot, 2003).

In addition to neurotransmitter, vesicles have also been proposed to store acetylcholine precursors in the form of phosphatidylcholine in their membranes (Parducz et al., 1976). Upon demand, the phosphatidylcholine might be hydrolyzed and the vesicle dissolved, thereby releasing both acetylcholine and choline into the cytoplasm (as reviewed in Israel et al., 1979), but the experimental evidence for such a scenario is quite limited. Another proposed function for the surplus vesicles is removal of calcium after stimulation-induced influx (Israel et al., 1979), but this seems to be performed by ATP-dependent calcium pumps and sodium-calcium exchangers (Nicholls et al., 2001).

In summary, several arguments from my work and the work of others contradict the previously presented hypotheses for the function of the majority of vesicles. Instead, I propose that these vesicles function as a molecular buffer for soluble proteins (Denker et al., 2011b), as will be discussed in the next section.

4.4.2 The Buffer Model

The basic idea underlying the concept of a vesicular protein buffer derives from the observation that many neurons have an extended structure, with the cell body connected to the nerve terminals by long axons. The neuron could in principle fill the whole cell volume with the molecules required for vesicle recycling, but this would be highly uneconomic, as these molecules are only required at very specialized sites, i.e. the synapses (Denker et al., 2011b). As evident from the immunostainings (refer to Figure 3.26 for an example), these proteins are indeed selectively localized at the synapses (note however that this is less evident for complexin, Figure 3.35). Therefore, the neuron must have developed some anchoring mechanism which retains these proteins in the synapse and prevents them from diffusing into the much larger volume of the axon. As described in Denker et al., 2011b, the volume ratio between the effective axonal volume (i.e. calculated from the effective length which a protein can cover in its lifetime) and the synaptic volume can be on the scale of a few hundreds, indicating the strength of the sink the anchoring or buffer mechanism needs to cope with. This buffer could be provided by the surplus vesicles, with their importance underlined by the fact that they are evolutionarily conserved among distinctly related organisms (as mentioned above).

Although there are probably molecular differences between the actively recycling and buffer vesicles (see Section 4.3), they seem to be so similar that nearly all proteins involved in the synaptic vesicle cycle display a certain affinity for the buffer vesicles, as shown by the immunostaining and Western Blotting experiments presented in Figures 3.20 to 3.25. Also, disruption of the vesicle clusters by BWSV application caused the diffusion of most of these proteins into the axon (Table 4.1); with the exception of many molecular players of the clathrin pathway, which would bind to the fused vesicles in the plasma membrane after BWSV treatment, and complexin, which seems to rely much less on buffering than the other proteins and therefore is required to be present at high concentrations throughout the axon under control conditions (Figure 3.35).

The buffer vesicles therefore mimic the actively recycling vesicles to be able to bind all the different molecules interacting at some point of the vesicle cycle with the actively recycling vesicles, whereas they at the same time cannot bind them with too high affinity, as they need to be able to provide these molecules upon demand. This limited affinity (albeit strong enough to retain detectable protein levels even after the extensive vesicle isolation procedure; Figure 3.25) could explain why such a large number of buffer vesicles is required.

Table 4.1: Vesicle clusters retain a plethora of soluble proteins in the synapse
(see also Denker et al., 2011b)

Protein	Function on vesicle cluster	Localization on vesicle cluster	Loss from synapse upon BWSV treatment
Synapsin	+	+	+
Rab3	-	+	+
Rabphilin	-	+	+
Complexin	-	+	+/-
CSP	-	+	+
NSF	-	+	+
RIM2	-	+	+
Clathrin	-	+	+
Dynamin	-	+	-
Endophilin	-	+	-
Synaptojanin	-	+	-
Amphiphysin	-	+	-
AP180	-	+	-
Hsc70	-	+	+

An interesting observation in favor of the buffer pool model comes from ribbon synapses, which seem to define their vesicle pools differently (i.e. by localization, as the vesicles on the ribbons are released first, being then refilled from a cytoplasmic vesicle pool; Holt et al., 2004) and display high rates of intermixing between the cytoplasmic and ribbon-bound vesicle populations. These synapses therefore do not seem to have a reserve vesicle pool in the conventional sense and might therefore eventually use all of their vesicles for neurotransmission, allowing them to sustain the high rates of release (see Section 4.2). Consequently, these synapses probably do not reserve a fraction of their vesicles as a buffer. Importantly, they prevent protein diffusion from the synapse by the fact that they either have a very short axon, or no axon at all (Cowan et al., 2001), explaining why they might not depend on a molecular buffer as much as the synapses investigated here.

The molecular buffer provides the cell the possibility to tightly regulate when endocytosis should take place (i.e. after exocytosis and the associated calcium influx; the role of calcium in the control of buffering will be further discussed in the next section). For instance, if a readily retrievable vesicle population would exist at the plasma membrane, this could already provide the necessary binding sites for the clathrin machinery. However, I never observed such pre-formed structures (such as pre-assembled clathrin coats) in EM,

possibly due to the fact that the endocytic players are retained at a distance from the plasma membrane, i.e. in the vesicle cluster, to prevent premature endocytosis (note however that protein localization is not the only factor regulating endocytosis, as several of the proteins of the clathrin machinery require calcium-dependent dephosphorylation to be functional, see next section). Therefore, the vesicle cluster might serve a double function as a molecular buffer, by retaining the accessory factors in the synapse and by temporally controlling their function.

For many of the proteins investigated, a reversible interaction with synaptic vesicles has already been proposed (Sudhof, 2004). Also, several endocytic proteins have been observed bound to the vesicle cluster. Interestingly, as discussed in Shupliakov, 2009, several of these proteins have been described to migrate from the vesicle cluster to the periactive zone during synaptic activity, possibly triggered by calcium influx (see Section 4.4.3). Among these proteins is for instance the scaffolding protein intersectin, as shown in the lamprey giant reticulospinal synapse (Evergren et al., 2007). Similar observations have been reported for many dephosphins, proteins which become dephosphorylated upon calcium influx (Cousin and Robinson, 2001; see also next section), including dynamin (Evergren et al., 2007), amphiphysin (Evergren et al., 2004), epsin (Jakobsson et al., 2008), synaptojanin (Haffner et al., 1997), endophilin (Bai et al., 2010), and Eps 15 (Koh et al., 2007). As mentioned above, synapsin also disperses from the vesicle cluster upon synaptic activity (Chi et al., 2001) and also seems to migrate to the periactive zone (Bloom et al., 2003).

Recently, it has been proposed that these proteins form a proteinaceous inter-vesicular matrix (IVM), which restricts vesicle mobility (Shupliakov, 2009; Pechstein and Shupliakov, 2010). As several of these proteins have been reported to interact with the actin cytoskeleton either directly or indirectly (Hilfiker et al., 1999; Qualmann and Kelly, 2000; McPherson, 2002; see also Merrifield et al., 2002; Murthy and De Camilli, 2003), it was proposed that the IVM, in conjunction with the cytoskeleton, forms a cage to retain the vesicles at the active zones (note that actin is largely excluded from the interior of the vesicle cluster and seems to surround it instead; Dunaevsky and Connor, 2000; Shupliakov et al., 2002; Sankaranarayanan et al., 2003). According to Shupliakov, 2009, and Pechstein and Shupliakov, 2010, the (calcium-dependent) phosphorylation (for synapsin) or dephosphorylation (for dephosphins) of proteins of the IVM would disrupt the vesicle cluster and increase vesicle mobility upon stimulation (in agreement with the many studies linking vesicle mobility to phosphorylation status; Betz and Henkel, 1994; Kraszewski et al., 1995; Henkel et al., 1996b; Gaffield et al., 2006; Gaffield and Betz, 2007). Indeed, CaMKII was found to be excluded from the interior of the vesicle cluster at rest, but dispersed during stimulation, intermingling with the declustered vesicles (Tao-Cheng et al., 2006). In a way,

this model represents an extension of the classical synapsin hypothesis, which has also been reported to be involved in vesicle clustering and to be regulated by phosphorylation (Sections 1.1.3 and 4.3.1), to the endocytic proteins found within the vesicle cluster.

However, in view of my data, it seems highly unlikely that the vesicle cluster and the IVM become disrupted under physiological stimulation conditions. In addition, there does not seem to be a need for maintaining a large vesicle reservoir in front of the active zones *in vivo*, as neurotransmission is driven by only very few mobile vesicles in the living animal. Finally, it is difficult to envision how the molecular composition of the IVM could enable efficient vesicle cross-linking, especially in view of the fact that the role of the actin cytoskeleton in controlling vesicle dynamics is quite controversial, considering that preventing actin polymerization by latrunculin had no apparent effect on vesicle mobility in the frog (Gaffield et al., 2006) or mouse NMJs (Gaffield and Betz, 2007). Therefore, I regard the role of a molecular buffer as the most likely function of the vesicle cluster (note, however, that actin itself has also been proposed to retain regulatory molecules within the terminals; Sankaranarayanan et al., 2003; see also Pechstein and Shupliakov, 2010, for a discussion of the functional role of actin in the synapse).

4.4.3 The Role of Calcium in Controlling Molecular Buffering

When investigating the effects of calcium on protein buffering by ionomycin application and immunostaining (Figure 3.29) or by employing biochemical assays (Figures 3.30 to 3.35), it became evident that calcium regulates the binding and unbinding of a plethora of structurally and functionally distinct proteins from the vesicle cluster. Obviously, such a regulation mechanism would be an elegant solution to controlling the binding behavior of these different proteins: first, if electrostatic interactions were involved, the binding and distribution of very diverse proteins could be controlled, as described in Zilly et al., 2011, and discussed in Section 5. If this was not the case, a separate regulatory pathway would need to be generated and controlled in the synapse for every protein to be buffered. Also, if calcium mediated unbinding of the accessory molecules from the vesicle buffer, the same signal which drives exocytosis would at the same time ensure efficient endocytosis, thereby coupling these two processes.

Indeed, a role of calcium in triggering endocytosis is well established (as reviewed for instance in Shupliakov, 2009). This was for example shown at the lamprey giant reticulospinal synapse, where exocytosis and endocytosis were separated by removal of extracellular calcium after strong stimulation (Gad et al., 1998). This procedure arrested endocytosis, which was only resumed after the addition of low concentrations of calcium. Importantly, the amount of calcium required to trigger endocytosis is much lower than the

calcium concentration required to induce exocytosis: vesicles fuse at concentrations of 10-25 µM calcium (Schneggenburger and Neher, 2005), but the calcium concentration can also exceed 100 µM locally (as reviewed in Neher, 1998). Endocytosis, on the other hand, proceeds at submicromolar concentrations and is inhibited at a calcium concentration above 1 µM (Yao et al., 2009; see also Shupliakov, 2009). This distinct calcium requirements of exo- and endocytosis indicate that the calcium sensors of the two processes are likely different. Whereas synaptotagmin and other sensors have been implicated in triggering exocytosis, the calcium sensor for endocytosis seems to be calmodulin (Artalejo et al., 1996), which induces dephosphorylation of the dephosphins (Cousin and Robinson, 2001; for instance dynamin, amphiphysin, AP180, Eps15, epsin, and synaptojanin) by calcineurin (Marks and McMahon, 1998; Cousin and Robinson, 2001). Note that the dephosphins are not structurally related but are all similarly dephosphorylated upon stimulation, which is to some degree similar to their regulated unbinding from the vesicle cluster upon calcium influx. Note also that the process of calmodulin/calcineurin-mediated dephosphin dephosphorylation might be less straight-forward than depicted here, as calcineurin inhibition by cyclosporin A accelerates, instead of inhibits, endocytosis (Artalejo et al., 1996; Kuromi et al., 1997; Denker et al., 2009).

Importantly, calcium and calmodulin initiate not only clathrin-mediated endocytosis (CME), but seem to be involved in all forms of synaptic vesicle endocytosis during depolarization (Wu et al., 2009). Interestingly, a calcium channel controlling endocytosis upon exocytosis has recently been identified, which is formed by the multimerization of the vesicle-transmembrane protein Flower (Yao et al., 2009).

Consequently, the hypothesis that calcium influx might link exo- and endocytosis, possibly by regulating the unbinding of molecules required for vesicle recycling from the vesicle cluster, is in agreement with many previous studies (see also Hosoi et al., 2009). However, my data also indicate that the regulation of protein buffering might be more complex: different accessory molecules displayed quite different buffering behavior and responsiveness to regulation by calcium (Figures 3.31 to 3.35). Also, the loss of protein from the synapses upon BWSV application obviously represented a different level of regulation of protein binding to vesicles, as it occurred in the absence of calcium. Further experiments to clarify the role of calcium or other factors in the control of the vesicular buffer are therefore required. As a first experiment, it would be desirable to repeat the ionomycin application to mouse NMJs (Figure 3.29) and to investigate the effect on protein localization while ensuring that exocytosis is indeed blocked by using the SNARE-cleaving tetanus or botulinum toxins (alternatively, the toxin application could be combined with stimulation instead of ionomycin treatment).

5. Summary and Outlook

The aim of this project was to investigate synaptic vesicle recycling *in vivo*, with special emphasis on the amount of vesicles used for neurotransmission in living animals. The results presented in this thesis further complement our understanding of synaptic function by placing our knowledge on how synapses can react under certain stimulation conditions into the context of a behaving organism. This study may therefore serve as a point of reference for the numerous working models of vesicle pools and vesicle recycling derived from *in vitro* investigations.

Many of these studies have described the release and recycling properties of the reserve vesicle pool, which has been proposed to drive neurotransmission under strong stimulation. My investigations of vesicle use *in vivo*, using injection of FM dye and subsequent photo-oxidation, imaging of pHluorin *Drosophila* larvae and electron microscopy of the temperature-sensitive *Drosophila* dynamin mutant *shibire*, demonstrate that these vesicles are not directly involved in synaptic transmission in the living animal. Instead, at any one point in time, organisms rely on a very small population of vesicles which recycle repeatedly, although there seems to be a very slow turnover between the actively recycling and inactive vesicle pools over time (on the time scale of hours). This limited vesicle use was conserved among distantly related organisms (*C. elegans*, *Drosophila*, locust, cricket, zebrafish, frog, chicken embryo, mouse and rat) and preparations (i.e. NMJs as well as CNS synapses). It therefore probably reflects a general concept of synaptic function. Importantly, this use of only a small actively recycling vesicle population also persisted under stress, as shown for the predation of locusts by frogs, albeit the percentage of recycling vesicles was significantly increased as compared to non-stressed animals, revealing increased synaptic activity.

In a second part of the project, I investigated the molecular mechanism distinguishing the recycling from the non-recycling vesicle population. From the spatially intermixed distribution of the active and inactive vesicles, it was proposed that the former might be mobile, allowing them to reach the active zones and fuse, whereas the latter should be clustered and immobile. As synapsin had been proposed to cluster vesicles, vesicle mobility in synapsin-null *Drosophila* larvae was investigated by FRAP. Indeed, vesicle mobility was increased when synapsin was absent, and this also correlated with a significantly higher number of actively recycling vesicles. Therefore, it was concluded that synapsin is one, albeit not the only, molecular player distinguishing between the recycling and inactive vesicles, probably by binding and immobilizing the latter, thereby preventing them from reaching the active zones and undergoing fusion.

Finally, I turned to the function of the majority of synaptic vesicles (95-99% in most synapses) which do not participate in neurotransmission *in vivo*. Due to the extended structure of most neurons, the hypothesis was developed that the surplus vesicles might function as a molecular buffer, concentrating molecules required for synaptic vesicle recycling in the synapses and preventing their diffusion into the axon. Whereas it was difficult to test this function directly (this would require a stable and selective removal of only the non-recycling vesicles, preferably *in vivo*), several experiments revealed that the vesicle cluster fulfils the basic requirements of a molecular buffer, in that it enriches the above-mentioned proteins (ranging from molecules involved in exocytosis to molecules implicated in endocytosis; as shown by immunostaining in combination with high-resolution microscopy and by immunoblotting of purified synaptic vesicles) and in that its disruption (by BWSV in mouse NMJs) causes protein loss into the axon. If the vesicle cluster maintained soluble accessory molecules in the synapse, it should also be able to provide them to a recycling vesicle upon demand. Indeed, it was found by triggering calcium influx in mouse NMJs through ionomycin application and by biochemical assays that the buffering reaction could be regulated by calcium, which causes protein loss from the vesicles.

From the data presented in this study, a new model for synaptic function *in vivo* was deduced (Figure 4.1), also encompassing recent data on vesicle mobility (Kamin et al., 2010) and vesicle recycling (Hoopmann et al., 2010) (note however that these latter data were obtained *in vitro*). Briefly, it states that only very few vesicles undergo active recycling. These vesicles are highly mobile, enabling them to reach the active zones and undergo fusion. The actively recycling vesicles might be recycled via an endosomal intermediate (not depicted in Figure 4.1, as it was also not observed in EM; see also Section 4.1.3). The majority of the vesicles are cross-linked and immobilized by synapsin and other cross-linking molecules of unknown identity. They do not participate in recycling, but serve to buffer molecules required for exo- and endocytosis of the active vesicle population. These two vesicle populations undergo at least partial slow turnover.

The buffer model proposes an entirely new function for the majority of synaptic vesicles. Instead of undergoing recycling themselves, they support synaptic transmission indirectly by ensuring an adequate supply of required molecules. This reflects a rather simple but effective principle: once a cell has acquired the ability to produce a certain cellular entity, such as organelles or proteins, it might not only use them for their original function, but it could for instance also use them to concentrate reaction partners at a specific site. The elegance of such an approach lies in the similarity of the buffer entities and the active members of the population, as the buffering organelles or proteins will display an inherent affinity for all required reaction partners.

This concept of molecular buffering developed here for synaptic vesicles could well be applicable to other cellular processes and structures. For example, as discussed in Lang and Rizzoli, 2010, the advent of super-resolution microscopy has revealed that many proteins are found in clusters instead of being homogeneously distributed. These proteins include synaptotagmin, which remains clustered at the plasma membrane after vesicle exocytosis (Willig et al., 2006), syntaxin 1 (Sieber et al., 2007), vinculin at focal adhesions (Betzig et al., 2006), membrane proteins of lysosomes (Betzig et al., 2006) and endosomes (Geumann et al., 2010), mitochondrial proteins (Betzig et al., 2006; Donnert et al., 2007; Schmidt et al., 2009) and the nuclear lamina component lamin B (Schermelleh et al., 2008). Such clusters could for instance accumulate reaction partners and at the same time prevent undesired molecular interactions by maintaining the cluster-integrated proteins in an inactive state, as has been proposed for syntaxin (Bar-On et al., 2009; see also Sieber et al., 2007). Note, however, that clusters can also simply reflect a need to locally increase protein concentration, for instance to reach a signalling threshold (as reviewed in Lang and Rizzoli, 2010).

As mentioned above, the regulation of the vesicular buffering function by calcium could well be mediated by electrostatic interactions. Again, this might represent a more general concept of cell and molecular biology, as it has recently been shown that the distribution of structurally very diverse plasma membrane proteins can be regulated by calcium (Zilly et al., 2011). Here, calcium was shown to rapidly and reversibly induce protein clustering via electrostatic effects. It remains to be seen whether such electrostatic interactions play a more general role in cellular processes in which a plethora of different proteins need to be controlled in a parallel manner.

Finally, the basic approach behind the here-described project was to investigate a cellular process, here the recycling of synaptic vesicles, under as physiological conditions as possible (as performed by FM dye injection, with the animals being afterwards allowed to behave freely). In allusion to the investigation of animal behavior, this approach was termed cellular ethology. This by definition implies that experimental conditions are less precisely defined as compared to *in vitro* experiments. For instance, using the approaches described here, I cannot control the stimulation frequencies experienced by the organs of interest. However, the cellular ethology approach provides results of greater physiological relevance than the experimental manipulations associated with the more traditional approaches of studying vesicle recycling. To further improve our understanding of cellular functions and to evaluate the relevance of *in vitro* results for the *in vivo* situation, more studies encompassing the cellular ethology approach would be desirable.

While the decades of *in vitro* synaptic research have been invaluable for teaching us the versatile reactions the synapse is capable of under different conditions, the field now

needs to define which of the deduced models of vesicle pools, mobility and recycling play a role for neurotransmission *in vivo* and to what extent. Only when this is achieved will we also be able to detect, understand and possibly cure associated diseases.

Bibliography

Abbe E (1873) Beiträge zur Theorie des Mikroskops und der mikroskopischen Wahrnehmung. Arch. Mikr. Anat. 9:55.

Ahnert-Hilger G, Holtje M, Pahner I, Winter S, Brunk I (2003) Regulation of vesicular neurotransmitter transporters. Rev Physiol Biochem Pharmacol 150:140-160.

Akbergenova Y, Bykhovskaia M (2010) Synapsin regulates vesicle organization and activity-dependent recycling at Drosophila motor boutons. Neuroscience 170:441-452.

Akbergenova Y, Bykhovskaia M (2009) Stimulation-induced formation of the reserve pool of vesicles in Drosophila motor boutons. J Neurophysiol 101:2423-2433.

Angaut-Petit D, Molgo J, Connold AL, Faille L (1987) The levator auris longus muscle of the mouse: a convenient preparation for studies of short- and long-term presynaptic effects of drugs or toxins. Neurosci Lett 82:83-88.

Angleson JK, Betz WJ (2001) Intraterminal Ca(2+) and spontaneous transmitter release at the frog neuromuscular junction. J Neurophysiol 85:287-294.

Antonin W, Fasshauer D, Becker S, Jahn R, Schneider TR (2002) Crystal structure of the endosomal SNARE complex reveals common structural principles of all SNAREs. Nat Struct Biol 9:107-111.

Antonin W, Riedel D, von Mollard GF (2000) The SNARE Vti1a-beta is localized to small synaptic vesicles and participates in a novel SNARE complex. J Neurosci 20:5724-5732.

Araki S, Kikuchi A, Hata Y, Isomura M, Takai Y (1990) Regulation of reversible binding of smg p25A, a ras p21-like GTP-binding protein, to synaptic plasma membranes and vesicles by its specific regulatory protein, GDP dissociation inhibitor. J Biol Chem 265:13007-13015.

Aravanis AM, Pyle JL, Tsien RW (2003) Single synaptic vesicles fusing transiently and successively without loss of identity. Nature 423:643-647.

Artalejo CR, Elhamdani A, Palfrey HC (1996) Calmodulin is the divalent cation receptor for rapid endocytosis, but not exocytosis, in adrenal chromaffin cells. Neuron 16:195-205.

Ashmore JF, Copenhagen DR (1983) An analysis of transmission from cones to hyperpolarizing bipolar cells in the retina of the turtle. J Physiol 340:569-597.

Bai J, Hu Z, Dittman JS, Pym EC, Kaplan JM (2010) Endophilin functions as a membrane-bending molecule and is delivered to endocytic zones by exocytosis. Cell 143:430-441.

Bar-On D, Gutman M, Mezer A, Ashery U, Lang T, Nachliel E (2009) Evaluation of the heterogeneous reactivity of the syntaxin molecules on the inner leaflet of the plasma membrane. J Neurosci 29:12292-12301.

Barysch SV, Jahn R, Rizzoli SO (2010) A fluorescence-based in vitro assay for investigating early endosome dynamics. Nat Protoc 5:1127-1137.

Bauerfeind R, Takei K, De Camilli P (1997) Amphiphysin I is associated with coated endocytic intermediates and undergoes stimulation-dependent dephosphorylation in nerve terminals. J Biol Chem 272:30984-30992.

Bear MF, Connors BW, Paradiso MA (2006) Neuroscience: Exploring the brain. 3rd edition. Philadelphia, Lippincott Williams & Wilkins.

Benfenati F, Greengard P, Brunner J, Bahler M (1989) Electrostatic and hydrophobic interactions of synapsin I and synapsin I fragments with phospholipid bilayers. J Cell Biol 108:1851-1862.

Bennett MK, Calakos N, Scheller RH (1992) Syntaxin: a synaptic protein implicated in docking of synaptic vesicles at presynaptic active zones. Science 257:255-259.

Betz WJ, Bewick GS (1992) Optical analysis of synaptic vesicle recycling at the frog neuromuscular junction. Science 255:200-203.

Betz WJ, Bewick GS, Ridge RM (1992a) Intracellular movements of fluorescently labeled synaptic vesicles in frog motor nerve terminals during nerve stimulation. Neuron 9:805-813.

Betz WJ, Henkel AW (1994) Okadaic acid disrupts clusters of synaptic vesicles in frog motor nerve terminals. J Cell Biol 124:843-854.

Betz WJ, Mao F, Bewick GS (1992b) Activity-dependent fluorescent staining and destaining of living vertebrate motor nerve terminals. J Neurosci 12:363-375.

Betz WJ, Wu LG (1995) Synaptic transmission. Kinetics of synaptic-vesicle recycling. Curr Biol 5:1098-1101.

Betzig E, Patterson GH, Sougrat R, Lindwasser OW, Olenych S, Bonifacino JS, Davidson MW, Lippincott-Schwartz J, Hess HF (2006) Imaging intracellular fluorescent proteins at nanometer resolution. Science 313:1642-1645.

Bewick GS (2003) Maintenance of transmitter release from neuromuscular junctions with different patterns of usage "in vivo". J Neurocytol 32:473-487.

Bigland-Ritchie B, Kukulka CG, Lippold OC, Woods JJ (1982) The absence of neuromuscular transmission failure in sustained maximal voluntary contractions. J Physiol 330:265-278.

Birks RI, MacIntosh FC (1961) Acetylcholine metabolism of a sympathetic ganglion. Can J Biochem Physiol 39:787-827.

Blioch ZL, Glagoleva IM, Liberman EA, Nenashev VA (1968) A study of the mechanism of quantal transmitter release at a chemical synapse. J Physiol 199:11-35.

Block MR, Glick BS, Wilcox CA, Wieland FT, Rothman JE (1988) Purification of an N-ethylmaleimide-sensitive protein catalyzing vesicular transport. Proc Natl Acad Sci U S A 85:7852-7856.

Bloom O, Evergren E, Tomilin N, Kjaerulff O, Low P, Brodin L, Pieribone VA, Greengard P, Shupliakov O (2003) Colocalization of synapsin and actin during synaptic vesicle recycling. J Cell Biol 161:737-747.

Bock JB, Matern HT, Peden AA, Scheller RH (2001) A genomic perspective on membrane compartment organization. Nature 409:839-841.

Brenner S (1974) The genetics of Caenorhabditis elegans. Genetics 77:71-94.

Brodin L, Low P, Shupliakov O (2000) Sequential steps in clathrin-mediated synaptic vesicle endocytosis. Curr Opin Neurobiol 10:312-320.

Brose N, Petrenko AG, Sudhof TC, Jahn R (1992) Synaptotagmin: a calcium sensor on the synaptic vesicle surface. Science 256:1021-1025.

Buckers J, Wildanger D, Vicidomini G, Kastrup L, Hell SW (2011) Simultaneous multi-lifetime multi-color STED imaging for colocalization analyses. Opt Express 19:3130-3143.

Bykhovskaia M (2011) Synapsin regulation of vesicle organization and functional pools. Semin Cell Dev Biol 22:387-392.

Cabin DE, Shimazu K, Murphy D, Cole NB, Gottschalk W, McIlwain KL, Orrison B, Chen A, Ellis CE, Paylor R, Lu B, Nussbaum RL (2002) Synaptic vesicle depletion correlates with attenuated synaptic responses to prolonged repetitive stimulation in mice lacking alpha-synuclein. J Neurosci 22:8797-8807.

Caldwell JC, Miller MM, Wing S, Soll DR, Eberl DF (2003) Dynamic analysis of larval locomotion in Drosophila chordotonal organ mutants. Proc Natl Acad Sci U S A 100:16053-16058.

Catterall WA (1992) Cellular and molecular biology of voltage-gated sodium channels. Physiol Rev 72:S15-48.

Ceccarelli B, Hurlbut WP (1980) Vesicle hypothesis of the release of quanta of acetylcholine. Physiol Rev 60:396-441.

Ceccarelli B, Hurlbut WP, Mauro A (1972) Depletion of vesicles from frog neuromuscular junctions by prolonged tetanic stimulation. J Cell Biol 54:30-38.

Ceccarelli B, Hurlbut WP, Mauro A (1973) Turnover of transmitter and synaptic vesicles at the frog neuromuscular junction. J Cell Biol 57:499-524.

Cesca F, Baldelli P, Valtorta F, Benfenati F (2010) The synapsins: key actors of synapse function and plasticity. Prog Neurobiol 91:313-348.

Chen X, Barg S, Almers W (2008) Release of the styryl dyes from single synaptic vesicles in hippocampal neurons. J Neurosci 28:1894-1903.

Chen X, Tomchick DR, Kovrigin E, Arac D, Machius M, Sudhof TC, Rizo J (2002) Three-dimensional structure of the complexin/SNARE complex. Neuron 33:397-409.

Chi P, Greengard P, Ryan TA (2001) Synapsin dispersion and reclustering during synaptic activity. Nat Neurosci 4:1187-1193.

Chung C, Barylko B, Leitz J, Liu X, Kavalali ET (2010) Acute dynamin inhibition dissects synaptic vesicle recycling pathways that drive spontaneous and evoked neurotransmission. J Neurosci 30:1363-1376.

Clayton EL, Cousin MA (2009) The molecular physiology of activity-dependent bulk endocytosis of synaptic vesicles. J Neurochem 111:901-914.

Clayton EL, Evans GJ, Cousin MA (2008) Bulk synaptic vesicle endocytosis is rapidly triggered during strong stimulation. J Neurosci 28:6627-6632.

Clements AN, May TE (1974) Studies on locust neuromuscular physiology in relation to glutamic acid. J Exp Biol 60:673-705.

Coleman WL, Bykhovskaia M (2009a) Rab3a-mediated vesicle recruitment regulates short-term plasticity at the mouse diaphragm synapse. Mol Cell Neurosci 41:286-296.

Coleman WL, Bykhovskaia M (2009b) Synapsin I accelerates the kinetics of neurotransmitter release in mouse motor terminals. Synapse 63:531-533.

Courtoy PJ, Quintart J, Baudhuin P (1984) Shift of equilibrium density induced by 3,3'-diaminobenzidine cytochemistry: a new procedure for the analysis and purification of peroxidase-containing organelles. J Cell Biol 98:870-876.

Cousin MA, Robinson PJ (2001) The dephosphins: dephosphorylation by calcineurin triggers synaptic vesicle endocytosis. Trends Neurosci 24:659-665.

Cowan WM, Sudhof TC, Stevens CF (2001) Synapses. Baltimore, Johns Hopkins University Press.

Darcy KJ, Staras K, Collinson LM, Goda Y (2006) Constitutive sharing of recycling synaptic vesicles between presynaptic boutons. Nat Neurosci 9:315-321.

David C, McPherson PS, Mundigl O, de Camilli P (1996) A role of amphiphysin in synaptic vesicle endocytosis suggested by its binding to dynamin in nerve terminals. Proc Natl Acad Sci U S A 93:331-335.

De Camilli P, Cameron R, Greengard P (1983a) Synapsin I (protein I), a nerve terminal-specific phosphoprotein. I. Its general distribution in synapses of the central and peripheral nervous system demonstrated by immunofluorescence in frozen and plastic sections. J Cell Biol 96:1337-1354.

De Camilli P, Harris SM, Jr., Huttner WB, Greengard P (1983b) Synapsin I (Protein I), a nerve terminal-specific phosphoprotein. II. Its specific association with synaptic vesicles demonstrated by immunocytochemistry in agarose-embedded synaptosomes. J Cell Biol 96:1355-1373.

De Camilli P, Takei K (1996) Molecular mechanisms in synaptic vesicle endocytosis and recycling. Neuron 16:481-486.

de Lange RP, de Roos AD, Borst JG (2003) Two modes of vesicle recycling in the rat calyx of Held. J Neurosci 23:10164-10173.

Deak F, Shin OH, Tang J, Hanson P, Ubach J, Jahn R, Rizo J, Kavalali ET, Sudhof TC (2006) Rabphilin regulates SNARE-dependent re-priming of synaptic vesicles for fusion. Embo J 25:2856-2866.

Deerinck TJ, Martone ME, Lev-Ram V, Green DP, Tsien RY, Spector DL, Huang S, Ellisman MH (1994) Fluorescence photooxidation with eosin: a method for high resolution immunolocalization and in situ hybridization detection for light and electron microscopy. J Cell Biol 126:901-910.

Del Castillo J, Katz B (1954) Quantal components of the end-plate potential. J Physiol 124:560-573.

Delgado R, Maureira C, Oliva C, Kidokoro Y, Labarca P (2000) Size of vesicle pools, rates of mobilization, and recycling at neuromuscular synapses of a Drosophila mutant, shibire. Neuron 28:941-953.

Denker A, Bethani I, Kröhnert K, Körber C, Horstmann H, Wilhelm BG, Barysch SV, Kuner T, Neher E, Rizzoli SO (2011a) A small pool of vesicles maintains synaptic activity in vivo. Proc Natl Acad Sci U S A (epub ahead of print)

Denker A, Kröhnert K, Bückers J, Neher E, Rizzoli SO (2011b) The reserve pool of synaptic vesicles acts as a buffer for proteins involved in synaptic vesicle recycling. Proc Natl Acad Sci U S A (epub ahead of print)

Denker A, Krohnert K, Rizzoli SO (2009) Revisiting synaptic vesicle pool localization in the Drosophila neuromuscular junction. J Physiol 587:2919-2926.

Denker A, Rizzoli SO (2010) Synaptic vesicle pools: an update. Front Synaptic Neurosci 2:135.

Di Paolo G, De Camilli P (2006) Phosphoinositides in cell regulation and membrane dynamics. Nature 443:651-657.

Donnert G, Keller J, Medda R, Andrei MA, Rizzoli SO, Luhrmann R, Jahn R, Eggeling C, Hell SW (2006) Macromolecular-scale resolution in biological fluorescence microscopy. Proc Natl Acad Sci U S A 103:11440-11445.

Donnert G, Keller J, Wurm CA, Rizzoli SO, Westphal V, Schonle A, Jahn R, Jakobs S, Eggeling C, Hell SW (2007) Two-color far-field fluorescence nanoscopy. Biophys J 92:L67-69.

Duffy JB (2002) GAL4 system in Drosophila: a fly geneticist's Swiss army knife. Genesis 34:1-15.

Dulubova I, Lou X, Lu J, Huryeva I, Alam A, Schneggenburger R, Sudhof TC, Rizo J (2005) A Munc13/RIM/Rab3 tripartite complex: from priming to plasticity? Embo J 24:2839-2850.

Dulubova I, Sugita S, Hill S, Hosaka M, Fernandez I, Sudhof TC, Rizo J (1999) A conformational switch in syntaxin during exocytosis: role of munc18. Embo J 18:4372-4382.

Dulubova I, Yamaguchi T, Gao Y, Min SW, Huryeva I, Sudhof TC, Rizo J (2002) How Tlg2p/syntaxin 16 'snares' Vps45. Embo J 21:3620-3631.

Dunaevsky A, Connor EA (2000) F-actin is concentrated in nonrelease domains at frog neuromuscular junctions. J Neurosci 20:6007-6012.

Elmqvist D, Quastel DM (1965) A quantitative study of end-plate potentials in isolated human muscle. J Physiol 178:505-529.

Esser L, Wang CR, Hosaka M, Smagula CS, Sudhof TC, Deisenhofer J (1998) Synapsin I is structurally similar to ATP-utilizing enzymes. Embo J 17:977-984.

Evans GJ, Morgan A, Burgoyne RD (2003) Tying everything together: the multiple roles of cysteine string protein (CSP) in regulated exocytosis. Traffic 4:653-659.

Evergren E, Gad H, Walther K, Sundborger A, Tomilin N, Shupliakov O (2007) Intersectin is a negative regulator of dynamin recruitment to the synaptic endocytic zone in the central synapse. J Neurosci 27:379-390.

Evergren E, Marcucci M, Tomilin N, Low P, Slepnev V, Andersson F, Gad H, Brodin L, De Camilli P, Shupliakov O (2004) Amphiphysin is a component of clathrin coats formed during synaptic vesicle recycling at the lamprey giant synapse. Traffic 5:514-528.

Fasshauer D, Antonin W, Subramaniam V, Jahn R (2002) SNARE assembly and disassembly exhibit a pronounced hysteresis. Nat Struct Biol 9:144-151.

Fasshauer D, Sutton RB, Brunger AT, Jahn R (1998) Conserved structural features of the synaptic fusion complex: SNARE proteins reclassified as Q- and R-SNAREs. Proc Natl Acad Sci U S A 95:15781-15786.

Fatt P, Katz B (1952) Spontaneous subthreshold activity at motor nerve endings. J Physiol 117:109-128.

Ferguson SM, Brasnjo G, Hayashi M, Wolfel M, Collesi C, Giovedi S, Raimondi A, Gong LW, Ariel P, Paradise S, O'Toole E, Flavell R, Cremona O, Miesenbock G, Ryan TA, De Camilli P (2007) A selective activity-dependent requirement for dynamin 1 in synaptic vesicle endocytosis. Science 316:570-574.

Fernandez-Alfonso T, Kwan R, Ryan TA (2006) Synaptic vesicles interchange their membrane proteins with a large surface reservoir during recycling. Neuron 51:179-186.

Fernandez-Alfonso T, Ryan TA (2004) The kinetics of synaptic vesicle pool depletion at CNS synaptic terminals. Neuron 41:943-953.

Fernandez-Alfonso T, Ryan TA (2008) A heterogeneous "resting" pool of synaptic vesicles that is dynamically interchanged across boutons in mammalian CNS synapses. Brain Cell Biol 36:87-100.

Fernandez-Chacon R, Konigstorfer A, Gerber SH, Garcia J, Matos MF, Stevens CF, Brose N, Rizo J, Rosenmund C, Sudhof TC (2001) Synaptotagmin I functions as a calcium regulator of release probability. Nature 410:41-49.

Fernandez I, Arac D, Ubach J, Gerber SH, Shin O, Gao Y, Anderson RG, Sudhof TC, Rizo J (2001) Three-dimensional structure of the synaptotagmin 1 C2B-domain: synaptotagmin 1 as a phospholipid binding machine. Neuron 32:1057-1069.

Fesce R, Grohovaz F, Valtorta F, Meldolesi J (1994) Neurotransmitter release: fusion or 'kiss-and-run'? Trends Cell Biol 4:1-4.

Fischer von Mollard G, Stahl B, Walch-Solimena C, Takei K, Daniels L, Khoklatchev A, De Camilli P, Sudhof TC, Jahn R (1994) Localization of Rab5 to synaptic vesicles identifies endosomal intermediate in synaptic vesicle recycling pathway. Eur J Cell Biol 65:319-326.

Fischer von Mollard G, Sudhof TC, Jahn R (1991) A small GTP-binding protein dissociates from synaptic vesicles during exocytosis. Nature 349:79-81.

Flucher BE, Daniels MP (1989) Distribution of Na+ channels and ankyrin in neuromuscular junctions is complementary to that of acetylcholine receptors and the 43 kd protein. Neuron 3:163-175.

Foster M, Sherrington CS (1897) A textbook of physiology, part three: The central nervous system. 7th edition. London, MacMillan & Co. Ltd.

Fredj NB, Burrone J (2009) A resting pool of vesicles is responsible for spontaneous vesicle fusion at the synapse. Nat Neurosci 12:751-758.

Furshpan EJ, Potter DD (1959) Transmission at the giant motor synapses of the crayfish. J Physiol 145:289-325.

Gad H, Low P, Zotova E, Brodin L, Shupliakov O (1998) Dissociation between Ca2+-triggered synaptic vesicle exocytosis and clathrin-mediated endocytosis at a central synapse. Neuron 21:607-616.

Gaffield MA, Betz WJ (2007) Synaptic vesicle mobility in mouse motor nerve terminals with and without synapsin. J Neurosci 27:13691-13700.

Gaffield MA, Rizzoli SO, Betz WJ (2006) Mobility of synaptic vesicles in different pools in resting and stimulated frog motor nerve terminals. Neuron 51:317-325.

Gaffield MA, Tabares L, Betz WJ (2009) Preferred sites of exocytosis and endocytosis colocalize during high- but not lower-frequency stimulation in mouse motor nerve terminals. J Neurosci 29:15308-15316.

Galarreta M, Hestrin S (1999) A network of fast-spiking cells in the neocortex connected by electrical synapses. Nature 402:72-75.

Gandhi SP, Stevens CF (2003) Three modes of synaptic vesicular recycling revealed by single-vesicle imaging. Nature 423:607-613.

Gennaro JF, Jr., Nastuk WL, Rutherford DT (1978) Reversible depletion of synaptic vesicles induced by application of high external potassium to the frog neuromuscular junction. J Physiol 280:237-247.

Geppert M, Goda Y, Hammer RE, Li C, Rosahl TW, Stevens CF, Sudhof TC (1994) Synaptotagmin I: a major Ca2+ sensor for transmitter release at a central synapse. Cell 79:717-727.

Geumann U, Schafer C, Riedel D, Jahn R, Rizzoli SO (2010) Synaptic membrane proteins form stable microdomains in early endosomes. Microsc Res Tech 73:606-617.

Giovedi S, Vaccaro P, Valtorta F, Darchen F, Greengard P, Cesareni G, Benfenati F (2004) Synapsin is a novel Rab3 effector protein on small synaptic vesicles. I. Identification and characterization of the synapsin I-Rab3 interactions in vitro and in intact nerve terminals. J Biol Chem 279:43760-43768.

Gitler D, Takagishi Y, Feng J, Ren Y, Rodriguiz RM, Wetsel WC, Greengard P, Augustine GJ (2004) Different presynaptic roles of synapsins at excitatory and inhibitory synapses. J Neurosci 24:11368-11380.

Glyvuk N, Tsytsyura Y, Geumann C, D'Hooge R, Huve J, Kratzke M, Baltes J, Boening D, Klingauf J, Schu P (2010) AP-1/sigma1B-adaptin mediates endosomal synaptic vesicle recycling, learning and memory. Embo J 29:1318-1330.

Godenschwege TA, Reisch D, Diegelmann S, Eberle K, Funk N, Heisenberg M, Hoppe V, Hoppe J, Klagges BR, Martin JR, Nikitina EA, Putz G, Reifegerste R, Reisch N, Rister J, Schaupp M, Scholz H, Schwarzel M, Werner U, Zars TD, Buchner S, Buchner E

(2004) Flies lacking all synapsins are unexpectedly healthy but are impaired in complex behaviour. Eur J Neurosci 20:611-622.

Gorassini M, Eken T, Bennett DJ, Kiehn O, Hultborn H (2000) Activity of hindlimb motor units during locomotion in the conscious rat. J Neurophysiol 83:2002-2011.

Grabenbauer M, Geerts WJ, Fernadez-Rodriguez J, Hoenger A, Koster AJ, Nilsson T (2005) Correlative microscopy and electron tomography of GFP through photooxidation. Nat Methods 2:857-862.

Gracheva EO, Hadwiger G, Nonet ML, Richmond JE (2008) Direct interactions between C. elegans RAB-3 and Rim provide a mechanism to target vesicles to the presynaptic density. Neurosci Lett 444:137-142.

Granseth B, Odermatt B, Royle SJ, Lagnado L (2006) Clathrin-mediated endocytosis is the dominant mechanism of vesicle retrieval at hippocampal synapses. Neuron 51:773-786.

Greengard P, Benfenati F, Valtorta F (1994) Synapsin I, an actin-binding protein regulating synaptic vesicle traffic in the nerve terminal. Adv Second Messenger Phosphoprotein Res 29:31-45.

Grigliatti TA, Hall L, Rosenbluth R, Suzuki DT (1973) Temperature-sensitive mutations in Drosophila melanogaster. XIV. A selection of immobile adults. Mol Gen Genet 120:107-114.

Groemer TW, Klingauf J (2007) Synaptic vesicles recycling spontaneously and during activity belong to the same vesicle pool. Nat Neurosci 10:145-147.

Groffen AJ, Martens S, Diez Arazola R, Cornelisse LN, Lozovaya N, de Jong AP, Goriounova NA, Habets RL, Takai Y, Borst JG, Brose N, McMahon HT, Verhage M (2010) Doc2b is a high-affinity Ca2+ sensor for spontaneous neurotransmitter release. Science 327:1614-1618.

Guatimosim C, Hull C, Von Gersdorff H, Prado MA (2002) Okadaic acid disrupts synaptic vesicle trafficking in a ribbon-type synapse. J Neurochem 82:1047-1057.

Haffner C, Takei K, Chen H, Ringstad N, Hudson A, Butler MH, Salcini AE, Di Fiore PP, De Camilli P (1997) Synaptojanin 1: localization on coated endocytic intermediates in nerve terminals and interaction of its 170 kDa isoform with Eps15. FEBS Lett 419:175-180.

Hagiwara S, Chichibu S, Simpson N (1968) Neuromuscular mechanisms of wing beat in hummingbirds. Zeitschrift für vergleichende Physiologie 60:209-218.

Hamburger V, Hamilton HL (1951) A series of normal stages in the development of the chick embryo. J Morphol 88:49-92.

Hanson PI, Heuser JE, Jahn R (1997) Neurotransmitter release - four years of SNARE complexes. Curr Opin Neurobiol 7:310-315.

Hanson PI, Otto H, Barton N, Jahn R (1995) The N-ethylmaleimide-sensitive fusion protein and alpha-SNAP induce a conformational change in syntaxin. J Biol Chem 270:16955-16961.

Hao W, Luo Z, Zheng L, Prasad K, Lafer EM (1999) AP180 and AP-2 interact directly in a complex that cooperatively assembles clathrin. J Biol Chem 274:22785-22794.

Harata N, Pyle JL, Aravanis AM, Mozhayeva M, Kavalali ET, Tsien RW (2001a) Limited numbers of recycling vesicles in small CNS nerve terminals: implications for neural signaling and vesicular cycling. Trends Neurosci 24:637-643.

Harata N, Ryan TA, Smith SJ, Buchanan J, Tsien RW (2001b) Visualizing recycling synaptic vesicles in hippocampal neurons by FM 1-43 photoconversion. Proc Natl Acad Sci U S A 98:12748-12753.

Harata NC, Choi S, Pyle JL, Aravanis AM, Tsien RW (2006) Frequency-dependent kinetics and prevalence of kiss-and-run and reuse at hippocampal synapses studied with novel quenching methods. Neuron 49:243-256.

Hayashi T, Yamasaki S, Nauenburg S, Binz T, Niemann H (1995) Disassembly of the reconstituted synaptic vesicle membrane fusion complex in vitro. Embo J 14:2317-2325.

Hell SW (2007) Far-field optical nanoscopy. Science 316:1153-1158.

Hell SW, Wichmann J (1994) Breaking the diffraction resolution limit by stimulated emission: stimulated-emission-depletion fluorescence microscopy. Opt Lett 19:780-782.

Henkel AW, Betz WJ (1995a) Monitoring of black widow spider venom (BWSV) induced exo- and endocytosis in living frog motor nerve terminals with FM1-43. Neuropharmacology 34:1397-1406.

Henkel AW, Betz WJ (1995b) Staurosporine blocks evoked release of FM1-43 but not acetylcholine from frog motor nerve terminals. J Neurosci 15:8246-8258.

Henkel AW, Lubke J, Betz WJ (1996a) FM1-43 dye ultrastructural localization in and release from frog motor nerve terminals. Proc Natl Acad Sci U S A 93:1918-1923.

Henkel AW, Simpson LL, Ridge RM, Betz WJ (1996b) Synaptic vesicle movements monitored by fluorescence recovery after photobleaching in nerve terminals stained with FM1-43. J Neurosci 16:3960-3967.

Hennig R, Lømo T (1985) Firing patterns of motor units in normal rats. Nature 314:164-166.

Heuser JE, Reese TS (1973) Evidence for recycling of synaptic vesicle membrane during transmitter release at the frog neuromuscular junction. J Cell Biol 57:315-344.

Hilfiker S, Pieribone VA, Czernik AJ, Kao HT, Augustine GJ, Greengard P (1999) Synapsins as regulators of neurotransmitter release. Philos Trans R Soc Lond B Biol Sci 354:269-279.

Hilfiker S, Schweizer FE, Kao HT, Czernik AJ, Greengard P, Augustine GJ (1998) Two sites of action for synapsin domain E in regulating neurotransmitter release. Nat Neurosci 1:29-35.

Hinshaw JE, Schmid SL (1995) Dynamin self-assembles into rings suggesting a mechanism for coated vesicle budding. Nature 374:190-192.

Hirokawa N, Sobue K, Kanda K, Harada A, Yorifuji H (1989) The cytoskeletal architecture of the presynaptic terminal and molecular structure of synapsin 1. J Cell Biol 108:111-126.

Hoffer JA, Sugano N, Loeb GE, Marks WB, O'Donovan MJ, Pratt CA (1987) Cat hindlimb motoneurons during locomotion. II. Normal activity patterns. J Neurophysiol 57:530-553.

Holt M, Cooke A, Neef A, Lagnado L (2004) High mobility of vesicles supports continuous exocytosis at a ribbon synapse. Curr Biol 14:173-183.

Honegger HW (1977) Interommatidial hair receptor axons extending into the ventral nerve cord in the cricket Gryllus campestris. Cell Tissue Res 182:281-285.

Honegger HW, Schurmann FW (1975) Cobalt sulphide staining of optic fibres in the brain of the cricket, Gryllus campestris. Cell Tissue Res 159:213-225.

Hoopmann P, Punge A, Barysch SV, Westphal V, Buckers J, Opazo F, Bethani I, Lauterbach MA, Hell SW, Rizzoli SO (2010) Endosomal sorting of readily releasable synaptic vesicles. Proc Natl Acad Sci U S A 107:19055-19060.

Hormuzdi SG, Filippov MA, Mitropoulou G, Monyer H, Bruzzone R (2004) Electrical synapses: a dynamic signaling system that shapes the activity of neuronal networks. Biochim Biophys Acta 1662:113-137.

Hosaka M, Hammer RE, Sudhof TC (1999) A phospho-switch controls the dynamic association of synapsins with synaptic vesicles. Neuron 24:377-387.

Hosoi N, Holt M, Sakaba T (2009) Calcium dependence of exo- and endocytotic coupling at a glutamatergic synapse. Neuron 63:216-229.

Hua Y, Sinha R, Martineau M, Kahms M, Klingauf J (2010) A common origin of synaptic vesicles undergoing evoked and spontaneous fusion. Nat Neurosci 13:1451-1453.

Hua Y, Sinha R, Thiel CS, Schmidt R, Huve J, Martens H, Hell SW, Egner A, Klingauf J (2011a) A readily retrievable pool of synaptic vesicles. Nat Neurosci 14:833-839.

Hua Z, Leal-Ortiz S, Foss SM, Waites CL, Garner CC, Voglmaier SM, Edwards RH (2011b) v-SNARE Composition Distinguishes Synaptic Vesicle Pools. Neuron 71:474-487.

Huttner WB, DeGennaro LJ, Greengard P (1981) Differential phosphorylation of multiple sites in purified protein I by cyclic AMP-dependent and calcium-dependent protein kinases. J Biol Chem 256:1482-1488.

Huttner WB, Schiebler W, Greengard P, De Camilli P (1983) Synapsin I (protein I), a nerve terminal-specific phosphoprotein. III. Its association with synaptic vesicles studied in a highly purified synaptic vesicle preparation. J Cell Biol 96:1374-1388.

Ikeda K, Bekkers JM (2009) Counting the number of releasable synaptic vesicles in a presynaptic terminal. Proc Natl Acad Sci U S A 106:2945-2950.

Israel M, Dunant Y, Manaranche R (1979) The present status of the vesicular hypothesis. Prog Neurobiol 13:237-275.

Itoh T, De Camilli P (2006) BAR, F-BAR (EFC) and ENTH/ANTH domains in the regulation of membrane-cytosol interfaces and membrane curvature. Biochim Biophys Acta 1761:897-912.

Jahn R, Lang T, Sudhof TC (2003) Membrane fusion. Cell 112:519-533.

Jahn R, Scheller RH (2006) SNAREs--engines for membrane fusion. Nat Rev Mol Cell Biol 7:631-643.

Jakobsson J, Gad H, Andersson F, Low P, Shupliakov O, Brodin L (2008) Role of epsin 1 in synaptic vesicle endocytosis. Proc Natl Acad Sci U S A 105:6445-6450.

Jan LY, Jan YN (1976) Properties of the larval neuromuscular junction in Drosophila melanogaster. J Physiol 262:189-214.

Kaeser PS (2011) Pushing synaptic vesicles over the RIM. Cell Logist 1:106-110.

Kamin D, Lauterbach MA, Westphal V, Keller J, Schonle A, Hell SW, Rizzoli SO (2010) High- and low-mobility stages in the synaptic vesicle cycle. Biophys J 99:675-684.

Katz B (1969) The release of neural transmitter substances. Liverpool, Liverpool Univ Press.

Katz B (2003) Neural transmitter release: from quantal secretion to exocytosis and beyond. J Neurocytol 32:437-446.

Katz B, Miledi R (1979) Estimates of quantal content during 'chemical potentiation' of transmitter release. Proc R Soc Lond B Biol Sci 205:369-378.

Kawasaki F, Hazen M, Ordway RW (2000) Fast synaptic fatigue in shibire mutants reveals a rapid requirement for dynamin in synaptic vesicle membrane trafficking. Nat Neurosci 3:859-860.

Khvotchev MV, Ren M, Takamori S, Jahn R, Sudhof TC (2003) Divergent functions of neuronal Rab11b in Ca2+-regulated versus constitutive exocytosis. J Neurosci 23:10531-10539.

Kirchhausen T, Harrison SC, Heuser J (1986) Configuration of clathrin trimers: evidence from electron microscopy. J Ultrastruct Mol Struct Res 94:199-208.

Kirov SA, Petrak LJ, Fiala JC, Harris KM (2004) Dendritic spines disappear with chilling but proliferate excessively upon rewarming of mature hippocampus. Neuroscience 127:69-80.

Klingauf J, Kavalali ET, Tsien RW (1998) Kinetics and regulation of fast endocytosis at hippocampal synapses. Nature 394:581-585.

Koenig JH, Ikeda K (1980) Flight pattern induced by temperature in a single-gene mutant of Drosophila melanogaster. J Neurobiol 11:509-517.

Koenig JH, Ikeda K (1996) Synaptic vesicles have two distinct recycling pathways. J Cell Biol 135:797-808.

Koenig JH, Ikeda K (1999) Contribution of active zone subpopulation of vesicles to evoked and spontaneous release. J Neurophysiol 81:1495-1505.

Koenig JH, Saito K, Ikeda K (1983) Reversible control of synaptic transmission in a single gene mutant of Drosophila melanogaster. J Cell Biol 96:1517-1522.

Koh TW, Korolchuk VI, Wairkar YP, Jiao W, Evergren E, Pan H, Zhou Y, Venken KJ, Shupliakov O, Robinson IM, O'Kane CJ, Bellen HJ (2007) Eps15 and Dap160 control synaptic vesicle membrane retrieval and synapse development. J Cell Biol 178:309-322.

Kopp-Scheinpflug C, Tolnai S, Malmierca MS, Rubsamen R (2008) The medial nucleus of the trapezoid body: comparative physiology. Neuroscience 154:160-170.

Kraszewski K, Daniell L, Mundigl O, De Camilli P (1996) Mobility of synaptic vesicles in nerve endings monitored by recovery from photobleaching of synaptic vesicle-associated fluorescence. J Neurosci 16:5905-5913.

Kraszewski K, Mundigl O, Daniell L, Verderio C, Matteoli M, De Camilli P (1995) Synaptic vesicle dynamics in living cultured hippocampal neurons visualized with CY3-conjugated antibodies directed against the lumenal domain of synaptotagmin. J Neurosci 15:4328-4342.

Kuromi H, Kidokoro Y (1998) Two distinct pools of synaptic vesicles in single presynaptic boutons in a temperature-sensitive Drosophila mutant, shibire. Neuron 20:917-925.

Kuromi H, Kidokoro Y (1999) The optically determined size of exo/endo cycling vesicle pool correlates with the quantal content at the neuromuscular junction of Drosophila larvae. J Neurosci 19:1557-1565.

Kuromi H, Kidokoro Y (2000) Tetanic stimulation recruits vesicles from reserve pool via a cAMP-mediated process in Drosophila synapses. Neuron 27:133-143.

Kuromi H, Kidokoro Y (2002) Selective replenishment of two vesicle pools depends on the source of Ca2+ at the Drosophila synapse. Neuron 35:333-343.

Kuromi H, Kidokoro Y (2003) Two synaptic vesicle pools, vesicle recruitment and replenishment of pools at the Drosophila neuromuscular junction. J Neurocytol 32:551-565.

Kuromi H, Kidokoro Y (2005) Exocytosis and endocytosis of synaptic vesicles and functional roles of vesicle pools: lessons from the Drosophila neuromuscular junction. Neuroscientist 11:138-147.

Kuromi H, Yoshihara M, Kidokoro Y (1997) An inhibitory role of calcineurin in endocytosis of synaptic vesicles at nerve terminals of Drosophila larvae. Neurosci Res 27:101-113.

Landis DM, Hall AK, Weinstein LA, Reese TS (1988) The organization of cytoplasm at the presynaptic active zone of a central nervous system synapse. Neuron 1:201-209.

Lang T, Rizzoli SO (2010) Membrane protein clusters at nanoscale resolution: more than pretty pictures. Physiology (Bethesda) 25:116-124.

Lee AK, Manns ID, Sakmann B, Brecht M (2006) Whole-cell recordings in freely moving rats. Neuron 51:399-407.

Lemke EA, Klingauf J (2005) Single synaptic vesicle tracking in individual hippocampal boutons at rest and during synaptic activity. J Neurosci 25:11034-11044.

Lenzi D, von Gersdorff H (2001) Structure suggests function: the case for synaptic ribbons as exocytotic nanomachines. Bioessays 23:831-840.

Leveque C, Hoshino T, David P, Shoji-Kasai Y, Leys K, Omori A, Lang B, el Far O, Sato K, Martin-Moutot N, et al. (1992) The synaptic vesicle protein synaptotagmin associates with calcium channels and is a putative Lambert-Eaton myasthenic syndrome antigen. Proc Natl Acad Sci U S A 89:3625-3629.

Li C, Ullrich B, Zhang JZ, Anderson RG, Brose N, Sudhof TC (1995) Ca(2+)-dependent and - independent activities of neural and non-neural synaptotagmins. Nature 375:594-599.

Lonart G, Simsek-Duran F (2006) Deletion of synapsins I and II genes alters the size of vesicular pools and rabphilin phosphorylation. Brain Res 1107:42-51.

Lonart G, Sudhof TC (1998) Region-specific phosphorylation of rabphilin in mossy fiber nerve terminals of the hippocampus. J Neurosci 18:634-640.

Lorteije JA, Rusu SI, Kushmerick C, Borst JG (2009) Reliability and precision of the mouse calyx of Held synapse. J Neurosci 29:13770-13784.

Mandell JW, Townes-Anderson E, Czernik AJ, Cameron R, Greengard P, De Camilli P (1990) Synapsins in the vertebrate retina: absence from ribbon synapses and heterogeneous distribution among conventional synapses. Neuron 5:19-33.

Marks B, McMahon HT (1998) Calcium triggers calcineurin-dependent synaptic vesicle recycling in mammalian nerve terminals. Curr Biol 8:740-749.

Martin AR (1994) Amplification of neuromuscular transmission by postjunctional folds. Proc Biol Sci 258:321-326.

Maycox PR, Link E, Reetz A, Morris SA, Jahn R (1992) Clathrin-coated vesicles in nervous tissue are involved primarily in synaptic vesicle recycling. J Cell Biol 118:1379-1388.

McMahon HT, Missler M, Li C, Sudhof TC (1995) Complexins: cytosolic proteins that regulate SNAP receptor function. Cell 83:111-119.

McPherson PS (2002) The endocytic machinery at an interface with the actin cytoskeleton: a dynamic, hip intersection. Trends Cell Biol 12:312-315.

McPherson PS, Garcia EP, Slepnev VI, David C, Zhang X, Grabs D, Sossin WS, Bauerfeind R, Nemoto Y, De Camilli P (1996) A presynaptic inositol-5-phosphatase. Nature 379:353-357.

Merrifield CJ, Feldman ME, Wan L, Almers W (2002) Imaging actin and dynamin recruitment during invagination of single clathrin-coated pits. Nat Cell Biol 4:691-698.

Meyers JR, MacDonald RB, Duggan A, Lenzi D, Standaert DG, Corwin JT, Corey DP (2003) Lighting up the senses: FM1-43 loading of sensory cells through nonselective ion channels. J Neurosci 23:4054-4065.

Michels B, Diegelmann S, Tanimoto H, Schwenkert I, Buchner E, Gerber B (2005) A role for Synapsin in associative learning: the Drosophila larva as a study case. Learn Mem 12:224-231.

Micheva KD, Ramjaun AR, Kay BK, McPherson PS (1997) SH3 domain-dependent interactions of endophilin with amphiphysin. Febs Letters 414:308-312.

Micheva KD, Smith SJ (2005) Strong effects of subphysiological temperature on the function and plasticity of mammalian presynaptic terminals. J Neurosci 25:7481-7488.

Miesenbock G, De Angelis DA, Rothman JE (1998) Visualizing secretion and synaptic transmission with pH-sensitive green fluorescent proteins. Nature 394:192-195.

Miller TM, Heuser JE (1984) Endocytosis of synaptic vesicle membrane at the frog neuromuscular junction. J Cell Biol 98:685-698.

Monaldi I, Vassalli M, Bachi A, Giovedi S, Millo E, Valtorta F, Raiteri R, Benfenati F, Fassio A (2010) The highly conserved synapsin domain E mediates synapsin dimerization and phospholipid vesicle clustering. Biochem J 426:55-64.

Monosov EZ, Wenzel TJ, Luers GH, Heyman JA, Subramani S (1996) Labeling of peroxisomes with green fluorescent protein in living P. pastoris cells. J Histochem Cytochem 44:581-589.

Morgan JR, Zhao X, Womack M, Prasad K, Augustine GJ, Lafer EM (1999) A role for the clathrin assembly domain of AP180 in synaptic vesicle endocytosis. J Neurosci 19:10201-10212.

Murthy VN, De Camilli P (2003) Cell biology of the presynaptic terminal. Annu Rev Neurosci 26:701-728.

Murthy VN, Sejnowski TJ, Stevens CF (1997) Heterogeneous release properties of visualized individual hippocampal synapses. Neuron 18:599-612.

Nagy A, Baker RR, Morris SJ, Whittaker VP (1976) The preparation and characterization of synaptic vesicles of high purity. Brain Res 109:285-309.

Neher E (1998) Vesicle pools and Ca2+ microdomains: new tools for understanding their roles in neurotransmitter release. Neuron 20:389-399.

Neher E (2010) What is Rate-Limiting during Sustained Synaptic Activity: Vesicle Supply or the Availability of Release Sites. Front Synaptic Neurosci 2:144.

Neves G, Lagnado L (1999) The kinetics of exocytosis and endocytosis in the synaptic terminal of goldfish retinal bipolar cells. J Physiol 515:181-202.

Nguyen D, Sargent PB (2002) Synaptic vesicle recycling at two classes of release sites in giant nerve terminals of the embryonic chicken ciliary ganglion. J Comp Neurol 448:128-137.

Nicholls DG (1978) Calcium transport and porton electrochemical potential gradient in mitochondria from guinea-pig cerebral cortex and rat heart. Biochem J 170:511-522.

Nicholls JG, Martin AR, Wallace BG, Fuchs PA (2001) From neuron to brain. 4th edition. Sunderland, Sinauer Associates, Inc.

Opazo F, Punge A, Buckers J, Hoopmann P, Kastrup L, Hell SW, Rizzoli SO (2010) Limited intermixing of synaptic vesicle components upon vesicle recycling. Traffic 11:800-812.

Opazo F, Rizzoli SO (2010) Studying synaptic vesicle pools using photoconversion of styryl dyes. J Vis Exp 36:e1790.

Paddenberg R, Wiegand C, Jockusch BM (1990) Characterization of the coated vesicle uncoating ATPase: tissue distribution, association with and activity on intact coated vesicles. Eur J Cell Biol 52:60-66.

Paillart C, Li J, Matthews G, Sterling P (2003) Endocytosis and vesicle recycling at a ribbon synapse. J Neurosci 23:4092-4099.

Pakkenberg B, Gundersen HJ (1997) Neocortical neuron number in humans: effect of sex and age. J Comp Neurol 384:312-320.

Parducz A, Kiss Z, Joo F (1976) Changes of the phosphatidylcholine content and the number of synaptic vesicles in relation to the neurohumoral transmission in sympathetic ganglia. Experientia 32:1520-1521.

Park S, Hwang H, Nam SW, Martinez F, Austin RH, Ryu WS (2008) Enhanced Caenorhabditis elegans locomotion in a structured microfluidic environment. PLoS One 3:e2550.

Parsons TD, Sterling P (2003) Synaptic ribbon. Conveyor belt or safety belt? Neuron 37:379-382.

Pechstein A, Shupliakov O (2010) Taking a back seat: synaptic vesicle clustering in presynaptic terminals. Front Synaptic Neurosci 2:143.

Petrucci TC, Morrow JS (1987) Synapsin I: an actin-bundling protein under phosphorylation control. J Cell Biol 105:1355-1363.

Petzold GC, Albeanu DF, Sato TF, Murthy VN (2008) Coupling of neural activity to blood flow in olfactory glomeruli is mediated by astrocytic pathways. Neuron 58:897-910.

Pieribone VA, Shupliakov O, Brodin L, Hilfiker-Rothenfluh S, Czernik AJ, Greengard P (1995) Distinct pools of synaptic vesicles in neurotransmitter release. Nature 375:493-497.

Plaut I (2000) Effects of fin size on swimming performance, swimming behaviour and routine activity of zebrafish Danio rerio. J Exp Biol 203:813-820.

Pockett S, Macdonald JA (1986) Temperature dependence of neurotransmitter release in the antarctic fish Pagothenia borchgrevinki. Experientia 42:414-415.

Popov VI, Bocharova LS, Bragin AG (1992) Repeated changes of dendritic morphology in the hippocampus of ground squirrels in the course of hibernation. Neuroscience 48:45-51.

Poskanzer KE, Davis GW (2004) Mobilization and fusion of a non-recycling pool of synaptic vesicles under conditions of endocytic blockade. Neuropharmacology 47:714-723.

Potter LT (1970) Synthesis, storage and release of [14C]acetylcholine in isolated rat diaphragm muscles. J Physiol 206:145-166.

Pyle JL, Kavalali ET, Piedras-Renteria ES, Tsien RW (2000) Rapid reuse of readily releasable pool vesicles at hippocampal synapses. Neuron 28:221-231.

Pyott SJ, Rosenmund C (2002) The effects of temperature on vesicular supply and release in autaptic cultures of rat and mouse hippocampal neurons. J Physiol 539:523-535.

Qualmann B, Kelly RB (2000) Syndapin isoforms participate in receptor-mediated endocytosis and actin organization. J Cell Biol 148:1047-1062.

Rea R, Li J, Dharia A, Levitan ES, Sterling P, Kramer RH (2004) Streamlined synaptic vesicle cycle in cone photoreceptor terminals. Neuron 41:755-766.

Redenti S, Chappell RL (2003) Zinc chelation enhances the sensitivity of the ERG b-wave in dark-adapted skate retina. Biol Bull 205:213-214.

Reiff DF, Ihring A, Guerrero G, Isacoff EY, Joesch M, Nakai J, Borst A (2005) In vivo performance of genetically encoded indicators of neural activity in flies. J Neurosci 25:4766-4778.

Reist NE, Buchanan J, Li J, DiAntonio A, Buxton EM, Schwarz TL (1998) Morphologically docked synaptic vesicles are reduced in synaptotagmin mutants of Drosophila. J Neurosci 18:7662-7673.

Richards DA, Bai J, Chapman ER (2005) Two modes of exocytosis at hippocampal synapses revealed by rate of FM1-43 efflux from individual vesicles. J Cell Biol 168:929-939.

Richards DA, Guatimosim C, Betz WJ (2000) Two endocytic recycling routes selectively fill two vesicle pools in frog motor nerve terminals. Neuron 27:551-559.

Richards DA, Guatimosim C, Rizzoli SO, Betz WJ (2003) Synaptic vesicle pools at the frog neuromuscular junction. Neuron 39:529-541.

Rittweger E, Han KY, Irvine SE, Eggeling C, Hell SW (2009) STED microscopy reveals crystal colour centres with nanometric resolution. Nature Photonics 3:144-147.

Rizzoli SO, Bethani I, Zwilling D, Wenzel D, Siddiqui TJ, Brandhorst D, Jahn R (2006) Evidence for early endosome-like fusion of recently endocytosed synaptic vesicles. Traffic 7:1163-1176.

Rizzoli SO, Betz WJ (2002) Effects of 2-(4-morpholinyl)-8-phenyl-4H-1-benzopyran-4-one on synaptic vesicle cycling at the frog neuromuscular junction. J Neurosci 22:10680-10689.

Rizzoli SO, Betz WJ (2004) The structural organization of the readily releasable pool of synaptic vesicles. Science 303:2037-2039.

Rizzoli SO, Betz WJ (2005) Synaptic vesicle pools. Nat Rev Neurosci 6:57-69.

Rizzoli SO, Jahn R (2007) Kiss-and-run, collapse and 'readily retrievable' vesicles. Traffic 8:1137-1144.

Roelandse M, Matus A (2004) Hypothermia-associated loss of dendritic spines. J Neurosci 24:7843-7847.

Roos A, Boron WF (1981) Intracellular pH. Physiol Rev 61:296-434.

Roos J, Kelly RB (1999) The endocytic machinery in nerve terminals surrounds sites of exocytosis. Curr Biol 9:1411-1414.

Rossi V, Banfield DK, Vacca M, Dietrich LE, Ungermann C, D'Esposito M, Galli T, Filippini F (2004) Longins and their longin domains: regulated SNAREs and multifunctional SNARE regulators. Trends Biochem Sci 29:682-688.

Ruiz R, Cano R, Casanas JJ, Gaffield MA, Betz WJ, Tabares L (2011) Active zones and the readily releasable pool of synaptic vesicles at the neuromuscular junction of the mouse. J Neurosci 31:2000-2008.

Ryan TA, Reuter H, Smith SJ (1997) Optical detection of a quantal presynaptic membrane turnover. Nature 388:478-482.

Sabatini BL, Regehr WG (1996) Timing of neurotransmission at fast synapses in the mammalian brain. Nature 384:170-172.

Sankaranarayanan S, Atluri PP, Ryan TA (2003) Actin has a molecular scaffolding, not propulsive, role in presynaptic function. Nat Neurosci 6:127-135.

Sankaranarayanan S, De Angelis D, Rothman JE, Ryan TA (2000) The use of pHluorins for optical measurements of presynaptic activity. Biophys J 79:2199-2208.

Sara Y, Virmani T, Deak F, Liu X, Kavalali ET (2005) An isolated pool of vesicles recycles at rest and drives spontaneous neurotransmission. Neuron 45:563-573.

Satzler K, Sohl LF, Bollmann JH, Borst JG, Frotscher M, Sakmann B, Lubke JH (2002) Three-dimensional reconstruction of a calyx of Held and its postsynaptic principal neuron in the medial nucleus of the trapezoid body. J Neurosci 22:10567-10579.

Schermelleh L, Carlton PM, Haase S, Shao L, Winoto L, Kner P, Burke B, Cardoso MC, Agard DA, Gustafsson MG, Leonhardt H, Sedat JW (2008) Subdiffraction multicolor imaging of the nuclear periphery with 3D structured illumination microscopy. Science 320:1332-1336.

Schiavo G, Stenbeck G, Rothman JE, Sollner TH (1997) Binding of the synaptic vesicle v-SNARE, synaptotagmin, to the plasma membrane t-SNARE, SNAP-25, can explain docked vesicles at neurotoxin-treated synapses. Proc Natl Acad Sci U S A 94:997-1001.

Schiebler W, Jahn R, Doucet JP, Rothlein J, Greengard P (1986) Characterization of synapsin I binding to small synaptic vesicles. J Biol Chem 261:8383-8390.

Schikorski T, Stevens CF (1997) Quantitative ultrastructural analysis of hippocampal excitatory synapses. J Neurosci 17:5858-5867.

Schikorski T, Stevens CF (2001) Morphological correlates of functionally defined synaptic vesicle populations. Nat Neurosci 4:391-395.

Schluter OM, Basu J, Sudhof TC, Rosenmund C (2006) Rab3 superprimes synaptic vesicles for release: implications for short-term synaptic plasticity. J Neurosci 26:1239-1246.

Schluter OM, Khvotchev M, Jahn R, Sudhof TC (2002) Localization versus function of Rab3 proteins. Evidence for a common regulatory role in controlling fusion. J Biol Chem 277:40919-40929.

Schluter OM, Schnell E, Verhage M, Tzonopoulos T, Nicoll RA, Janz R, Malenka RC, Geppert M, Sudhof TC (1999) Rabphilin knock-out mice reveal that rabphilin is not required for rab3 function in regulating neurotransmitter release. J Neurosci 19:5834-5846.

Schmidt R, Wurm CA, Punge A, Egner A, Jakobs S, Hell SW (2009) Mitochondrial cristae revealed with focused light. Nano Lett 9:2508-2510.

Schneggenburger R, Meyer AC, Neher E (1999) Released fraction and total size of a pool of immediately available transmitter quanta at a calyx synapse. Neuron 23:399-409.

Schneggenburger R, Neher E (2000) Intracellular calcium dependence of transmitter release rates at a fast central synapse. Nature 406:889-893.

Schneggenburger R, Neher E (2005) Presynaptic calcium and control of vesicle fusion. Curr Opin Neurobiol 15:266-274.

Schneider H, Sulner B (2006) Innervation of dorsal and caudal fin muscles in adult zebrafish Danio rerio. J Comp Neurol 497:702-716.

Schwartz SL, Cao C, Pylypenko O, Rak A, Wandinger-Ness A (2007) Rab GTPases at a glance. J Cell Sci 120:3905-3910.

Shen KF, Schwartzkroin PA (1988) Effects of temperature alterations on population and cellular activities in hippocampal slices from mature and immature rabbit. Brain Res 475:305-316.

Shirataki H, Kaibuchi K, Sakoda T, Kishida S, Yamaguchi T, Wada K, Miyazaki M, Takai Y (1993) Rabphilin-3A, a putative target protein for smg p25A/rab3A p25 small GTP-binding protein related to synaptotagmin. Mol Cell Biol 13:2061-2068.

Shtrahman M, Yeung C, Nauen DW, Bi GQ, Wu XL (2005) Probing vesicle dynamics in single hippocampal synapses. Biophys J 89:3615-3627.

Shupliakov O (2009) The synaptic vesicle cluster: a source of endocytic proteins during neurotransmitter release. Neuroscience 158:204-210.

Shupliakov O, Bloom O, Gustafsson JS, Kjaerulff O, Low P, Tomilin N, Pieribone VA, Greengard P, Brodin L (2002) Impaired recycling of synaptic vesicles after acute perturbation of the presynaptic actin cytoskeleton. Proc Natl Acad Sci U S A 99:14476-14481.

Shupliakov O, Low P, Grabs D, Gad H, Chen H, David C, Takei K, De Camilli P, Brodin L (1997) Synaptic vesicle endocytosis impaired by disruption of dynamin-SH3 domain interactions. Science 276:259-263.

Sieber JJ, Willig KI, Kutzner C, Gerding-Reimers C, Harke B, Donnert G, Rammner B, Eggeling C, Hell SW, Grubmuller H, Lang T (2007) Anatomy and dynamics of a supramolecular membrane protein cluster. Science 317:1072-1076.

Siksou L, Rostaing P, Lechaire JP, Boudier T, Ohtsuka T, Fejtova A, Kao HT, Greengard P, Gundelfinger ED, Triller A, Marty S (2007) Three-dimensional architecture of presynaptic terminal cytomatrix. J Neurosci 27:6868-6877.

Slater CR (2003) Structural determinants of the reliability of synaptic transmission at the vertebrate neuromuscular junction. J Neurocytol 32:505-522.

Slater CR, Lyons PR, Walls TJ, Fawcett PR, Young C (1992) Structure and function of neuromuscular junctions in the vastus lateralis of man. A motor point biopsy study of two groups of patients. Brain 115:451-478.

Slepnev VI, De Camilli P (2000) Accessory factors in clathrin-dependent synaptic vesicle endocytosis. Nat Rev Neurosci 1:161-172.

Smith JE, Reese TS (1980) Use of aldehyde fixatives to determine the rate of synaptic transmitter release. J Exp Biol 89:19-29.

Sollner T, Bennett MK, Whiteheart SW, Scheller RH, Rothman JE (1993a) A protein assembly-disassembly pathway in vitro that may correspond to sequential steps of synaptic vesicle docking, activation, and fusion. Cell 75:409-418.

Sollner T, Whiteheart SW, Brunner M, Erdjument-Bromage H, Geromanos S, Tempst P, Rothman JE (1993b) SNAP receptors implicated in vesicle targeting and fusion. Nature 362:318-324.

Staras K, Branco T (2010) Sharing vesicles between central presynaptic terminals: implications for synaptic function. Front Synaptic Neurosci 2:20.

Staras K, Branco T, Burden JJ, Pozo K, Darcy K, Marra V, Ratnayaka A, Goda Y (2010) A vesicle superpool spans multiple presynaptic terminals in hippocampal neurons. Neuron 66:37-44.

Sterling P, Matthews G (2005) Structure and function of ribbon synapses. Trends Neurosci 28:20-29.

Stevens CF, Williams JH (2000) "Kiss and run" exocytosis at hippocampal synapses. Proc Natl Acad Sci U S A 97:12828-12833.

Sudhof TC (2002) Synaptotagmins: why so many? J Biol Chem 277:7629-7632.

Sudhof TC (2004) The synaptic vesicle cycle. Annu Rev Neurosci 27:509-547.

Sudhof TC, Czernik AJ, Kao HT, Takei K, Johnston PA, Horiuchi A, Kanazir SD, Wagner MA, Perin MS, De Camilli P, et al. (1989) Synapsins: mosaics of shared and individual domains in a family of synaptic vesicle phosphoproteins. Science 245:1474-1480.

Sugita S, Shin OH, Han W, Lao Y, Sudhof TC (2002) Synaptotagmins form a hierarchy of exocytotic Ca(2+) sensors with distinct Ca(2+) affinities. Embo J 21:270-280.

Sumakovic M, Hegermann J, Luo L, Husson SJ, Schwarze K, Olendrowitz C, Schoofs L, Richmond J, Eimer S (2009) UNC-108/RAB-2 and its effector RIC-19 are involved in dense core vesicle maturation in Caenorhabditis elegans. J Cell Biol 186:897-914.

Sun JY, Wu XS, Wu LG (2002) Single and multiple vesicle fusion induce different rates of endocytosis at a central synapse. Nature 417:555-559.

Sutton RB, Fasshauer D, Jahn R, Brunger AT (1998) Crystal structure of a SNARE complex involved in synaptic exocytosis at 2.4 A resolution. Nature 395:347-353.

Svoboda K, Denk W, Kleinfeld D, Tank DW (1997) In vivo dendritic calcium dynamics in neocortical pyramidal neurons. Nature 385:161-165.

Takamori S, Holt M, Stenius K, Lemke EA, Gronborg M, Riedel D, Urlaub H, Schenck S, Brugger B, Ringler P, Muller SA, Rammner B, Grater F, Hub JS, De Groot BL, Mieskes G, Moriyama Y, Klingauf J, Grubmuller H, Heuser J, Wieland F, Jahn R (2006) Molecular anatomy of a trafficking organelle. Cell 127:831-846.

Takei K, McPherson PS, Schmid SL, De Camilli P (1995a) Tubular membrane invaginations coated by dynamin rings are induced by GTP-gamma S in nerve terminals. Nature 374:186-190.

Takei Y, Harada A, Takeda S, Kobayashi K, Terada S, Noda T, Takahashi T, Hirokawa N (1995b) Synapsin I deficiency results in the structural change in the presynaptic terminals in the murine nervous system. J Cell Biol 131:1789-1800.

Tao-Cheng JH (2006) Activity-related redistribution of presynaptic proteins at the active zone. Neuroscience 141:1217-1224.

Tao-Cheng JH, Dosemeci A, Winters CA, Reese TS (2006) Changes in the distribution of calcium calmodulin-dependent protein kinase II at the presynaptic bouton after depolarization. Brain Cell Biol 35:117-124.

Teng H, Wilkinson RS (2000) Clathrin-mediated endocytosis near active zones in snake motor boutons. J Neurosci 20:7986-7993.

Thomas JK, Janz DM (2011) Dietary selenomethionine exposure in adult zebrafish alters swimming performance, energetics and the physiological stress response. Aquat Toxicol 102:79-86.

Thompson SM, Masukawa LM, Prince DA (1985) Temperature dependence of intrinsic membrane properties and synaptic potentials in hippocampal CA1 neurons in vitro. J Neurosci 5:817-824.

Ubach J, Zhang X, Shao X, Sudhof TC, Rizo J (1998) Ca2+ binding to synaptotagmin: how many Ca2+ ions bind to the tip of a C2-domain? Embo J 17:3921-3930.

Ungewickell E, Ungewickell H, Holstein SE, Lindner R, Prasad K, Barouch W, Martin B, Greene LE, Eisenberg E (1995) Role of auxilin in uncoating clathrin-coated vesicles. Nature 378:632-635.

Uytterhoeven V, Kuenen S, Kasprowicz J, Miskiewicz K, Verstreken P (2011) Loss of skywalker reveals synaptic endosomes as sorting stations for synaptic vesicle proteins. Cell 145:117-132.

Van der Kloot W (2003) Loading and recycling of synaptic vesicles in the Torpedo electric organ and the vertebrate neuromuscular junction. Prog Neurobiol 71:269-303.

Vautrin J, Mambrini J (1989) Synaptic current between neuromuscular junction folds. J Theor Biol 140:479-498.

Venance L, Rozov A, Blatow M, Burnashev N, Feldmeyer D, Monyer H (2000) Connexin expression in electrically coupled postnatal rat brain neurons. Proc Natl Acad Sci U S A 97:10260-10265.

Voglmaier SM, Kam K, Yang H, Fortin DL, Hua Z, Nicoll RA, Edwards RH (2006) Distinct endocytic pathways control the rate and extent of synaptic vesicle protein recycling. Neuron 51:71-84.

Volgushev M, Vidyasagar TR, Chistiakova M, Eysel UT (2000a) Synaptic transmission in the neocortex during reversible cooling. Neuroscience 98:9-22.

Volgushev M, Vidyasagar TR, Chistiakova M, Yousef T, Eysel UT (2000b) Membrane properties and spike generation in rat visual cortical cells during reversible cooling. J Physiol 522:59-76.

Von Kriegstein K, Schmitz F, Link E, Sudhof TC (1999) Distribution of synaptic vesicle proteins in the mammalian retina identifies obligatory and facultative components of ribbon synapses. Eur J Neurosci 11:1335-1348.

Wang Y, Okamoto M, Schmitz F, Hofmann K, Sudhof TC (1997) Rim is a putative Rab3 effector in regulating synaptic-vesicle fusion. Nature 388:593-598.

Weiler M, Roed IS, Whittaker VP (1982) The kinetics of acetylcholine turnover in a resting cholinergic nerve terminal and the magnitude of the cytoplasmic compartment. J Neurochem 38:1187-1191.

Weimer RM, Gracheva EO, Meyrignac O, Miller KG, Richmond JE, Bessereau JL (2006) UNC-13 and UNC-10/rim localize synaptic vesicles to specific membrane domains. J Neurosci 26:8040-8047.

Westphal V, Rizzoli SO, Lauterbach MA, Kamin D, Jahn R, Hell SW (2008) Video-rate far-field optical nanoscopy dissects synaptic vesicle movement. Science 320:246-249.

Whittaker VP (1987) Cholinergic synaptic vesicles from the electromotor nerve terminals of Torpedo. Composition and life cycle. Ann N Y Acad Sci 493:77-91.

Wienisch M, Klingauf J (2006) Vesicular proteins exocytosed and subsequently retrieved by compensatory endocytosis are nonidentical. Nat Neurosci 9:1019-1027.

Wilhelm BG, Groemer TW, Rizzoli SO (2010) The same synaptic vesicles drive active and spontaneous release. Nat Neurosci 13:1454-1456.

Willig KI, Rizzoli SO, Westphal V, Jahn R, Hell SW (2006) STED microscopy reveals that synaptotagmin remains clustered after synaptic vesicle exocytosis. Nature 440:935-939.

Wood SJ, Slater CR (2001) Safety factor at the neuromuscular junction. Prog Neurobiol 64:393-429.

Wu W, Wu LG (2007) Rapid bulk endocytosis and its kinetics of fission pore closure at a central synapse. Proc Natl Acad Sci U S A 104:10234-10239.

Wu W, Xu J, Wu XS, Wu LG (2005) Activity-dependent acceleration of endocytosis at a central synapse. J Neurosci 25:11676-11683.

Wu XS, McNeil BD, Xu J, Fan J, Xue L, Melicoff E, Adachi R, Bai L, Wu LG (2009) Ca(2+) and calmodulin initiate all forms of endocytosis during depolarization at a nerve terminal. Nat Neurosci 12:1003-1010.

Wucherpfennig T, Wilsch-Brauninger M, Gonzalez-Gaitan M (2003) Role of Drosophila Rab5 during endosomal trafficking at the synapse and evoked neurotransmitter release. J Cell Biol 161:609-624.

Yamashita T, Hige T, Takahashi T (2005) Vesicle endocytosis requires dynamin-dependent GTP hydrolysis at a fast CNS synapse. Science 307:124-127.

Yao CK, Lin YQ, Ly CV, Ohyama T, Haueter CM, Moiseenkova-Bell VY, Wensel TG, Bellen HJ (2009) A synaptic vesicle-associated Ca2+ channel promotes endocytosis and couples exocytosis to endocytosis. Cell 138:947-960.

Zhai RG, Bellen HJ (2004) The architecture of the active zone in the presynaptic nerve terminal. Physiology (Bethesda) 19:262-270.

Zhang B, Koh YH, Beckstead RB, Budnik V, Ganetzky B, Bellen HJ (1998a) Synaptic vesicle size and number are regulated by a clathrin adaptor protein required for endocytosis. Neuron 21:1465-1475.

Zhang JZ, Davletov BA, Sudhof TC, Anderson RG (1994) Synaptotagmin I is a high affinity receptor for clathrin AP-2: implications for membrane recycling. Cell 78:751-760.

Zhang Q, Li Y, Tsien RW (2009) The dynamic control of kiss-and-run and vesicular reuse probed with single nanoparticles. Science 323:1448-1453.

Zhang X, Rizo J, Sudhof TC (1998b) Mechanism of phospholipid binding by the C2A-domain of synaptotagmin I. Biochemistry 37:12395-12403.

Zhu Y, Stevens CF (2008) Probing synaptic vesicle fusion by altering mechanical properties of the neuronal surface membrane. Proc Natl Acad Sci U S A 105:18018-18022.

Zilly FE, Halemani ND, Walrafen D, Spitta L, Schreiber A, Jahn R, Lang T (2011) Ca2+ induces clustering of membrane proteins in the plasma membrane via electrostatic interactions. Embo J 30:1209-1220.

Zinsmaier KE, Bronk P (2001) Molecular chaperones and the regulation of neurotransmitter exocytosis. Biochem Pharmacol 62:1-11.

Curriculum Vitae

Personal Information

Name: Annette Denker

Date of birth: January 29th 1985

Place of birth: Aachen, Germany

Address: Fabrikweg 3, 37075 Göttingen, Germany

Email: a.denker@eni-g.de

Education

04/2009 – 09/2011	MSc/PhD Program Molecular Biology PhD thesis in the group of Dr. S. Rizzoli (STED Microscopy of Synaptic Function) at the European Neuroscience Institute, Göttingen
10/2009	Master of Science in Molecular Biology; Degree: 1.08 = A
10/2008 – 03/2009	MSc/PhD Program Molecular Biology (Integrated) Master's thesis in the group of Dr. S. Rizzoli (STED Microscopy of Synaptic Function) at the European Neuroscience Institute, Göttingen
10/2007– 09/2008	MSc/PhD Program Molecular Biology, International Max Planck Research School, University of Göttingen First segment of theoretical and practical Master's studies
08/2007	Bachelor of Science in Molecular Biotechnology; Degree: 1.2 = A
10/2004 – 09/2007	Studies in Molecular Biotechnology at the University of Heidelberg
08/2002 – 06/2004	Gymnasium Essen-Werden Higher Education Entrance Diploma (Abitur); Grade: 1.0 = A
08/2001 – 07/2002	Saint Andrew's-Sewanee School in Sewanee, Tennessee, USA (Scholarship provided by ASSIST Germany)
08/1995 – 07/2001	Gymnasium Essen-Werden

Research Experience and Internships

04/2009 – present	PhD thesis in the group of Dr. S. Rizzoli (STED Microscopy of Synaptic Function) at the European Neuroscience Institute, Göttingen Title: *Synaptic vesicle recycling in vivo*
10/2008 – 03/2009	(Integrated) Master's thesis in the group of Dr. S. Rizzoli (STED Microscopy of Synaptic Function) at the European Neuroscience Institute, Göttingen Title: *Ultrastructural investigation of synaptic vesicle pools in Drosophila melanogaster*
05/2008 – 06/2008	European Neuroscience Institute, Göttingen, Research Group STED Microscopy of Synaptic Function with Dr. S. Rizzoli: *Styryl dye photoconversion in the Drosophila larval neuromuscular junction*
03/2008 – 05/2008	University of Göttingen, Institute for Human Genetics, Department of Molecular Developmental Genetics with Prof. Dr. H. Hahn and Dr. A. Zibat: *Regulation of Wnt5a expression and investigation of Wnt5a-mediated signaling in basal cell carcinoma*
01/2008 – 02/2008	Max Planck Institute for Biophysical Chemistry, Göttingen, Department of Molecular Developmental Biology with Prof. Dr. H. Jäckle and Dr. A. Herzig: *Visualization of chromatin organization and localization by fluorescence in situ hybridization*
04/2007 – 06/2007	University of Heidelberg, Institute for Pharmacy and Molecular Biotechnology with Prof. Dr. S. Wölfl: *Apoptosis in yeast and mammalian cells*
08/2006 – 09/2006	Michigan State University, Lansing, MI, USA, Department of Biochemistry and Molecular Biology with Prof. Dr. W. Wedemeyer: *Toxin secretion system of cholera bacteria*
09/2005 – 10/2005	German Cancer Research Center (DKFZ), Heidelberg, Department of Molecular Genetics with Prof. Dr. H. Herrmann-Lerdon: *Laminopathies*
06/2004 – 08/2004	Bayer AG, Wuppertal, Department of Microbiology (HealthCare-Pharma-Biotechnology) with Dr. H. Wehlmann: Fermentation (*Saccharomyces cerevisiae*), drug production

Fellowships and Awards

06/2011	Best scientific talk award at the "ScieTalk" student congress in Göttingen, Germany (title: Synaptic vesicle recycling *in vivo*)
05/2011	Best student poster award at the "Neurizons" Neuroscience Conference in Göttingen, Germany (title: Investigation of synaptic vesicle recycling *in vivo*)
08/2009 – 09/2011	Boehringer Ingelheim Fonds PhD Fellowship
08/2009	PhD Scholarship of the University of Göttingen (Dorothea Schlözer Program)
11/2004 – 03/2009	Studienstiftung des deutschen Volkes (German National Academic Foundation) (Fellowship awarded to the top 0.5% of German students)

Travel Grants

07/2011	Boehringer Ingelheim Fonds Travel Grant, financing poster presentation at the 8th World Congress of Neuroscience of the International Brain Research Organization in Florence, Italy
06/2011	Participation in the 61st Nobel Laureate Meeting at Lindau, Germany
11/2010	Boehringer Ingelheim Fonds Travel Grant, financing talk at the 40th Annual Meeting of the Society for Neuroscience, San Diego, California, USA
01/2009	GGNB Travel Grant, financing poster presentation at the 42nd Winter Conference on Brain Research, Copper Mountain, Colorado, USA
08/2006 – 09/2006	Grant from the Studienstiftung des deutschen Volkes to finance the internship at Michigan State University, Lansing, Michigan, USA

Publications

09/2011	**Denker A**, Kröhnert K, Bückers J, Neher E, Rizzoli SO. The reserve pool of synaptic vesicles acts as a buffer for proteins involved in synaptic vesicle recycling. Proc Natl Acad Sci USA *(epub ahead of print)*
09/2011	**Denker A**, Bethani I, Kröhnert K, Körber C, Horstmann H, Wilhelm BG, Barysch SV, Kuner T, Neher E, Rizzoli SO. A small pool of vesicles maintains synaptic activity *in vivo*. Proc Natl Acad Sci USA *(epub ahead of print)*
10/2010	**Denker A**, Rizzoli SO. Synaptic vesicle pools: an update. Review. Front Synaptic Neurosci 2:135. doi:10.3389/fnsyn.2010.00135
06/2009	**Denker A**, Kröhnert K, Rizzoli SO. Revisiting synaptic vesicle pool localization in the *Drosophila* neuromuscular junction. J Physiol 587:2919-2926.

Presentations

07/2011   Poster presentation (title: Synaptic vesicle recycling in living animals) at the 8th World Congress of Neuroscience of the International Brain Research Organization in Florence, Italy

06/2011   Talk (title: Synaptic vesicle recycling *in vivo*) at the "ScieTalk" student congress in Göttingen, Germany

05/2011   Poster presentation (title: Investigation of synaptic vesicle recycling *in vivo*) at the "Neurizons" Neuroscience Conference in Göttingen, Germany

04/2011   Talk and poster presentation (title: Investigation of synaptic vesicle recycling in living animals) at the Molecular Mechanisms of Exocytosis and Endocytosis Meeting, Edinburgh, Scotland, UK

11/2010   Talk (title: Synaptic vesicle recycling *in vivo*) at the 40th Annual Meeting of the Society for Neuroscience, San Diego, California, USA

11/2009   Poster presentation (title: Revisiting synaptic vesicle pool localization in the *Drosophila* neuromuscular junction) at the Science Day of the Göttingen Graduate School for Neurosciences and Molecular Biosciences (GGNB)

01/2009   Poster presentation (title: Ultrastructural investigation of synaptic vesicle pools in *Drosophila melanogaster*) at the 42nd Winter Conference on Brain Research, Colorado, USA

01/2009   Invited Talk (title: Ultrastructural investigation of synaptic vesicle pools in *Drosophila melanogaster*) at the University of Colorado, Denver, USA, Department of Physiology and Biophysics (Prof. Dr. W. Betz)

Teaching Experience

05/2011 – 06/2011   Teaching of practical advanced methods course
(title: High resolution microscopy in synapses)

01/2011 – 02/2011   Supervision of lab rotation project
(title: Techniques to investigate synaptic vesicle recycling)

10/2010   Teaching of practical advanced methods course
(title: High resolution microscopy in synapses)

06/2010   Teaching of practical advanced methods course
(title: High resolution microscopy in synapses)

05/2010 – 06/2010   Supervision of lab rotation project
(title: Establishment of the Lumio^{TM} technique in mammalian PC12 cells)

05/2009   Supervision of lab rotation project (together with Dr. S. Rizzoli)
(title: Examining neurons and glia with high resolution imaging techniques)

Memberships

Society for Neuroscience (SFN; since 2010)

Academic Engagement

12/2010 – 11/2011	Organization of the "Women's Careers and Networks" symposium; www.wocanet.uni-goettingen.de
04/2010 – 05/2011	Student representative of the MSc/PhD Program Molecular Biology, International Max Planck Research School, University of Göttingen
01/2009 – 09/2010	Organization of the annual international PhD student symposium "Horizons in Molecular Biology"; www.horizons.uni-goettingen.de